Dissertation

submitted to the

Combined Faculties of the Natural Sciences and Mathematics

of Ruperto-Carola-University of Heidelberg. Germany

for the degree of

Doctor of Natural Sciences

Put forward by

Filippo Fratini

born in: Fano, Italy

Oral examination: 14 December 2011

Title of thesis

Polarization and correlation phenomena

in the two-photon absorption and decay

of heavy ions

Referees: Priv-Doz. Dr. Andrey Surzhykov

                             Priv-Doz. Dr. Antonino Di Piazza

Zusammenfassung

In dieser Arbeit untersuchen wir Zwei-Photonenbergänge zwischen gebunden Zustnden in Atomen und Ionen. Nach einer Einfhrung in die relativistische Diracgleichung und Störungstheorie erster und zweiter Ordnung, analysieren wir die spektrale Verteilung sowie die Winkel- und Polarisationseigenschaften der emittierten Photonen. Die Arbeit beinhaltet eine Untersuchung der Quantenkorrelation (Verschränkung), die der Polarisationszustand der Photonen besitzt, wie auch mgliche Anwendungen der Zwei-Photonenbergnge im Hinblick auf Studien zur Parittsverletzung.

Abstract

In this thesis we investigate two-photon bound-bound transitions in atoms and ions. After a formal introduction to the relativistic Dirac equation and to first- and second-order perturbation theory, we analyze the spectral distribution as well as the angular and polarization properties of the emitted photons. The thesis includes an analysis on the quantum correlation (entanglement) that the polarization state of the photons possesses as well as applications of two-photon transitions toward parity violation studies.

During my PhD studies, the papers which bear my name and which have been published in scientific journals of international standing are the following :

I) A. Surzhykov, A. Volotka, F. Fratini, J. P. Santos, P. Indelicato, G. Plunien, Th. Stöhlker and S. Fritzsche
Angular correlations in the two-photon decay of heliumlike heavy ions
Phys. Rev. A **81** 042510 (2010);

II) F. Fratini and A. Surzhykov
Polarization correlations in the twophoton decay of hydrogenlike ions
Hyp. Int. **199**, 85 (2011);

III) F. Fratini, M.C. Tichy, Th. Jahrsetz, A. Buchleitner, S. Fritzsche and Andrey Surzhykov
Quantum correlations in the two-photon decay of few-electron ions
Phys. Rev. A **83**, 032506 (2011);

IV) F. Fratini, S. Trotsenko, S. Tashenov, Th. Stöhlker and Andrey Surzhykov
Photon-photon polarization correlations as a tool for studying parity nonconservation in heliumlike uranium
Phys. Rev. A **83**, 052505 (2011).

Acknowledgments

CONTENT

Chapter 1

Introduction

Studies of two-photon decay have a long history in Physics. The possibility of a two-photon process was first pointed out by Max Born's PhD student Göppert Mayer in 1931 [1]. At the early stages of these studies (up until the 70s'), most of the research interest has been toward the measurements and the theoretical description of lifetimes of atoms and ions which preferably decay via two-photon emission. An important advance in these studies was achieved in 1940 by Breit and Teller who derived that the double photon emission in Hydrogen has a decay rate of approximately 8 sec^{-1} [2]. Few years later, Shapiro and Breit refined the calculations and explained, therewith, the decay of interstellar hydrogen atoms [3]. Soon after, it has been understood that, in addition to lifetimes studies, the spectral distribution of the two-photon continuum emission could provides richer information concerning the inner structure of the atom. Thus, physicists began measuring such spectral distributions and, with the advent of computer power, highly accurate theoretical calculations could also be made to support these experiments [4–7]. Accurate calculations of two-photon decay rates and spectral distributions are, still nowadays, current challenges for the research physics community.

More recently, the angular properties of the two emitted photons have been investigated [8–10]. Contrarily to energetic and lifetime studies, angle-resolved calculations and measurements give access to vectorial physical quantities of the emitted photons, such as their linear momenta and polarizations. These characteristics may thus provide unique information on the dynamics of atoms and ions. As a matter of fact, by studying spectral and angular distributions of the emitted photons, the statistical properties of electron (Fermi-Dirac statistics) as well as of photons (Bose-Einstein statistics) could be studied and tested [11–15].

In addition, due to the remarkable advances in detector technology that have been

achieved in the last decades, nowadays it is possible to record, in coincidence, energy as well as polarization properties of highly energetic (X-ray) photons [16]. This ability paves the way to a wide field of polarization research studies aimed at testing fundamental principles of quantum mechanics, like quantum correlation (entanglement) [17–19] and parity violation effects in atomic physics [20].

This thesis contributes to, and is part of, these advanced studies. In Chapter 2 we introduce the relativistic theory of particles, atoms and electromagnetic radiation. In Chapter 3 we analyze first- and second-order perturbation theory, as it is the theory at the base of single- and double-photon emission from bound systems. In Chapter 4 a brief introduction to density matrix theory and its applications is made. In Chapter 5, the original results of this thesis are displayed and discussed, together with the advanced studies that have been carried out in the last decade, prior to the present thesis, pertaining two-photon decay. All these studies analyze in detail the energetic, angular, polarization and entanglement properties of the two emitted photons. Finally, a summary is given in Chapter 6, together with an outlook and some perspectives.

Notation
Vectors are denoted with boldface, *e.g.* $\boldsymbol{A}$, while unit vectors with underline, *e.g.* $\underline{A}$. In the quantum space, operators are denoted with hat, *e.g.* $\hat{\mathbf{O}}$ (vector operator) and $\hat{O}$ (scalar operator).
The Einstein summation convention on indices

$$\sum_i A_i \, B_i = A_i \, B_i$$

is adopted.
The notation $J_1 \otimes J_2 = J_3$, where $J_{1,2,3}$ are angular momenta, will be used to denote the triangle rule $|J_1 - J_2| \leq J_3 \leq J_1 + J_2$.
SI units are used throughout, unless differently stated.

CHAPTER 2

RELATIVISTIC THEORY OF PARTICLES, IONS AND ELECTROMAGNETIC RADIATION

The miracle of appropriateness of the language of mathematics for the formulation of the laws of physics is a wonderful gift which we neither undestand nor deserve.

Eugene Wigner, 1960

Due to the strength of the electromagnetic fields, the kinetic energy of the electrons in highly charged ions approaches the rest mass energy. A relativistic theory is therefore required to adequately describe the state and properties of highly-charged ions.

In 1928, the British physicist Paul Dirac proposed a relativistic (covariant) wave equation for the description of elementary charged particles of spin-1/2, such as the electron [21]. One of the remarkable advantages of such equation is that it provides a description of particles where their spin properties are coming out spontaneously from the theory. At that time, this was completely new in comparison with the non-relativistic theory, where the spin, if considered, was added "by hands" to the spatial wavefunction by multiplying it by the spin wavefunction. Since Dirac's work, the spin has been considered a characteristic feature of relativistic quantum mechanics. The second remarkable property of the Dirac equation is that it is single differential in both space and time, so as to allow to interpret the squared modulus of the wavefunction as a probability density.

From now on, we will exclusively refer to electrons, although the treatment holds true for any elementary spin-1/2 charged particle.

3

2.1 RELATIVISTIC DESCRIPTION OF FREE-STATES

2.1.1 DIRAC EQUATION FOR FREE-STATES

If the electron is not affected by any force, i.e we are in the free case, the Dirac equation
reads

$$\left(-i\hbar c\boldsymbol{\alpha}\cdot\boldsymbol{\nabla} + \beta mc^2\right)\Psi(\boldsymbol{r},t) = i\hbar\frac{\partial}{\partial t}\Psi(\boldsymbol{r},t) \ , \tag{2.1}$$

where m is the electronic mass and $\Psi(\boldsymbol{r},t)$ denotes the wavefunction of the electron
at the position $\boldsymbol{r}$ and time t. The matrices $\boldsymbol{\alpha}$ and β are called Dirac matrices. In the
Dirac representation, they read

$$\boldsymbol{\alpha} = \left(\begin{array}{cc} 0 & \boldsymbol{\sigma} \\ \boldsymbol{\sigma} & 0 \end{array}\right) \qquad \beta = \left(\begin{array}{cc} \mathbb{1}_2 & 0 \\ 0 & \mathbb{1}_2 \end{array}\right) \ ,$$

where $\boldsymbol{\sigma}$ is the vector of Pauli matrices and $\mathbb{1}_2$ is the unitary 2x2 matrix. The Dirac
matrices satisfy the relations

$$\begin{aligned}
\{\alpha_i, \alpha_j\} &= 2\delta_{ij} \\
\{\alpha_i, \beta\} &= 0 \\
\alpha_i^2 = \beta^2 &= 1 \\
\alpha_i^\dagger &= \alpha_i \\
\beta^\dagger &= \beta \ ,
\end{aligned} \tag{2.2}$$

for any $i,j = \{1,2,3\}$. Here and in the following, $\{a,b\}$ denotes the anticommutator
between a and b.
The last two properties ensure that the Dirac Hamiltonian

$$\hat{\mathrm{H}}_D = c\boldsymbol{\alpha}\cdot\hat{\mathbf{p}} + \beta mc^2 \tag{2.3}$$

is hermitian.
Since $\boldsymbol{\alpha}$ and β are 4x4 matrices, the electronic wavefuntion is consequently a 4x1 matrix
which is called "Dirac-spinor" (or briefly "spinor").

2.1.2 KLEIN GORDON EQUATION FROM DIRAC EQUATION

It is easy to show that *each* component of the Dirac spinor satisfies the Klein-Gordon
(KG) equation for the free case. We can indeed write

$$-\hbar^2\frac{\partial^2}{\partial^2 t}\Psi(\boldsymbol{r},t) = \left(-i\hbar c\boldsymbol{\alpha}\cdot\boldsymbol{\nabla} + \beta mc^2\right)\left(-i\hbar c\boldsymbol{\alpha}\cdot\boldsymbol{\nabla} + \beta mc^2\right)\Psi(\boldsymbol{r},t) =$$

$$\left(-\hbar^2 c^2\sum_{i,j=1}^{3}\frac{\alpha_i\alpha_j + \alpha_j\alpha_i}{2}\frac{\partial^2}{\partial x_i\partial x_j} - i\hbar mc^3\sum_{i=1}^{3}(\alpha_i\beta + \beta\alpha_i)\frac{\partial}{\partial x_i} + \beta^2 mc^2\right)\Psi(\boldsymbol{r},t) =$$

$$\left(-\hbar^2 c^2\sum_{i,j=1}^{3}\delta_{ij}\frac{\partial^2}{\partial x_i\partial x_j} + 0 + m^2 c^4\right)\Psi(\boldsymbol{r},t) = \left(-\hbar^2 c^2\nabla^2 + mc^2\right)\Psi(\boldsymbol{r},t) \ .$$

$$\tag{2.4}$$

The properties (2.2) have been used together with the equation

$$\alpha_i\alpha_j\frac{\partial^2}{\partial x_i\partial x_j} = \alpha_j\alpha_i\frac{\partial^2}{\partial x_j\partial x_i} = \alpha_j\alpha_i\frac{\partial^2}{\partial x_i\partial x_j} = \frac{\alpha_i\alpha_j + \alpha_j\alpha_i}{2}\frac{\partial^2}{\partial x_i\partial x_j} \ ,$$

which follows from using the Schwarz theorem on the wavefunction $\Psi(\boldsymbol{r}, t)$[1].

Since the differential operator in Eq. (2.4) is scalar, for each scalar component f_μ of the spinor $\Psi(\boldsymbol{r}, t)$ ($\mu = 0, 1, 2, 3$) it must be true that

$$\left(-\hbar^2 c^2 \nabla^2 + mc^2\right) f_\mu = -\hbar^2 \frac{\partial^2}{\partial^2 t} f_\mu \; ,$$

which is the KG equation (in the free case) for the function f_μ.

This has been the first evidence that the Dirac equation was on the right track. The KG equation represents in fact the first attempt to formulate a relativistic equation in quantum mechanics and it is still the equation that rules the relativistic wavefunction evolution of scalar particles (particles with zero spin).

2.1.3 Eigenfunctions of the free Dirac Hamiltonian

Since H_D does not depend on time, we can make use of the ansatz $\Psi(\boldsymbol{r}, t) = \varphi(\boldsymbol{r}) e^{\frac{1}{\hbar} E t}$ and equation (2.1) simplifies to

$$\left(-i\hbar c \boldsymbol{\alpha} \cdot \boldsymbol{\nabla} + \beta mc^2\right) \Psi(\boldsymbol{r}, t) = E \Psi(\boldsymbol{r}, t) \; , \tag{2.5}$$

where E is the energy of the state described by the wavefunction $\Psi(\boldsymbol{r}, t)$.

Prior to deriving the solutions of the above equation, we like to show which quantum numbers are conserved in the free Dirac theory, i.e which quantum numbers commute with the Dirac Hamiltonian (2.3). Those will be the quantum numbers by which we will label our solutions.

We start out by noticing that the operator $\hat{\mathbf{p}}$ trivially commutes with the Dirac Hamiltonian: $[\hat{\mathbf{p}}, c\, \boldsymbol{\alpha} \cdot \hat{\mathbf{p}} + \beta mc^2] = c\, \alpha_i [\hat{\mathbf{p}}, \hat{p}_i] = 0$. The same is true for the helicity operator $\hat{h} = \frac{\hat{\boldsymbol{\Sigma}} \hat{\mathbf{p}}}{|\hat{\mathbf{p}}|}$, where

$$\hat{\boldsymbol{\Sigma}} = \left(\begin{array}{cc} \boldsymbol{\sigma} & 0 \\ 0 & \boldsymbol{\sigma} \end{array} \right) \; .$$

We can indeed write

$$\left[\frac{\hat{\boldsymbol{\Sigma}} \hat{\mathbf{p}}}{|\hat{\mathbf{p}}|}, c\, \boldsymbol{\alpha} \cdot \hat{\mathbf{p}} + \beta mc^2 \right] = \frac{c}{|\hat{\mathbf{p}}|} \hat{p}_i \hat{p}_j [\hat{\Sigma}_i, \alpha_j] + \frac{mc^2}{|\hat{\mathbf{p}}|} \hat{p}_i [\hat{\Sigma}_i, \beta]$$

$$= \frac{c}{|\hat{\mathbf{p}}|} \hat{p}_i \hat{p}_j 2i\epsilon_{i,j,k} \alpha_k + 0 = \frac{2c}{|\hat{\mathbf{p}}|} i \underbrace{\epsilon_{ijk}}_{\text{antisimm.}} \underbrace{\hat{p}_i \hat{p}_j}_{\text{simm.}} \alpha_k = 0 \; .$$

We will therefore use the eigenvalues of $\hat{\mathbf{p}}$ and $\hat{h}$ to label the eigenfunctions of $\hat{H}_D$, so as to denote the eigenfunctions as $\Psi^{\boldsymbol{p} h}(\boldsymbol{r}, t)$. We proceed now to find them.

Being eigenfunctions of the operator $\hat{\mathbf{p}}$, in addition of being solution of Eq. (2.5), they must satisfy the equation:

$$-i\hbar \frac{\partial}{\partial x_i} \Psi^{\boldsymbol{p} h}(\boldsymbol{r}, t) = p_i \Psi^{\boldsymbol{p} h}(\boldsymbol{r}, t) \; , \tag{2.6}$$

---

[1] In order to apply the Schwartz theorem to exchange the partial derivatives, the wavefunction is supposed to be regular: $\Psi \in C_{\geq 2}$.

for any $i = \{1, 2, 3\}$.

Both equations (2.5) and (2.6) are satisfied by a function of the type

$$\Psi^{\boldsymbol{p}h}(\boldsymbol{r}, t) = \Psi_0^{\boldsymbol{p}h} e^{-\frac{i}{\hbar}(\boldsymbol{p}\boldsymbol{r} - Et)} = \Psi_0^{\boldsymbol{p}h} e^{\frac{i}{\hbar}p_\mu x^\mu} \;, \tag{2.7}$$

where $\Psi_0^{\boldsymbol{p}h}$ is to be determined. For this purpose, noticing the 2x2 modular shape of
the Dirac matrices, we write for convenience $\Psi_0^{\boldsymbol{p}h}$ as

$$\Psi_0^{\boldsymbol{p}h} = \begin{pmatrix} \Phi_0 \\ \chi_0 \end{pmatrix} \;.$$

By combining Eq. (2.5) and Eq. (2.7), we find the equations for Φ_0 and χ_0 to be

$$\begin{cases} c\,\boldsymbol{\sigma}\boldsymbol{p}\,\chi_0 + mc^2\,\Phi_0 & = & E\,\Phi_0 \\ c\,\boldsymbol{\sigma}\boldsymbol{p}\,\Phi_0 - mc^2\,\chi_0 & = & E\,\chi_0 \end{cases},$$

for which solutions are

$$E = \pm\sqrt{c^2\boldsymbol{p}^2 + m^2 c^4} \equiv \lambda E_p$$

$$\Phi_0 = \text{any}$$

$$\chi_0 = c\frac{\boldsymbol{\sigma}\boldsymbol{p}}{E_p + mc^2}\Phi_0 \quad.$$

We arbitrarily choose Φ_0 as Pauli spinor representing the helicity state of the particle.
That means that, if the particle runs along the $\hat{z}$ direction and has positive helicity,
the function Φ_0 will be $\begin{pmatrix} 1 \\ 0 \end{pmatrix}$. We will soon see that this is an appropriate choice.

In the first of the above equations, we have defined $E_p = \sqrt{c^2\boldsymbol{p}^2 + m^2 c^4} > 0$, while λ
can assume the two values $+1$ and -1.

In conclusion, the wavefunctions solutions of the Dirac equation for the free case can
be written as

$$\Psi_\lambda^{\boldsymbol{r}h}(\boldsymbol{p}, t) = N \begin{pmatrix} \Phi_0 \\ \dfrac{c\boldsymbol{\sigma}\boldsymbol{p}}{E + mc^2}\Phi_0 \end{pmatrix} e^{\frac{i}{\hbar}x_\mu p^\mu} \;,$$

where λ has been added to the wavefunction's labels to specify whether the function is
positively or negatively energy defined. N is a constant which can be easily shown to
be $N = \sqrt{\dfrac{mc^2 + \lambda E_p}{2\lambda E_p}} = \sqrt{\dfrac{mc^2 + E}{2E}}$ by imposing the normalization of the wavefunc-
tion in space.

Since trivially $\left[\dfrac{\boldsymbol{\sigma}\hat{\mathbf{p}}}{|\boldsymbol{p}|}, \boldsymbol{\sigma}\hat{\mathbf{p}}\right] = 0$, by acting from the left with the helicity operator on the
Dirac wavefunction, we can easily verify that our choice of Φ_0 to be the (conserved)
helicity state of the particle holds true: $\hat{\mathrm{h}}\Psi(\boldsymbol{r}, t) = h\Psi(\boldsymbol{r}, t)$.

As remarked above, two different kinds of states come out from the theory: the positive
and the negative energy states. Although a detailed discussion of this duality exceeds
the scope of this thesis, we may remind that this fact arose, at the beginning, several
doubts toward the Dirac theory.

In accordance with Dirac solutions, the lowest energetic state is the state with infinite

negative energy. This evidently implies that the all matter would continuously decay down to a (so-called) "negative sea", without stability. For this reason, Wolfgang Pauli himself [22], as well as many other eminent physicists of that time, were initially reluctant to accept Dirac's theory, although this latter had been successful in explaining many characteristics of the electron, like its spin.

By making use of the Pauli exclusion principle as inherent property of spin-1/2 particles, Dirac replied to their critics by postulating a nifty conjecture [23]: Since the matter is undoubtly stable, the negative sea must be totally full of electrons, so that the lowest *available* state is of positive energy. The electrons possessing negative energy are evidently not visible and must represent what we call the physical vacuum. When a negative energy electron is lifted to any positive energy state, we should be able to observe both the electron with now positive energy and the hole left in the negative sea, where the latter will be then interpreted as a moving free particle with the same electronic characteristics but with positive charge.

This imaginative hypothesis looked, to many physicist of that time, very far from something real, until "the positive electron" (which has been afterwards called *positron*) was effectively discovered by C.D. Anderson in 1933 [24][2]. Dirac was forthwith awarded with the Nobel Prize together with Erwin Schrödinger.

2.2   RELATIVISTIC DESCRIPTION OF BOUND-STATES

If a time-independent scalar potential $V(\boldsymbol{r})$ is present, the Dirac equation reads

$$\left(-i\hbar c\boldsymbol{\alpha} \cdot \boldsymbol{\nabla} + V(\boldsymbol{r}) + \beta mc^2\right)\Psi(\boldsymbol{r},t) = E\,\Psi(\boldsymbol{r},t)\ .$$

In many cases of interest, the scalar potential is of central type. Thus we will henceforth consider $V(\boldsymbol{r}) = V(r)$.

Analogously as we did for the free case, prior to deriving the solution of the above equation, we look for the good (conserved) quantum numbers by which to describe the solutions. In other words, we look for the operators which commute with the Dirac Hamiltonian. The Dirac Hamiltonian in the bound case reads

$$\hat{\mathrm{H}}_D = c\boldsymbol{\alpha} \cdot \hat{\mathbf{p}} + V(\hat{\mathrm{r}}) + \beta mc^2\ .$$

As a general argument, being the potential central, the total angular momentum is expected to be conserved in contrast to the linear momentum. We therefore start our search by analyzing spin, orbital angular and total angular momenta, separately.

The spin operator is $\hat{\mathbf{S}} = \dfrac{\hbar}{2}\hat{\boldsymbol{\Sigma}}$, where $\hat{\boldsymbol{\Sigma}}$ has been defined in Sec. 2.1.3. We have

$$[\frac{\hbar}{2}\hat{\Sigma}_i, c\,\boldsymbol{\alpha}\cdot\hat{\mathbf{p}} + V(\hat{\mathrm{r}}) + \beta mc^2] = \frac{\hbar}{2}c\hat{\mathrm{p}}_j[\hat{\Sigma}_i, \alpha_j] + 0 + mc^2\frac{\hbar}{2}[\hat{\Sigma}_i, \beta] =$$

$$\frac{\hbar}{2}c\hat{\mathrm{p}}_j\,2i\epsilon_{ijk}\alpha_k + 0 = -i\hbar c\epsilon_{ikj}\alpha_k\hat{\mathrm{p}}_j = -i\hbar c(\boldsymbol{\alpha}\times\hat{\mathbf{p}})_i$$

$$\Rightarrow [\hat{\mathbf{S}}, \hat{\mathrm{H}}_D] = -i\hbar c\boldsymbol{\alpha}\times\hat{\mathbf{p}}\ .$$

---

[2] "The positive electron" was precisely the title of Anderson's paper in 1933.

The orbital angular momentum operator $\hat{\mathbf{L}} = \hat{\mathbf{r}} \times \hat{\mathbf{p}}$ has a similar behaviour:

$$[(\hat{\mathbf{r}} \times \hat{\mathbf{p}})_i, c\,\boldsymbol{\alpha} \cdot \hat{\mathbf{p}} + V(\hat{\mathbf{r}}) + \beta mc^2] = c\,\alpha_V[\hat{\mathbf{r}}_j \hat{\mathbf{p}}_k \epsilon_{ijk}, \hat{\mathbf{p}}_V] = c\,\alpha_V \hat{\mathbf{p}}_k \epsilon_{ijk}[\hat{\mathbf{r}}_j, \hat{\mathbf{p}}_V] =$$

$$c\,\alpha_V \hat{\mathbf{p}}_k \epsilon_{ijk}(i\hbar\delta_{j,V}) = ci\hbar\alpha_j \hat{\mathbf{p}}_k \epsilon_{ijk} = i\hbar c(\boldsymbol{\alpha} \times \hat{\mathbf{p}})_i \ ,$$

$$\Rightarrow [\hat{\mathbf{L}}, \hat{\mathrm{H}}_D] = i\hbar c\boldsymbol{\alpha} \times \hat{\mathbf{p}} \ ,$$

where we naturally used $[\hat{\mathbf{L}}, V(\hat{\mathbf{r}})] = 0^3$.

Thus we found that the spin as well as the orbital angular momentum vectors are not good quantum numbers.

However, it straightforwardly follows that the total angular momentum operator $\hat{\mathbf{J}} = \hat{\mathbf{L}} + \hat{\mathbf{S}}$ commutes with the Hamiltonian, i.e. the total angular momentum is, in contrast with orbital and spin angular momenta, a conserved quantum number. We may pictorially say that a Dirac particle is able to exchange spin angular momentum for getting orbital angular momentum, so that the two physical quantities $\mathbf{S}$ and $\mathbf{L}$ are separately not conserved, while the sum of the two is.

It is moreover interesting to show that, while the spin operator $(\frac{\hbar}{2}\hat{\boldsymbol{\Sigma}})^2 = \frac{3}{4}\hbar^2\hat{\mathbb{1}}$ trivially commutes with the Hamiltonian, the operator $\hat{\mathbf{L}}^2$ does not:

$$[\hat{\mathbf{L}}^2, \hat{\mathrm{H}}_D] = \hat{\mathbf{L}}[\hat{\mathbf{L}}, \hat{\mathrm{H}}_D] + [\hat{\mathbf{L}}, \hat{\mathrm{H}}_D]\hat{\mathbf{L}} = c\,i\,\hbar\,\alpha_j \underbrace{\epsilon_{ist}\epsilon_{ijk}}_{\delta_{sj}\delta_{tk} - \delta_{sk}\delta_{tj}} (\hat{\mathbf{r}}_s \hat{\mathbf{p}}_t \hat{\mathbf{p}}_k + \hat{\mathbf{p}}_k \hat{\mathbf{r}}_s \hat{\mathbf{p}}_t)$$

$$= c\,i\,\hbar\,\alpha_j \left(\hat{\mathbf{r}}_j \hat{\mathbf{p}}_k \hat{\mathbf{p}}_k - \hat{\mathbf{r}}_k \hat{\mathbf{p}}_j \hat{\mathbf{p}}_k + \hat{\mathbf{p}}_k \hat{\mathbf{r}}_j \hat{\mathbf{p}}_k - \hat{\mathbf{p}}_k \hat{\mathbf{r}}_k \hat{\mathbf{p}}_j \right)$$

$$= c\,i\,\hbar\,\alpha \left(\hat{\mathbf{r}}_j \hat{\mathbf{p}}_k \hat{\mathbf{p}}_j - \hat{\mathbf{r}}_k \hat{\mathbf{p}}_k \hat{\mathbf{p}}_j + (\hat{\mathbf{r}}_j \hat{\mathbf{p}}_k - i\,\hbar\,\delta_{jk})\hat{\mathbf{p}}_k - (\hat{\mathbf{r}}_k \hat{\mathbf{p}}_k - i\,\hbar\,\delta_{kk})\hat{\mathbf{p}}_j \right)$$

$$= 2ic\hbar\left((\boldsymbol{\alpha} \cdot \hat{\mathbf{r}})(\hat{\mathbf{p}} \cdot \hat{\mathbf{p}}) - (\hat{\mathbf{r}} \cdot \hat{\mathbf{p}})(\boldsymbol{\alpha} \cdot \hat{\mathbf{p}}) \right) \ .$$

Consequently, the modulus of the orbital angular momentum is not a good quantum number, while the modulus of the spin angular momentum is^4. In other words, the spin of the electron keeps being $\hbar/2$, while the magnitude as well as the direction of the orbital angular momentum change with time.

As last, we study the operator $\hat{\mathrm{P}} = \beta\hat{\Pi}$, where $\hat{\Pi}$ is the operator which brings $\boldsymbol{r} \rightarrow -\boldsymbol{r}$. It can be shown that $\hat{\mathrm{P}}$ represents the correct parity operator for the Dirac wavefuntion if one imposes the modulus squared of the wavefunctions to be a probability density. We have

$$[\beta\hat{\Pi}, c\,\boldsymbol{\alpha} \cdot \hat{\mathbf{p}} + V(\hat{\mathbf{r}}) + \beta mc^2] = \beta\hat{\Pi}\boldsymbol{\alpha} \cdot \hat{\mathbf{p}} - \boldsymbol{\alpha} \cdot \hat{\mathbf{p}}\beta\hat{\Pi}$$

$$= \boldsymbol{\alpha} \cdot (-1)(-1)\hat{\mathbf{p}}\beta\hat{\Pi} - \boldsymbol{\alpha} \cdot \hat{\mathbf{p}}\beta\hat{\Pi} = 0 \quad ,$$

where the relations (2.2) and the properties $\{\hat{\Pi}, \hat{\mathbf{r}}\} = \{\hat{\Pi}, \hat{\mathbf{p}}\} = 0$ have been used [25]. In the light of what found above, we state that parity is a symmetry for the Dirac Hamiltonian, as naturally expected.

$^3\hat{\mathbf{L}}$ is an operator which involves only angular differential forms. Since $\dfrac{\partial V(r)}{\partial\theta} = \dfrac{\partial V(r)}{\partial\varphi} = 0$, then $\hat{\mathbf{L}}\hat{V} = \hat{V}\hat{\mathbf{L}}$.

^{4}This in turn implies that the operator $\hat{\mathbf{L}}\hat{\mathbf{S}}$ (also known as spin-orbit term) does not commute with the Hamiltonian, since the operator $\hat{\mathbf{J}}^2 = \hat{\mathbf{S}}^2 + 2\hat{\mathbf{L}}\hat{\mathbf{S}} + \hat{\mathbf{L}}^2$ must evidently commute with the Hamiltonian.

Since the eigenfunctions in a central field problem are expected to be proportional to spherical harmonics, it is wise to define l as the quantum number by which to label our eigenfunctions such that $(-1)^l$ is the eigenvalue of the operator $\hat{P}$ when acting on the wavefunction $\Psi(\boldsymbol{r}, t)$. Analogously, we define the quantum numbers j and m_j such that $\hbar^2 j(j+1)$ and $\hbar m_j$ are respectively the eigenvalues of $\hat{\mathbf{J}}^2$ and $\hat{\mathbf{J}}_z$ when acting on the wavefunction $\Psi(\boldsymbol{r}, t)$.

Since we found $[\hat{\mathbf{J}}_i, \hat{\mathbf{H}}_D] = 0$ for $i = 1, 2, 3$, we can arbitrarily choose the axis along which to quantize the eigenfunctions. Most naturally, we choose the $\hat{z}$ axis for that purpose. In other words, we will find the basis states on which $\hat{\mathbf{J}}_z$ is diagonal.

By now, our list of quantum numbers by which to label the solutions of Eq. (2.2) is j, m_j and l. In addition to these, it must exist another quantum number which directly differentiates energetically the eigenstates, similarly to the Bohr principal quantum number in the non-relativistic Coulomb case. We will denote such a quantum number by n. Finally, our list of quantum numbers by which to label the solutions of Eq. (2.2) is n, j, l and m_j. We now proceed to find those solutions.

We make the ansatz

$$\Psi_{njlm_j}(\boldsymbol{r}, t) = \begin{pmatrix} g_{nj}(r)\Omega_{jlm_j}(\theta, \varphi) \\ if_{nj}(r)\Omega_{jl'm_j}(\theta, \varphi) \end{pmatrix} e^{\frac{i}{\hbar} Et} \quad , \tag{2.8}$$

where $g_{nj}(r)$ and $f_{nj}(r)$ are radial functions to be determined, while $\Omega_{jlm_j}(\theta, \varphi)$ and $\Omega_{jl'm_j}(\theta, \varphi)$ are defined through

$$\Omega_{jlm_j}(\theta, \varphi) = \sum_{m_l=-l}^{l} \sum_{\substack{m_s=-1/2, \\ +1/2}} \langle l, m_l, 1/2, m_s | j, m_j \rangle Y_l^{m_l}(\theta, \varphi) \chi_{1/2}(m_s) \quad , \tag{2.9}$$

for which $\langle l, m_l, 1/2, m_s | j, m_j \rangle$ are Clebsh-Gordan coefficients, $Y_l^{m_l}$ are Spherical Harmonics and the functions $\chi_{1/2}(m_s)$ are Pauli spinors

$$\chi_{1/2}(+1/2) = \begin{pmatrix} 1 \\ 0 \end{pmatrix} \quad , \quad \chi_{1/2}(-1/2) = \begin{pmatrix} 0 \\ 1 \end{pmatrix} \quad .$$

The relation between l and l' is taken to be

$$l' = 2j - l = \begin{cases} l+1 & \text{for } j = l+1/2 \\ l-1 & \text{for } j = l-1/2 \end{cases} \quad .$$

We now explain the motivations at the basis of this ansatz. The exponential term must be present since $\Psi(\boldsymbol{r}, t)$ is eigenfunction of the Hamiltonian. The definitions of $\Omega_{jlm_j}(\theta, \varphi)$ and $\Omega_{jl'm_j}(\theta, \varphi)$ ensure that the total angular momentum $\mathbf{J}$ is conserved. In addition, the relation between l and l' ensures that the wavefunction Ψ_{njlm_j} has a defined parity, specifically it ensures that Ψ_{njlm_j} is eigenfunction of the operator $\hat{P}$ with eigenvalue $(-1)^l$.

By plugging Eq. (2.8) into Eq. (2.2), we find an equivalence for the angular part of the spinor (which indicates that the angular part of our ansatz is right) and the following equations for the radial functions:

$$\begin{aligned} \left[E - V(r) - mc^2\right] g_{nj}(r) &= \hbar c \left[-\left(\frac{d}{dr} + \frac{1}{r}\right) + \frac{\kappa}{r} \right] f_{nj}(r) \\ \left[E - V(r) + mc^2\right] f_{nj}(r) &= \hbar c \left[\frac{d}{dr} + \frac{1}{r} + \frac{\kappa}{r} \right] g_{nj}(r) \quad , \end{aligned} \tag{2.10}$$

where κ is called Dirac quantum number and is defined as follows

$$
\begin{aligned}
\kappa &= \begin{cases} -(l+1) & \text{for } j = l + 1/2 \\ l & \text{for } j = l - 1/2 \end{cases} \\
&= l(l+1) - 1/4 - j(j+1) \\
&= -l'(l'+1) + 1/4 + j(j+1) \quad .
\end{aligned}
$$

Only by specifying the potential $V(r)$, one can solve the two radial equations (2.10). In contrast, the angular part of the wavefunction does not depend on the potential, as long as the potential is radial.

We suppose now to have a Coulombic potential: $V(r) = -\dfrac{Z\alpha\hbar c}{r}$, where α (not to be confused with $\boldsymbol{\alpha}$) represents the electromagnetic coupling constant, which is $\approx \dfrac{1}{137}$. In this case, the solutions for g_{nj} and f_{nj} can be found to be [26]

$$
\begin{aligned}
\left.\begin{array}{c} g_{nj} \\ f_{nj} \end{array}\right\} &= \frac{\pm(2\lambda)^{3/2}}{\Gamma(2\gamma+1)} \sqrt{\frac{(mc^2 \pm E)\Gamma(2\gamma + n' + 1)}{4mc^2 \frac{(n'+\gamma)mc^2}{E}\left(\frac{(n'+\gamma)mc^2}{E} - \kappa\right)n'!}} (2\lambda r)^{\gamma-1}e^{-\lambda r} \\
&\times \left\{ \left(\frac{(n'+\gamma)mc^2}{E} - \kappa\right) {}_1F_1(-n', 2\gamma+1; 2\lambda r) \mp n'\,{}_1F_1(1-n', 2\gamma+1; 2\lambda r) \right\} \quad ,
\end{aligned}
\tag{2.11}
$$

where the energy is

$$
E = \frac{mc^2}{\left(1 + \dfrac{(Z\alpha)^2}{\left(n' + \sqrt{(j+1/2)^2 - (Z\alpha)^2}\right)^2}\right)^{1/2}} \equiv E_{nj}
\tag{2.12}
$$

and

$$
\begin{aligned}
n' &= n - j - 1/2 = n - |\kappa| \quad , \\
\lambda &= \frac{(m^2c^4 - E^2)^{1/2}}{\hbar c} \quad , \\
\gamma &= \frac{Z\alpha E}{\hbar c \lambda} - n' \quad .
\end{aligned}
$$

In Eq. (2.11), ${}_1F_1(a, c; x)$ are Kummer confluent hypergeometric functions while $\Gamma(y)$ is the Gamma function

$$
\Gamma(z) = \int_0^{+\infty} t^{z-1} e^{-t} \mathrm{d}t \quad .
$$

Ions with nuclear charge Z and one electron are called hydrogenlike (or hydrogen-like) ions, for obvious reasons[5].

2.3 RELATIVISTIC GREEN'S FUNCTION

In two-photon transitions, as well as in many other atomic processes, the computation of the Green function for the process is needed and is the core of the theoretical

---

[5]In the same way, it is denoted with helium-like ions, those ions with two electrons but arbitrary atomic number Z. And so on.

description of the process.

The Green function for a certain Hamiltonian $\hat{H}$ is the solution of the equation

$$(\hat{H} - E)G_E(\boldsymbol{r}_1, \boldsymbol{r}_2) = \delta(\boldsymbol{r}_1 - \boldsymbol{r}_2) \quad . \tag{2.13}$$

Given the (complete) set of eigenfunctions $\Psi_\nu(\boldsymbol{r})$ of the Hamiltonian operator, the Green function can be formally written as

$$G_E(\boldsymbol{r}_1, \boldsymbol{r}_2) = \sum_\nu \frac{\Psi_\nu(\boldsymbol{r}_1)\Psi_\nu^\dagger(\boldsymbol{r}_2)}{E_\nu - E} \quad , \tag{2.14}$$

where the summation $\sum_\nu$ runs over the whole spectrum of the operator $\hat{H}$. In fact, by plugging this expression into the left hand side (lhs) of Eq. (2.13), we get:

$$\begin{aligned}
(\hat{H} - E)G_E(\boldsymbol{r}_1, \boldsymbol{r}_2) &= \sum_\nu (E_\nu - E)\frac{\Psi_\nu(\boldsymbol{r}_1)\Psi_\nu^\dagger(\boldsymbol{r}_2)}{E_\nu - E} \\
&= \sum_\nu \Psi_\nu(\boldsymbol{r}_1)\Psi_\nu^\dagger(\boldsymbol{r}_2) = \sum_\nu \langle \boldsymbol{r}_1|\nu\rangle\langle\nu|\boldsymbol{r}_2\rangle \\
&= \langle\boldsymbol{r}_1|\boldsymbol{r}_2\rangle = \delta(\boldsymbol{r}_1 - \boldsymbol{r}_2) \quad ,
\end{aligned}$$

where the identity $\sum_\nu |\nu\rangle\langle\nu| = \hat{\mathbb{1}}$ has been used.

By looking carefully at Eq. (2.14), it can be easily understood that the computation of the Green function is usually not a trivial task since, in general, the operator $\hat{H}$ may possess an infinite spectrum, as in the case of real atoms and molecules. Several attempts devoted to most accurately solve such infinite summation have been made in the past century (for example, in hydrogenlike ions, see Refs. [27–33]).

From now on, we will focus on deriving the Dirac-Coulomb Green function (DCGF), i.e. the Green function for the Dirac-Coulomb Hamiltonian.

On inserting the Dirac-Coulomb Hamiltonian into Eq. (2.13), we get

$$\left(-i\hbar c \boldsymbol{\alpha} \cdot \boldsymbol{\nabla} - \frac{\alpha Z \hbar c}{r} + \beta mc^2 - E\right)G_E(\boldsymbol{r}_1, \boldsymbol{r}_2) = \delta(\boldsymbol{r}_1 - \boldsymbol{r}_2)\mathbb{1}_4 \,, \tag{2.15}$$

where $\mathbb{1}_4$ is the 4x4 unitary matrix.

We try a solution of the form

$$\begin{aligned}
G_E(\boldsymbol{r}_1, \boldsymbol{r}_2) &= \sum_{\kappa\, m_j} \\
&\times \begin{pmatrix} g_{\kappa E}^{11}(r_1, r_2)\Omega_{\kappa m_j}(\hat{r}_1)\Omega_{\kappa m_j}^\dagger(\hat{r}_2) & -ig_{\kappa E}^{12}(r_1, r_2)\Omega_{\kappa m_j}(\hat{r}_1)\Omega_{-\kappa m_j}^\dagger(\hat{r}_2) \\ ig_{\kappa E}^{21}(r_1, r_2)\Omega_{-\kappa m_j}(\hat{r}_1)\Omega_{\kappa m_j}^\dagger(\hat{r}_2) & g_{\kappa E}^{22}(r_1, r_2)\Omega_{-\kappa m_j}(\hat{r}_1)\Omega_{-\kappa m_j}^\dagger(\hat{r}_2) \end{pmatrix} \,,
\end{aligned} \tag{2.16}$$

with g^{ij} to be determined. For the sake of simplicity, we re-labeled $\Omega_{\kappa m_j} \equiv \Omega_{jlm_j}$, where Ω_{jlm_j} are defined in Eq. (2.9).

In order to go further, we must rewrite the right hand side (rhs) of Eq. (2.15) in

spherical coordinates. This is accomplished by using

$$\delta(\boldsymbol{r}_1 - \boldsymbol{r}_2)\mathbb{1}_4 = \frac{\delta(r_1 - r_2)}{r_1 r_2}$$

$$\times \sum_{\kappa m_j} \begin{pmatrix} \Omega_{\kappa m_j}(\hat{r}_1)\Omega_{\kappa m_j}^\dagger(\hat{r}_2) & 0 \\ 0 & \Omega_{-\kappa m_j}(\hat{r}_1)\Omega_{-\kappa m_j}^\dagger(\hat{r}_2) \end{pmatrix} \quad . \tag{2.17}$$

Combining Eqs. (2.16), (2.15) and (2.17), we get an equivalence for the angular part (which means that our angular part of the trial solution is, once again, correct) and the following radial equation for the determination of g^{ij}:

$$\begin{pmatrix} [\epsilon_0 - \epsilon - \frac{\alpha Z}{r_1}] & [-\frac{1}{r_1}\frac{\mathrm{d}}{\mathrm{d}r_1}r_1 + \frac{\kappa}{r_1}] \\ [\frac{1}{r_1}\frac{\mathrm{d}}{\mathrm{d}r_1}r_1 + \frac{\kappa}{r_1}] & [-\epsilon_0 - \epsilon - \frac{\alpha Z}{r_1}] \end{pmatrix} \begin{pmatrix} g_{\kappa E}^{11}(r_1,r_2) & g_{\kappa E}^{12}(r_1,r_2) \\ g_{\kappa E}^{21}(r_1,r_2) & g_{\kappa E}^{22}(r_1,r_2) \end{pmatrix}$$

$$= \frac{1}{\hbar c}\frac{\delta(r_1 - r_2)}{r_1 r_2}\mathbb{1}_2 \quad , \tag{2.18}$$

where $\epsilon_0 = mc^2/\hbar c$ and $\epsilon = E/\hbar c$.

The derivation of the solution for these equations that we here present follows Ref. [34].

We define the following linear transformation

$$\begin{pmatrix} f_\kappa^{11}(r_1,r_2) & f_\kappa^{12}(r_1,r_2) \\ f_\kappa^{21}(r_1,r_2) & f_\kappa^{22}(r_1,r_2) \end{pmatrix} = \underline{X}\begin{pmatrix} g_{\kappa E}^{11}(r_1,r_2) & g_{\kappa E}^{12}(r_1,r_2) \\ g_{\kappa E}^{21}(r_1,r_2) & g_{\kappa E}^{22}(r_1,r_2) \end{pmatrix} \quad ,$$

where the matrix $\underline{X}$ is

$$\underline{X} = \begin{pmatrix} 1 & X \\ X & 1 \end{pmatrix} \quad ,$$

and X is a real number. Since

$$\underline{X}^{-1} = (1 - X^2)^{-1}\begin{pmatrix} 1 & -X \\ -X & 1 \end{pmatrix} \quad ,$$

the radial equations (2.18) are written in terms of f^{ij} as

$$\begin{pmatrix} [\epsilon_0 - \epsilon - \frac{\alpha Z + X\kappa - X}{r_1} + X\frac{\mathrm{d}}{\mathrm{d}r_1}] & [-X\epsilon_0 + X\epsilon + \frac{\alpha ZX + \kappa - 1}{r_1} - \frac{\mathrm{d}}{\mathrm{d}r_1}] \\ [X\epsilon_0 + X\epsilon + \frac{\alpha ZX + \kappa + 1}{r_1} + \frac{\mathrm{d}}{\mathrm{d}r_1}] & [-\epsilon_0 - \epsilon - \frac{\alpha Z + X\kappa + X}{r_1} - X\frac{\mathrm{d}}{\mathrm{d}r_1}] \end{pmatrix}$$

$$\times \begin{pmatrix} f_\kappa^{11}(r_1,r_2) & f_\kappa^{12}(r_1,r_2) \\ f_\kappa^{21}(r_1,r_2) & f_\kappa^{22}(r_1,r_2) \end{pmatrix} = \frac{1 - X^2}{\hbar c}\frac{\delta(r_1 - r_2)}{r_1 r_2}\mathbb{1}_2 \quad .$$

On multiplying by the matrix $\underline{X}^{-1}$ from the lhs, the derivatives disappear from the diagonal terms and we are left with

$$
\begin{pmatrix}
\left[(1-X^2)\epsilon_0 - (1+X^2)\epsilon - \dfrac{A}{r_1} \right] & \left[2X\epsilon + \dfrac{B}{r_1} - (1-X^2)\dfrac{\mathrm{d}}{\mathrm{d}r_1} \right] \\[2ex]
\left[2X\epsilon + \dfrac{B}{r_1} + (1-X^2)\dfrac{\mathrm{d}}{\mathrm{d}r_1} \right] & \left[(X^2-1)\epsilon_0 - (1+X^2)\epsilon - \dfrac{A}{r_1} \right]
\end{pmatrix}
$$

$$
\times \begin{pmatrix} f_\kappa^{11}(r_1,r_2) & f_\kappa^{12}(r_1,r_2) \\ f_\kappa^{21}(r_1,r_2) & f_\kappa^{22}(r_1,r_2) \end{pmatrix} = \frac{(1-X^2)^2}{\hbar c} \frac{\delta(r_1-r_2)}{r_1 r_2} \underline{X}^{-1} \quad ,
$$

where $A = (1+X^2)\alpha Z + 2X\kappa$ and $B = 2\alpha Z X + (1+X^2)\kappa - (1-X^2)$.
Then, we choose X in such a way that A vanishes, i.e. $X = (-\kappa + \gamma)/\alpha Z$, with $\gamma = \sqrt{\kappa^2 - \alpha^2 Z^2}$. With this choice, the radial equations simplify to

$$
\begin{pmatrix}
\left[\epsilon_0 - \dfrac{\epsilon\kappa}{\gamma} \right] & \left[-\dfrac{\alpha Z\epsilon}{\gamma} + \dfrac{\gamma-1}{r} - \dfrac{\mathrm{d}}{\mathrm{d}r_1} \right] \\[2ex]
\left[-\dfrac{\alpha Z\epsilon}{\gamma} + \dfrac{\gamma+1}{r} + \dfrac{\mathrm{d}}{\mathrm{d}r_1} \right] & \left[-\epsilon_0 - \dfrac{\epsilon\kappa}{\gamma} \right]
\end{pmatrix}
$$

$$
\times \begin{pmatrix} f_\kappa^{11}(r_1,r_2) & f_\kappa^{12}(r_1,r_2) \\ f_\kappa^{21}(r_1,r_2) & f_\kappa^{22}(r_1,r_2) \end{pmatrix} = \frac{(1-X^2)^2}{\hbar c} \frac{\delta(r_1-r_2)}{r_1 r_2} \underline{X}^{-1} \quad .
$$

We diagonalize the rhs of the above equation by multiplying from the right with the matrix $\underline{X}$ and by defining

$$
\begin{aligned}
\begin{pmatrix} h_\kappa^{11}(r_1,r_2) & h_\kappa^{12}(r_1,r_2) \\ h_\kappa^{21}(r_1,r_2) & h_\kappa^{22}(r_1,r_2) \end{pmatrix} &= \begin{pmatrix} f_\kappa^{11}(r_1,r_2) & f_\kappa^{12}(r_1,r_2) \\ f_\kappa^{21}(r_1,r_2) & f_\kappa^{22}(r_1,r_2) \end{pmatrix} \underline{X} \\[2ex]
&= \underline{X} \begin{pmatrix} g_{\kappa E}^{11}(r_1,r_2) & g_{\kappa E}^{12}(r_1,r_2) \\ g_{\kappa E}^{21}(r_1,r_2) & g_{\kappa E}^{22}(r_1,r_2) \end{pmatrix} \underline{X} \quad ,
\end{aligned}
\tag{2.19}
$$

so that we have

$$
\begin{pmatrix}
\left[\epsilon_0 - \dfrac{\epsilon\kappa}{\gamma} \right] & \left[-\dfrac{\alpha Z\epsilon}{\gamma} + \dfrac{\gamma-1}{r} - \dfrac{\mathrm{d}}{\mathrm{d}r_1} \right] \\[2ex]
\left[-\dfrac{\alpha Z\epsilon}{\gamma} + \dfrac{\gamma+1}{r} + \dfrac{\mathrm{d}}{\mathrm{d}r_1} \right] & \left[-\epsilon_0 - \dfrac{\epsilon\kappa}{\gamma} \right]
\end{pmatrix}
\tag{2.20}
$$

$$
\times \begin{pmatrix} h_\kappa^{11}(r_1,r_2) & h_\kappa^{12}(r_1,r_2) \\ h_\kappa^{21}(r_1,r_2) & h_\kappa^{22}(r_1,r_2) \end{pmatrix} = \frac{(1-X^2)^2}{\hbar c} \frac{\delta(r_1-r_2)}{r_1 r_2} \mathbb{1}_2 \quad .
$$

We can consider now the four equations embodied in Eq. (2.20) in two pairs, since there is no mixing of the columns of the h-matrix any more.
The first one reads:

$$
\begin{cases}
\left[\epsilon_0 - \epsilon\dfrac{\kappa}{\gamma} \right] h_\kappa^{11}(r_1,r_2) + \left[-\dfrac{\alpha Z\epsilon}{\gamma} + \dfrac{\gamma-1}{r_1} - \dfrac{\mathrm{d}}{\mathrm{d}r_1} \right] h_\kappa^{21} &= \dfrac{(1-X^2)}{\hbar c} \dfrac{\delta r_1 - r_2}{r_1 r_2} \\[2ex]
\left[-\dfrac{\alpha Z\epsilon}{\gamma} + \dfrac{\gamma+1}{r_1} + \dfrac{\mathrm{d}}{\mathrm{d}r_1} \right] h_\kappa^{11}(r_1,r_2) - \left[\epsilon_0 + \epsilon\dfrac{\kappa}{\gamma} \right] h_\kappa^{21} &= 0 \quad ,
\end{cases}
$$

from which we get

$$
\begin{cases}
\left[\dfrac{d^2}{dr_1^2} + \dfrac{2}{r_1}\dfrac{d}{dr_1} - \dfrac{\gamma(\gamma+1)}{r_1^2} + \dfrac{2\alpha Z\epsilon}{r_1} + \epsilon^2 - \epsilon_0^2 \right] h_\kappa^{11}(r_1,r_2) = \left(\epsilon_0 + \epsilon\dfrac{\kappa}{\gamma} \right) \dfrac{X^2-1}{\hbar c}\dfrac{\delta(r_1-r_2)}{r_1 r_2} \\[3mm]
h_\kappa^{21}(r_1,r_2) = \dfrac{\gamma}{\epsilon\kappa+\epsilon_0\gamma}\left[-\dfrac{\alpha Z\epsilon}{\gamma} + \dfrac{\gamma+1}{r_1} + \dfrac{d}{dr_1} \right] h^{11}(r_1,r_2) \quad .
\end{cases}
$$

Analogously, we get the second pair of equations to be

$$
\begin{cases}
\left[\dfrac{d^2}{dr_1^2} + \dfrac{2}{r_1}\dfrac{d}{dr_1} - \dfrac{\gamma(\gamma-1)}{r_1^2} + \dfrac{2\alpha Z\epsilon}{r_1} + \epsilon^2 - \epsilon_0^2 \right] h_\kappa^{22}(r_1,r_2) = \left(\epsilon_0 - \epsilon\dfrac{\kappa}{\gamma} \right) \dfrac{1-X^2}{\hbar c}\dfrac{\delta(r_1-r_2)}{r_1 r_2} \\[3mm]
h_\kappa^{12}(r_1,r_2) = \dfrac{\gamma}{\epsilon\kappa-\epsilon_0\gamma}\left[-\dfrac{\alpha Z\epsilon}{\gamma} + \dfrac{\gamma-1}{r_1} - \dfrac{d}{dr_1} \right] h^{22}(r_1,r_2) \quad .
\end{cases}
$$
$$(2.21)$$

It can be shown that the solution for h_κ^{11} and h_κ^{22} in the above equations can be expressed in the form [34]

$$
h_\kappa^{11}(r_1,r_2) = (1-X^2)\frac{\epsilon\kappa+\epsilon_0\gamma}{\hbar c\gamma}g_{\nu\gamma}(r_1,r_2;\omega)
$$
$$(2.22)$$
$$
h_\kappa^{22}(r_1,r_2) = (1-X^2)\frac{\epsilon\kappa-\epsilon_0\gamma}{\hbar c\gamma}g_{\nu\gamma-1}(r_1,r_2;\omega) \quad ,
$$

where

$$
g_{\nu\gamma}(r_1,r_2;\omega) = (2\omega)^{2\gamma+1}(r_1 r_2)^\gamma e^{-(r_1+r_2)\omega}
$$
$$
\times \sum_{v=0}^{+\infty} \frac{v!(v+1+\gamma-\nu)^{-1}}{\Gamma(2\gamma+2+v)}L_v^{2\gamma+1}(2r_1\omega)L_v^{2\gamma+1}(2r_2\omega) \quad ,
$$
$$(2.23)$$

$\omega = \sqrt{\epsilon_0^2-\epsilon^2}$, $\nu = \alpha Z\epsilon/\sqrt{\epsilon_0^2-\epsilon^2}$ and $L_\alpha^\beta(x)$ are associated Laguerre polynomials. By using Eqs. (2.21) and (2.22), we get also

$$
h_\kappa^{21}(r_1,r_2) = h_\kappa^{12}(r_2,r_1)
$$
$$
= \frac{1-X^2}{2\hbar c\gamma}\left(\frac{\delta(r_1-r_2)}{\sqrt{r_1 r_2}} + (2\omega)^{2\gamma+1}r_1^{\gamma-1}r_2^\gamma \right.
$$
$$
\left. \times\, e^{-\omega(r_1+r_2)}\sum_{v=0}^{+\infty}\frac{(v+1)!\,(\gamma+v+1-\nu)^{-1}}{\Gamma(2\gamma+1+v)}L_{v+1}^{2\gamma-1}(2\omega r_1)L_v^{2\gamma+1}(2\omega r_2) \right) \quad .
$$
$$(2.24)$$

With the help of Eq. (2.19), we come back to the initial functions g_κ^{ij} :

$$
\begin{pmatrix} g_{\kappa E}^{11}(r_1,r_2) & g_{\kappa E}^{12}(r_1,r_2) \\ g_{\kappa E}^{21}(r_1,r_2) & g_{\kappa E}^{22}(r_1,r_2) \end{pmatrix} = (1-X^2)^{-2}
$$
$$
\times \begin{pmatrix} h_\kappa^{11}-Xh_\kappa^{12}-Xh_\kappa^{21}+X^2h_\kappa^{22} & -Xh_\kappa^{11}+h_\kappa^{12}+X^2h_\kappa^{21}-Xh_\kappa^{22} \\ -Xh_\kappa^{11}+X^2h_\kappa^{12}+h_\kappa^{21}-Xh_\kappa^{22} & X^2h_\kappa^{11}-Xh_\kappa^{12}-Xh_\kappa^{21}+h_\kappa^{22} \end{pmatrix} \quad .
$$
$$(2.25)$$

We recall here all the parameters involved in the written solutions:

$$
\begin{aligned}
X &= \frac{\gamma - \kappa}{\alpha Z}\,, & \gamma &= \sqrt{\kappa^2 - \alpha^2 Z^2}\,, \\
\omega &= \sqrt{\epsilon_0^2 - \epsilon^2}\,, & \nu &= \frac{\alpha Z \epsilon}{\sqrt{\epsilon_0^2 - \epsilon^2}}\,, \\
\epsilon &= \frac{E}{\hbar c}\,, & \epsilon_0 &= \frac{mc^2}{\hbar c}\,.
\end{aligned}
\tag{2.26}
$$

The set of equations (2.26), (2.25), (2.24), (2.23), (2.22) and (2.16) complete the analysis of the Green function for the Dirac-Coulomb problem.

2.4 FROM ONE- TO MANY-ELECTRON ATOMS: THE INDEPENDENT PARTICLE MODEL

The complexity of atoms and ions critically increases as soon as the number of bound electrons that the atom or ion possesses gets bigger than one. For the case of two or more electrons (many-electron systems), the Dirac equation is not solvable. For instance, the time independent Dirac equation for heliumlike ions reads

$$
\left(-i\hbar c \boldsymbol{\alpha} \cdot \boldsymbol{\nabla}_{r_1} - i\hbar c \boldsymbol{\alpha} \cdot \boldsymbol{\nabla}_{r_2} - \frac{Z\alpha\hbar c}{r_1} - \frac{Z\alpha\hbar c}{r_2} + \frac{\alpha\hbar c}{|\boldsymbol{r}_1 - \boldsymbol{r}_2|} + 2\beta mc^2 \right) \Psi(\boldsymbol{r}_1, \boldsymbol{r}_2)
$$
$$
= E\,\Psi(\boldsymbol{r}_1, \boldsymbol{r}_2) \quad,
\tag{2.27}
$$

where we have neglected any magnetic electron-electron interaction.

This equation cannot be solved analytically. Approximations are (generally) required if one wants to describe static as well as dynamic characteristics of many-electron systems. We will now focus on describing the states of two-electron bound systems, i.e. heliumlike systems.

The first approximation one can make is wholly neglecting the electron-electron (static) interaction term. This is called "zero-order" approximation and is the core assumption of the *Independent Particle Model*. The differential equation (2.27) then becomes

$$
\left(-i\hbar c \boldsymbol{\alpha} \cdot \boldsymbol{\nabla}_{r_1} - i\hbar c \boldsymbol{\alpha} \cdot \boldsymbol{\nabla}_{r_2} - \frac{Z\alpha\hbar c}{r_1} - \frac{Z\alpha\hbar c}{r_2} + 2\beta mc^2 \right) \Psi(\boldsymbol{r}_1, \boldsymbol{r}_2) = E\Psi(\boldsymbol{r}_1, \boldsymbol{r}_2) \quad.
\tag{2.28}
$$

This equation is fully separable so that the eigenfunction $\Psi(\boldsymbol{r}_1, \boldsymbol{r}_2)$ can be trivially written in the form of product of relativistic hydrogenic wave functions. In particular, for discrete states we have

$$
\Psi(\boldsymbol{r}_1, \boldsymbol{r}_2) = \Psi_{n_1 \kappa_1 m_{j_1}}(\boldsymbol{r}_1) \Psi_{n_2 \kappa_2 m_{j_2}}(\boldsymbol{r}_2) \quad,
\tag{2.29}
$$

where $\Psi_{n\kappa m_j}(\boldsymbol{r})$ is shown in Eq. (2.8). The corresponding energies are

$$
E \equiv E_{n_1 j_1\, n_2 j_2} = E_{n_1 j_1} + E_{n_2 j_2} \quad,
\tag{2.30}
$$

where E_{nj} is shown in Eq. (2.12).

However, our solution of Eq. (2.29), though it satisfies the IPM equation (2.28), it does not satisfy two other requirements we must demand:

1. the wavefunction must be eigenfunction of the total angular momentum operator $\hat{\mathbf{J}} = \hat{\mathbf{j}}_1 + \hat{\mathbf{j}}_2$, where $\hat{\mathbf{j}}_1$ and $\hat{\mathbf{j}}_2$ are angular momentum operators of the first and second electron, respectively.
   Motivation: The solution (2.29) has defined quantum numbers for j_1^2, $j_{1\,z}$, j_2^2 and $j_{2\,z}$. We wrote that wavefunction being conscious that both $\hat{\mathbf{j}}_1$ and $\hat{\mathbf{j}}_2$ commute with the Hamiltonian so that they are good quantum numbers. What we did is correct. However, we must consider that also $\hat{\mathbf{J}}$, analogously, commutes with the Hamiltonian. Thus, we know from pure Quantum Mechanics that we can build our solutions in two equivalent bases: the single particles basis $\{j_1^2, j_{1\,z}, j_2^2, j_{2\,z}\}$ or the coupled basis $\{j_1^2, j_2^2, J^2, J_z\}$. We can freely choose the one we like most or the one which suits more the physics we wish to describe. We accidentally chose the single particle basis. Nonetheless, we reconsider our choice and try to think as smart as we can: Even though in our zero-order approximation there is not any electron-electron interaction, a heliumlike ion is a system of two interacting electrons in a central (nuclear) field. In addition, the electron-electron interaction is central as well. In such a system, we know, again from pure quantum mechanics, that the total angular momentum is always (vectorially) conserved. Therefore, by building our eigenfunctions on the coupled basis, we argue that we will get a better, more realistic description.

2. the wavefunction must change sign under the permutation symmetry $\boldsymbol{r}_1 \leftrightarrow \boldsymbol{r}_2$.
   Motivation: The Pauli principle dictates that the wavefunction of two identical fermions (as two electrons are) must be antisymmetric with respect to the exchange of the spatial coordinates.

We will derive, step by step, a wavefunction which fulfills the two above requirements *and* which is solution of Eq. (2.28).
A wavefunction that is eigenfunction of the operators $\{\hat{\mathbf{j}}_1^2, \hat{\mathbf{j}}_2^2, \hat{\mathbf{J}}^2, \hat{\mathbf{J}}_z\}$ can be easily written as

$$\Phi_{n_1\kappa_1 n_2\kappa_2}^{Jm_J}(\boldsymbol{r}_1, \boldsymbol{r}_2) = \sum_{m_{j_1}\,m_{j_2}} \langle j_1, m_{j_1}, j_2, m_{j_2} | J, m_J \rangle \Psi_{n_1\kappa_1 m_{j_1}}(\boldsymbol{r}_1) \Psi_{n_2\kappa_2 m_{j_2}}(\boldsymbol{r}_2) \quad . \quad (2.31)$$

However, the permutation symmetry of this wavefunction is generally not defined. We can simply build a function which is antisymmetric with respect to $\boldsymbol{r}_1 \leftrightarrow \boldsymbol{r}_2$ by combining Φ wavefunctions:

$$\Psi_{n_1\kappa_1 n_2\kappa_2}^{Jm_J}(\boldsymbol{r}_1, \boldsymbol{r}_2) = \frac{1}{\sqrt{2}} \left(\Phi_{n_1\kappa_1 n_2\kappa_2}^{Jm_J}(\boldsymbol{r}_1, \boldsymbol{r}_2) - \Phi_{n_1\kappa_1 n_2\kappa_2}^{Jm_J}(\boldsymbol{r}_2, \boldsymbol{r}_1) \right) \quad . \quad\quad (2.32)$$

Such a combination of wavefunctions has been named after John C. Slater [35], as "Slater determinant", since it can be trivially obtained as determinant of a 2x2 matrix composed by one-particle wavefunctions:

$$\Psi_{n_1\kappa_1 n_2\kappa_2}^{Jm_J}(\boldsymbol{r}_1, \boldsymbol{r}_2) = \frac{1}{\sqrt{2}} \sum_{m_{j_1}\,m_{j_2}} \langle j_1, m_{j_1}, j_2, m_{j_2} | J, m_J \rangle$$

$$\times \begin{vmatrix} \Psi_{n_1\kappa_1 m_{j_1}}(\boldsymbol{r}_1) & \Psi_{n_2\kappa_2 m_{j_2}}(\boldsymbol{r}_1) \\ \Psi_{n_1\kappa_1 m_{j_1}}(\boldsymbol{r}_2) & \Psi_{n_2\kappa_2 m_{j_2}}(\boldsymbol{r}_2) \end{vmatrix} \quad . \quad\quad (2.33)$$

The antisymmetric nature of the matrix determinant, ensures the right fermionic symmetry for the electronic states.

Since both the actions of the operator $\hat{\mathbf{J}} = \hat{\mathbf{j}}_1 + \hat{\mathbf{j}}_2$ and of the differential operator in Eq. (2.28) are linear, we can verify that the above wavefunctions satisfy all the wanted requirements:

$$\left(-i\hbar\boldsymbol{\alpha}\cdot\boldsymbol{\nabla}_{r_1} - i\hbar\boldsymbol{\alpha}\cdot\boldsymbol{\nabla}_{r_2} - \frac{Z\alpha\hbar c}{r_1} - \frac{Z\alpha\hbar c}{r_2} + 2\beta mc^2\right)\Psi^{Jm_J}_{n_1\kappa_1 n_2\kappa_2}(\boldsymbol{r}_1, \boldsymbol{r}_2)$$
$$= E_{n_1\kappa_1 n_2\kappa_2}\Psi^{Jm_J}_{n_1\kappa_1 n_2\kappa_2}(\boldsymbol{r}_1, \boldsymbol{r}_2)$$

$$\hat{\mathbf{J}}^2\Psi^{Jm_J}_{n_1\kappa_1 n_2\kappa_2}(\boldsymbol{r}_1, \boldsymbol{r}_2) = \hbar^2 J(J+1)\Psi^{Jm_J}_{n_1\kappa_1 n_2\kappa_2}(\boldsymbol{r}_1, \boldsymbol{r}_2)$$

$$\hat{\mathbf{J}}_z\Psi^{Jm_J}_{n_1\kappa_1 n_2\kappa_2}(\boldsymbol{r}_1, \boldsymbol{r}_2) = \hbar m_J\Psi^{Jm_J}_{n_1\kappa_1 n_2\kappa_2}(\boldsymbol{r}_1, \boldsymbol{r}_2)$$

$$\hat{\mathbf{P}}_{12}\Psi^{Jm_J}_{n_1\kappa_1 n_2\kappa_2}(\boldsymbol{r}_1, \boldsymbol{r}_2) = -\Psi^{Jm_J}_{n_1\kappa_1 n_2\kappa_2}(\boldsymbol{r}_1, \boldsymbol{r}_2) \quad ,$$

where the $\hat{\mathbf{P}}_{12}$ is the *permutation operator* that interchanges the spatial coordinates of the electrons: $\hat{\mathbf{P}}_{12}\Psi^{Jm_J}_{n_1\kappa_1 n_2\kappa_2}(\boldsymbol{r}_1, \boldsymbol{r}_2) = \Psi^{Jm_J}_{n_1\kappa_1 n_2\kappa_2}(\boldsymbol{r}_2, \boldsymbol{r}_1) = -\Psi^{Jm_J}_{n_1\kappa_1 n_2\kappa_2}(\boldsymbol{r}_1, \boldsymbol{r}_2)$.

If we calculated the energies in Eq. (2.30), we would notice that the effective bound states (with energy $< 2mc^2$) are only those ones with the wavefunctions of the form

$$\Psi^{Jm_J}_{1-1n_2\kappa_2}(\boldsymbol{r}_1, \boldsymbol{r}_2) = \frac{1}{\sqrt{2}}\left(\Phi^{Jm_J}_{1-1n_2\kappa_2}(\boldsymbol{r}_1, \boldsymbol{r}_2) - \Phi^{Jm_J}_{1-1n_2\kappa_2}(\boldsymbol{r}_2, \boldsymbol{r}_1)\right) \quad . \tag{2.34}$$

Pictorially, we can evidently interpret these states as if one electron were fixed at the ground state $(1s_{1/2})$, while the other one could assume excited states. This kind of states forms the so-called *genuine discrete* part of the spectrum. They are also called *single excited states*. As remarked, these are the only bound-states of the spectrum, if we define bound states as the states with energy $< 2mc^2$. Nevertheless, *double excited* as well as continuum states are also part of the ionic spectrum and they do describe some (not bound) states which exist in nature. Particularly, the double excited states are the essential ingredient of *Auger processes* [36], for which the energy coming from one decay of the two excited electrons is internally converted to ionize the ion. In the following we will restrict ourselves to genuine discrete states.

The function Ψ for the ground state $(n_1 = n_2 = 1, \kappa_1 = \kappa_2 = -1)$, from Eq. (2.34), is

$$\Psi^{Jm_J}_{1-11-1}(\boldsymbol{r}_1, \boldsymbol{r}_2) = \begin{cases} 0 & J = 1, \; m_J = -1, 0, 1 \quad , \\[2mm] \left(\Psi_{1-1+\frac{1}{2}}(\boldsymbol{r}_1)\Psi_{1-1-\frac{1}{2}}(\boldsymbol{r}_2) \right. & J = 0, \; m_J = 0 \quad . \\ \left. - \Psi_{1-1-\frac{1}{2}}(\boldsymbol{r}_1)\Psi_{1-1+\frac{1}{2}}(\boldsymbol{r}_2)\right) & \end{cases}$$

We realize that the Pauli principles forbids the electron configuration with $J = 1$. At the same time we notice that, in order to have a normalized wavefunction for the ground state, we must additionally insert a factor $\frac{1}{\sqrt{2}}$ in front. Then, specifically for the ground state, the wavefunction is

$$\Psi^{0m_J}_{1-11-1}(\boldsymbol{r}_1, \boldsymbol{r}_2) = \frac{1}{\sqrt{2}}\left(\Psi_{1-1+\frac{1}{2}}(\boldsymbol{r}_1)\Psi_{1-1-\frac{1}{2}}(\boldsymbol{r}_2) - \Psi_{1-1-\frac{1}{2}}(\boldsymbol{r}_1)\Psi_{1-1+\frac{1}{2}}(\boldsymbol{r}_2)\right)$$
$$\tag{2.35}$$
$$= \frac{1}{2}\left(\Phi^{0m_J}_{1-11-1}(\boldsymbol{r}_1, \boldsymbol{r}_2) - \Phi^{0m_J}_{1-11-1}(\boldsymbol{r}_2, \boldsymbol{r}_1)\right) \quad .$$

The two equations (2.34) and (2.35) complete the description of the genuine discrete
states of heliumlike systems within the Independent Particle Model (IPM).

The goodness of IPM strongly depends on the atomic number Z. Since, for large Z
($Z \gtrsim 50$), the electron-electron interaction term becomes quite smaller than the two
electron-nucleus interaction terms in the Hamiltonian, the approximation of neglecting
the former should be (and is indeed) quite good. For highly-charged ions, IPM is in
fact widely and successfully used.
On the other hand, for small Z ($Z \lesssim 20$) the approximation of neglecting the electron-
electron interaction term in the Hamiltonian is not well-founded, although IPM anyway
keeps being a rough approximation which may be good enough in many practical cases.

As a conclusive note, we discuss the quantum numbers needed and commonly used to
describe the two-particle ionic states. We discuss also the commonly used notations.
First and foremost, we point out the fact that, by demanding negative permutation
symmetry of the two-electron wavefunction (as the Pauli principle demand), we lost
the modulus of the angular momentum of the first and second electrons (respectively
represented by the operators $\hat{\mathbf{j}}_1^2$ and $\hat{\mathbf{j}}_2^2$) as good quantum numbers. This can be directly
verified:

$$\hat{\mathbf{j}}_1^2 \Psi_{n_1\kappa_1 n_2\kappa_2}^{Jm_J}(\boldsymbol{r}_1, \boldsymbol{r}_2) = \frac{1}{\sqrt{2}} \sum_{m_{j_1} m_{j_2}} \langle j_1, m_{j_1}, j_2, m_{j_2}|J, m_J\rangle$$

$$\times \left[\left(\hat{\mathbf{j}}_1^2 \Psi_{n_1\kappa_1 m_{j_1}}(\boldsymbol{r}_1)\right) \Psi_{n_2\kappa_2 m_{j_2}}(\boldsymbol{r}_2) - \Psi_{n_1\kappa_1 m_{j_1}}(\boldsymbol{r}_2)\left(\hat{\mathbf{j}}_1^2 \Psi_{n_2\kappa_2 m_{j_2}}(\boldsymbol{r}_1)\right) \right]$$

$$= \frac{1}{\sqrt{2}} \sum_{m_{j_1} m_{j_2}} \langle j_1, m_{j_1}, j_2, m_{j_2}|J, m_J\rangle$$

$$\times \left(\hbar^2(|\kappa_1| - 1/2)(|\kappa_1| + 1/2)\Psi_{n_1\kappa_1 m_{j_1}}(\boldsymbol{r}_1)\Psi_{n_2\kappa_2 m_{j_2}}(\boldsymbol{r}_2) \right.$$

$$\left. - \hbar^2(|\kappa_2| - 1/2)(|\kappa_2| + 1/2)\Psi_{n_1\kappa_1 m_{j_1}}(\boldsymbol{r}_2)\Psi_{n_2\kappa_2 m_{j_2}}(\boldsymbol{r}_1) \right) \quad ,$$

which in general implies $\hat{\mathbf{j}}_1^2 \Psi_{n_1\kappa_1 n_2\kappa_2}^{Jm_J} \neq \lambda \Psi_{n_1\kappa_1 n_2\kappa_2}^{Jm_J}$, unless $|\kappa_1| = |\kappa_2|$. In conclusion,
κ_1 and κ_2 are still good quantum numbers but they are not, in general, anymore
correlated to the total angular momentum and parity of the two electrons. In other
words, we will still write

$$\begin{aligned}
|\kappa_1| &= j_1 + 1/2 \\
\kappa_1 &= l_1(l_1 + 1) - 1/4 - j_1(j_1 + 1) \\
&= -l_1'(l_1' + 1) + 1/4 + j_1(j_1 + 1) \\
|\kappa_2| &= j_2 + 1/2 \\
\kappa_2 &= l_2(l_2 + 1) - 1/4 - j_2(j_2 + 1) \\
&= -l_2'(l_2' + 1) + 1/4 + j_2(j_2 + 1) \quad ,
\end{aligned}$$

but $j_{1(2)}$ and $l_{1(2)}$ will not represent anymore the angular momentum and parity of
the first (second) electron. Rather, they will be normal quantum numbers (like n_1 and
n_2) by which to label the ionic state. Actually, speaking about quantities of the *first*
and *second* electron does not make sense in two-electron systems, since we imposed the
electrons to be not distinguishable. Following this reasoning, we notice that the parity

of the ionic state is given by $\Pi = (-1)^{l_1}(-1)^{l_2}$. Then, we may define Π as quantum number by which to describe the ionic state in replacement of l_2 or l_1. We may argue that Π has at least a clear physics meaning, while $l_{1(2)}$ has not. However, what is normally used by physicists is $l_{1(2)}$.

Thus, the quantum numbers by which the ionic states are normally labeled are

$$n_1 \ , \ j_1 \ , \ l_1 \ , \ n_2 \ , \ j_2 \ , \ l_2 \ , \ J \ , \ J_z \quad .$$

The relativistic notation used by the atomic community refers to these quantum numbers: The hydrogenlike ionic states are thus normally labeled by

$$n_1 \, L1_{j_1} \, n_2 \, L2_{j_2} \ : \ J^{m_J} \quad , \tag{2.36}$$

where J, m_J are naturally related to $\hat{\mathbf{J}}^2$, $\hat{\mathbf{J}}_z$ by $\hat{\mathbf{J}}^2\Psi = \hbar^2 J(J+1)\Psi$, $\hat{\mathbf{J}}_z\Psi = \hbar m_J\Psi$. $L1$ and $L2$ represent l_1 and l_2 in spectroscopic notation, i.e.

L	l
s	0
p	1
d	2
f	3
g	4
...	

From f on, the column on the left follows the roman alphabet, i.e. h corresponds to $l = 5$ and so on. For genuine discrete states, the notation above reduces to $1s_{1/2} \, n \, L_j \ : \ J^{m_J}$.

The nature of the notation (2.36) comes from the fact that the ionic states are obtained by coupling the two total angular momenta of the single electrons ($\boldsymbol{j}_1$ and $\boldsymbol{j}_2$) to give birth to $\boldsymbol{J}$ (see Eq. (2.31)). There exist another notation by which to label the ionic states which is inherited from non-relativistic theory. We know that each electron has itself two angular momenta, $\boldsymbol{S}$ and $\boldsymbol{L}$, which are already coupled by the Dirac formalism to give birth to $\boldsymbol{j}$. However, in the non-relativistic theory, this is not so. The orbital and spin angular momenta are *not* coupled by the formalism but simply by Clebsch-Gordan coefficients. Then, working non-relativistically with two electrons, one may choose to couple either

- step 1) $\boldsymbol{S}_1$ with $\boldsymbol{L}_1$ to get $\boldsymbol{j}_1$
  step 2) $\boldsymbol{S}_2$ with $\boldsymbol{L}_2$ to get $\boldsymbol{j}_2$ $\qquad\qquad \boldsymbol{j} - \boldsymbol{j} \textbf{ coupling}$
  step 3) $\boldsymbol{j}_1$ with $\boldsymbol{j}_2$ to get $\boldsymbol{J}$

or

- step 1) $\boldsymbol{L}_1$ with $\boldsymbol{L}_2$ to get $\boldsymbol{L}$
  step 2) $\boldsymbol{S}_1$ with $\boldsymbol{S}_2$ to get $\boldsymbol{S}$ $\qquad\qquad \boldsymbol{L} - \boldsymbol{S} \textbf{ coupling}$
  step 3) $\boldsymbol{L}$ with $\boldsymbol{S}$ to get $\boldsymbol{J}$ $\quad$.

The non-relativistic ionic states which emerge from the two proceedings are similar but not equal. They are linked by a linear transformation which involves Racah coefficients

[37].

The $j-j$ coupling is most similar to the relativistic framework, where spin and orbital angular momenta are already coupled by the Dirac formalism. Indeed, it turns out that the $j-j$ coupling scheme gives a better (non-relativistic) description than the $L-S$ scheme for states of highly or medium charged ions, where relativistic effects are important. On the other hand, it is also known that the $L-S$ coupling scheme gives a better (non-relativistic) description than the $j-j$ scheme for the states of low charged ions. What is believed to happen is that, in low Z regime, the spin-orbit interactions (L_1-S_1 and L_2-S_2) are smaller in comparison with the orbit-orbit (L_1-L_2) interactions, so that coupling at "the first round" the orbital angular momenta ($L_1+L_2=L$), and consequently also the spin angular momenta ($S_1+S_2=S$), turns out to work better. In other words, the electron-electron interaction term in the non-relativistic Hamiltonian plays a bigger role that the spin-orbit relativistic correction term, which sounds indeed reasonable.

The non-relativistic common notation which is used in spectroscopy refers to the $L-S$ coupling and therefore uses the good quantum numbers in that coupling scheme: $\{n_1, l_1, n_2, l_2, L, S, J, m_J\}$. In spectroscopic notation, the genuine discrete states are thus labeled by[6]

$$(1s \, , \, n_2 \, L \,)^{(2S+1)} L_J^{m_J} \quad , \tag{2.37}$$

or, more shortly,

$$n_2^{(2S+1)} L_J^{m_J} \quad . \tag{2.38}$$

From the foregoing discussion we may catch the concept that i) heliumlike systems have in nature many states, ii) if the physicist describes them by using non-relativistic $L-S$ coupling scheme, that physicist should denote the states by the spectroscopic notation (2.37) or (2.38), iii) if the physicist describes them by using the non-relativistic $j-j$ coupling scheme or by using the relativistic IPM explained above, that physicist should denote the states by the relativistic notation in equation (2.36).

Unfortunately, this is not a strict rule. Even though, as remarked, the $j-j$ and the $L-S$ coupled states are not equal, they are of course of the same number, so that one can build a one-to-one correspondence between the two bases. For the levels with $n \leq 3$ such correspondence reads

$$
\begin{array}{llll|lll}
1s_{1/2}1s_{1/2} : & J=0 & 1^1S_0 & & 1s_{1/2}3s_{1/2} : & J=0 & 3^1S_0 \\
1s_{1/2}2s_{1/2} : & J=1 & 2^3S_1 & & 1s_{1/2}3p_{1/2} : & J=0 & 3^3P_0 \\
1s_{1/2}2p_{1/2} : & J=1 & 2^3P_1 & & 1s_{1/2}3p_{3/2} : & J=2 & 3^3P_2 \\
1s_{1/2}2s_{1/2} : & J=0 & 2^1S_0 & & 1s_{1/2}3d_{3/2} : & J=2 & 3^3D_2 \\
1s_{1/2}2p_{1/2} : & J=0 & 2^3P_0 & & 1s_{1/2}3d_{3/2} : & J=1 & 3^3D_1 \\
1s_{1/2}2p_{3/2} : & J=2 & 2^3P_2 & & 1s_{1/2}3p_{3/2} : & J=1 & 3^1P_1 \\
1s_{1/2}2p_{3/2} : & J=1 & 2^1P_1 & & 1s_{1/2}3d_{5/2} : & J=3 & 3^3D_3 \\
1s_{1/2}3s_{1/2} : & J=1 & 3^3S_1 & & 1s_{1/2}3d_{5/2} : & J=2 & 3^1D_2 \\
1s_{1/2}3p_{1/2} : & J=1 & 3^3P_1 & & ... & &
\end{array}
\tag{2.39}
$$

By virtue of this correspondence, one may denote by the non-relativistic spectroscopic notation some physical states that have been then actually in theory treated with the $j-j$ coupling scheme or the relativistic IPM[7].

---

[6]Note that in the genuine discrete states $l_2 = L$.

[7]I remark this fact, since I did the same "abuse of notation" in two of my papers.

2.5 Electromagnetic radiation

The electromagnetic fields $\boldsymbol{E}$ and $\boldsymbol{B}$ are described by Maxwell's equations. In vacuum, these equations read

$$
\begin{cases}
\boldsymbol{\nabla} \times \boldsymbol{E} & = & -\dfrac{\partial \boldsymbol{B}}{\partial t} \\[2mm]
\boldsymbol{\nabla} \cdot \boldsymbol{B} & = & 0 \\[2mm]
\boldsymbol{\nabla} \times \boldsymbol{B} & = & \dfrac{1}{c^2}\dfrac{\partial \boldsymbol{E}}{\partial t} \\[2mm]
\boldsymbol{\nabla} \cdot \boldsymbol{E} & = & 0 \quad .
\end{cases}
\tag{2.40}
$$

The scalar (Φ) and vector ($\boldsymbol{A}$) potentials are related to the fields by

$$
\begin{aligned}
\boldsymbol{E} & = & -\boldsymbol{\nabla}\Phi - \dfrac{\partial \boldsymbol{A}}{\partial t} \\[2mm]
\boldsymbol{B} & = & \boldsymbol{\nabla} \times \boldsymbol{A} \quad .
\end{aligned}
\tag{2.41}
$$

The two above equations do not fully specify the potentials. As known, given a regular scalar function λ, the Maxwell's equations remain invariant under a transformation of the type

$$
\begin{aligned}
\boldsymbol{A} & \rightarrow & \boldsymbol{A} + \boldsymbol{\nabla}\lambda \\[2mm]
\Phi & \rightarrow & \Phi - \dfrac{\partial \lambda}{\partial t} \quad .
\end{aligned}
$$

We may therefore choose another further condition to wholly specify the potentials: the so-called *gauge condition*. Common gauge choices are the Coulomb condition

$$
\boldsymbol{\nabla} \cdot \boldsymbol{A} = 0 \quad ,
\tag{2.42}
$$

and the Lorentz condition

$$
\boldsymbol{\nabla} \cdot \boldsymbol{A} + \dfrac{1}{c^2}\dfrac{\partial \Phi}{\partial t} = 0 \quad .
$$

We shall work within the Coulomb gauge with the further condition $\Phi = 0$, which can be imposed as long as we are in the vacuum. See App. A for a proof. This choice is also referred to as *radiation gauge* or *solenoidal gauge*. With this choice, the Lorentz and Coulomb gauges represent the same gauge choice.

By combining Eqs. (2.41) and (2.40), in App. A it is shown that we get the following wave equation for the vector potential:

$$
\boldsymbol{\nabla}^2 \boldsymbol{A} - \dfrac{1}{c^2}\dfrac{\partial^2 \boldsymbol{A}}{\partial t^2} = 0 \quad .
$$

The general solution of it is

$$
\boldsymbol{A}(\boldsymbol{r}, t) = A_0 \left(\underline{\epsilon} e^{i(\boldsymbol{k}\boldsymbol{r} - \omega t + \delta_\omega)} + \underline{\epsilon}^* e^{-i(\boldsymbol{k}\boldsymbol{r} - \omega t + \delta_\omega)} \right) \quad ,
\tag{2.43}
$$

where δ_ω, A_0 and $\underline{\epsilon}$ are integration constants to be fixed, $\boldsymbol{k}$ and ω are the propagation vector and the angular frequency of the electromagnetic wave respectively. $\boldsymbol{k}$ and ω are related by the equations

$$
\begin{aligned}
|\boldsymbol{k}| & = & \dfrac{2\pi}{\lambda} = 2\pi\dfrac{\nu}{c} & \equiv k \\[2mm]
\omega & = & 2\pi\nu & ,
\end{aligned}
$$

where λ and ν are the wavelength and the frequency of the electromagnetic wave respectively.

From now on, without loss of generality, we consider, unless differently stated, the electromagnetic wave as traveling along the $\underline{z}$ direction: $\boldsymbol{k} = (0, 0, k)$. The phase δ_ω can be fixed by declaring the initial state. For our purposes, we can freely set $\delta_\omega = 0$. Since we inserted A_0 in Eq. (2.43), we can evidently freely also set $\underline{\epsilon}$ as unit vector, i.e. $|\underline{\epsilon}| = 1$. We shall call this unit vector the *polarization vector* of the electromagnetic wave, for reasons which will be clearer in a few lines. The appearance of both $\underline{\epsilon}$ and $\underline{\epsilon}^*$ in the rhs of Eq. (2.43) is forced by the reality of the fields which from the potentials are derived.

The choice of the polarization vector can be limited by the gauge condition. Indeed, the gauge condition $\boldsymbol{\nabla} \cdot \boldsymbol{A} = 0$ implies

$$0 = \boldsymbol{\nabla} \cdot \boldsymbol{A} = iA_0 \left(\boldsymbol{k} \cdot \underline{\epsilon} e^{i(\boldsymbol{kr} - \omega t + \delta_\omega)} - \boldsymbol{k} \cdot \underline{\epsilon}^* e^{-i(\boldsymbol{kr} - \omega t + \delta_\omega)} \right) \quad .$$

By explicitly writing the polarization vector in its real and complex parts, $\underline{\epsilon} = \boldsymbol{a}_\epsilon + i\boldsymbol{b}_\epsilon$, the above equation leads to

$$0 = \left(\boldsymbol{k}\boldsymbol{a}_\epsilon \right) \sin(\boldsymbol{kr} - \omega t) + \left(\boldsymbol{k}\boldsymbol{b}_\epsilon \right) \cos(\boldsymbol{kr} - \omega t) \quad , \tag{2.44}$$

which must be true for any time t and any position $\boldsymbol{r}$. This can be fulfilled only if $\boldsymbol{k}\boldsymbol{a}_\epsilon = \boldsymbol{k}\boldsymbol{b}_\epsilon = 0$, which directly means $\boldsymbol{k}\underline{\epsilon} = 0$. In conclusion, the Coulomb gauge condition implies the transversality of the potential vector $\boldsymbol{A}$.

Though the choices for $\underline{\epsilon}$ are still infinite, they can be divided in two groups[8]:

$$\begin{aligned} \underline{\epsilon}_L &= (\cos\theta_s , \sin\theta_s , 0) &&\textbf{type L} \\ \underline{\epsilon}_C &= (\cos\theta_s , i\sin\theta_s , 0) &&\textbf{type C} \quad , \end{aligned} \tag{2.45}$$

where we added the subscript $_s$ to make it clear that the angle θ_s has nothing to do with momentum or cartesian spaces.

The electromagnetic waves of type L are said to be *linearly polarized*, while the electromagnetic waves of type C are said to be *circularly polarized*.

The vector potential for these two cases can be easily written

$$\begin{aligned} \boldsymbol{A}_L(\boldsymbol{r}, t) &= A_0 \left(\underline{\epsilon}_L e^{i(\boldsymbol{kr} - \omega t + \delta_\omega)} + \underline{\epsilon}_L^* e^{-i(\boldsymbol{kr} - \omega t + \delta_\omega)} \right) \\ &= 2\underline{\epsilon}_L A_0 \cos(\boldsymbol{kr} - \omega t) = 2A_0 \cos(\boldsymbol{kr} - \omega t)\left(\cos\theta , \sin\theta , 0 \right) \quad \textbf{type L} \end{aligned}$$

$$\begin{aligned} \boldsymbol{A}_C(\boldsymbol{r}, t) &= A_0 \left(\underline{\epsilon}_C e^{i(\boldsymbol{kr} - \omega t + \delta_\omega)} + \underline{\epsilon}_C^* e^{-i(\boldsymbol{kr} - \omega t + \delta_\omega)} \right) \\ &= 2A_0 \left(\cos\theta \cos(\boldsymbol{kr} - \omega t), \ -\sin\theta \sin(\boldsymbol{kr} - \omega t), \ 0 \right) \quad\quad \textbf{type C} \quad . \end{aligned}$$

At this point, one can in principle start associating electromagnetic waves to photon particles. Then, on analyzing the angular momentum carried by the electromagnetic wave, that is given by

$$\boldsymbol{M} = \frac{1}{\mu_0} \int \mathrm{d}^3 r \quad \boldsymbol{r} \times (\boldsymbol{E} \times \boldsymbol{B}) \quad ,$$

---

[8]By considering that the polarization vector must satisfy $|\underline{\epsilon}| = 1$ and that any overall phase can be absorbed into the constant A_0, these two groups fully represent any possible polarization vector.

it can be showed, after some quite tedious but elementary analysis, that: If we want to define a Spin operator in the photons' quantum space (which will be denoted by $\hat{\mathbf{S}}$), then that operator must be defined by the equation [38]

$$\hat{S}_\alpha \epsilon_\beta = -i \epsilon_{\alpha\beta\gamma} \epsilon_\gamma \quad , \tag{2.46}$$

where ϵ_β is the β component of the polarization vector $\underline{\epsilon}$, while $\epsilon_{\alpha\beta\gamma}$ is the total antisymmetric tensor (also called Levi-Civita symbol). $\hat{S}_\alpha$ is the α component of the spin operator $\hat{\mathbf{S}}$.

We may now verify that the two circular polarization vectors

$$
\begin{aligned}
\underline{\epsilon}_C^+ &= \frac{1}{\sqrt{2}}(1,i,0) \\
&= \frac{1}{\sqrt{2}}(\underline{x} + i\underline{y}) \quad \doteq \quad \frac{1}{\sqrt{2}}\big(|x\rangle + i\,|y\rangle\big) = |\lambda = +1\rangle \\
\underline{\epsilon}_C^- &= \frac{1}{\sqrt{2}}(1,-i,0) \\
&= \frac{1}{\sqrt{2}}(\underline{x} - i\underline{y}) \quad \doteq \quad \frac{1}{\sqrt{2}}\big(|x\rangle - i\,|y\rangle\big) = |\lambda = -1\rangle
\end{aligned}
\tag{2.47}
$$

are eigenstates of the $\hat{S}_z$ operator with eigenvalue $+1$ and -1 respectively:

$$
\begin{aligned}
\hat{S}_z\,\epsilon_{C\,x}^+ &= -i\,\epsilon_{zxy}\,\epsilon_{C\,y}^+ = -i \cdot 1 \cdot \left(\frac{i}{\sqrt{2}}\right) = \frac{1}{\sqrt{2}} = (+1)\,\epsilon_{C\,x}^+ \\
\hat{S}_z\,\epsilon_{C\,y}^+ &= -i\,\epsilon_{zyx}\,\epsilon_{C\,x}^+ = -i \cdot (-1) \cdot \left(\frac{1}{\sqrt{2}}\right) = \frac{i}{\sqrt{2}} = (+1)\,\epsilon_{C\,y}^+ \\
&\Rightarrow \hat{S}_z\,\underline{\epsilon}_C^+ = (\hat{S}_z\,\epsilon_{C\,x}^+, \hat{S}_z\,\epsilon_{C\,y}^+, 0) = (+1)\underline{\epsilon}_C^+ \quad ,
\end{aligned}
$$

$$
\begin{aligned}
\hat{S}_z\,\epsilon_{C\,x}^- &= -i\,\epsilon_{zxy}\,\epsilon_{C\,y}^- = -i \cdot 1 \cdot \left(-\frac{i}{\sqrt{2}}\right) = -\frac{1}{\sqrt{2}} = (-1)\,\epsilon_{C\,x}^- \\
\hat{S}_z\,\epsilon_{C\,y}^- &= -i\,\epsilon_{zyx}\,\epsilon_{C\,x}^- = -i \cdot (-1) \cdot \left(\frac{1}{\sqrt{2}}\right) = \frac{i}{\sqrt{2}} = (-1)\,\epsilon_{C\,y}^- \\
&\Rightarrow \hat{S}_z\,\underline{\epsilon}_C^- = (\hat{S}_z\,\epsilon_{C\,x}^-, \hat{S}_z\,\epsilon_{C\,y}^-, 0) = (-1)\underline{\epsilon}_C^- \quad .
\end{aligned}
$$

As we wrote in Eq. (2.47), it is natural to associate, in quantum mechanics, the polarization states $\underline{\epsilon}_C^+$ and $\underline{\epsilon}_C^-$ respectively with the positive ($|\lambda = +1\rangle$) and negative ($|\lambda = -1\rangle$) spin-1 states for massless particles along the $\underline{z}$ direction (the propagation direction). The analytic structure is indeed the same. However, we must here point out an important issue: Due to the transversality of the vector potential (in the Coulomb gauge) and of the electromagnetic fields (in any gauge), the direction of the polarization vector must always be orthogonal to the propagation direction. As it happens in the relativistic description of electrons, the photon spin space is *not* fully separated from the photon spatial space. We must then be careful in dealing with photon plane waves. For example, when we want to rotate the vector potential along a given axis, the polarization vector must rotate correspondingly.

Since our photon is traveling along the $\underline{z}$ direction, λ corresponds to the photon helicity. It is moreover interesting to notice that $\underline{\epsilon}_C^{-*} = \underline{\epsilon}_C^+$. Because of this, for example, the potential vector $\mathbf{A}_C^{\lambda=\pm 1}$ is not eigenstate of the spin operator $\hat{S}_z$, while the single

vector plane waves $\underline{\epsilon}_C^{\pm 1} e^{\pm i\boldsymbol{k}\boldsymbol{r}}$ and $\underline{\epsilon}_C^{\pm 1 *} e^{\pm i\boldsymbol{k}\boldsymbol{r}}$ are. From this reasoning, we infer that, if we wanted to construct the photon wavefunction, such wavefunction would be proportional to a single vector plane wave $\underline{\epsilon}_C^\lambda e^{\pm i\boldsymbol{k}\boldsymbol{r}}$. Since the construction of the photon wavefunction exits the scope of this thesis, we will not further investigate toward this direction.

We have in conclusion demonstrated that the correct association between the polarization state of an electromagnetic wave and the spin of a particle must be an association to a massless spin-1 particle. What about the spin state $|\lambda = 0\rangle$? To which polarization vector does it correspond? Vector massless particles cannot have, as known, spin state $|\lambda = 0\rangle$. This condition indeed is in line with the characteristics of the electromagnetic wave. The spin state $|\lambda = 0\rangle$ by definition satisfies the equation

$$\hat{\mathrm{S}}_z^{J=1} |\lambda = 0\rangle = 0 \, |\lambda = 0\rangle = 0 \quad .$$

By looking at the action that the spin operator $\hat{\mathrm{S}}_z$ does on the polarization vector of the electromagnetic wave (see Eq. (2.46)), we deduce that the polarization vector with vanishing eigenvalue can only be

$$\underline{\epsilon}_C^0 = (0, 0, 1) \quad .$$

However, as discussed above, such a polarization vector cannot characterize the photon since our gauge choice (2.42) forces the polarization vector to be orthogonal to the propagation direction $\hat{z}$ (see Eq. (2.44)). Thus, we can safely state that an electromagnetic wave characterized by the polarization state $\underline{\epsilon}_C^0$ does not exist, or, what is the same, that the polarization state $\underline{\epsilon}_C^0$ is forbidden for any electromagnetic wave[9].

Now that we have well understood what the polarization vector $\underline{\epsilon}$ means, we can come back to equation (2.43) to fix A_0. For doing that, it is useful to derive the fields $\boldsymbol{E}$ and $\boldsymbol{B}$ of a linearly polarized wave by using Eq. (2.41) and by remembering furthermore our gauge choice $\Phi = 0$:

$$
\begin{aligned}
\boldsymbol{E}_L(\boldsymbol{r}, t) &= -\frac{\partial \boldsymbol{A}_L}{\partial t} = i\omega A_0 \, \underline{\epsilon}_L \left(e^{i(\boldsymbol{k}\boldsymbol{r} - \omega t)} - e^{-i(\boldsymbol{k}\boldsymbol{r} - \omega t)} \right) \\
&= -2\omega A_0 \, \underline{\epsilon}_L \sin(\boldsymbol{k}\boldsymbol{r} - \omega t) \quad ,
\end{aligned}
$$

$$
\begin{aligned}
\boldsymbol{B}_L(\boldsymbol{r}, t) &= \nabla \times \boldsymbol{A}_L = i\boldsymbol{k} \times A_0 \underline{\epsilon}_L \left(e^{i(\boldsymbol{k}\boldsymbol{r} - \omega t)} - e^{-i(\boldsymbol{k}\boldsymbol{r} - \omega t)} \right) \\
&= -2A_0 \boldsymbol{k} \times \underline{\epsilon}_L \sin(\boldsymbol{k}\boldsymbol{r} - \omega t) \quad .
\end{aligned}
$$

We see from the above equations that $\boldsymbol{E}_L$ and $\boldsymbol{B}_L$ are in phase, orthogonal to each other and to $\boldsymbol{k}$ (these features are true in any gauge) and that $\boldsymbol{E}_L$ is proportional to $\boldsymbol{A}_L$ (this is a characteristic of the Coulomb gauge). We moreover notice that the electric and magnetic fields' directions do not change in time (this feature is characteristic of linearly polarized electromagnetic waves).

In order to determine A_0 from measurable characteristics, we may write explicitly the energy density of the radiation [39]

$$\rho(\omega) = \frac{1}{2} \left(\epsilon_0 \boldsymbol{E}_L^2 + \frac{1}{\mu_0} \boldsymbol{B}_L^2 \right) = 4\epsilon_0 \omega^2 A_0^2 \sin^2(\boldsymbol{k}\boldsymbol{r} - \omega t) \quad ,$$

---

[9]Although we worked within the Coulomb gauge, the spin state $|\lambda = 0\rangle$ is forbidden, for any electromagnetic wave, in any gauge.

where ϵ_0 and μ_0 are respectively the electric and magnetic permeabilities of vacuum ($\dfrac{1}{\epsilon_0 \mu_0} = c^2$).

The average energy density over a period $T = 2\pi/\omega$ is then

$$\overline{\rho}(\omega) = 2\epsilon_0 \omega^2 A_0^2 \quad . \tag{2.48}$$

The average energy density of the electromagnetic wave cannot reasonably depend on its polarization. Although we found $\overline{\rho}(\omega)$ for linearly polarized waves, the relation (2.48) must hold for any electromagnetic wave, irrespectively of its polarization.

We now impose that the energy density must be equal to the number of photons (N_γ) per volume (V) times the single photon energy[10]:

$$\overline{\rho}(\omega) = \frac{N_\gamma \hbar \omega}{V} \quad . \tag{2.49}$$

By combining Eq. (2.48) with Eq. (2.49), we get

$$A_0 = \sqrt{\frac{\hbar N_\gamma}{2\epsilon_0 \omega V}} \quad . \tag{2.50}$$

From Eq. (2.43) we can now finally write the general electromagnetic vector potential as given by N_γ photons having the same characteristics:

$$\boldsymbol{A}(\boldsymbol{r}, t) = \sqrt{\frac{\hbar N_\gamma}{2\epsilon_0 \omega V}} \left(\underline{\epsilon}\, e^{i(\boldsymbol{k}\boldsymbol{r} - \omega t)} + \underline{\epsilon}^*\, e^{-i(\boldsymbol{k}\boldsymbol{r} - \omega t)} \right) \quad .$$

The vector potential due to the presence of one single photon having propagation vector $\boldsymbol{k}$ and polarization $\underline{\epsilon}$ is then given by

$$\boldsymbol{A}(\boldsymbol{r}, t) = \sqrt{\frac{\hbar}{2\epsilon_0 \omega V}} \left(\underline{\epsilon}\, e^{i(\boldsymbol{k}\boldsymbol{r} - \omega t)} + \underline{\epsilon}^*\, e^{-i(\boldsymbol{k}\boldsymbol{r} - \omega t)} \right) \quad . \tag{2.51}$$

It may be instructive showing also $\boldsymbol{E}$ and $\boldsymbol{B}$ fields as given by one single photon having propagation vector $\boldsymbol{k}$ and polarization $\underline{\epsilon}$. By using Eq. (2.41) we get

$$
\begin{aligned}
\boldsymbol{E}_L(\boldsymbol{r}, t) &= -\sqrt{\frac{2\hbar\omega}{\epsilon_0 V}}\, \underline{\epsilon}_L\, \sin(\boldsymbol{k}\boldsymbol{r} - \omega t) \\
\boldsymbol{B}_L(\boldsymbol{r}, t) &= -\sqrt{\frac{2\hbar}{\epsilon_0 \omega V}}\, \boldsymbol{k} \times \underline{\epsilon}_L\, \sin(\boldsymbol{k}\boldsymbol{r} - \omega t)
\end{aligned}
\right] \quad \textbf{linearly polarized photon}
$$

$$
\begin{aligned}
\boldsymbol{E}_C(\boldsymbol{r}, t) &= -\sqrt{\frac{2\hbar\omega}{\epsilon_0 V}} \left(\underline{\epsilon}_C \circ \boldsymbol{\eta} \right) \\
\boldsymbol{B}_C(\boldsymbol{r}, t) &= -\sqrt{\frac{2\hbar}{\epsilon_0 \omega V}}\, \boldsymbol{k} \times \left(\underline{\epsilon}_C \circ \boldsymbol{\eta} \right)
\end{aligned}
\right] \quad \textbf{circularly polarized photon}
$$

---

[10]This is a crucial step. So far we have dealt with classical electrodynamics with some associations of the wave polarization states to particle spin states in quantum mechanics. We have never imposed that the electromagnetic wave is given by any quanta, nor imposed any quantum mechanical rule. Only now we do such a step.

where $\boldsymbol{\eta} = (\sin(\boldsymbol{kr} - \omega t), -i\cos(\boldsymbol{kr} - \omega t), 0)$ and the symbol $\circ$ stands for the Hadamard
product between vectors and it is defined such that

$$\boldsymbol{A} \circ \boldsymbol{B} = (A_1 B_1, \ A_2 B_2, \ A_3 B_3)$$

for any two vectors $\boldsymbol{A} = (A_1, A_2, A_3)$, $\boldsymbol{B} = (B_1, B_2, B_3)$.

The expression (2.51) is general and can be used for a photon having any propagation
direction, as long as the polarization vector $\underline{\epsilon}$ fulfills the gauge condition $\boldsymbol{k}\underline{\epsilon} = 0$.
The electromagnetic vector potential is integral part of the electron-photon interaction
Hamiltonian, which is the core of the dynamics of the two-photon transitions in atoms
and ions. Thus, Eq. (2.51) will be much used in the following.

Prior to turning to solve atomic problems, we make now a decomposition of the vector
plane wave $\underline{\epsilon}e^{i\boldsymbol{kr}}$. We are interested in investigating the angular momentum properties
of this quantity. As underlined above, the polarization vector $\underline{\epsilon}$ represents the photon
spin state and therefore it has well defined angular momentum properties. On the
other hand, the exponential part of the vector plane wave has *not* well defined angular
momentum properties. Rather it has well defined linear momentum properties. Since,
in atomic physics, we deal with states with defined angular momentum (and not linear
momentum), we should better make a plane wave decomposition of the exponential
(Rayleigh expansion) in terms of elements with defined angular momentum properties
[38]:

$$e^{i\boldsymbol{kr}} = (4\pi) \sum_{L=0}^{+\infty} \sum_{m=-L}^{L} i^L j_L(kr) Y_L^m(\theta_r, \varphi_r) Y_L^{m*}(\theta_k, \varphi_k) \quad , \tag{2.52}$$

where j_L are Spherical Bessel functions of the first kind and Y_L^m are spherical harmon-
ics. Each addend of this summation has well defined orbital angular momentum.
Summarizing, in the whole vector plane wave, we have i) the photon spin angular
momentum contained in the polarization vector and ii) a summation of terms, com-
ing from the Rayleigh expansion, where each one of them has defined orbital angular
momentum. We can easily also derive that the orbital and spin angular momenta
quantum spaces are well separated for photons, i.e. $\left[\hat{\mathbf{L}}, \hat{\mathbf{S}}\right] = 0$:

$$\hat{\mathrm{L}}_i \hat{\mathrm{S}}_j \, \epsilon_V e^{i\boldsymbol{kr}} = \hat{\mathrm{L}}_i (-i\epsilon_{j\,V\,\gamma}) \epsilon_\gamma e^{i\boldsymbol{kr}} = (-i\epsilon_{j\,V\,\gamma})(-i\hbar\,\hat{\mathbf{r}} \times \boldsymbol{\nabla}_r)_i \, \epsilon_\gamma e^{i\boldsymbol{kr}}$$

$$= (-i\epsilon_{j\,V\,\gamma}) \epsilon_\gamma (-i\hbar\,\hat{\mathbf{r}} \times \boldsymbol{\nabla}_r)_i \, e^{i\boldsymbol{kr}} = \hat{\mathrm{S}}_j \, \epsilon_V \, (-i\hbar\,\hat{\mathbf{r}} \times \boldsymbol{\nabla}_r)_i \, e^{i\boldsymbol{kr}}$$

$$= \hat{\mathrm{S}}_j \, \hat{\mathrm{L}}_i \, \epsilon_V e^{i\boldsymbol{kr}} \quad .$$

Hence, we can treat independently spin and orbital quantum spaces, i.e we can describe
the photon angular momentum state by giving, for instance, separately the quantum
numbers L, m, $S = 1$ and λ, where λ is the photon helicity. We also emphasize that,
since spin properties of the photon are contained solely in the polarization vector, a
measure of the polarization state gives a measure of the spin state.

Now we are partially satisfied since, for instance, in non-relativistic quantum mechanics
the states are described by giving separately the orbital angular momentum L (with its
projection m_l) and the spin angular momentum S (with its projection m_s). A standard
atomic transition amplitude would then separate into spin and angular momentum

parts, allowing a fast evaluation.

Notwithstanding the efforts we made, our analysis cannot be applied to relativistic states or to many-electron states. In these cases, in fact, the quantum numbers we use to characterize the atomic spectrum are total angular momentum and parity. We must give a description of the vector potential in terms of total photon angular momentum and parity. We now proceed to find such a description.

Let us define the unit vector

$$
\xi_p = \begin{cases}
\dfrac{1}{\sqrt{2}}(\underline{x} - i\underline{y}) & \text{if } p = -1 \\[2mm]
\underline{z} & \text{if } p = 0 \\[2mm]
-\dfrac{1}{\sqrt{2}}(\underline{x} + i\underline{y}) & \text{if } p = +1
\end{cases} \quad .
$$

By comparing with Eq. (2.47), we see that $\underline{\epsilon}_C^p = -p\,\xi_p$. Therefore, by using the association (2.47), we see that ξ_p represents the three photon spin states, included the not physical state with zero projection. By virtue of this, we can state that ξ_p transforms like a spherical tensor of rank 1 [37].

Now, let us fix the photon direction along $\underline{z}$. Thus, the vector plane wave for this circularly polarized photon is, using Eq. (2.52),

$$
\begin{aligned}
\underline{\epsilon}_C^\lambda\, e^{ik\,z} &= -\lambda\,\xi_\lambda\,(4\pi) \sum_{L=0}^{+\infty} \sum_{m=-L}^{L} i^L j_L(kr) Y_L^m(\theta_r, \varphi_r) Y_L^{m\,*}(0,0) \\[2mm]
&= -\lambda\,\xi_\lambda\,(4\pi) \sum_{L=0}^{+\infty} \sum_{m=-L}^{L} i^L j_L(kr) Y_L^m(\theta_r, \varphi_r) \sqrt{\frac{2L+1}{4\pi}}\, \delta_{m0} \qquad (2.53) \\[2mm]
&= -\lambda\,(4\pi)^{1/2} \sum_{L=0}^{+\infty} i^L (2L+1)^{1/2} j_L(kr)\, \xi_\lambda\, Y_L^0(\underline{r}) \quad ,
\end{aligned}
$$

where the angles (φ_r, θ_r) have been denoted by the unit vector $\underline{r}$ for the sake of brevity. Now, let us define the so-called "vector spherical harmonics", $\boldsymbol{T}_{JLM}(\underline{r})$:

$$
\begin{aligned}
\boldsymbol{T}_{JLM}(\underline{r}) &= \sum_{m=-1}^{1} \sum_{\mu=-L}^{L} < L, \mu, 1, m | J, M > Y_L^\mu(\underline{r})\, \xi_m \\[2mm]
&= \sum_{m=-1}^{1} < L, M-m, 1, m | J, M > Y_L^{M-m}(\underline{r})\, \xi_m \quad .
\end{aligned}
\qquad (2.54)
$$

By recalling the theorem of composition of spherical tensors [25], we recognize that $\boldsymbol{T}_{JLM}(\underline{r})$ is a spherical tensor of rank J, since it couples through Clebsch-Gordan coefficients the spherical tensors Y_L^μ (which contains the orbital angular momentum) with the spherical tensor ξ_m (which contains the spin angular momentum). We remark here the fact that $\boldsymbol{T}_{JLM}^*(\underline{r})$ is *not* a spherical tensor, since, for example, $Y_L^{\mu\,*}$ is not a spherical tensor. It can be easily showed, in fact, that $Y_L^{\mu\,*}$ does not transform as a spherical tensor of rank L, while Y_L^μ does.

It follows that $\boldsymbol{T}_{JLM}$ has well defined total angular momentum J, projection M,

orbital angular momentum L and spin angular momentum 1. Moreover, L denotes also something else relevant in $\boldsymbol{T}_{JLM}$: its parity. The parity of $\boldsymbol{T}_{JLM}$ turns trivially out to be given by $(-1)^{L+1}$, since the parity of Y_L^μ and ξ are $(-1)^L$ and (-1) respectively. $\boldsymbol{T}_{JLM}$ is therefore what we are looking for! It contains the quantum numbers we need. Let us find a way to plug it inside our vector plane wave.
We derive the inverse relation

$$\sum_{\eta=L-1}^{L+1} \langle L,0,1,\lambda|\eta,\lambda\rangle \boldsymbol{T}_{\eta\,L\,\lambda}(\underline{r}) = \xi_\lambda\, Y_L^0(\underline{r}) \quad . \tag{2.55}$$

Proof:

$$\sum_{\eta=L-1}^{L+1} \langle L,0,1,\lambda|\eta,\lambda\rangle \boldsymbol{T}_{\eta\,L\,\lambda} = \sum_{\eta=L-1}^{L+1} \sum_{m=-1}^{1} \langle L,0,1,\lambda|\eta,\lambda\rangle \langle L,\lambda-m,1,m|\eta,\lambda\rangle$$
$$\times\; Y_L^{\lambda-m}(\underline{r})\,\xi_m$$

$$= \sum_{m=-1}^{1} \sum_{\eta=L-1}^{L+1} \sum_{s=-\eta}^{+\eta} \langle L,0,1,\lambda|\eta,s\rangle \langle L,\lambda-m,1,m|\eta,s\rangle$$
$$\times\; Y_L^{\lambda-m}(\underline{r})\,\xi_m$$

$$= \sum_{m=-1}^{1} \delta_{L\,L}\delta_{0\,\lambda-m}\delta_{1\,1}\delta_{\lambda\,m}\, Y_L^{\lambda-m}(\underline{r})\,\xi_m = \; Y_L^0(\underline{r})\,\xi_p \quad .$$

Therefore, we can plug Eq. (2.55) into Eq. (2.53) to obtain

$$\underline{\epsilon}_C^\lambda\, e^{ik\,z} = -\lambda\,(4\pi)^{1/2} \sum_{L=0}^{+\infty} i^L(2L+1)^{1/2} j_L(kr) \sum_{\eta=L-1}^{L+1} \langle L,0,1,\lambda|\eta,\lambda\rangle \boldsymbol{T}_{\eta\,L\,\lambda}(\underline{r})$$

$$= (4\pi)^{1/2} \sum_{L=0}^{+\infty} i^L(-p)(2L+1)^{1/2} j_L(kr)\Big[\langle L,0,1,\lambda|L-1,\lambda\rangle \boldsymbol{T}_{L-1\,L\,\lambda}(\underline{r})$$
$$+\; \langle L,0,1,\lambda|L,\lambda\rangle \boldsymbol{T}_{L\,L\,\lambda}(\underline{r}) \;+\; \langle L,0,1,\lambda|L+1,\lambda\rangle \boldsymbol{T}_{L+1\,L\,\lambda}(\underline{r})\Big]$$

$$= (4\pi)^{1/2} \sum_{L=0}^{+\infty} i^L(-\lambda)(2L+1)^{1/2} j_L(kr)\left[\left(\frac{L-1}{2(2L+1)}\right)^{1/2} \boldsymbol{T}_{L-1\,L\,\lambda}(\underline{r})\right.$$
$$\left. -\; \frac{\lambda}{\sqrt{2}}\, \boldsymbol{T}_{L\,L\,\lambda}(\underline{r}) \;+\; \left(\frac{L+2}{2(2L+1)}\right)^{1/2} \boldsymbol{T}_{L+1\,L\,\lambda}(\underline{r})\right]$$

$$= (2\pi)^{1/2} \sum_{L=0}^{+\infty} i^L j_L(kr)\Big[-\lambda\,(L-1)^{1/2}\, \boldsymbol{T}_{L-1\,L\,\lambda}(\underline{r})$$
$$+\; (2L+1)^{1/2}\, \boldsymbol{T}_{L\,L\,\lambda}(\underline{r}) \;-\; \lambda\,(L+2)^{1/2}\, \boldsymbol{T}_{L+1\,L\,\lambda}(\underline{r})\Big] \quad ,$$

where it has been used $\lambda^2 = 1$, since $\lambda = \pm 1$.
The first term enclosed in parentheses results vanishing for $L=0$ (since $\boldsymbol{T}_{-1\,0\,p}=0$) and for $L=1$ (since, in that case, $(L-1)=0$). The second term enclosed in parentheses

results vanishing for $L = 0$ (since $\boldsymbol{T}_{0\,0\,p} = 0$). Therefore we are left with

$$
\underline{\epsilon}_C^\lambda \, e^{ik\,z} = (2\pi)^{1/2} \Big[-\lambda \sum_{L=2}^{+\infty} i^L j_L(kr)(L-1)^{1/2} \, \boldsymbol{T}_{L-1\,L\,\lambda}(\underline{r})
$$
$$
+ \sum_{L=1}^{+\infty} i^L j_L(kr)(2L+1)^{1/2} \, \boldsymbol{T}_{L\,L\,\lambda}(\underline{r}) - \lambda \sum_{L=0}^{+\infty} i^L j_L(kr)(L+2)^{1/2} \, \boldsymbol{T}_{L+1\,L\,\lambda}(\underline{r}) \Big] \quad .
$$

Now, we rename $L \to L + 1$ in the first term, $L \to L - 1$ in the third term. The summations modify correspondingly.
After all, we get

$$
\underline{\epsilon}_C^\lambda \, e^{ik\,z} \;\; = \;\; \sqrt{2\pi} \sum_{L=1}^{+\infty} i^L (2L+1)^{1/2} \left(\boldsymbol{A}_{L\lambda}^{(m)}(k,\boldsymbol{r}) + i\lambda \boldsymbol{A}_{L\lambda}^{(e)}(k,\boldsymbol{r}) \right) \quad , \qquad (2.56)
$$

where

$$
\boldsymbol{A}_{L\lambda}^{(m)}(k,\boldsymbol{r}) \;\; = \;\; j_L(kr) \boldsymbol{T}_{L\,L\,\lambda}(\underline{r})
$$
$$
\boldsymbol{A}_{L\lambda}^{(e)}(k,\boldsymbol{r}) \;\; = \;\; j_{L-1}(kr) \sqrt{\frac{L+1}{2L+1}} \boldsymbol{T}_{L\,L-1\,\lambda}(\underline{r}) - j_{L+1}(kr) \sqrt{\frac{L}{2L+1}} \boldsymbol{T}_{L\,L+1\,p}(\underline{r}) \quad .
$$

Since the elements $\boldsymbol{A}_{L\lambda}^{(m,e)}$ are spherical tensors with total angular momentum L and projection λ, we can safely obtain the potential vector for an arbitrary direction $\boldsymbol{k}$ by rotating, with a Wigner-D matrix, each term with defined angular momentum L in the summation of Eq. (2.56) [25].
By doing that, we get:

$$
\underline{\epsilon}_C^\lambda \, e^{i\boldsymbol{k}\boldsymbol{r}} \;\; = \;\; \sqrt{2\pi} \sum_{L=1}^{+\infty} \sum_{M=-L}^{L} i^L (2L+1)^{1/2} \left(\boldsymbol{A}_{LM}^{(m)}(k,\boldsymbol{r}) + i\lambda \boldsymbol{A}_{LM}^{(e)}(k,\boldsymbol{r}) \right) \, D_{M\lambda}^L(\varphi_k,\theta_k,0)
$$
$$
= \;\; \sqrt{2\pi} \sum_{L=1}^{+\infty} \sum_{M=-L}^{L} \sum_{p=0,1} i^L (2L+1)^{1/2} (i\lambda)^p \, \boldsymbol{a}_{LM}^p(k,\boldsymbol{r}) \, D_{M\lambda}^L(\varphi_k,\theta_k,0) \quad ,
$$
$$
(2.57)
$$

with, in summary,

$$\boldsymbol{A}_{LM}^{(m)}(k,\boldsymbol{r}) = j_L(kr)\boldsymbol{T}_{L,L,M}(\underline{r})$$

$$\boldsymbol{A}_{LM}^{(e)}(k,\boldsymbol{r}) = j_{L-1}(kr)\sqrt{\frac{L+1}{2L+1}}\boldsymbol{T}_{LL-1M}(\underline{r}) - j_{L+1}(kr)\sqrt{\frac{L}{2L+1}}\boldsymbol{T}_{LL+1M}(\underline{r})$$

$$\boldsymbol{T}_{JLM}(\underline{r}) = \sum_{m=-1}^{1} <L,M-m,1,m|J,M> Y_L^{M-m}(\varphi_r,\theta_r)\boldsymbol{\xi}_m$$

$$\xi_m = \begin{cases} \dfrac{1}{\sqrt{2}}(\underline{x}-iy) & \text{if } m=-1 \\ \underline{z} & \text{if } m=0 \\ -\dfrac{1}{\sqrt{2}}(\underline{x}+iy) & \text{if } m=+1 \end{cases}$$

$$\lambda = \textbf{helicity of the photon}$$

$$\boldsymbol{a}_{LM}^p(k,\boldsymbol{r}) = \begin{cases} \boldsymbol{A}_{LM}^{(m)}(k,\boldsymbol{r}) & \text{if } p=0 \\ \boldsymbol{A}_{LM}^{(e)}(k,\boldsymbol{r}) & \text{if } p=1 \end{cases}.$$

The spherical angles (φ_k,θ_k), of course, correspond to the spherical angles of the vector $\boldsymbol{p}$, since $\boldsymbol{k}$ and $\boldsymbol{p}$ differ by a constant (see Eq. (2.43) and the paragraph afterwards). This decomposition is referred to as *multipole decomposition*.

From what said previously, it turns evidently out that each term $\boldsymbol{a}_{LM}^p$ has total angular momentum L, total angular momentum projection M and parity $(-1)^{L+1+p}$ well defined. Analogously, each term $\boldsymbol{T}_{JLM}$ has total angular momentum J, total angular momentum projection M, orbital angular momentum L and parity $(-1)^{L+1}$ well defined.

We also underline that, even though the spin state $|\lambda=0\rangle$, which corresponds to the element $\xi_{m=0}$, is forbidden for the photon, the rotation of the vector plane wave includes it since the definition of spherical harmonics tensor makes use of the completeness of the basis set $\xi_{m=-1,0,1}$.

The multipole decomposition is useful in atomic physics since each term of it has defined parity and total angular momentum properties. Due to the radial nature of the atomic potential, the electronic wavefunctions which correspond to atomic states have also defined parity and angular momentum. The invariance of the overall Hamiltonian under rotations and parity transformation ensures that both angular momentum and parity are conserved quantum numbers in atomic transitions. It can be thus easily understood that the decomposition (2.57) is particularly useful to discern terms which have contribution in atomic transitions from terms which have not.

Following standard notation, we define

$$
\begin{aligned}
\underline{\epsilon}_C^\lambda \, e^{i\boldsymbol{k}\boldsymbol{r}} &= \sqrt{2\pi} \sum_{L=1}^{+\infty} \sum_{M=-L}^{L} i^L (2L+1)^{1/2} \boldsymbol{A}_{LM}^{(m)}(k,\boldsymbol{r}) D_{M\lambda}^L(\varphi_k,\theta_k,0) \\
&+ \sqrt{2\pi} \sum_{L=1}^{+\infty} \sum_{M=-L}^{L} i^L (2L+1)^{1/2} i\lambda \boldsymbol{A}_{LM}^{(e)}(k,\boldsymbol{r}) D_{M\lambda}^L(\varphi_k,\theta_k,0) \\
&= M1 + M2 + M3 + ... \\
&+ \quad E1 + E2 + E3 + ... \qquad ,
\end{aligned}
$$

where ML and EL are respectively called magnetic and electric multipole of order L. As said in the foregoing discussion, these multipoles have parity and total angular momentum well defined, i.e. they are eigenfunctions of parity and total angular momentum operators. We summarize their properties for a quick view:

multipole	Parity	Angular momentum
ML	$(-1)^{L+1}$	L
EL	$(-1)^{L}$	L

We emphasize that, as discussed in Eq. (2.47), the photon spin is entirely contained in the polarization vector (ϵ) of the electromagnetic wave. The plane wave $e^{\pm i\boldsymbol{k}\boldsymbol{r}}$ indeed contains naturally only orbital angular momentum components. Measuring the polarization state of a light quanta equals to measuring the photon spin.

Generally, the higher multipole we consider the smaller contribution in atomic transitions we get. This is due to the fact that high multipoles are characterized by Bessel functions of high order. These latter are small for small values of kr (which is the argument), which, in turn, are characteristic values for atomic and ionic transitions. To better explain, we will make a concrete example. The magnetic quadrupole $M2$ contains the spherical Bessel function $j_2(kr)$. Since this spherical Bessel function is nearly vanishing for $0 \leq kr \lesssim 1$, in order to have a sizeable contribution from $M2$ in atomic transitions, we must have $kr \gtrsim 1$, which implies $r \gtrsim \dfrac{\hbar c}{E}$, where E is the energy of the photon. Due to energy conservation, the photon energy must be equal to the transition energy, for single-photon transitions. For multi-photon transitions, the photon energy will be anyway of the same order of magnitude of the transition energy. In Hydrogen atom, the characteristic energies for transitions are of order $\sim eV$. Thus, the condition $r \gtrsim \dfrac{\hbar c}{E}$ implies $r \gtrsim 200 \dfrac{\text{MeV fm}}{\text{eV}} = 2 \cdot 10^{-7} \, \text{m} = 2 \cdot 10^5 \, \text{pm}$. The electronic wavefunctions for Hydrogen are nearly zero if evaluated in $r \gtrsim 2 \cdot 10^5$ pm, as the Hydrogen size is roughly 25 pm [40]. The contribution of the $M2$ multipole results therefore negligible.

The same story is followed for any multipole with the exception of $E1$ (electric dipole), which is the only one that contains the spherical Bessel function $j_0(kr)$. This spherical Bessel function has its maximum value at $kr = 0$ and it gives not negligible values for the whole interval $0 \leq r \leq 2 \cdot 10^5$ pm, which is the region where the electronic wavefunctions of the hydrogen atom are not vanishing. Thus, by following this reasoning, we understand that the dynamics of atomic transitions in Hydrogen, as well as in any low-charged ion, is totally dominated by the electric dipole $E1$, apart from cases

where parity or angular momentum conservation rules forbid it. Apart from these latter cases, where either multi-photon transitions or the next multipole ($M1$) single-photon transition will be important, the $E1$ multipole gives the leading contribution and it is therefore common to stop the multipole expansion (2.57) at this term. This approximation is commonly referred to as *electric dipole approximation*.

As the atomic number increases, the transition energy in hydrogenlike ions increases as well, since it approximately scales as Z^2. At some point, the product kr will be of order ~ 1 even for small values of r, where the electronic wavefunction is not vanishing. For such ions, high multipoles will play a sizeable role in atomic transitions. We will see in detail such effects in Chapter 5.

Now, we analyze more in detail the electric dipole approximation. By including only the leading term ($E1$) in the summation of Eq. (2.57), we get

$$\underline{\epsilon}_C^\lambda \, e^{i\boldsymbol{kr}} \quad \approx \quad \sqrt{2\pi} \sum_{M=-1}^{+1} i\left(\sqrt{3}\right) i\lambda \, \boldsymbol{A}_{1M}^{(e)}(k,\boldsymbol{r}) \, D_{M\lambda}^1(\varphi_k,\theta_k,0) \quad . \tag{2.58}$$

For simplicity, we suppose the photon's direction to be $\hat{z}$. Consequently, $D_{M\lambda}^1(\varphi_k,\theta_k,0) \to D_{M\lambda}^1(0,0,0)=\delta_{M\lambda}$ and we are left with

$$\underline{\epsilon}_C^\lambda \, e^{i\boldsymbol{kr}} \quad = \quad -\sqrt{6\pi}\,\lambda\,\boldsymbol{A}_{1\lambda}^{(e)}(k,\boldsymbol{r}) \quad . \tag{2.59}$$

On analyzing $\boldsymbol{A}_{1\lambda}^{(e)}(k,\boldsymbol{r})$ we find

$$
\begin{aligned}
\boldsymbol{A}_{1\lambda}^{(e)}(k,\boldsymbol{r}) \quad = \quad & j_0(kr)\sqrt{\frac{2}{3}}\left(\sum_{m=-1}^{+1}\langle 0,\lambda-m,1,m|1,\lambda\rangle\, Y_0^{\lambda-m}(\underline{r})\,\boldsymbol{\xi}_m\right) \\
& -j_2(kr)\sqrt{\frac{1}{3}}\left(\sum_{m=-1}^{+1}\langle 2,\lambda-m,1,m|1,\lambda\rangle\, Y_2^{\lambda-m}(\underline{r})\boldsymbol{\xi}_m\right) \\
= \quad & j_0(kr)\sqrt{\frac{2}{3}}\left(\sum_{m=-1}^{+1}\delta_{m,\lambda}\, Y_0^{\lambda-m}(\underline{r})\,\boldsymbol{\xi}_m\right) - j_2(kr)\boldsymbol{X}_\lambda \quad ,
\end{aligned}
$$

where we have defined $\boldsymbol{X}_\lambda = \sqrt{\dfrac{1}{3}}\left(\displaystyle\sum_{m=-1}^{+1}\langle 2,\lambda-m,1,m|1,\lambda\rangle\, Y_2^{\lambda-m}(\underline{r})\boldsymbol{\xi}_m\right)$.

Proceeding with the calculation we get

$$
\begin{aligned}
\boldsymbol{A}_{1\lambda}^{(e)}(\boldsymbol{k},\boldsymbol{r}) \quad = \quad & j_0(kr)\sqrt{\frac{2}{3}}\frac{1}{2}\frac{1}{\sqrt{\pi}}\,\boldsymbol{\xi}_\lambda - j_2(kr)\boldsymbol{X}_\lambda \\
= \quad & j_0(kr)\frac{1}{\sqrt{6\pi}}\,\boldsymbol{\xi}_\lambda - j_2(kr)\boldsymbol{X}_\lambda \quad .
\end{aligned}
$$

Coming back to Eq. (2.59), we can now write

$$\underline{\epsilon}_C^\lambda \, e^{i\boldsymbol{kr}} \quad \approx \quad -\lambda\left(j_0(kr)\,\boldsymbol{\xi}_\lambda - \sqrt{6\pi}j_2(kr)\boldsymbol{X}_\lambda\right) \quad . \tag{2.60}$$

Thus, the electric dipole approximation consists of, roughly speaking, approximating the complex exponential with the first two parity-even spherical Bessel functions.
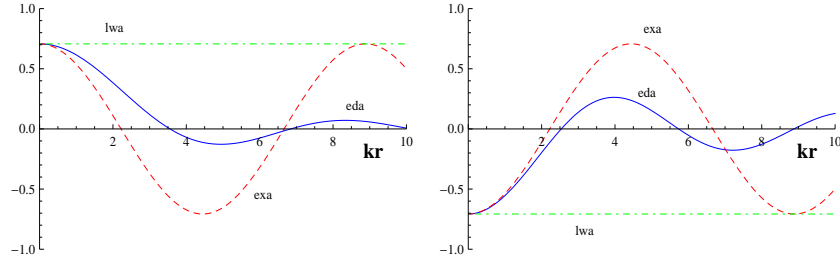
Figure 2.1: Real part of the $\hat{x}$-component (left-panel) and the imaginary part of the $\hat{y}$-component (right-panel) of the vector plane wave for a photon traveling along the $\underline{z}$-direction with negative helicity. The (electron) polar angle θ is fixed equal to $\pi/4$. The blue-solid and red-dashed curves respectively correspond to the exact value and the electric dipole approximation of the vector plane wave. The green-dot-dashed curve corresponds to the long-wavelength approximation of the vector plane wave (discussed in the text).

From Eq. (2.60), if we make further approximations, the expression simplifies considerably. In the low-Z regime, we already discussed that it is allowed to consider $kr \ll 1$. Within this limit, we have

$$
\begin{aligned}
j_0(kr) &\rightarrow 1 - \frac{1}{6}(kr)^2 \quad, \\
j_2(kr) &\rightarrow \frac{1}{15}(kr)^2 \quad.
\end{aligned}
$$

Equation (2.60) then becomes

$$
\underline{\epsilon}_C^\lambda \, e^{i\boldsymbol{kr}} \quad \approx \quad -\lambda \, \xi_\lambda + \lambda \, \frac{1}{6} \xi_\lambda (kr)^2 + \lambda \frac{\sqrt{6\pi}}{15}(kr)^2 \boldsymbol{X}_\lambda \quad. \tag{2.61}
$$

We can further simplify the above equation by neglecting the terms proportional to $(kr)^2$, which are, in the chosen approximation ($kr \ll 1$), of course much weaker than the others. By doing that, we end up with

$$
\underline{\epsilon}_C^\lambda \, e^{i\boldsymbol{kr}} \quad \approx \quad -\lambda \, \xi_\lambda = \underline{\epsilon}_C^\lambda \quad. \tag{2.62}
$$

At this point we realize that all the approximations we made up to here are equivalent to considering the first term of the Taylor expansion of the exponential

$$
\underline{\epsilon}_C^\lambda \, e^{i\boldsymbol{kr}} \quad = \quad \underline{\epsilon}_C^\lambda \left(1 \, + \, i\boldsymbol{k} \cdot \boldsymbol{r} \, + \, \frac{(i\boldsymbol{k} \cdot \boldsymbol{r})^2}{2!} + ... \right) \quad.
$$

The approximation of considering the first term of the Taylor expansion for the vector plane wave, i.e. the approximation of considering the rhs in replacement of the lhs in Eq. (2.62), will be here and henceforth called "long-wavelength approximation"[11].

---

[11]In the literature there is a little confusion about the notation concerning this issue. Sometimes, what we call here *long-wavelength* approximation is called by other authors *non-relativistic electric dipole* approximation, or, some other times, simply *electric dipole* approximation, so that the notation may become confusing.

By now it must be clear that the electric dipole approximation, as evident from Eq.
(2.60) and (2.61), is a less stringent approximation than the long-wavelength approx-
imation. In other words, the goodness of the electric dipole approximation is higher
than the one of considering the first term of the Taylor expansion for the exponential.
Qualitatively, we may say that the electric dipole approximation must comprehend
more terms than the first one of the Taylor expansion, as it is already evident from
Eq. (2.61), where part of the second term of the Taylor expansion shows explicitly up
in the approximation $kr \ll 1$.

Anyway, since the terms in the Taylor expansion do not have defined angular momen-
tum properties (though they have defined parity) while $E1$ multipole has, we cannot
pin down which terms of the expansion the full electric dipole approximation includes.
In fact, Taylor and multipole expansions have different analytical properties, so that
it is not possible to compare them term by term. The sum of the all terms in the two
expansions leads anyway of course to the same result.

For underlining and evaluating the goodness of the various approximations that we
have considered in the present analysis, in Fig. 2.1 we show i) the real part of the
$\hat{x}$-component (left panel) and ii) the imaginary part of the $\hat{y}$-component (right panel)
of the total vector planewave $\underline{\epsilon}_C^\lambda \, e^{i\boldsymbol{kr}}$, for the case $\lambda = -1$ and $\theta = \dfrac{\pi}{4}$, where θ is the
angle defined in $\boldsymbol{r} = r(\sin\theta\cos\varphi, \sin\theta\sin\varphi, \cos\theta)$. Since the photon' direction is as-
sumed to be $\hat{z}$, any dependence on the angle φ vanishes. The curves which correspond
to the exact term (the lhs of Eq. (2.60)), the electric dipole approximation (the rhs of
Eq. (2.60)) and the long-wavelength approximation (the rhs of Eq. (2.62)) are showed.
The labels "exa", "eda" and "lwa" naturally refer respectively to "exact", "electric
dipole approximation" and "long-wavelength approximation".

Looking at the figure, we can now better estimate the goodness of eda and lwa in ap-
proximating exa. As also remarked above, we clearly notice that eda resembles more
efficiently the exact curve than lwa, or, in other words, that eda is a better approxi-
mation with respect to lwa. In particular, while lwa loses validity already for $kr \gtrsim 0.3$
or 0.4, eda keeps being a good approximation roughly for $0 \lesssim kr \lesssim 1$.

As kr increases, the goodness of both lwa and eda decreases till the point that, for
large values of kr, both approximations become completely misleading. Particularly,
the sign and the concavity of the curves corresponding to the exact vector planewave
and eda (or lwa) are different. For transitions in highly-charged ions, we can infer that
the inclusion of high order multipoles can therefore change qualitatively the dynamics
of the transition, as recently showed [41].

CHAPTER 3

SINGLE- AND TWO-PHOTON DECAYS IN ATOMS AND IONS

*The state of mind which enables a man to do work of this kind
is akin to that of the religious worshiper or the lover;
the daily effort comes from no deliberate intention
or program, but straight from the heart.*

Albert Einstein, 1918

Few problems in Quantum Mechanics can be solved exactly. Because of this, approximation methods are a strong core of quantum mechanics.

When I was a student at the university, the lecture on quantum perturbation theory has been a magical surprise. I learnt how many quantum mechanical problems without exact solutions could be approximately solved up to the wished accuracy. Since we are physicists and not mathematicians, for me this actually equaled to solving the problems.

3.1 TIME-DEPENDENT PERTURBATION THEORY

Although physicists are usually more familiar with the Schrödinger representation of quantum mechanics, the perturbative approach is usually introduced in the *Interaction representation* (or *Interaction picture*) of quantum mechanics. We recall here the basic equations which link the two representations.

Any state α at the time t is denoted in the Schrödinger representation by the ket vector $|\alpha, t\rangle_S$, where the variable t explicitly denotes the time dependence of the state. The words "ket", "ket vector" and "ket state" will be hereafter used interchangeably.

The evolution of this ket vector is ruled by the evolution operator:

$$|\alpha, t\rangle_S = \hat{U}(t_0, t) |\alpha, t_0\rangle_S \quad . \tag{3.1}$$

The evolution operator satisfies the operator equation

$$i\hbar\frac{\partial}{\partial t}\hat{U}(t_0, t) = \hat{H}(t)\hat{U}(t_0, t) \quad , \tag{3.2}$$

where $\hat{H}(t)$ is the Hamiltonian operator, which generally may depend on time. The
operator $\hat{U}(t_0, t)$ will therefore depend on $\hat{H}(t)$.
Let us suppose that the time dependent part of the Hamiltonian is represented by a
term $\lambda\hat{V}(t)$, where λ is a dimensionless constant that represents the strength of the
potential $\hat{V}(t)$. Hence, we suppose the Hamiltonian to have the form

$$\hat{H}(t) = \hat{H}_0 + \lambda\hat{V}(t) \quad . \tag{3.3}$$

We moreover suppose to known the eigenstates of the unperturbed Hamiltonian $\hat{H}_0$,
i.e. we know the ket vectors $\{|n^0\rangle_S\}$ which are solutions of the equation

$$\hat{H}_0 |n^0\rangle_S = E_n |n^0\rangle_S$$

where E_n is a real number.
Suppose we start at the initial time t_0 with the eigenstate $|i^0\rangle_S$ of the unperturbed
Hamiltonian. We then have

$$|\alpha, t_0\rangle_S = |i^0\rangle_S \quad .$$

What we would like to know is the probability of measuring, at the time t, the eigenstate
of the unperturbed Hamiltonian $|f^0\rangle_S$. In quantum mechanics this quantity is equal
to

$$\begin{aligned}
\mathcal{P} &= \left| {}_S\langle f^0| \hat{U}(t_0, t) |\alpha, t_0\rangle_S \right|^2 \\
&= \left| {}_S\langle f^0| \hat{U}(t_0, t) |i^0\rangle_S \right|^2 \quad .
\end{aligned}$$

The two ket states $|f^0\rangle_S$ and $|i^0\rangle_S$ are not necessarily different. In order to find such
a quantity, we will make use of the Interaction representation.

Let us define a new set of ket states and operators through the equations

$$\begin{aligned}
|\alpha, t\rangle_I &\equiv e^{\frac{i}{\hbar}\hat{H}_0 t} |\alpha, t\rangle_S \\
\hat{O}_I(t) &\equiv e^{\frac{i}{\hbar}\hat{H}_0 t}\hat{O}(t)e^{-\frac{i}{\hbar}\hat{H}_0 t} \quad ,
\end{aligned} \tag{3.4}$$

where $\hat{O}(t)$ is any operator (which may depend on time) in the Schrödinger represen-
tation.
The ket vector $|\alpha, t\rangle_I$ and the operator $\hat{O}_I(t)$ are called ket vector and operator in the
Interaction representation, respectively. We can easily $|\alpha, t\rangle_I$, which is related to to
$|i\rangle_S$:

$$|\alpha, t_0\rangle_I = e^{\frac{i}{\hbar}\hat{H}_0 t} |\alpha, t_0\rangle_S = e^{\frac{i}{\hbar}\hat{H}_0 t} |i\rangle_S = e^{\frac{i}{\hbar}E_i t} |i\rangle_S \quad .$$

Considering the form of the Hamiltonian in Eq. (3.2), let us follow the evolution of the ket state at the time t, in the Interaction representation:

$$
\begin{aligned}
i\hbar \frac{\partial}{\partial t} \left| \alpha, t \right\rangle_I &= i\hbar \left(\frac{\partial}{\partial t} e^{\frac{i}{\hbar}\hat{H}_0 t} \right) \left| \alpha, t \right\rangle_S + i\hbar e^{\frac{i}{\hbar}\hat{H}_0 t} \left(\frac{\partial}{\partial t} \left| \alpha, t \right\rangle_S \right) \\
&= -\hat{H}_0 e^{\frac{i}{\hbar}\hat{H}_0 t} \left| \alpha, t \right\rangle_S + i\hbar e^{\frac{i}{\hbar}\hat{H}_0 t} \left(-\frac{i}{\hbar} \hat{H}(t) \left| \alpha, t \right\rangle_S \right) \\
&= e^{\frac{i}{\hbar}\hat{H}_0 t} \left(-\hat{H}_0 + \hat{H}(t) \right) \left| \alpha, t \right\rangle_S = e^{\frac{i}{\hbar}\hat{H}_0 t} \lambda \hat{V}(t) \left| \alpha, t \right\rangle_S \\
&= \lambda\, e^{\frac{i}{\hbar}\hat{H}_0 t} \hat{V}(t) e^{-\frac{i}{\hbar}\hat{H}_0 t} e^{\frac{i}{\hbar}\hat{H}_0 t} \left| \alpha, t \right\rangle_S \\
&= \lambda \hat{V}_I(t) \left| \alpha, t \right\rangle_I \quad ,
\end{aligned}
\tag{3.5}
$$

where we made use of the Schrödinger equation for the ket $\left| \alpha, t \right\rangle_S$ and of the fact that $e^{\frac{i}{\hbar}\hat{H}_0 t}$ naturally commutes with $\hat{H}_0$.

By looking at Eq. (3.5), we can euristically say that the evolution equation for the ket states in the Interaction representation is equal to the evolution equation for the ket states in the Schrödinger representation with $\hat{H}(t)$ replaced with $\lambda \hat{V}_I(t)$.

We define also the evolution operator $\hat{U}_I(t_0, t)$ for the ket states in the Interaction representation:

$$
\left| \alpha, t \right\rangle_I = \hat{U}_I(t_0, t) \left| \alpha, t_0 \right\rangle_I \quad .
\tag{3.6}
$$

We see that this definition is compatible with Eq. (3.4), since

$$
\begin{aligned}
\left| \alpha, t \right\rangle_I &= e^{\frac{i}{\hbar}\hat{H}_0 t} \left| \alpha, t \right\rangle_S = e^{\frac{i}{\hbar}\hat{H}_0 t} \hat{U}(t_0, t) \left| \alpha, t_0 \right\rangle_S \\
&= \underbrace{e^{\frac{i}{\hbar}\hat{H}_0 t} \hat{U}(t_0, t) e^{-\frac{i}{\hbar}\hat{H}_0 t}}_{\hat{U}_I(t_0, t)} \left| \alpha, t_0 \right\rangle_I \\
&= \hat{U}_I(t_0, t) \left| \alpha, t_0 \right\rangle_I \quad .
\end{aligned}
$$

It follows also that

$$
\begin{aligned}
\left| {}_S\langle f^0 | \hat{U}_I(t_0, t) | i^0 \rangle_S \right| &= \left| {}_S\langle f^0 | e^{\frac{i}{\hbar}\hat{H}_0 t} \hat{U}(t_0, t) e^{-\frac{i}{\hbar}\hat{H}_0 t} | i^0 \rangle_S \right| \\
&= \left| {}_S\langle f^0 | e^{\frac{i}{\hbar}E_f t} \hat{U}(t_0, t) e^{-\frac{i}{\hbar}E_i t} | i^0 \rangle_S \right| \\
&= \left| {}_S\langle f^0 | \hat{U}(t_0, t) | i^0 \rangle_S \right| \quad .
\end{aligned}
$$

By using the above equation, we can write the remarkable equation

$$
\begin{aligned}
\mathcal{P} &= \left| {}_S\langle f^0 | \hat{U}(t_0, t) | i^0 \rangle_S \right|^2 \\
&= \left| {}_S\langle f^0 | \hat{U}_I(t_0, t) | i^0 \rangle_S \right|^2 \quad .
\end{aligned}
\tag{3.7}
$$

We must then find the expression for $\hat{U}_I(t_0, t)$.

By combining Eqs. (3.5) and (3.6), we get

$$
\begin{aligned}
i\hbar \frac{\partial}{\partial t} \left| \alpha, t \right\rangle_I &= i\hbar \frac{\partial}{\partial t} \hat{U}_I(t_0, t) \left| \alpha, t_0 \right\rangle_I \\
&= \lambda \hat{V}_I(t) \hat{U}_I(t_0, t) \left| \alpha, t_0 \right\rangle_I \quad .
\end{aligned}
$$

Since this equation must hold for any ket state $|\alpha, t_0\rangle_I$, $\hat{U}_I(t_0, t)$ must satisfy the
following operator equation

$$i\hbar\frac{\partial}{\partial t}\hat{U}_I(t_0, t) = \lambda\hat{V}_I(t)\hat{U}_I(t_0, t) \quad . \tag{3.8}$$

Hence, the equation for the evolution operator $\hat{U}_I(t_0, t)$ is, again, similar to Eq. (3.2)
with $\hat{H}(t)$ replaced with $\lambda\hat{V}_I(t)$.
We can surely impose the initial condition

$$\hat{U}_I(t_0, t_0) = \hat{\mathbb{1}} \quad ,$$

so that

$$|\alpha, t_0\rangle_I = \hat{U}_I(t_0, t_0)\,|\alpha, t_0\rangle_I = \hat{\mathbb{1}}\,|\alpha, t_0\rangle_I = |\alpha, t_0\rangle_I \quad ,$$

as it should be. With this, we can rewrite the differential equation (3.8) in the form
of an integral equation:

$$\hat{U}_I(t_0, t) = \hat{\mathbb{1}} + \left(-\frac{i}{\hbar}\lambda\right)\int_{t_0}^{t}dt_1\hat{V}_I(t_1)\hat{U}_I(t_0, t_1) \quad .$$

To solve the above equation we proceed iteratively

$$\begin{aligned}
\hat{U}_I(t_0, t) &= \hat{\mathbb{1}} + \left(-\frac{i}{\hbar}\lambda\right)\int_{t_0}^{t}dt_1\hat{V}_I(t_1)\left(\hat{\mathbb{1}} + \left(-\frac{i}{\hbar}\lambda\right)\int_{t_0}^{t_1}dt_2\hat{V}_I(t_2)\hat{U}_I(t_0, t_2)\right) \\
&= \hat{\mathbb{1}} + \left(-\frac{i}{\hbar}\lambda\right)\int_{t_0}^{t}dt_1\hat{V}_I(t_1) + \left(-\frac{i}{\hbar}\lambda\right)^2\int_{t_0}^{t}dt_1\int_{t_0}^{t_1}dt_2\hat{V}_I(t_1)\hat{V}_I(t_2) \\
&\quad + ... + \left(-\frac{i}{\hbar}\lambda\right)^n\int_{t_0}^{t}dt_1\int_{t_0}^{t_1}dt_2\,...\int_{t_0}^{t_{n-1}}dt_n\hat{V}_I(t_1)\hat{V}_I(t_2)\,...\,\hat{V}_I(t_n) \\
&\quad + ... \quad .
\end{aligned}$$

This series is known as the *Dyson series* and represents our final expression for the
operator $\hat{U}_I(t_0, t)$.
Plugging this expression for $\hat{U}_I(t_0, t)$ into Eq. (3.7), we can now write the probability
function as

$$\begin{aligned}
\mathcal{P} = \Big|\ &_S\langle f^0|i^0\rangle_S \\
&+ \left(-\frac{i}{\hbar}\lambda\right)\int_{t_0}^{t}dt_1\ {}_S\langle f^0|\,\hat{V}_I(t_1)\,|i^0\rangle_S \\
&+ \left(-\frac{i}{\hbar}\lambda\right)^2\int_{t_0}^{t}dt_1\int_{t_0}^{t_1}dt_2\ {}_S\langle f^0|\,\hat{V}_I(t_1)\hat{V}_I(t_2)\,|i^0\rangle_S \\
&+ ... \\
&+ \left(-\frac{i}{\hbar}\lambda\right)^n\int_{t_0}^{t}dt_1\int_{t_0}^{t_1}dt_2\,...\int_{t_0}^{t_{n-1}}dt_n\ {}_S\langle f^0|\,\hat{V}_I(t_1)\hat{V}_I(t_2)\,...\,\hat{V}_I(t_n)\,|i^0\rangle_S \\
&+ \ ... \ \Big|^2 \quad .
\end{aligned}$$

$$\tag{3.9}$$

In order to further simplify the above equation, we first notice that

$$
{}_S\langle n^0| \,\hat{V}_I(t_1)\,|m^0\rangle_S = {}_S\langle n^0|\, e^{\frac{i}{\hbar}\hat{H}_0 t_1}\hat{V}(t_1)e^{-\frac{i}{\hbar}\hat{H}_0 t_1}\,|m^0\rangle_S
$$

$$
= e^{\frac{i}{\hbar}(E_n - E_m)t_1}\, {}_S\langle n^0|\,\hat{V}(t_1)\,|m^0\rangle_S \qquad = e^{i\omega_{nm}\,t_1} V_{nm}(t_1) \quad,
$$

where we defined $\omega_{nm} = \dfrac{E_n - E_m}{\hbar}$ and $V_{nm}(t_1) = {}_S\langle n^0|\,\hat{V}(t_1)\,|m^0\rangle_S$.

By using the completeness of the unperturbed states, we finally rewrite Eq. (3.9) as

$$
\begin{aligned}
\mathcal{P} \;=\; & \Big| \; {}_S\langle f^0|i^0\rangle_S \\
& + \Big(-\frac{i}{\hbar}\lambda\Big)\int_{t_0}^{t}\mathrm{d}t_1\, e^{i\omega_{fi}\,t_1}V_{fi}(t_1) \\
& + \Big(-\frac{i}{\hbar}\lambda\Big)^2\int_{t_0}^{t}\mathrm{d}t_1\int_{t_0}^{t_1}\mathrm{d}t_2\sum_{\nu_1}e^{i\omega_{f\nu_1}\,t_1}e^{i\omega_{\nu_1 i}\,t_2}\,V_{f\nu_1}(t_1)V_{\nu_1 i}(t_2) \\
& + ... \\
& + \Big(-\frac{i}{\hbar}\lambda\Big)^N\int_{t_0}^{t}\mathrm{d}t_1\int_{t_0}^{t_1}\mathrm{d}t_2\,...\int_{t_0}^{t_{N-1}}\mathrm{d}t_N\sum_{\nu_1,\nu_2,...\nu_N} \\
& \qquad \times\Big(e^{i\omega_{f\nu_1}\,t_1}e^{i\omega_{\nu_1\nu_2}\,t_2}...\,e^{i\omega_{\nu_{N-1}\nu_N}\,t_N}\Big)\Big(V_{f\nu_1}(t_1)V_{\nu_1\nu_2}(t_2)...\,V_{\nu_N i}(t_N)\Big) \\
& + \;\; ... \;\; \Big|^2 \quad.
\end{aligned}
$$

$$(3.10)$$

In the above equation, the first term of the rhs corresponds to the zero-order approximation. If the initial and final states are different (as it is usually the case), this term is of course vanishing. By adding the second term, the first order approximation is achieved, and so on. It is easy to understand that, provided that $\lambda < 1$, the series will converge. We can then stop the series at term which corresponds to the wished accuracy.

In a case experiment, the measurement will be done at a large t in comparison with the time scale of the system. Therefore one generally measures the probability of transition for a large time t. What it is actually measured is the transition rate for a large time t, that is

$$
\Gamma = \lim_{t\to+\infty}\frac{\mathrm{d}\mathcal{P}}{\mathrm{d}t} \quad.
$$

$$(3.11)$$

This will be the quantity we will investigate. The first natural application of perturbation theory is for the decays of atoms and ions.

3.2 Single-photon decay rate

We start out by evaluating the single-photon decay rate, believing that, due to its simplicity, it may give deeper insights on the interaction between atoms and radiation. By single-photon decay, we mean that only one photon is emitted as consequence of the de-excitation of the ion or atom.

In Quantum Electrodynamics, the Hamiltonian which accounts for the electron-photon interaction is

$$
\hat{H}'(t) = c\,e\,\boldsymbol{\alpha}\cdot\hat{\boldsymbol{A}}(\boldsymbol{r},t) \quad,
$$

$$(3.12)$$

where $-e$ is the charge of the electron ($e > 0$), $\hat{\boldsymbol{A}}$ is the vector potential given by one single photon (the one showed in Eq. (2.51)) promoted to operator. $\hat{\mathrm{H}}'(t)$ is $\equiv -\lambda \hat{\mathrm{V}}(t)$ in the notation used in Eq. (3.3).

We can therefore rewrite the above equation as

$$
\begin{aligned}
\hat{\mathrm{H}}'(t) &= \boldsymbol{\alpha} \cdot \sqrt{\frac{2\pi\hbar^2 c^3 \alpha}{\omega V}} \left(\underline{\epsilon} e^{i(\boldsymbol{k}\hat{\boldsymbol{r}} - \omega t)} + \underline{\epsilon}^* e^{-i(\boldsymbol{k}\hat{\boldsymbol{r}} - \omega t)} \right) \\
&\equiv \bar{\lambda} \boldsymbol{\alpha} \cdot \left(\underline{\epsilon} e^{i(\boldsymbol{k}\hat{\boldsymbol{r}} - \omega t)} + \underline{\epsilon}^* e^{-i(\boldsymbol{k}\hat{\boldsymbol{r}} - \omega t)} \right) \quad ,
\end{aligned}
\tag{3.13}
$$

where $\bar{\lambda} = \sqrt{\dfrac{2\pi\hbar^2 c^3 \alpha}{\omega V}}$.

As explicitly displayed, only $\hat{\boldsymbol{r}}$ is operator in the definition of $\hat{\boldsymbol{A}}$, since $\boldsymbol{k}$, ω and $\underline{\epsilon}$ are inherent characteristics of the photon which carries the vector potential.

If we have more than one electron which undergo the interaction, the interaction Hamiltonian is naturally given by the sum of the one-particle interaction Hamiltonians:

$$
\hat{\mathrm{H}}'(t) = c\,e\,\boldsymbol{\alpha} \cdot \hat{\mathbf{A}}(\boldsymbol{r}_1, t) + c\,e\,\boldsymbol{\alpha} \cdot \hat{\mathbf{A}}(\boldsymbol{r}_2, t) + \dots \quad ,
\tag{3.14}
$$

since any single electron feels the radiation. This is the same prescription that it is most usually applied to write the total Coulombic scalar potential for many-particle systems: $\hat{\mathrm{H}}_C = \dfrac{Z\alpha\hbar c}{r_1} + \dfrac{Z\alpha\hbar c}{r_2} + \dots$.

We can safely apply perturbation theory with the Hamiltonian in Eq. (3.13) thanks to the presence of the electromagnetic coupling constant α, which is far smaller than 1: $\alpha = \dfrac{e^2}{4\pi\epsilon_0 \hbar c} \approx \dfrac{1}{137}$. We can assign the role that λ has in Eq. (3.3) to $\bar{\lambda}$, even though the latter is not dimensionless. Trivially, it does not really matter.

We look for processes where the initial state is different from the final state and where only one photon is involved. Looking at our master equation (3.10), we understand that the first term (which corresponds to the zero-approximation) is vanishing and that the second term (which corresponds to the first order approximation) is the term we are looking for, since it is the only one that involves one photon[1].

The probability function $\mathcal{P}$ is then given by

$$
\begin{aligned}
\mathcal{P} &= \left| \left(-\frac{i}{\hbar} \bar{\lambda} \right) \int_{t_0}^{t} dt_1 e^{i\omega_{fi}t_1} \langle f | \boldsymbol{\alpha} \cdot \left(\underline{\epsilon} e^{i(\boldsymbol{k}\hat{\boldsymbol{r}} - \omega t_1)} + \underline{\epsilon}^* e^{-i(\boldsymbol{k}\hat{\boldsymbol{r}} - \omega t_1)} \right) | i \rangle \right|^2 \\
&= \left| \left(\frac{\bar{\lambda}}{\hbar} \right) \left(\langle f | \boldsymbol{\alpha} \cdot \underline{\epsilon} e^{i\boldsymbol{k}\hat{\boldsymbol{r}}} | i \rangle \int_{t_0}^{t} dt_1 e^{it_1(\omega_{fi} - \omega)} \right. \right. \\
&\qquad \left. \left. + \langle f | \boldsymbol{\alpha} \cdot \underline{\epsilon}^* e^{-i\boldsymbol{k}\hat{\boldsymbol{r}}} | i \rangle \int_{t_0}^{t} dt_1 e^{it_1(\omega_{fi} + \omega)} \right) \right|^2 \quad ,
\end{aligned}
$$

where, in comparison with the notation used in Eq. (3.10), we dropped for simplicity the subscript $_S$ and the superscript ^{0}, since we leave understood that the initial and final states we speak about hereinafter are eigenstates of the unperturbed Hamiltonian, in the Schrödinger representation.

---

[1] Each vector potential which appears in Eq. (3.10) is brought by one photon. Therefore each vector potential corresponds to one photon.

Since, further on, we will take $t \to \infty$ (in order to follow the prescription (3.11)), we see that the first term in the rhs will be evidently proportional to $\sim \delta(\omega_{fi} - \omega)$, while the second term will be proportional to $\sim \delta(\omega_{fi} + \omega)$. The first term then must correspond to the photon absorption as the energy of the final atomic state is higher than the energy of the initial atomic state. The delta function will in fact impose $0 = \omega_{fi} - \omega = \frac{1}{\hbar}(E_f - E_i - E_\gamma)$, where we denoted with E_γ the photon energy. Analogously, the second term must correspond to the photon emission as the energy of the final atomic state is lower than the energy of the initial atomic state. Since we want to consider the single photon emission process, the energy of the final atomic state will be always lower than the one of the initial atomic state. This entails that the first term will be thus vanishing. From now on, we will therefore consider exclusively the second term. We will look for the probability function

$$
\begin{aligned}
\mathcal{P} &= \left| \left(\frac{\bar{\lambda}}{\hbar} \right) \langle f | \, \boldsymbol{\alpha} \cdot \underline{\epsilon}^* e^{-i\boldsymbol{k}\hat{\boldsymbol{r}}} \, | i \rangle \int_{t_0}^t dt_1 e^{it_1(\omega_{fi}+\omega)} \right|^2 \\
&\equiv \left(\frac{\bar{\lambda}}{\hbar} \right)^2 |\mathcal{M}^\gamma(i \to f)|^2 \left| \int_{t_0}^t dt_1 e^{it_1(\omega_{fi}+\omega)} \right|^2 \quad,
\end{aligned}
\tag{3.15}
$$

where we defined $\mathcal{M}^\gamma(i \to f) = \langle f | \, \boldsymbol{\alpha} \cdot \underline{\epsilon}^* e^{-i\boldsymbol{k}\hat{\boldsymbol{r}}} \, | i \rangle$, which is generally referred to as the matrix element for the single-photon transition between the initial state i and the final state f.

Let us evaluate the last factor of the rhs of Eq. (3.15). By choosing $t_0 = 0$ as the time we prepare the initial state $|i\rangle$, we get

$$
\begin{aligned}
\left| \int_{t_0}^t dt_1 e^{it_1(\omega_{fi}+\omega)} \right|^2 &= \left| \frac{e^{it(\omega_{fi}+\omega)} - 1}{i(\omega_{fi}+\omega)} \right|^2 = \left| \frac{i}{\omega_{fi}+\omega} \left(1 - e^{it(\omega_{fi}+\omega)} \right) \right|^2 \\
&= \left(\frac{1}{\omega_{fi}+\omega} \right)^2 \left| e^{\frac{i}{2}t(\omega_{fi}+\omega)} \left(e^{-\frac{i}{2}t(\omega_{fi}+\omega)} - e^{\frac{i}{2}t(\omega_{fi}+\omega)} \right) \right|^2 \\
&= \left(\frac{1}{\omega_{fi}+\omega} \right)^2 \left| -2i \sin\left[\frac{t(\omega_{fi}+\omega)}{2} \right] \right|^2 = 4 \frac{\sin^2\left[\frac{t(\omega_{fi}+\omega)}{2} \right]}{(\omega_{fi}+\omega)^2} \quad.
\end{aligned}
$$

On introducing the above element into Eq. (3.15), we get

$$
\mathcal{P} = 4 \left(\frac{\bar{\lambda}}{\hbar} \right)^2 |\mathcal{M}^\gamma(i \to f)|^2 \frac{\sin^2\left[\frac{t(\omega_{fi}+\omega)}{2} \right]}{(\omega_{fi}+\omega)^2} \quad.
$$

Now, we follow the prescription of Eq. (3.11), to get the transition rate:

$$
\begin{aligned}
\frac{d\mathcal{P}}{dt} &= 4 \left(\frac{\bar{\lambda}}{\hbar} \right)^2 |\mathcal{M}^\gamma(i \to f)|^2 \frac{2 \sin\left[\frac{t(\omega_{fi}+\omega)}{2} \right] \cos\left[\frac{t(\omega_{fi}+\omega)}{2} \right] \left(\frac{\omega_{fi}+\omega}{2} \right)}{(\omega_{fi}+\omega)^2} \\
&= 2 \left(\frac{\bar{\lambda}}{\hbar} \right)^2 |\mathcal{M}^\gamma(i \to f)|^2 \frac{\sin\left[t(\omega_{fi}+\omega) \right]}{\omega_{fi}+\omega} \quad.
\end{aligned}
$$

By making use of the identity

$$
\lim_{t \to +\infty} \frac{\sin\left[a\, t \right]}{a} = \pi\, \delta(a) \quad,
$$

we finally get

$$
\begin{aligned}
\Gamma &= \lim_{t \to +\infty} \frac{\mathrm{d}\mathcal{P}}{\mathrm{d}t} = 2\pi \left(\frac{\bar{\lambda}}{\hbar}\right)^2 |\mathcal{M}^\gamma(i \to f)|^2 \, \delta(\omega_{fi} + \omega) \\
&= 2\pi \frac{\bar{\lambda}^2}{\hbar} |\mathcal{M}^\gamma(i \to f)|^2 \, \delta(E_f - E_i + E_\gamma) \quad,
\end{aligned}
\tag{3.16}
$$

where we used, in the last step, the identity $\delta\left(\dfrac{E_f - E_i + E_\gamma}{\hbar}\right) = |\hbar|\delta(E_f - E_i + E_\gamma)$.
We must still do something for obtaining the final decay rate: We must sum over all the final states. Now, one could argue: "We select both the initial and final atomic states, the photon momentum is well defined...there is nothing to sum over!". The reply to this arguing is that, while the atomic spectrum is discrete and we can successfully identify initial and final state, we cannot actually distinguish between an emitted photon with momentum $\boldsymbol{p}_\gamma$ and another one with momentum $\boldsymbol{p}_\gamma + \mathrm{d}^3 p_\gamma$. So, we must sum over all the photons between $\boldsymbol{p}_\gamma$ and $\boldsymbol{p}_\gamma + \mathrm{d}^3 p_\gamma$. Now, one can still argue: "Then, how many photons are there between $\boldsymbol{p}_\gamma$ and $\boldsymbol{p}_\gamma + \mathrm{d}^3 p_\gamma$?". To answer this question we make use of a prescription which is presumably due to Enrico Fermi since it is known under the name "Fermi's Golden Rule". The statement is the following. We know that a photon (as any particle) cannot have both linear momentum and position well defined. If $\triangle^3 x$ is its indefiniteness in the cartesian space and $\triangle^3 p_\gamma$ its indefiniteness in linear momentum, then they must satisfy the equation [42, 43]

$$
\triangle^3 x \, \triangle^3 p_\gamma = h^3 = (2\pi)^3 \, \hbar^3 \quad.
$$

We can think of having a spatial-momentum quantum space made of minimal cells of size h^3. Each one of those cells specifies the characteristics of the photon. Then it is easy to understand that the number of photons in the total element $V \, \mathrm{d}^3 p$ must be

$$
\begin{aligned}
N_\gamma &= \frac{V \, \mathrm{d}^3 p_\gamma}{h^3} = \frac{V \, \mathrm{d}^3 p_\gamma}{(2\pi)^3 \hbar^3} = \frac{V \, p_\gamma^2}{(2\pi)^3 \hbar^3} \, \mathrm{d}p_\gamma \, \mathrm{d}\Omega_{\boldsymbol{p}_\gamma} \\
&= \frac{V \, E_\gamma^2}{(2\pi)^3 c^3 \hbar^3} \, \mathrm{d}E_\gamma \, \mathrm{d}\Omega_{\boldsymbol{p}_\gamma} \quad.
\end{aligned}
\tag{3.17}
$$

The solid angle $\mathrm{d}\Omega_{\boldsymbol{p}_\gamma}$ is equal, of course, to the solid angle $\mathrm{d}\Omega_{\boldsymbol{k}}$, since $\boldsymbol{k}$ and $\boldsymbol{p}_\gamma$, like ω and E_γ, differ by a constant (see Eq. (2.43)):

$$
\boldsymbol{k} = \frac{\boldsymbol{p}_\gamma}{\hbar} \quad,
$$

$$
\omega = \frac{E_\gamma}{\hbar} \quad.
$$

From the foregoing discussion, it is easy to understand that we must multiply the transition probability (3.16), which is $\boldsymbol{p}_\gamma$ dependent, by the number of photons between $\boldsymbol{p}_\gamma$ and $\boldsymbol{p}_\gamma + \mathrm{d}^3 p_\gamma$, which is N_γ. By doing so, the decay rate naturally becomes differential:

$$
\begin{aligned}
\mathrm{d}\Gamma &= 2\pi \frac{\bar{\lambda}^2}{\hbar} N_\gamma \, |\mathcal{M}^\gamma(i \to f)|^2 \, \delta(E_f - E_i + E_\gamma) \\
&= 2\pi \frac{\bar{\lambda}^2}{\hbar} \frac{V \, E_\gamma^2}{(2\pi)^3 c^3 \hbar^3} \, |\mathcal{M}^\gamma(i \to f)|^2 \, \delta(E_f - E_i + E_\gamma) \, \mathrm{d}E_\gamma \, \mathrm{d}\Omega_{\boldsymbol{p}_\gamma} \quad.
\end{aligned}
$$

By using the definition of $\bar{\lambda}$, we get

$$
\mathrm{d}\Gamma = \frac{\alpha E_\gamma}{(2\pi)\hbar} |\mathcal{M}^\gamma(i \to f)|^2 \, \delta(E_f - E_i + E_\gamma) \, \mathrm{d}E_\gamma \, \mathrm{d}\Omega_{\boldsymbol{p}_\gamma} \quad .
$$

Integrating over the photon energy, the above equation finally leads to

$$
\frac{\mathrm{d}\Gamma^\lambda}{\mathrm{d}\Omega_{\boldsymbol{p}_\gamma}} = \frac{\alpha(E_i - E_f)}{(2\pi)\hbar} |\mathcal{M}^\gamma(i \to f)|^2_{E_\gamma = E_i - E_f} \quad , \tag{3.18}
$$

with

$$
\mathcal{M}^\gamma(i \to f) = \langle f| \, \boldsymbol{\alpha} \cdot \underline{\epsilon}^* \, e^{-i\boldsymbol{k}\hat{\boldsymbol{r}}} \, |i\rangle \quad , \tag{3.19}
$$

and where the notation $\big|_{E_\gamma = E_i - E_f}$ means that the expression standing before must be calculated with $E_\gamma = E_i - E_f$. We have furthermore added the label λ to the decay rate to make explicit the fact that it depends on the polarization of the emitted photon. λ is here intended to denote the photon helicity.

We may see that the result we found for $\mathrm{d}\Gamma$ has the correct dimensions (sec^{-1}), since the element $\mathcal{M}^\gamma(i \to f)$ is dimensionless. This also means that we can calculate the matrix element $\mathcal{M}^\gamma(i \to f)$ in the unit system we find more comfortable and then plug the result into the above formula for finding the correct decay rate.

3.3 EVALUATION OF THE FIRST-ORDER MATRIX ELEMENT

3.3.1 GENERAL EXPRESSION

If we want to study the polarization and angular properties of the emitted photon with respect to a fixed axis (which could be, for instance, the polarization axis of the atom), we will need to write the vector plane wave for a photon which propagates in an arbitrary direction. This can be safely done by using the multipole decomposition showed in Eq. (2.57):

$$
\begin{aligned}
\mathcal{M}^\gamma(i \to f) = \ & \sqrt{2\pi} \sum_{L=1}^{+\infty} \sum_{M=-L}^{L} \sum_{p=0,1} i^{-L-p}(2L+1)^{1/2}(\lambda)^p \\
& \times D_{M\lambda}^{L\,*}(\varphi_k, \theta_k, 0) \langle f| \, \boldsymbol{\alpha} \cdot \boldsymbol{a}_{LM}^{p\,*}(k, \hat{\boldsymbol{r}}) \, |i\rangle \quad .
\end{aligned} \tag{3.20}
$$

The atomic states $|f\rangle$ and $|i\rangle$ will have, in general, defined angular momentum properties. We can hence write them respectively as $|\beta_f, J_f, m_{J_f}\rangle$ and $|\beta_i, J_i, m_{J_i}\rangle$, where β is a collective label to denote all the quantum numbers needed to specify the atomic states but for J and m_J. As we underlined in Eq. (2.54), the operator $\boldsymbol{\alpha} \cdot \boldsymbol{a}_{LM}^p(\boldsymbol{k}, \hat{\boldsymbol{r}})$ is an irriducible tensor operator of rank L, while the operator $\boldsymbol{\alpha} \cdot \boldsymbol{a}_{LM}^{p\,*}(\boldsymbol{k}, \hat{\boldsymbol{r}})$ is not. In order to apply the Wigner-Eckart theorem on the matrix element, we must therefore make the transformation $\boldsymbol{a}_{LM}^{p\,*} = (-1)^{M+p+1} \boldsymbol{a}_{L-M}^p$ (see App. B). We obtain

$$
\begin{aligned}
\mathcal{M}^\gamma(i \to f) = \ & \sqrt{2\pi} \sum_{L=1}^{+\infty} \sum_{M=-L}^{L} \sum_{p=0,1} i^{-L-p}(2L+1)^{1/2}(\lambda)^p D_{M\lambda}^{L\,*}(\varphi_k, \theta_k, 0) \\
& \times (-1)^{M+p+1} \frac{\langle J_i, m_{J_i}, L, -M | J_f, m_{J_f}\rangle}{\sqrt{2J_i+1}} \langle \beta_f, J_f \| \boldsymbol{\alpha} \cdot \boldsymbol{a}_L^p(k, \hat{\boldsymbol{r}}) \| \beta_i, J_i \rangle \quad ,
\end{aligned} \tag{3.21}
$$

where $\langle \beta_1, J_1 \| \boldsymbol{\alpha} \cdot \boldsymbol{a}_L^p(k, \hat{\boldsymbol{r}}) \| \beta_2, J_2 \rangle$ is a scalar that does not depend upon geometrical
properties of the system (it does not depend upon the angular momenta projections
m_{J_1}, m_{J_2} and M).

In writing the above equation, it has been used the fact that Clebsch-Gordan coefficients are real.

3.3.2 Integrating over the photon direction

Equation (3.20) simplifies considerably if we integrate over the photon direction, i.e.
if we look for the decay rate irrespectively of the photon direction.
We define $V_M^L(k)$ as

$$V_M^L(k) = \sqrt{2\pi} \sum_p (-i)^{L+p} \sqrt{2L+1} (\lambda)^p \langle f | \boldsymbol{\alpha} \cdot \boldsymbol{a}_{LM}^{p\,*}(k, \hat{\boldsymbol{r}}) | i \rangle \quad ,$$

so that we can rewrite the matrix element $\mathcal{M}^\gamma(i \to f)$ as

$$\mathcal{M}^\gamma(i \to f) = \sum_L \sum_M V_M^L(k) D_{M\lambda}^{L\,*}(\varphi_k, \theta_k, 0) \quad .$$

Here, we notice that only the Wigner matrix depends on the spherical angles of the
photon direction, while V_M^L depends only on the magnitude of the vector $\boldsymbol{k}$. Thus,
from Eq. (3.18), using the equivalence $\mathrm{d}\Omega_{\boldsymbol{p}_\gamma} = \mathrm{d}\Omega_{\boldsymbol{k}}$ (as discussed in Eq. (3.17)), we
can write

$$
\begin{aligned}
\Gamma^\lambda &= \frac{\alpha(E_i - E_f)}{(2\pi)\hbar} \sum_{LM} \sum_{L'M'} V_M^L(k) V_{M'}^{L'\,*}(k) \\
&\quad \times \left(\int \mathrm{d}\Omega_{\boldsymbol{k}} D_{M\lambda}^{L\,*}(\varphi_k, \theta_k, 0) D_{M'\lambda}^{L'}(\varphi_k, \theta_k, 0) \right) \\
&= \frac{\alpha(E_i - E_f)}{(2\pi)\hbar} \sum_{LM} \sum_{L'M'} V_M^L(k) V_{M'}^{L'\,*}(k) \frac{4\pi}{2L+1} \delta_{LL'} \delta_{MM'} \\
&= \frac{\alpha(E_i - E_f)}{(2\pi)\hbar} \sum_{LM} \frac{4\pi}{2L+1} \left| V_M^L(k) \right|^2 \quad .
\end{aligned}
$$

We can eventually write

$$\Gamma^\lambda = \frac{\alpha(E_i - E_f)}{(2\pi)\hbar} \sum_{LM} \left| \tilde{\mathcal{M}}^\gamma(i \to f) \right|^2 \quad , \tag{3.22}$$

where we defined[2]

$$\tilde{\mathcal{M}}^\gamma(i \to f) = (2\pi)\sqrt{2} \sum_{p=0,1} (-i)^p (\lambda)^p \langle f | \boldsymbol{\alpha} \cdot \boldsymbol{a}_{LM}^{p\,*}(k, \hat{\boldsymbol{r}}) | i \rangle \quad .$$

As done for Eq. (3.21), in case we have atomic or ionic states, we can always make the
transformation $\boldsymbol{a}_{LM}^{p\,*} = (-1)^{M+p+1} \boldsymbol{a}_{L-M}^p$ (see App. B) and apply the Wigner-Eckart
theorem to obtain

$$
\begin{aligned}
\tilde{\mathcal{M}}^\gamma(i \to f) &= (2\pi)\sqrt{2} \sum_{p=0,1} (-i)^p (\lambda)^p (-1)^{M+p+1} \frac{\langle J_i, m_{J_i}, L, -M | J_f, m_{J_f} \rangle}{\sqrt{2J_i+1}} \\
&\quad \times \langle \beta_f, J_f \| \boldsymbol{\alpha} \cdot \boldsymbol{a}_L^p(k, \hat{\boldsymbol{r}}) \| \beta_i, J_i \rangle \quad .
\end{aligned}
$$

---

[2]The element $(-i)^L$ drops off because of the modulus squared.

3.3.3 INTEGRATING OVER THE PHOTON DIRECTION AND SUMMING OVER PHOTON POLARIZATIONS: THE TOTAL DECAY RATE

We may be interested in summing the decay rate over the photon polarizations to obtain the total decay rate. In other words, we look for single-photon emission irrespectively of both the direction and the polarization of the emitted photon.
We obtain the total decay rate from Eq. (3.22) as

$$\Gamma \;=\; \frac{\alpha(E_i - E_f)}{(2\pi)\hbar} \sum_{L\,M} \sum_{\lambda=\pm1} \left| \tilde{\mathcal{M}}^{\gamma}(i \to f) \right|^2 \quad. \tag{3.23}$$

We may explicitly write

$$\sum_{\lambda=\pm1} \left| \tilde{\mathcal{M}}^{\gamma}(i \to f) \right|^2 \;=\; 2(2\pi)^2 \sum_{p,p'=0,1} (-i)^{p-p'} \sum_{\lambda=\pm1} (\lambda)^{p+p'}$$
$$\times \left(\langle f | \,\boldsymbol{\alpha} \cdot \boldsymbol{a}_{LM}^{p\,*}(k,\hat{\boldsymbol{r}}) \,|i\rangle \right) \left(\langle f | \,\boldsymbol{\alpha} \cdot \boldsymbol{a}_{LM}^{p'\,*}(k,\hat{\boldsymbol{r}}) \,|i\rangle \right)^*$$

Now, by considering that p and p' are either 0 or 1, it follows that

$$\sum_{\lambda=\pm1} (\lambda)^{p+p'} = (-1)^{p+p'} + (+1)^{p+p'} = \left(2\delta_{p,p'} - 1\right) + 1$$
$$= 2\delta_{p,p'} \quad. \tag{3.24}$$

Then, we have

$$\sum_{\lambda=\pm1} \left| \tilde{\mathcal{M}}^{\gamma}(i \to f) \right|^2 \;=\; 4(2\pi)^2 \sum_{p,p'=0,1} (-i)^{p-p'} \delta_{p,p'}$$
$$\times \left(\langle f | \,\boldsymbol{\alpha} \cdot \boldsymbol{a}_{LM}^{p\,*}(k,\hat{\boldsymbol{r}}) \,|i\rangle \right) \left(\langle f | \,\boldsymbol{\alpha} \cdot \boldsymbol{a}_{LM}^{p'\,*}(k,\hat{\boldsymbol{r}}) \,|i\rangle \right)^*$$
$$=\; \sum_{p} \left| \tilde{\tilde{\mathcal{M}}}^{\gamma}(i \to f) \right|^2 \quad,$$

where

$$\tilde{\tilde{\mathcal{M}}}^{\gamma}(i \to f) = 4\pi \, \langle f | \,\boldsymbol{\alpha} \cdot \boldsymbol{a}_{LM}^{p\,*}(k,\hat{\boldsymbol{r}}) \,|i\rangle \quad.$$

Furthermore, from Eq. (3.23) we have

$$\Gamma \;=\; \frac{\alpha(E_i - E_f)}{(2\pi)\hbar} \sum_{L\,M} \sum_{p=0,1} \left| \tilde{\tilde{\mathcal{M}}}^{\gamma}(i \to f) \right|^2 \quad.$$

3.3.4 NON-RELATIVISTIC AND LONG WAVELENGTH APPROXIMATIONS

Normal approach

The non-relativistic interaction Hamiltonian is

$$\hat{H}'_{NR} = -e\,\frac{\hat{\mathbf{P}}}{m} \cdot \hat{\mathbf{A}}(\boldsymbol{r},t) + e^2 \hat{\mathbf{A}}^2(\boldsymbol{r},t) \quad. \tag{3.25}$$

Then, by looking at Eq. (3.12), we easily understand that, in order to get the non-relativistic matrix amplitude, we must replace $c\boldsymbol{\alpha} \to -\hat{\boldsymbol{p}}/m + e\hat{\mathbf{A}}^2$.

Fortunately, the second term in Eq. (3.25) is evidently proportional to α^2 and is therefore (normally) much smaller than the first term, which is proportional to α. Thus, we may here neglect it and simply make the replacement $c\boldsymbol{\alpha} \rightarrow -\hat{\boldsymbol{p}}/m$. We must however bring into notice that this approximation cannot be made in the two-photon decay, since, trivially, the second order expansion term due to $e\,\dfrac{\hat{\mathbf{p}}}{m}\!\cdot\!\hat{\mathbf{A}}(\boldsymbol{r},t)$ turns out to be of the same order in α as the first order expansion term due to $e^2\,\hat{\mathbf{A}}^2(\boldsymbol{r},t)$. In addition and in fact, we may also notice that $e^2\,\hat{\mathbf{A}}^2(\boldsymbol{r},t)$ contains two vector plane waves, so that it is directly related to two-photon emission.

From the foregoing discussion, it follows that the non-relativistic matrix element for one photon decay will be obtained by coming back to Eq. (3.19) and by making the replacement $c\boldsymbol{\alpha} \rightarrow -\hat{\boldsymbol{p}}/m$:

$$\mathcal{M}^{\gamma}_{NR}(i \rightarrow f) \;\; = \;\; -\frac{\langle f|\,\hat{\boldsymbol{p}}\cdot\underline{\epsilon}^{*}\,e^{-i\boldsymbol{k}\hat{\boldsymbol{r}}}\,|i\rangle}{m\,c} \;\; . \tag{3.26}$$

One may think that, at this point, we have some problems related to the not commutativity of $\hat{\mathbf{p}}$ and $\hat{\mathbf{r}}$, so that we may find it troublesome deciding to define the non-relativistic interaction Hamiltonian as $\propto \hat{\boldsymbol{p}}\cdot\underline{\epsilon}^{*}\,e^{-i\boldsymbol{k}\hat{\boldsymbol{r}}}$ or as $\propto \underline{\epsilon}^{*}\,e^{-i\boldsymbol{k}\hat{\boldsymbol{r}}}\cdot\hat{\mathbf{p}}$. However, one of the most valuable benefits of working within the Coulomb gauge is that $\hat{\mathbf{p}}$ and $\hat{\mathbf{A}}$ commute:

$$\hat{\mathbf{p}}\cdot\hat{\mathbf{A}} = i\hbar\boldsymbol{\nabla}\cdot\hat{\mathbf{A}} + i\hbar\hat{\mathbf{A}}\cdot\boldsymbol{\nabla} = 0 + \hat{\mathbf{A}}\cdot\hat{\mathbf{p}} \;\; .$$

Therefore, we do not have any problem in writing Eq. (3.26).

From here, if we further make the long wavelength approximation (see Eq. (2.62)), which is approximating the exponential with unity, we get

$$\begin{aligned} \mathcal{M}^{\gamma}_{NR\&lwa}(i \rightarrow f) \;\; &= \;\; -\underline{\epsilon}^{*}\cdot\frac{\langle f|\,\hat{\boldsymbol{p}}\,|i\rangle}{m\,c} \;\; = \;\; -\underline{\epsilon}^{*}\cdot\frac{\langle f|\,\hat{\dot{\boldsymbol{r}}}\,|i\rangle}{c} \\ &= \;\; -(-i)\frac{E_i - E_f}{\hbar c}\,\underline{\epsilon}^{*}\cdot\langle f|\,\hat{\boldsymbol{r}}\,|i\rangle \;\; , \end{aligned} \tag{3.27}$$

where the Heisemberg equation for $\hat{\boldsymbol{r}}$ has been used.

The long wavelength approximation is evidently assuming that the wavelength of the photon $(1/k)$ is much larger than the electron spatial coordinate $\sim r$, which is roughly the atomic size.

Joining with Eq. (3.19), the differential decay rate, within non-relativistic and long wavelength approximations, turns out to be

$$\frac{\mathrm{d}\Gamma^{\lambda}}{\mathrm{d}\Omega_{\boldsymbol{p}_{\gamma}}}\bigg|_{NR\&lwa} \;\; = \;\; \frac{\alpha(E_i - E_f)^3}{(2\pi)\hbar^3 c^2}\,|\underline{\epsilon}^{*}\cdot\langle f|\,\hat{\boldsymbol{r}}\,|i\rangle|^2 \;\; , \tag{3.28}$$

which is equal to equation [4.70] in Ref. [44], where the single-photon emission is treated non-relativistically from the outset.

Alternative approach

To have deeper insight and for further considerations, we may obtain the electric and magnetic fields carried by the photon, within *lwa*. Both fields are, prior to any

approximation, exactly equal to

$$
\begin{aligned}
\boldsymbol{E}(\boldsymbol{r},t) &= -\frac{\partial \boldsymbol{A}}{\partial t} = -\frac{\bar{\lambda}}{c\,e}\frac{\partial}{\partial t}\Big(\underline{\epsilon}e^{+i(\boldsymbol{kr}+\omega t)}+\underline{\epsilon}^{*}e^{-i(\boldsymbol{kr}+\omega t)}\Big) \\
&= -i\frac{\bar{\lambda}\omega}{c\,e}\Big(\underline{\epsilon}e^{+i(\boldsymbol{kr}+\omega t)}-\underline{\epsilon}^{*}e^{-i(\boldsymbol{kr}+\omega t)}\Big) \quad,\\[1em]
\boldsymbol{B}(\boldsymbol{r},t) &= \boldsymbol{\nabla}\times\boldsymbol{A} = \frac{\bar{\lambda}}{c\,e}\boldsymbol{\nabla}\times\Big(\underline{\epsilon}e^{+i(\boldsymbol{kr}+\omega t)}+\underline{\epsilon}^{*}e^{-i(\boldsymbol{kr}+\omega t)}\Big) \\
&= i\frac{\bar{\lambda}}{c\,e}\boldsymbol{k}\times\Big(\underline{\epsilon}e^{+i(\boldsymbol{kr}+\omega t)}-\underline{\epsilon}^{*}e^{-i(\boldsymbol{kr}+\omega t)}\Big) \quad,
\end{aligned}
\tag{3.29}
$$

where $\bar{\lambda}$ is defined in Eq. (3.13).

Now, we see that the exact electric field turns out to be proportional to ω, while the exact magnetic field turns out to be proportional to $\dfrac{\omega}{c}$, since $|\boldsymbol{k}| = \dfrac{\omega}{c}$. The latter is therefore suppressed by a factor c. Hence, we may neglect the whole magnetic field and just take the first term of the series expansion of the electric field. We get

$$
\begin{aligned}
\boldsymbol{E}\big|_{lwa} &= -i\frac{\bar{\lambda}\omega}{c\,e}\Big(\underline{\epsilon}e^{+i\omega t}-\underline{\epsilon}^{*}e^{-i\omega t}\Big) \quad,\\[1em]
\boldsymbol{B}\big|_{lwa} &= 0 \quad.
\end{aligned}
\tag{3.30}
$$

We will soon see that this approximation corresponds to what we called lwa. That is the reason for which we labeled the corresponding fields with lwa.

We know that the non relativistic Hamiltonian which accounts for the electron inter-action with a constant (in space) electric field is

$$
\hat{\mathrm{H}}_{e\boldsymbol{E}} = +\hat{\mathbf{d}}_{e}\cdot\boldsymbol{E} \quad,
\tag{3.31}
$$

where $\hat{\mathbf{d}}_{e} = e\hat{\mathbf{r}}$ is the electric dipole operator. Therefore, we can use Eq. (3.31) with the electric field $\boldsymbol{E}\big|_{lwa}$.

Then we should carry out again the evaluation of the first order term of the probability function $\mathcal{P}$, as we did in Sec. 3.2, by using the Hamiltonian $\hat{\mathrm{H}}_{e\boldsymbol{E}}$ instead of $\hat{\mathrm{H}}'$ showed in Eq. (3.12). What we would find is evidently that the term proportional to $e^{+i(\boldsymbol{kr}+\omega t)}$ drops off, as it is responsible for the photon absorption, and the new amplitude would read

$$
\mathcal{M}^{\gamma}_{NR\&lwa}(i\to f) = +i\frac{E_{i}-E_{f}}{e\hbar c}\,\langle f|\,\hat{\mathbf{d}}_{e}\cdot\boldsymbol{E}_{o}\,|i\rangle \quad,
\tag{3.32}
$$

where $\boldsymbol{E}_{o} = \underline{\epsilon}$ is the part of the photon electric field left after the evaluation.

Equation (3.32) is, as expected, equal to Eq. (3.27). Therefore, making the non-relativistic long wavelength approximation is effectively i) neglecting any magnetic field that the photon carries, ii) assuming the electric field to be constant in space and iii) assuming the interaction between electrons and photon to be given by the non-relativistic Hamiltonian in Eq. (3.31).

Integrating over the photon direction

In case the direction of the photon is not relevant, we should correctly come back to
Eq. (3.22), expanding with the multipole expansion and make there the non-relativistic
and long wavelength approximations. The calculation is easily carried out by looking
at Eq. (2.60) where we have seen that "long wavelength approximation" is effectively
equal to *eda* with the further approximations $J_0(kr) \to 1$ and $J_2(kr) \to 0$. We can
therefore first make *eda* to get

$$
\left| \tilde{\mathcal{M}}^\gamma(i \to f) \right|^2_{eda} = \left| (2\pi)\sqrt{2}\,(-i)\,(\lambda)\,\langle f| \, \boldsymbol{\alpha} \cdot \boldsymbol{A}^{(e)\,*}_{1\,M}(k,\hat{\boldsymbol{r}})\,|i\rangle \right|^2
$$

$$
= \left| (2\pi)\sqrt{2}\,(-i)\,(\lambda)\,\langle f| \, \boldsymbol{\alpha} \cdot (-1)^M \boldsymbol{A}^{(e)}_{1\,-M}(k,\hat{\boldsymbol{r}})\,|i\rangle \right|^2 \quad,
$$

where we used $\boldsymbol{A}^{(e)\,*}_{1\,M} = (-1)^M \boldsymbol{A}^{(e)}_{1\,-M}$ as showed in Sec. B.
From here, by neglecting $J_2(kr)$ and by replacing $J_0(kr) \to 1$ we easily get

$$
\left| \tilde{\mathcal{M}}^\gamma(i \to f) \right|^2_{lwa} = 8\pi^2 \Big| \langle f| \, \boldsymbol{\alpha} \cdot \sqrt{\frac{2}{3}} \sum_{m=-1}^{1} \langle 0, -M-m, 1, m|1, -M\rangle
$$

$$
\times\, Y_0^{-M-m}(\varphi_r, \theta_r)\xi_m\,|i\rangle \Big|^2
$$

$$
= \frac{4\pi}{3} \Big| \langle f| \, \boldsymbol{\alpha} \cdot \xi_{-M}\,|i\rangle \Big|^2 \quad.
$$

Introducing this term into Eq. (3.22) we get

$$
\Gamma^\lambda \Big|_{lwa} = \frac{\alpha(E_i - E_f)}{(2\pi)\hbar} \sum_{M=-1}^{1} \frac{4\pi}{3} \Big| \langle f| \, \boldsymbol{\alpha} \cdot \xi_{-M}\,|i\rangle \Big|^2 \quad.
$$

Adding the non-relativistic approximation is, as discussed, making the replacement
$c\boldsymbol{\alpha} \to \hat{\boldsymbol{p}}/m$. We get

$$
\Gamma^\lambda \Big|_{NR\&lwa} = \frac{\alpha(E_i - E_f)}{(2\pi)\hbar} \sum_{M=-1}^{1} \frac{4\pi}{3} \Big| \langle f| \, \frac{\hat{\boldsymbol{p}}}{mc} \cdot \xi_{-M}\,|i\rangle \Big|^2
$$

$$
= \frac{\alpha(E_i - E_f)^3}{(2\pi)\hbar^3\,c^2} \frac{4\pi}{3} \sum_{M=-1}^{1} \Big| \langle f| \, \hat{\boldsymbol{r}} \cdot \xi_{-M}\,|i\rangle \Big|^2 \quad.
$$

$$(3.33)$$

Now, by straightforward analysis, it is easy to show that, for any vector operator
$\hat{\boldsymbol{A}} = (\hat{A}_x, \hat{A}_y, \hat{A}_z)$, it follows

$$
\sum_{M=-1}^{1} \Big| \langle f| \, \hat{\boldsymbol{A}} \cdot \xi_{-M}\,|i\rangle \Big|^2 = \sum_{M=-1}^{1} \Big| \langle f| \, \hat{\boldsymbol{A}} \cdot \xi_{M}\,|i\rangle \Big|^2
$$

$$
= \Big| \langle f| \, \hat{A}_x\,|i\rangle \Big|^2 + \Big| \langle f| \, \hat{A}_y\,|i\rangle \Big|^2 + \Big| \langle f| \, \hat{A}_z\,|i\rangle \Big|^2 = \Big| \langle f| \, \hat{\boldsymbol{A}}\,|i\rangle \Big|^2 \quad,
$$

being ξ_m the unit vector showed in Eq. (2.57).
Using this relation in Eq. (3.33), we are lead to

$$
\Gamma^\lambda \Big|_{NR\&lwa} = \frac{2\alpha(E_i - E_f)^3}{3\hbar^3\,c^2} \Big| \langle f| \, \hat{\boldsymbol{r}}\,|i\rangle \Big|^2 \quad.
$$

$$(3.34)$$

This expression could be also more easily (but less intuitively) obtained from Eq. (3.28), by choosing a system of reference such that $\underline{\epsilon}^* \cdot \boldsymbol{r} = |\underline{\epsilon}^*||\boldsymbol{r}|\cos\theta_k = |\boldsymbol{r}|\cos\theta_k$, where θ_k is, as usual, the polar angle of the emitted photon and $\boldsymbol{r}$ is the electron coordinate. From Eq. (3.28) we get

$$
\begin{aligned}
\Gamma^\lambda\Big|_{NR\&lwa} &= \frac{\alpha(E_i - E_f)^3}{(2\pi)\hbar^3 c^2} \int_0^{2\pi}\int_{-1}^1 \cos^2\theta_k \, |\langle f|\,\hat{\boldsymbol{r}}\,|i\rangle|^2 \, \mathrm{d}\cos\theta_k \mathrm{d}\varphi_k \\
&= \frac{\alpha(E_i - E_f)^3}{\hbar^3 c^2} \int_{-1}^1 \cos^2\theta_k \, |\langle f|\,\hat{\boldsymbol{r}}\,|i\rangle|^2 \, \mathrm{d}\cos\theta_k \\
&= \frac{2\alpha(E_i - E_f)^3}{3\hbar^3 c^2} \, |\langle f|\,\hat{\boldsymbol{r}}\,|i\rangle|^2 \quad .
\end{aligned}
$$

Total decay rate

From Eq. (3.34) we see that, after having integrated over the photon direction, the decay rate does not depend anymore on the photon polarization. The total decay rate is then given by the sum over the two possible photon polarizations $\lambda = -1, +1$:

$$
\Gamma\Big|_{NR\&lwa} = \sum_{\substack{\lambda = -1, \\ +1}} \Gamma^\lambda\Big|_{NR\&lwa} = \frac{4\alpha(E_i - E_f)^3}{3\hbar^3 c^2} \left| \langle f|\,\hat{\boldsymbol{r}}\,|i\rangle \right|^2 \quad ,
$$

which matches Eq. (4.71) in Ref. [44].

Remarks and comments

As first remark, we point out that, since the matrix element

$$
\langle f|\,\hat{\boldsymbol{r}}\,|i\rangle = \int \mathrm{d}r^3 \Psi_f^*(\boldsymbol{r})\boldsymbol{r}\Psi_i(\boldsymbol{r}) \tag{3.35}
$$

is vanishing if parity of initial and final states are equal, only single-photon decays between states with different parity are allowed within non-relativistic and long wavelength approximations. This selection rule is known as *Laporte rule*.

As second remark: if we considered the spin part of the atomic wavefunction, we would notice that, within this approximation, single photon transitions are not able to link atomic states with different spin:

$$
\begin{aligned}
\langle f|\,\hat{\boldsymbol{r}}\,|i\rangle &= \int \mathrm{d}r^3 \Psi_f^*(\boldsymbol{r})\boldsymbol{\chi}_{S_f}^\dagger(m_{S_f}) \, \boldsymbol{r} \, \Psi_i(\boldsymbol{r})\boldsymbol{\chi}_{S_i}(m_{S_i}) \\
&= \left(\int \mathrm{d}r^3 \Psi_f^*(\boldsymbol{r})\boldsymbol{r}\Psi_i(\boldsymbol{r}) \right)\left(\boldsymbol{\chi}_{S_f}^\dagger(m_{S_f})\boldsymbol{\chi}_{S_i}(m_{S_i}) \right) \\
&= \delta_{S_i,S_f}\,\delta_{m_{S_i},m_{S_f}} \int \mathrm{d}r^3 \Psi_f^*(\boldsymbol{r})\boldsymbol{r}\Psi_i(\boldsymbol{r}) \quad ,
\end{aligned}
$$

where S and m_S are the atomic spin magnitude and its projection along the quantization axis respectively.

In other words, single photon transitions within NR&*lwa* do not account for "spin flip

transitions". This selection rule is a consequence of having neglected any magnetic field the photon carries. Higher order of the vector plane wave must be invoked so as to allow spin flip transitions to occur.

Anyway, being spin-flip transitions not encompassed at the first order, this means that they are normally far less probable than spin conserved transitions.

As third and last remark, we remind that the vector $\boldsymbol{r} = (x, y, z)$ can be decomposed in terms of spherical harmonics of first rank as

$$x = \frac{r}{2}\sqrt{\frac{8\pi}{3}}\left(Y_1^1 + Y_1^{-1}\right)$$

$$y = \frac{r}{2i}\sqrt{\frac{8\pi}{3}}\left(Y_1^1 - Y_1^{-1}\right) \tag{3.36}$$

$$z = r\sqrt{\frac{4\pi}{3}}Y_1^0 \quad .$$

Since the initial and final atomic eigenfunctions have normally defined angular momentum, on evaluating the amplitude (3.35), we will generally have an integral of the Gaunt type

$$\int Y_{J_f}^{m_f *}(\theta, \varphi)\, Y_1^m(\theta, \varphi)\, Y_{J_i}^{m_i}(\theta, \varphi)\, \mathrm{d}\varphi \sin\theta \mathrm{d}\theta$$

$$= (-1)^{m_f}\, 4\pi\sqrt{(2+1)(2J_i+1)(2J_f+1)}\begin{pmatrix} 1 & J_i & J_f \\ m & m_i & -m_f \end{pmatrix}\begin{pmatrix} 1 & J_i & J_f \\ 0 & 0 & 0 \end{pmatrix} \quad ,$$

where m could be -1, 0 or 1 and we employed the standard notation for the Wigner 3-j symbols.

Due to the symmetry properties of the 3-j symbols, the amplitude (3.35) would be vanishing if the triangle rule $J_{f(i)} \otimes 1 = J_{i(f)}$ were not satisfied. In short, we see from Eq. (3.36) that the operator $\hat{\mathbf{r}}$, being a superposition of spherical harmonics of rank 1, can only link states which fulfill the tringle rule $J_{f(i)} \otimes 1 = J_{i(f)}$.

In atomic systems for which the parity is given by a quantum number l as $(-1)^l$, we can in summary write the selection rules which hold in NR&lwa as

$$\begin{aligned} \Delta S &= 0 \\ \Delta m_S &= 0 \\ \Delta l &= 1 \\ J_{f(i)} \otimes 1 &= J_{i(f)} \quad . \end{aligned} \tag{3.37}$$

In the next section, we will investigate how to take into account some of the magnetic photon effects so as to allow spin flip transitions to occur.

3.3.5 Non-relativistic Pauli approximation

The amplitude in Eq. (3.27), as it is clear from the previous section, accounts for the electric dipole interaction between electron and photon, while it does not account at all for the electron-photon magnetic interaction given by the $\boldsymbol{B}$ field the photon carries (see Eq. (3.30)). Therefore, a better approximation than lwa would be obtained if we added some contribution from the photon magnetic field.

The exact magnetic field carried by the photon is given in Eq. (3.29) and it depends on $\boldsymbol{r}$. This may be rather uncomfortable during the calculation of transition amplitudes and therefore we would like to drop such a dependence without neglecting the magnetic field completely. If $\boldsymbol{k}\boldsymbol{r} << 1$, we can safely approximate the exponential with unity. In other words, we are again saying that the photon wavelength is much bigger than the atomic size, so that the atomic electrons feel a constant magnetic field. We get

$$\boldsymbol{B}\big|_{PA} \approx i\frac{\bar{\lambda}}{c\,e}\boldsymbol{k} \times \left(\underline{\epsilon}e^{+i\omega t} - \underline{\epsilon}^* e^{-i\omega t} \right) \quad .$$

This approximation will be hereinafter referred to as "Pauli approximation" (PA). Now, with a constant magnetic field, everything becomes much easier. As we derive in App. C, the non-relativistic Hamiltonian which accounts for the electron interaction with a constant magnetic field is

$$\hat{\mathrm{H}}_{e\boldsymbol{B}} = +\hat{\boldsymbol{\mu}}_e \cdot \boldsymbol{B} \quad , \tag{3.38}$$

where

$$\hat{\boldsymbol{\mu}}_e = \frac{\mu_B\,c}{\hbar}\left(\hat{\mathbf{L}} + g_s\hat{\mathbf{S}} \right)$$

is the magnetic dipole operator for the electron and $\mu_B = \dfrac{e\hbar}{2mc}$ is the Bohr magneton. We can therefore plug $\boldsymbol{B}\big|_{PA}$ into Eq. (3.38) to obtain the photon-electron magnetic interaction Hamiltonian.

From the previous section, we also know that the Hamiltonian which accounts for the electron interaction with the (approximately) constant electric field of the photon is

$$\hat{\mathrm{H}}_{e\boldsymbol{E}} = +\hat{\mathbf{d}}_e \cdot \boldsymbol{E} \quad ,$$

where

$$\hat{\mathbf{d}}_e \;=\; e\hat{\mathbf{r}} \quad ,$$

$$\boldsymbol{E} \;\approx\; i\frac{\bar{\lambda}\omega}{c\,e}\left(\underline{\epsilon}e^{+i\omega t} - \underline{\epsilon}^* e^{-i\omega t} \right) \quad .$$

Now, we should carry out again the evaluation of the first order term of the probability function $\mathcal{P}$, that we did in Sec. 3.2, by using the Hamiltonian $\hat{\mathrm{H}}_{e\boldsymbol{E}} + \hat{\mathrm{H}}_{e\boldsymbol{M}}$ instead of $\hat{\mathrm{H}}'$ of Eq. (3.12). What we would find is evidently that the terms proportional to $e^{+i(\boldsymbol{k}\boldsymbol{r}+\omega t)}$ drop off, as they are responsible for the photon absorption, and we would have the amplitude as

$$
\begin{aligned}
\mathcal{M}^{\gamma}_{NR\&PA}(i \to f) \;=\;& +i\frac{E_i - E_f}{\hbar c}\,\underline{\epsilon}^* \cdot \langle f|\,\hat{\mathbf{r}}\,|i\rangle + \frac{\mu_B\,c}{e\hbar}\,\langle f|\left(\hat{\mathbf{L}} + g_s\hat{\mathbf{S}} \right) \cdot \boldsymbol{B}|_{PA}\,|i\rangle \\
\;=\;& +i\frac{E_i - E_f}{\hbar c}\,\underline{\epsilon}^* \cdot \langle f|\,\hat{\mathbf{r}}\,|i\rangle - i\,\frac{\mu_B\,c}{e\hbar}\left(\boldsymbol{k} \times \underline{\epsilon}^* \right) \cdot \langle f|\,\hat{\mathbf{L}} + g_s\hat{\mathbf{S}}\,|i\rangle \quad .
\end{aligned}
\tag{3.39}
$$

The comparison with Eq. (3.27) is immediate. We see that, by adding the (first order) magnetic contribution to the vector potential, we have gained a new term in the amplitude which depends upon the orbital and spin angular momenta of the initial and final electronic states. By virtue of this term, single photon spin flip transitions, though with low probability, are now allowed. This term is therefore essential for studying the

polarization properties of the radiation as well as of the atom/ion which undergoes the transition.

From the proceeding we adopted in the previous section, it is straightforward the derivation of the quantities $\left.\dfrac{\mathrm{d}\Gamma^{\lambda}}{\mathrm{d}\Omega_{\boldsymbol{p}_{\gamma}}}\right|_{NR\&PA}$, $\left.\Gamma^{\lambda}\right|_{NR\&PA}$ and $\left.\Gamma\right|_{NR\&PA}$.

Remarks and comments

Despite the efforts we made, the amplitude (3.39) accounts only partially for spin-flip transitions. In fact, we know that the operator $\hat{\mathbf{L}}$ contains only the spherical angles operators $\hat{\varphi}$ and $\hat{\theta}$, while it does not contain contain the radial operator $\hat{\mathrm{r}}$ [45]. By virtue of this, the operator $\hat{\mathbf{L}}+g_s\hat{\mathbf{S}}$ cannot link states with different principal quantum number, since the radial wavefunctions of states with different principal quantum numbers are normally orthogonal. For example, in hydrogen-like ions, the matrix element of the last term in Eq. (3.39) would read

$$
\begin{aligned}
\langle n', l', m'_l, 1/2, m'_s | \left(\hat{\mathbf{L}} + g_s\hat{\mathbf{S}}\right) |n, l, m_l, 1/2, m_s\rangle &= \left(\int \mathrm{d}r\, r^2\, g_{n'l'}(r)g_{nl}(r)\right) \\
&\times \left(\int \mathrm{d}\varphi \sin\theta\mathrm{d}\theta\, \mathrm{Y}_{l'}^{m'_l *}(\varphi,\theta)\chi_{1/2}^{\dagger}(m'_s)\Big(\mathbf{L} + g_s\frac{\hbar}{2}\boldsymbol{\sigma}\Big)\mathrm{Y}_l^{m_l}(\varphi,\theta)\chi_{1/2}(m_s)\right) \\
&\propto \delta_{n,n'} \left(\int \mathrm{d}\varphi \sin\theta\mathrm{d}\theta\, \mathrm{Y}_{l'}^{m'_l *}(\varphi,\theta)\chi_{1/2}^{\dagger}(m'_s)\Big(\mathbf{L} + g_s\frac{\hbar}{2}\boldsymbol{\sigma}\Big)\mathrm{Y}_l^{m_l}(\varphi,\theta)\chi_{1/2}(m_s)\right) \quad ,
\end{aligned}
$$

where $g_{nl}(r)$ are the radial hydrogenic wavefunctions, $\mathrm{Y}_l^{m_l}$ are spherical harmonics and $\chi_{1/2}(m_s)$ are Pauli spinors.

Since the radial wavefunctions for equal n and different l are *not* orthogonal, spin-flip transitions between states with different orbital angular momentum lying on the same shell are in principle allowed. Evidently, in order to allow spin-flip transitions between states with different principal quantum number, higher order terms in the field and potential expansions must be taken into account.

Moreover, since both $\hat{\mathbf{L}}$ and $\hat{\mathbf{S}}$ have even parity, the right term of Eq. (3.39) accounts for transitions between states with equal parity and the same principal quantum number. For making a clear example, the Pauli term accounts for the single photon transition between the hydrogenic states $2p_{3/2}$ and $2p_{1/2}$, which are degenerate in the non-relativistic description of Hydrogen but are actually separated by the fine splitting correction.

3.4 TWO-PHOTON DECAY RATE

For the two-photon transition rate, we must go back to Eq. (3.10). We look for processes where i) the initial state is different from the final state and where ii) two photons are emitted with propagation vector $\boldsymbol{k}_1$ and $\boldsymbol{k}_2$. Looking at our master equation (3.10), we correspondingly discard i) the first term (which corresponds to the zero-order approximation) and ii) the second term (which corresponds to the first order approximation) since both are vanishing for the problem under consideration. The third term is what we are looking for, as it contains two vector potentials given by two different photons.

Since we are at the second order, we expect that the probability of two-photon emission is quite small in comparison with the one of single-photon emission which is at the first order. In other words, we expect that the atom mostly gets de-excited by single-photon emission, which is consistent with the original idea of the atomic Bohr model and which is what is usually studied in an introductory course on quantum mechanics. Indeed, this is the case. For many purposes, we can freely consider the single-photon decay as the only existing one. This is what physicists were also actually doing at the early stages of quantum mechanics. However, as usual in physics, there are a few transitions, between particular initial and final states, for which the single-photon emission is either strongly suppressed or vanishing. At the time when quantum mechanics was dawning, the Max Born's PhD student Maria Göppert-Mayer was the first one who formulated the theory of possible two-photon transitions in atoms, in 1931 [1].

Owing to the modern formulation of quantum mechanics explained in the previous sections, we do not have troubles nowadays in accepting the concept that two-photon processes can occur. The derivation of the two-photon decay rate comes indeed straightforwardly. By using the electron-photon Hamiltonian showed at the beginning of the previous section, the probability function for the two-photon decay is[3]

$$
\mathcal{P} = \left| \left(-\frac{i}{\hbar} \right)^2 \bar{\lambda}_1 \bar{\lambda}_2 \int_{t_0}^{t} \mathrm{d}t_1 \int_{t_0}^{t_1} \mathrm{d}t_2 \sum_{\nu_1} e^{i\omega_{f\nu_1}t_1} e^{i\omega_{\nu_1 i}t_2} \right.
$$
$$
\left. \times \langle f| \, \boldsymbol{\alpha} \cdot \underline{\epsilon}_1^* e^{-i(\boldsymbol{k}_1 \hat{\boldsymbol{r}} - \omega_1 t_1)} |\nu_1\rangle \langle \nu_1| \, \boldsymbol{\alpha} \cdot \underline{\epsilon}_2^* e^{-i(\boldsymbol{k}_2 \hat{\boldsymbol{r}} - \omega_2 t_1)} |i\rangle \right|^2 , \tag{3.40}
$$

where $\bar{\lambda}_j = \sqrt{\dfrac{2\pi \hbar^2 c^3 \alpha}{\omega_j V}}$ while the subscripts $_1$ and $_2$ label the first and second photon respectively. These labels are fictitious (they are merely an index in quantum mechanics), so that we cannot actually distinguish between the situation in which 'the first and second photon are detected respectively at the detector A and B' from the situation in which 'the second and first photon are detected respectively at the detector A and B'. Following one of the core principles of quantum mechanics [46], in this case we must sum the amplitudes, *nor* the probabilities, of the two processes. Therefore, the probability function that we must actually investigate is

$$
\mathcal{P} = \left| \left(-\frac{i}{\hbar} \right)^2 \bar{\lambda}_1 \bar{\lambda}_2 \int_{t_0}^{t} \mathrm{d}t_1 \int_{t_0}^{t_1} \mathrm{d}t_2 \sum_{\nu_1} e^{i\omega_{f\nu_1}t_1} e^{i\omega_{\nu_1 i}t_2} \right.
$$
$$
\times \left[\langle f| \, \boldsymbol{\alpha} \cdot \underline{\epsilon}_1^* e^{-i(\boldsymbol{k}_1 \hat{\boldsymbol{r}} - \omega_1 t_1)} |\nu_1\rangle \langle \nu_1| \, \boldsymbol{\alpha} \cdot \underline{\epsilon}_2^* e^{-i(\boldsymbol{k}_2 \hat{\boldsymbol{r}} - \omega_2 t_2)} |i\rangle \right.
$$
$$
\left. \left. + \langle f| \, \boldsymbol{\alpha} \cdot \underline{\epsilon}_2^* e^{-i(\boldsymbol{k}_2 \hat{\boldsymbol{r}} - \omega_2 t_1)} |\nu_1\rangle \langle \nu_1| \, \boldsymbol{\alpha} \cdot \underline{\epsilon}_1^* e^{-i(\boldsymbol{k}_1 \hat{\boldsymbol{r}} - \omega_1 t_2)} |i\rangle \right] \right|^2 .
$$
$$
\tag{3.41}
$$

The discussion which brought us from Eq. (3.40) to Eq. (3.41) is avoided in the formalism of Quantum Field Theory (QFT), where the action of creation and annihilation operators of photons provides the right multiplicity and amplitude types [47].

---

[3]We have dropped the terms corresponding to photons absorption.

We carry on our evaluation of the probability function re-labeling $\nu_1 \rightarrow \nu$:

$$
\begin{aligned}
\mathcal{P} = {} & \left| \frac{\bar{\lambda}_1 \bar{\lambda}_2}{\hbar^2} \sum_\nu \left[\langle f | \, \boldsymbol{\alpha} \cdot \underline{\boldsymbol{\epsilon}}_1^* e^{-i\boldsymbol{k}_1 \hat{\boldsymbol{r}}} \, | \nu \rangle \, \langle \nu | \, \boldsymbol{\alpha} \cdot \underline{\boldsymbol{\epsilon}}_2^* e^{-i\boldsymbol{k}_2 \hat{\boldsymbol{r}}} \, | i \rangle \right. \right. \\
& \left. \times \int_{t_0}^t \mathrm{d}t_1 \int_{t_0}^{t_1} \mathrm{d}t_2 \, e^{it_1(\omega_{f\nu} + \omega_1)} e^{it_2(\omega_{\nu i} + \omega_2)} \right. \\
& + \langle f | \, \boldsymbol{\alpha} \cdot \underline{\boldsymbol{\epsilon}}_2^* e^{-i\boldsymbol{k}_2 \hat{\boldsymbol{r}}} \, | \nu \rangle \, \langle \nu | \, \boldsymbol{\alpha} \cdot \underline{\boldsymbol{\epsilon}}_1^* e^{-i\boldsymbol{k}_1 \hat{\boldsymbol{r}}} \, | i \rangle \\
& \left. \left. \times \int_{t_0}^t \mathrm{d}t_1 \int_{t_0}^{t_1} \mathrm{d}t_2 \, e^{it_1(\omega_{f\nu} + \omega_2)} e^{it_2(\omega_{\nu i} + \omega_1)} \right] \right|^2 \quad , \\
= {} & \left| A_{12} \, B_{12} \, + \, A_{21} \, B_{21} \right|^2 \quad ,
\end{aligned}
$$

where

$$
A_{12} = \frac{\bar{\lambda}_1 \bar{\lambda}_2}{\hbar^2} \sum_\nu \langle f | \, \boldsymbol{\alpha} \cdot \underline{\boldsymbol{\epsilon}}_1^* e^{-i\boldsymbol{k}_1 \hat{\boldsymbol{r}}} \, | \nu \rangle \, \langle \nu | \, \boldsymbol{\alpha} \cdot \underline{\boldsymbol{\epsilon}}_2^* e^{-i\boldsymbol{k}_2 \hat{\boldsymbol{r}}} \, | i \rangle
$$

$$
B_{12} = \int_{t_0}^t \mathrm{d}t_1 \int_{t_0}^{t_1} \mathrm{d}t_2 \, e^{it_1(\omega_{f\nu} + \omega_1)} e^{it_2(\omega_{\nu i} + \omega_2)}
$$

and the elements A_{21}, B_{21} are just the same as the elements above with the photons' characteristics interchanged.

We choose $t_0 = 0$ (t_0 is the time when the experiments starts, when the atom is prepared in the excited state), as it is natural, as we have done in treating the single-photon decay. We focus on B_{12}:

$$
\begin{aligned}
B_{12} = {} & \int_0^t \mathrm{d}t_1 \, e^{it_1(\omega_{f\nu} + \omega_1)} \frac{e^{it_1(\omega_{\nu i} + \omega_2)} - 1}{i(\omega_{\nu i} + \omega_2)} \\
= {} & \frac{i}{\omega_{\nu i} + \omega_2} \int_0^t \mathrm{d}t_1 \, e^{it_1(\omega_{f\nu} + \omega_1)} \left(1 - e^{it_1(\omega_{\nu i} + \omega_2)} \right) \\
= {} & \frac{i}{\omega_{\nu i} + \omega_2} \int_0^t \mathrm{d}t_1 \left(e^{it_1(\omega_{f\nu} + \omega_1)} - e^{it_1(\overbrace{\omega_{f\nu} + \omega_{\nu i}}^{\omega_{fi}} + \omega_1 + \omega_2)} \right) \\
= {} & \frac{i}{\omega_{\nu i} + \omega_2} \left(\frac{e^{it(\omega_{f\nu} + \omega_1)} - 1}{i(\omega_{f\nu} + \omega_1)} - \frac{e^{it(\omega_{fi} + \omega_1 + \omega_2)} - 1}{i(\omega_{fi} + \omega_1 + \omega_2)} \right) \\
= {} & \frac{1}{\omega_{\nu i} + \omega_2} \left(\frac{e^{it(\omega_{f\nu} + \omega_1)} - 1}{\omega_{f\nu} + \omega_1} + \frac{1 - e^{it(\omega_{fi} + \omega_1 + \omega_2)}}{\omega_{fi} + \omega_1 + \omega_2} \right) \quad .
\end{aligned}
\tag{3.42}
$$

Bearing in mind that we must take the limit $t \rightarrow +\infty$ to get the decay rate from the first derivative in time of the probability function, we can easily understand that the first term in the rhs of the above equation will be proportional to $\sim \delta(\omega_{f\nu} + \omega_1)$, or, more explicitly to $\sim \delta(E_f - E_\nu + E_1)$, where we called E_n the energy of the n-th photon. As long as we detect only events far from any resonance of the type $E_{1,2} = E_\nu - E_f$ or, being the overall energy conserved, of the type $E_{1,2} = E_i - E_\nu$, we can safely discard this term both in B_{12} and in B_{21}. It is obvious, nonetheless, that if one wants to investigate the two-photon decays near resonances, he must come back to this equation and consider all the terms.

Neglecting the first term in the rhs of Eq. (3.42) brings also great advantage to the calculation, since the second term is almost symmetric in $1 \to 2$. We can therefore write

$$B_{12} \quad \simeq \quad \frac{1}{\omega_{\nu i} + \omega_2} \frac{1 - e^{it(\omega_{fi} + \omega_1 + \omega_2)}}{\omega_{fi} + \omega_1 + \omega_2}$$

$$B_{21} \quad \simeq \quad \frac{1}{\omega_{\nu i} + \omega_1} \frac{1 - e^{it(\omega_{fi} + \omega_1 + \omega_2)}}{\omega_{fi} + \omega_1 + \omega_2} \quad .$$

The probability function is then

$$\mathcal{P} \quad = \quad \left| A_{12} B_{12} + A_{21} B_{21} \right|^2$$

$$\simeq \quad \left| \overbrace{\left(\frac{A_{12}}{\omega_{\nu i} + \omega_2} + \frac{A_{21}}{\omega_{\nu i} + \omega_1} \right)}^{A} \frac{1 - e^{it(\omega_{fi} + \omega_1 + \omega_2)}}{\omega_{fi} + \omega_1 + \omega_2} \right|^2$$

$$= \quad |A|^2 \left| e^{i\frac{t}{2}(\omega_{fi} + \omega_1 + \omega_2)} \frac{e^{-i\frac{t}{2}(\omega_{fi} + \omega_1 + \omega_2)} - e^{i\frac{t}{2}(\omega_{fi} + \omega_1 + \omega_2)}}{\omega_{fi} + \omega_1 + \omega_2} \right|^2$$

$$= \quad \frac{|A|^2}{(\omega_{fi} + \omega_1 + \omega_2)^2} \left| -2i \sin\left[\frac{t(\omega_{fi} + \omega_1 + \omega_2)}{2} \right] \right|^2$$

$$= \quad 4 |A|^2 \frac{\sin^2\left[\frac{t(\omega_{fi} + \omega_1 + \omega_2)}{2} \right]}{(\omega_{fi} + \omega_1 + \omega_2)^2} \quad .$$

In order to find the decay rate, we proceed to take the first derivative in time,

$$\frac{\mathrm{d}P}{\mathrm{d}t} \quad = \quad 2 |A|^2 \frac{\sin\left[t(\omega_{fi} + \omega_1 + \omega_2) \right]}{\omega_{fi} + \omega_1 + \omega_2} \quad ,$$

from which we finally get

$$\Gamma \quad = \quad \lim_{t \to +\infty} \frac{\mathrm{d}P}{\mathrm{d}t} = (2\pi)|A|^2 \delta(\omega_{fi} + \omega_1 + \omega_2) \quad .$$

By writing explicitly the element A, we obtain

$$\Gamma \quad = \quad \left(2\pi \frac{\bar{\lambda}_1^2 \bar{\lambda}_2^2}{\hbar^3} \right) \left| \mathcal{M}^{\gamma\gamma}(i \to f) \right|^2 \delta(E_f - E_i + E_1 + E_2) \quad , \tag{3.43}$$

where

$$\mathcal{M}^{\gamma\gamma}(i \to f) \quad = \quad \sum_{\nu} \left(\frac{\langle f| \, \boldsymbol{\alpha} \cdot \underline{\epsilon}_1^* e^{-i\boldsymbol{k}_1 \hat{\boldsymbol{r}}} \, |\nu\rangle \, \langle \nu| \, \boldsymbol{\alpha} \cdot \underline{\epsilon}_2^* e^{-i\boldsymbol{k}_2 \hat{\boldsymbol{r}}} \, |i\rangle}{\omega_{\nu i} + \omega_2} \right.$$
$$\left. + \frac{\langle f| \, \boldsymbol{\alpha} \cdot \underline{\epsilon}_2^* e^{-i\boldsymbol{k}_2 \hat{\boldsymbol{r}}} \, |\nu\rangle \, \langle \nu| \, \boldsymbol{\alpha} \cdot \underline{\epsilon}_1^* e^{-i\boldsymbol{k}_1 \hat{\boldsymbol{r}}} \, |i\rangle}{\omega_{\nu i} + \omega_1} \right) \quad . \tag{3.44}$$

We may now compare Eq. (3.43) with Eq. (3.16) in order to notice a general structure. Writing explicitly the elements $\bar{\lambda}_{1,2}$, multiplying by the number of photons N_{γ_1} and N_{γ_2} (see Eq. (3.17)) and integrating over the second photon energy E_2, we get the final expression

$$\frac{\mathrm{d}\Gamma^{\lambda_1 \lambda_2}}{\mathrm{d}E_1 \mathrm{d}\Omega_{\boldsymbol{p}_1} \mathrm{d}\Omega_{\boldsymbol{p}_2}} \quad = \quad \left(\frac{\alpha^2 E_1 (E_i - E_f - E_1)}{(2\pi)^3 \hbar^3} \right) \left| \mathcal{M}^{\gamma\gamma}(i \to f) \right|^2 \Big|_{E_2 = E_i - E_f - E_1} \quad , \tag{3.45}$$

where the notation $\big|_{E_2 = E_i - E_f - E_1}$ means that the expression standing before must be calculated with $E_2 = E_i - E_f - E_1$. We have furthermore added the label $\lambda_1 \lambda_2$ to the decay rate to make explicit the fact that it depends on the polarization of the emitted photons. $\lambda_{1,2}$ are here intended to denote the photons helicities.

Contrarily to the single-photon decay case, the element $\mathcal{M}^{\gamma\gamma}$ is *not* dimensionless. Rather, $\mathcal{M}^{\gamma\gamma}$ has dimensions *sec*. By virtue of this, if the matrix element $\mathcal{M}^{\gamma\gamma}$ is calculated in unit systems different from SI, in order to get the right decay rate, one must first transform it into the correct value in SI (multiplying it by the unit time of that unit system) and then plug the result in Eq. (3.45). We may also notice that, being $\mathcal{M}^{\gamma\gamma}$ with dimensions *sec*, the rhs of Eq. (3.45) has the right dimensions $J^{-1} sec^{-1}$.

Coming back to Eq. (3.44), we can now identify the Green function for the transition:

$$
\begin{aligned}
\mathcal{M}^{\gamma\gamma}(i \to f) = \hbar \sum_\nu \int \mathrm{d}^3 r_1 \mathrm{d}^3 r_2 \, \Bigg(& \frac{\langle f | \boldsymbol{r}_1 \rangle \boldsymbol{\alpha} \cdot \underline{\epsilon}_1^* e^{-i\boldsymbol{k}_1 \boldsymbol{r}_1} \langle \boldsymbol{r}_1 | \nu \rangle \langle \nu | \boldsymbol{r}_2 \rangle \boldsymbol{\alpha} \cdot \underline{\epsilon}_2^* e^{-i\boldsymbol{k}_2 \boldsymbol{r}_2} \langle \boldsymbol{r}_2 | i \rangle}{E_\nu - E_i + E_2} \\
& + \frac{\langle f | \boldsymbol{r}_1 \rangle \boldsymbol{\alpha} \cdot \underline{\epsilon}_2^* e^{-i\boldsymbol{k}_2 \boldsymbol{r}_1} \langle \boldsymbol{r}_1 | \nu \rangle \langle \nu | \boldsymbol{r}_2 \rangle \boldsymbol{\alpha} \cdot \underline{\epsilon}_1^* e^{-i\boldsymbol{k}_1 \boldsymbol{r}_2} \langle \boldsymbol{r}_2 | i \rangle}{E_\nu - E_i + E_1} \Bigg) \\
= \hbar \int \mathrm{d}^3 r_1 \mathrm{d}^3 r_2 \, \Big(& \Psi_f^\dagger(\boldsymbol{r}_1) \boldsymbol{\alpha} \cdot \underline{\epsilon}_1^* e^{-i\boldsymbol{k}_1 \boldsymbol{r}_1} G_{E_2 - E_i}(\boldsymbol{r}_1, \boldsymbol{r}_2) \boldsymbol{\alpha} \cdot \underline{\epsilon}_2^* e^{-i\boldsymbol{k}_2 \boldsymbol{r}_2} \Psi_i(\boldsymbol{r}_2) \\
& + \Psi_f^\dagger(\boldsymbol{r}_1) \boldsymbol{\alpha} \cdot \underline{\epsilon}_2^* e^{-i\boldsymbol{k}_2 \boldsymbol{r}_1} G_{E_1 - E_i}(\boldsymbol{r}_1, \boldsymbol{r}_2) \boldsymbol{\alpha} \cdot \underline{\epsilon}_1^* e^{-i\boldsymbol{k}_1 \boldsymbol{r}_2} \Psi_i(\boldsymbol{r}_2) \Big) \quad ,
\end{aligned}
$$
(3.46)

where the identity $\int \mathrm{d}^3 r \, | \boldsymbol{r} \rangle \langle \boldsymbol{r} | = \hat{\mathbb{1}}$ and the equation $e^{-i\boldsymbol{k}_1 \hat{\boldsymbol{r}}} | \boldsymbol{r}_1 \rangle = e^{-i\boldsymbol{k}_1 \boldsymbol{r}_1} | \boldsymbol{r}_1 \rangle$ have been used.

Equations (3.44), (3.45) and (3.46) are general and can be used for analyzing the two-photon decay in any kind of atoms or ions.

In the next section, we will evaluate more explicitly $\mathcal{M}^{\gamma\gamma}$.

3.5 Evaluation of the second-order matrix element

3.5.1 General expression

In two-photon decays we have two photons to be detected. For treating the two-photon decay, we need to write the potential vector operator for a photon traveling along an arbitrary direction. For that purpose, we can safely use the multipole expansion in Eq. (2.57).

By employing Eq. (2.57) into Eq. (3.44), we find

$$
\begin{aligned}
\mathcal{M}^{\gamma\gamma}(i \to f) \;=\; & (2\pi) \sum_{L_1 L_2} \sum_{M_1 M_2} \sum_{p_1 p_2} (-i)^{L_1+L_2+p_1+p_2} \sqrt{(2L_1+1)(2L_2+1)} \\
& \times (\lambda_1)^{p_1}(\lambda_2)^{p_2} D^{L_1\,*}_{M_1\,\lambda_1}(\varphi_{k_1},\theta_{k_1},0) D^{L_2\,*}_{M_2\,\lambda_2}(\varphi_{k_2},\theta_{k_2},0) \\[4pt]
& \times \sum_\nu \Bigg(\frac{\langle f|\,\boldsymbol{\alpha}\cdot\boldsymbol{a}^{p_1\,*}_{L_1\,M_1}(k_1,\hat{\boldsymbol{r}})\,|\nu\rangle\,\langle\nu|\,\boldsymbol{\alpha}\cdot\boldsymbol{a}^{p_2\,*}_{L_2\,M_2}(k_2,\hat{\boldsymbol{r}})\,|i\rangle}{\omega_{\nu i}+\omega_2} \\
& \quad + \frac{\langle f|\,\boldsymbol{\alpha}\cdot\boldsymbol{a}^{p_2\,*}_{L_2\,M_2}(k_2,\hat{\boldsymbol{r}})\,|\nu\rangle\,\langle\nu|\,\boldsymbol{\alpha}\cdot\boldsymbol{a}^{p_1\,*}_{L_1\,M_1}(k_1,\hat{\boldsymbol{r}})\,|i\rangle}{\omega_{\nu i}+\omega_1} \Bigg) \quad .
\end{aligned}
\tag{3.47}
$$

In what follows, we will work with atomic states. Atomic states have, in general, defined angular momentum properties. They can be therefore described by ket of the type $|\beta, J, m_J\rangle$, where J and m_J are the magnitude and the projection along $\hat{z}$ of the angular momentum of the state, while β is a collective index to denote all the other quantum numbers needed to describe the state.

Now, since $\boldsymbol{a}^{p}_{L\,M}$ is an irreducible tensor of rank L [37], we can apply the transformation $\boldsymbol{a}^{p\,*}_{LM} = (-1)^{M+p+1} \boldsymbol{a}^{p}_{L-M}$ and, subsequently, the Wigner-Eckart theorem on the two matrix elements in the equation above:

$$
\begin{aligned}
\mathcal{M}^{\gamma\gamma}(i \to f) \;=\; & (2\pi) \sum_{L_1 L_2} \sum_{M_1 M_2} \sum_{p_1 p_2} (-i)^{L_1+L_2+p_1+p_2} \sqrt{(2L_1+1)(2L_2+1)} \\
& \times (\lambda_1)^{p_1}(\lambda_2)^{p_2} D^{L_1\,*}_{M_1\,\lambda_1}(\varphi_{k_1},\theta_{k_1},0) D^{L_2\,*}_{M_2\,\lambda_2}(\varphi_{k_2},\theta_{k_2},0)(-1)^{M_1+M_2+p_1+p_2} \\[4pt]
& \times \sum_\nu \Bigg(\frac{\langle J_\nu, m_{J_\nu}, L_1, -M_1 | J_f, m_{J_f}\rangle}{\sqrt{2J_\nu+1}} \frac{\langle J_i, m_{J_i}, L_2, -M_2 | J_\nu, m_{J_\nu}\rangle}{\sqrt{2J_i+1}} \\
& \times \frac{\langle \beta_f, J_f \| \boldsymbol{\alpha}\cdot\boldsymbol{a}^{p_1}_{L_1}(k_1,\hat{\boldsymbol{r}}) \| \beta_\nu, J_\nu\rangle \langle \beta_\nu, J_\nu \| \boldsymbol{\alpha}\cdot\boldsymbol{a}^{p_2}_{L_2}(k_2,\hat{\boldsymbol{r}}) \| \beta_i, J_i\rangle}{\omega_{\nu i}+\omega_2} \\
& + 1 \longleftrightarrow 2 \Bigg) \quad ,
\end{aligned}
\tag{3.48}
$$

where the symbol $1 \longleftrightarrow 2$ means the previous term enclosed in parentheses with the photon labels exchanged. We have furthermore used the fact that Clebsch-Gordan coefficients are real.

This general expression for the matrix element $\mathcal{M}^{\gamma\gamma}(i \to f)$ can be applied to study two-photon decays in any atom or ion.

3.5.2 INTEGRATING OVER THE PHOTONS DIRECTIONS

Equation (3.45) simplifies considerably if we integrate over the two photons' directions, i.e. if we look for the decay rate irrespectively of the photons' directions.

From Eq. (3.47), we define $V^{L_1 L_2}_{M_1 M_2}(k_1,k_2)$ as

$$
\begin{aligned}
V^{L_1 L_2}_{M_1 M_2}(k_1,k_2) = & (2\pi) \sum_{p_1 p_2} (-i)^{L_1+L_2+p_1+p_2} \sqrt{(2L_1+1)(2L_2+1)}(\lambda_1)^{p_1}(\lambda_2)^{p_2} \\
& \times \sum_\nu \Bigg(\frac{\langle f|\,\boldsymbol{\alpha}\cdot\boldsymbol{a}^{p_1\,*}_{L_1\,M_1}(k_1,\hat{\boldsymbol{r}})\,|\nu\rangle\,\langle\nu|\,\boldsymbol{\alpha}\cdot\boldsymbol{a}^{p_2\,*}_{L_2\,M_2}(k_2,\hat{\boldsymbol{r}})\,|i\rangle}{\omega_{\nu i}+\omega_2} + 1 \longleftrightarrow 2 \Bigg) \quad .
\end{aligned}
$$

With this, we can rewrite $\mathcal{M}^{\gamma\gamma}(i \to f)$ as

$$
\begin{aligned}
\mathcal{M}^{\gamma\gamma}(i \to f) \quad = \quad & \sum_{L_1 L_2} \sum_{M_1 M_2} V^{L_1 L_2}_{M_1 M_2}(k_1, k_2) \\
& \times D^{L_1 *}_{M_1 \lambda_1}(\varphi_{k_1}, \theta_{k_1}, 0) D^{L_2 *}_{M_2 \lambda_2}(\varphi_{k_2}, \theta_{k_2}, 0) \quad .
\end{aligned}
$$

The important thing to notice in the above equation is that only the Wigner matrices depend on the spherical angles of the photons' directions, while $V^{L_1 L_2}_{M_1 M_2}$ depends only on the magnitude of the vectors $\boldsymbol{k}_1$ and $\boldsymbol{k}_2$. Thus, by using Eq. (3.45) and the equivalence $\mathrm{d}\Omega_{\boldsymbol{p}_j} = \mathrm{d}\Omega_{\boldsymbol{k}_j}$ (as discussed in Eq. (3.17)), we can write

$$
\begin{aligned}
\frac{\mathrm{d}\Gamma^{\lambda_1 \lambda_2}}{\mathrm{d}E_1} = & \left(\frac{\alpha^2 E_1 (E_i - E_f - E_1)}{(2\pi)^3 \hbar^3} \right) \sum_{\substack{L_1 L_2 \\ M_1 M_2}} \sum_{\substack{L'_1 L'_2 \\ M'_1 M'_2}} V^{L_1 L_2}_{M_1 M_2}(k_1, k_2) V^{L'_1 L'_2 *}_{M'_1 M'_2}(k_1, k_2) \\
& \times \left(\int \mathrm{d}\Omega_{\boldsymbol{k}_1} D^{L_1 *}_{M_1 \lambda_1}(\varphi_{k_1}, \theta_{k_1}, 0) D^{L'_1}_{M'_1 \lambda_1}(\varphi_{k_1}, \theta_{k_1}, 0) \right) \\
& \times \left(\int \mathrm{d}\Omega_{\boldsymbol{k}_2} D^{L_2 *}_{M_2 \lambda_2}(\varphi_{k_2}, \theta_{k_2}, 0) D^{L'_2}_{M'_2 \lambda_2}(\varphi_{k_2}, \theta_{k_2}, 0) \right) \\
= & \left(\frac{\alpha^2 E_1 E_2}{(2\pi)^3 \hbar^3} \right) \sum_{\substack{L_1 L_2 \\ M_1 M_2}} \sum_{\substack{L'_1 L'_2 \\ M'_1 M'_2}} V^{L_1 L_2}_{M_1 M_2}(k_1, k_2) V^{L'_1 L'_2 *}_{M'_1 M'_2}(k_1, k_2) \\
& \times \frac{4\pi}{2L_1 + 1} \frac{4\pi}{2L_2 + 1} \delta_{L_1 L'_1} \delta_{M_1 M'_1} \delta_{L_2 L'_2} \delta_{M_2 M'_2} \\
= & \left(\frac{\alpha^2 E_1 E_2}{(2\pi)^3 \hbar^3} \right) \sum_{\substack{L_1 L_2 \\ M_1 M_2}} \frac{16\pi^2}{(2L_1 + 1)(2L_2 + 1)} \left| V^{L_1 L_2}_{M_1 M_2}(k_1, k_2) \right|^2 \quad .
\end{aligned}
$$

We can eventually write

$$
\frac{\mathrm{d}\Gamma^{\lambda_1 \lambda_2}}{\mathrm{d}E_1} \quad = \quad \left(\frac{\alpha^2 E_1 (E_i - E_f - E_1)}{(2\pi)^3 \hbar^3} \right) \sum_{L_1 L_2} \sum_{M_1 M_2} \left| \tilde{\mathcal{M}}^{\gamma\gamma}(i \to f) \right|^2_{E_2 = E_i - E_f - E_1}
$$

$$(3.49)$$

so that is has a structure similar to Eq. (3.45) but the matrix element involved is slightly different and reads[4]

$$
\begin{aligned}
\tilde{\mathcal{M}}^{\gamma\gamma}(i \to f) = & (8\pi^2) \sum_{p_1 p_2} (-i)^{p_1 + p_2} (\lambda_1)^{p_1} (\lambda_2)^{p_2} \\
& \times \sum_{\nu} \left(\frac{\langle f | \, \boldsymbol{\alpha} \cdot \boldsymbol{a}^{p_1 *}_{L_1 M_1}(k_1, \hat{\boldsymbol{r}}) \, | \nu \rangle \, \langle \nu | \, \boldsymbol{\alpha} \cdot \boldsymbol{a}^{p_2 *}_{L_2 M_2}(k_2, \hat{\boldsymbol{r}}) \, | i \rangle}{\omega_{\nu i} + \omega_2} + 1 \longleftrightarrow 2 \right) \quad .
\end{aligned}
$$

$$(3.50)$$

---

[4]The factor $(-i)^{L_1 + L_2}$ disappears because of the modulus squared.

Similarly to what done in Eq. (3.48), we can apply the the transformation $\boldsymbol{a}_{LM}^{p*} = (-1)^{M+p+1}\boldsymbol{a}_{L-M}^{p}$ and then use the Wigner-Eckart theorem to obtain

$$
\begin{aligned}
\tilde{\mathcal{M}}^{\gamma\gamma}(i \to f) \;=\; & (8\pi^2) \sum_{p_1\,p_2} (+i)^{p_1+p_2} (\lambda_1)^{p_1} (\lambda_2)^{p_2} \\
& \times \sum_{\nu} \Bigg(\frac{\langle J_\nu, m_{J_\nu}, L_1, -M_1 | J_f, m_{J_f}\rangle}{\sqrt{2J_\nu+1}} \frac{\langle J_i, m_{J_i}, L_2, -M_2 | J_\nu, m_{J_\nu}\rangle}{\sqrt{2J_i+1}} \\
& \times \frac{\langle \beta_f, J_f \| \boldsymbol{\alpha}\cdot\boldsymbol{a}_{L_1}^{p_1}(k_1,\hat{\boldsymbol{r}}) \| \beta_\nu, J_\nu\rangle \langle \beta_\nu, J_\nu \| \boldsymbol{\alpha}\cdot\boldsymbol{a}_{L_2}^{p_2}(k_2,\hat{\boldsymbol{r}}) \| \beta_i, J_i\rangle}{\omega_{\nu i} + \omega_2} \\
& + 1 \longleftrightarrow 2 \Bigg) \quad,
\end{aligned}
$$
(3.51)

where the phase $(-1)^{M_1+M_2}$ has been dropped because of the modulus squared and we have used $(-i)^p(-1)^p = (+i)^p$[5]. The elements $\langle \beta_1, J_1 \| \boldsymbol{\alpha}\cdot\boldsymbol{a}_L^p(k,\hat{\boldsymbol{r}}) \| \beta_2, J_2\rangle$ are scalars that do not depend upon geometrical properties of the system (they do not depend upon the angular momenta projections m_{J_1}, m_{J_2} and M).
We may now recall $M_1 \to -M_1$, $M_2 \to -M_2$ in $\tilde{\mathcal{M}}^{\gamma\gamma}$. The summations in Eq. (3.49) do not modify since they run from $-L_{1,2}$ to $L_{1,2}$. We get

$$
\begin{aligned}
\tilde{\mathcal{M}}^{\gamma\gamma}(i \to f) \;=\; & (8\pi^2) \sum_{p_1\,p_2} (+i)^{p_1+p_2} (\lambda_1)^{p_1} (\lambda_2)^{p_2} \\
& \times \sum_{\nu} \Bigg(\frac{\langle J_\nu, m_{J_\nu}, L_1, M_1 | J_f, m_{J_f}\rangle}{\sqrt{2J_\nu+1}} \frac{\langle J_i, m_{J_i}, L_2, M_2 | J_\nu, m_{J_\nu}\rangle}{\sqrt{2J_i+1}} \\
& \times \frac{\langle \beta_f, J_f \| \boldsymbol{\alpha}\cdot\boldsymbol{a}_{L_1}^{p_1}(k_1,\hat{\boldsymbol{r}}) \| \beta_\nu, J_\nu\rangle \langle \beta_\nu, J_\nu \| \boldsymbol{\alpha}\cdot\boldsymbol{a}_{L_2}^{p_2}(k_2,\hat{\boldsymbol{r}}) \| \beta_i, J_i\rangle}{\omega_{\nu i} + \omega_2} \\
& + 1 \longleftrightarrow 2 \Bigg) \quad,
\end{aligned}
$$

We can always explicitly write $\displaystyle\sum_{\nu}$ as $\displaystyle\sum_{\beta_\nu J_\nu m_{J_\nu}}$. Then, by defining,

$$
S^{J_\nu}(1,2) \equiv \sum_{\beta_\nu} \frac{\langle \beta_f, J_f \| \boldsymbol{\alpha}\cdot\boldsymbol{a}_{L_1}^{p_1}(k_1,\hat{\boldsymbol{r}}) \| \beta_\nu, J_\nu\rangle \langle \beta_\nu, J_\nu \| \boldsymbol{\alpha}\cdot\boldsymbol{a}_{L_2}^{p_2}(k_2,\hat{\boldsymbol{r}}) \| \beta_i, J_i\rangle}{\omega_{\nu i} + \omega_2} \qquad (3.52)
$$

and by using the 3-j symbol definition

$$
\langle J_1, m_{J_1}, J_2, m_{J_2} | J_3, m_{J_3}\rangle = (-1)^{J_1-J_2+m_{J_3}}\sqrt{2J_3+1}\begin{pmatrix} J_1 & J_2 & J_3 \\ m_{J_1} & m_{J_2} & -m_{J_3} \end{pmatrix}
$$

---

[5]we can do this since p is certainly integer.

we may rewrite Eq. (3.51) as

$$
\begin{aligned}
\tilde{\mathcal{M}}^{\gamma\gamma}(i \to f) \;=\; & (8\pi^2) \sum_{p_1\,p_2} (+i)^{p_1+p_2} (\lambda_1)^{p_1} (\lambda_2)^{p_2} \frac{(2J_f+1)^{1/2}}{(2J_i+1)^{1/2}} \\
& \times \sum_{J_\nu} \frac{(-1)^{-J_\nu}}{(2J_\nu+1)^{1/2}} \Big(\theta^{J_\nu}(1,2) S^{J_\nu}(1,2) + \theta^{J_\nu}(2,1) S^{J_\nu}(2,1) \Big) \;,
\end{aligned}
\tag{3.53}
$$

where we defined

$$
\begin{aligned}
\theta^{J_\nu}(1,2) \;=\; & (2J_\nu+1)^{1/2} \sum_{m_{J_\nu}} (-1)^{m_{J_f}+m_{J_\nu}+1} \\
& \times \begin{pmatrix} J_f & L_1 & J_\nu \\ -m_{J_f} & M_1 & m_{J_\nu} \end{pmatrix} \begin{pmatrix} J_\nu & L_2 & J_i \\ -m_{J_\nu} & M_2 & m_{J_i} \end{pmatrix} \;,
\end{aligned}
\tag{3.54}
$$

and where the $S^{j_\nu}_\omega$ elements, although not explicitly denoted, depend on p_1, p_2.
In deriving the above equation it has been used the symmetry properties of the 3-j symbols together with the fact that any phase of the type $(-1)^r$, where $r = L_1 + L_2, M_1 + M_2, J_i, m_{J_i}, J_f, m_{J_f}$ are inessential and can be dropped due to the modulus squared which wraps the amplitude, since they do not depend upon the summation over ν and are symmetric upon the exchange $1 \longleftrightarrow 2$. Indeed, the factor $(-1)^{m_{J_f}+1}$ in Eq. (3.54) can be dropped but it is left there for convenience since it allows to use the sum rules

$$
\sum_{M_1, M_2, m_{J_f}, m_{J_i}} \theta^{J_\nu}(1,2)\, \theta^{J'_\nu}(1,2) = \delta_{J_\nu, J'_\nu} \;\;,
$$

$$
\sum_{M_1, M_2, m_{J_f}, m_{J_i}} \theta^{J_\nu}(2,1)\, \theta^{J'_\nu}(2,1) = \delta_{J_\nu, J'_\nu} \;\;.
$$

We used also $(-1)^{3J_\nu} = (-1)^{4J_\nu}(-1)^{-J_\nu} = (-1)^{-J_\nu}$, being $4J_\nu$ certainly even integer.

3.5.3   INTEGRATING OVER PHOTONS DIRECTIONS AND SUMMING OVER PHOTONS POLARIZATIONS

Equations (3.50) and (3.53) further simplify if we sum over the photons polarizations, i.e. if we look for the decay rate irrespectively of photons directions and polarizations. By summing over photons polarizations (helicites), the differential decay rate (3.49) becomes

$$
\frac{\mathrm{d}\Gamma}{\mathrm{d}E_1} \;=\; \left(\frac{\alpha^2\, E_1(E_i - E_f - E_1)}{(2\pi)^3 \hbar^3} \right) \sum_{L_1 L_2} \sum_{M_1 M_2} \sum_{\lambda_1 \lambda_2} \Big| \tilde{\mathcal{M}}^{\gamma\gamma}(i \to f) \Big|^2_{E_2 = E_i - E_f - E_1} \;\;.
$$

Let us investigate in detail the above quantity. We have

$$\sum_{\lambda_1 \lambda_2} \left| \tilde{\mathcal{M}}^{\gamma\gamma}(i \to f) \right|^2 = (64\pi^4) \sum_{\substack{p_1 \, p_2 \\ p_1' \, p_2'}} (-i)^{p_1 + p_2 - p_1' - p_2'} \left(\sum_{\lambda_1 = \pm 1} (\lambda_1)^{p_1 + p_1'} \right) \left(\sum_{\lambda_2 = \pm 1} (\lambda_2)^{p_2 + p_2'} \right)$$

$$\times \sum_{\nu} \left(\frac{\langle f | \, \boldsymbol{\alpha} \cdot \boldsymbol{a}_{L_1 M_1}^{p_1 \, *}(k_1, \hat{\boldsymbol{r}}) \, | \nu \rangle \, \langle \nu | \, \boldsymbol{\alpha} \cdot \boldsymbol{a}_{L_2 M_2}^{p_2 \, *}(k_2, \hat{\boldsymbol{r}}) \, | i \rangle}{\omega_{\nu i} + \omega_2} + 1 \longleftrightarrow 2 \right)$$

$$\times \sum_{\nu'} \left(\frac{\langle f | \, \boldsymbol{\alpha} \cdot \boldsymbol{a}_{L_1 M_1}^{p_1' \, *}(k_1, \hat{\boldsymbol{r}}) \, | \nu' \rangle \, \langle \nu' | \, \boldsymbol{\alpha} \cdot \boldsymbol{a}_{L_2 M_2}^{p_2' \, *}(k_2, \hat{\boldsymbol{r}}) \, | i \rangle}{\omega_{\nu' i} + \omega_2} + 1 \longleftrightarrow 2 \right)^* \quad .$$

Now, similarly to Eq. (3.24), it follows that

$$\sum_{\lambda_1 = \pm 1} (\lambda_1)^{p_1 + p_1'} = 2\delta_{p_1, p_1'} \quad ,$$

$$\sum_{\lambda_2 = \pm 1} (\lambda_2)^{p_2 + p_2'} = 2\delta_{p_2, p_2'} \quad .$$

Then we have

$$\sum_{\lambda_1 \lambda_2} \left| \tilde{\mathcal{M}}^{\gamma\gamma}(i \to f) \right|^2 = 4(64\pi^4) \sum_{\substack{p_1 \, p_2 \\ p_1' \, p_2'}} (-i)^{p_1 + p_2 - p_1' - p_2'} \delta_{p_1, p_1'} \delta_{p_2, p_2'}$$

$$\times \sum_{\nu} \left(\frac{\langle f | \, \boldsymbol{\alpha} \cdot \boldsymbol{a}_{L_1 M_1}^{p_1 \, *}(k_1, \hat{\boldsymbol{r}}) \, | \nu \rangle \, \langle \nu | \, \boldsymbol{\alpha} \cdot \boldsymbol{a}_{L_2 M_2}^{p_2 \, *}(k_2, \hat{\boldsymbol{r}}) \, | i \rangle}{\omega_{\nu i} + \omega_2} + 1 \longleftrightarrow 2 \right)$$

$$\times \sum_{\nu'} \left(\frac{\langle f | \, \boldsymbol{\alpha} \cdot \boldsymbol{a}_{L_1 M_1}^{p_1' \, *}(k_1, \hat{\boldsymbol{r}}) \, | \nu' \rangle \, \langle \nu' | \, \boldsymbol{\alpha} \cdot \boldsymbol{a}_{L_2 M_2}^{p_2' \, *}(k_2, \hat{\boldsymbol{r}}) \, | i \rangle}{\omega_{\nu' i} + \omega_2} + 1 \longleftrightarrow 2 \right)^*$$

$$= \sum_{p_1 \, p_2} \left[4(64\pi^4) \right.$$

$$\times \sum_{\nu} \left(\frac{\langle f | \, \boldsymbol{\alpha} \cdot \boldsymbol{a}_{L_1 M_1}^{p_1 \, *}(k_1, \hat{\boldsymbol{r}}) \, | \nu \rangle \, \langle \nu | \, \boldsymbol{\alpha} \cdot \boldsymbol{a}_{L_2 M_2}^{p_2 \, *}(k_2, \hat{\boldsymbol{r}}) \, | i \rangle}{\omega_{\nu i} + \omega_2} + 1 \longleftrightarrow 2 \right)$$

$$\times \sum_{\nu'} \left. \left(\frac{\langle f | \, \boldsymbol{\alpha} \cdot \boldsymbol{a}_{L_1 M_1}^{p_1 \, *}(k_1, \hat{\boldsymbol{r}}) \, | \nu' \rangle \, \langle \nu' | \, \boldsymbol{\alpha} \cdot \boldsymbol{a}_{L_2 M_2}^{p_2 \, *}(k_2, \hat{\boldsymbol{r}}) \, | i \rangle}{\omega_{\nu' i} + \omega_2} + 1 \longleftrightarrow 2 \right)^* \right]$$

$$= \sum_{p_1 \, p_2} \left| \tilde{\tilde{\mathcal{M}}}^{\gamma\gamma}(i \to f) \right|^2 \quad ,$$

where

$$\tilde{\tilde{\mathcal{M}}}^{\gamma\gamma}(i \to f) = 16\pi^2 \sum_{\nu} \left(\frac{\langle f | \, \boldsymbol{\alpha} \cdot \boldsymbol{a}_{L_1 M_1}^{p_1 \, *}(k_1, \hat{\boldsymbol{r}}) \, | \nu \rangle \, \langle \nu | \, \boldsymbol{\alpha} \cdot \boldsymbol{a}_{L_2 M_2}^{p_2 \, *}(k_2, \hat{\boldsymbol{r}}) \, | i \rangle}{\omega_{\nu i} + \omega_2} \right.$$

$$+ \left. \frac{\langle f | \, \boldsymbol{\alpha} \cdot \boldsymbol{a}_{L_2 M_2}^{p_2 \, *}(k_2, \hat{\boldsymbol{r}}) \, | \nu \rangle \, \langle \nu | \, \boldsymbol{\alpha} \cdot \boldsymbol{a}_{L_1 M_1}^{p_1 \, *}(k_1, \hat{\boldsymbol{r}}) \, | i \rangle}{\omega_{\nu i} + \omega_1} \right) \quad .$$

In conclusion, the differential decay rate irrespectively of photons directions and polarizations is

$$\frac{\mathrm{d}\Gamma}{\mathrm{d}E_1} = \left(\frac{\alpha^2 \, E_1 (E_i - E_f - E_1)}{(2\pi)^3 \hbar^3} \right) \sum_{L_1 \, L_2} \sum_{M_1 \, M_2} \sum_{p_1 \, p_2} \left| \tilde{\tilde{\mathcal{M}}}^{\gamma\gamma}(i \to f) \right|^2 \Bigg|_{E_2 = E_i - E_f - E_1} .$$

As we have done in the previous section, we can express the amplitude $\tilde{\tilde{\mathcal{M}}}^{\gamma\gamma}$ in terms of the functions S^{J_ν} and θ^{J_ν}. We easily get

$$\tilde{\tilde{\mathcal{M}}}^{\gamma\gamma}(i \to f) = 16\pi^2 \frac{(2J_f + 1)^{1/2}}{(2J_i + 1)^{1/2}} \sum_\nu \frac{(-1)^{-J_\nu}}{(2J_\nu + 1)^{1/2}}$$
$$\times \left(\theta^{J_\nu}(1,2) S^{J_\nu}(1,2) + \theta^{J_\nu}(2,1) S^{J_\nu}(2,1) \right) .$$

The two above equations allow a direct comparison with Eq. (2.25) of Ref. [48].

3.5.4 NON-RELATIVISTIC AND LONG WAVELENGTH APPROXIMATIONS

The non-relativistic Hamiltonian is showed in Eq. (3.25) and it consists of two terms: The first term is proportional to α while the second term to α^2. By using that Hamiltonian in our master equation (3.10), we soon see that the first order term (second row) will contain a term proportional to α due to $e\dfrac{\hat{\mathbf{p}} \cdot \hat{\mathbf{A}}}{m}$ and a term proportional to α^2 due to $e^2 \hat{\mathbf{A}}^2$. On the other hand, the second order term (third row) will contain a term proportional to α^2 due to $e\dfrac{\hat{\mathbf{p}} \cdot \hat{\mathbf{A}}}{m}$ and a term proportional to α^4 due to $e^2 \hat{\mathbf{A}}^2$. In order to get the right terms for the description of the two-photon decay, we must evidently keep the two terms which are proportional to α^2. Since both terms have the same overall coefficient A_0 defined in Eq. (2.50), we are able to write the amplitude within non-relativistic approximation just readjusting the dimensions of the term due to $e^2 \hat{\mathbf{A}}$ to be "sec". We get

$$\mathcal{M}_{NR}^{\gamma\gamma}(i \to f) = \frac{\hbar}{mc^2} \langle f | \underline{\epsilon}_1^* \cdot \underline{\epsilon}_2^* \, e^{-i\boldsymbol{k}_1 \hat{\boldsymbol{r}}} e^{-i\boldsymbol{k}_2 \hat{\boldsymbol{r}}} | i \rangle$$
$$- \frac{1}{m^2 c^2} \sum_\nu \left(\frac{\langle f | \hat{\mathbf{p}} \cdot \underline{\epsilon}_1^* e^{-i\boldsymbol{k}_1 \hat{\boldsymbol{r}}} | \nu \rangle \langle \nu | \hat{\mathbf{p}} \cdot \underline{\epsilon}_2^* e^{-i\boldsymbol{k}_2 \hat{\boldsymbol{r}}} | i \rangle}{\omega_{\nu i} + \omega_2} \right.$$
$$\left. + \frac{\langle f | \hat{\mathbf{p}} \cdot \underline{\epsilon}_2^* e^{-i\boldsymbol{k}_2 \hat{\boldsymbol{r}}} | \nu \rangle \langle \nu | \hat{\mathbf{p}} \cdot \underline{\epsilon}_1^* e^{-i\boldsymbol{k}_1 \hat{\boldsymbol{r}}} | i \rangle}{\omega_{\nu i} + \omega_1} \right) .$$

In order to further simplify the amplitude, we make also *lwa* to get:

$$\mathcal{M}_{NR\&lwa}^{\gamma\gamma}(i \to f) = \frac{\hbar}{mc^2} \langle f | \underline{\epsilon}_1^* \cdot \underline{\epsilon}_2^* | i \rangle - \frac{1}{m^2 c^2} \sum_\nu \left(\frac{\langle f | \hat{\mathbf{p}} \cdot \underline{\epsilon}_1^* | \nu \rangle \langle \nu | \hat{\mathbf{p}} \cdot \underline{\epsilon}_2^* | i \rangle}{\omega_{\nu i} + \omega_2} \right.$$
$$\left. + \frac{\langle f | \hat{\mathbf{p}} \cdot \underline{\epsilon}_2^* | \nu \rangle \langle \nu | \hat{\mathbf{p}} \cdot \underline{\epsilon}_1^* | i \rangle}{\omega_{\nu i} + \omega_1} \right)$$
$$= \frac{\hbar}{mc^2} \langle f | \underline{\epsilon}_1^* \cdot \underline{\epsilon}_2^* | i \rangle + \frac{1}{c^2} \sum_\nu \omega_{f\nu} \omega_{\nu i} \left(\frac{\langle f | \hat{\mathbf{r}} \cdot \underline{\epsilon}_1^* | \nu \rangle \langle \nu | \hat{\mathbf{r}} \cdot \underline{\epsilon}_2^* | i \rangle}{\omega_{\nu i} + \omega_2} \right.$$
$$\left. + \frac{\langle f | \hat{\mathbf{r}} \cdot \underline{\epsilon}_2^* | \nu \rangle \langle \nu | \hat{\mathbf{r}} \cdot \underline{\epsilon}_1^* | i \rangle}{\omega_{\nu i} + \omega_1} \right) ,$$
$$(3.55)$$

where the Heisemberg equation

$$\langle s| \hat{\mathbf{p}} |t\rangle = i\, m\, \omega_{st}\, \langle s| \hat{\mathbf{r}} |t\rangle$$

has been used.

Now we make a nifty trick, which follows from the anticommutator relation between $\hat{\mathrm{r}}_i$ and $\hat{\mathrm{p}}_j$

$$\hat{\mathrm{r}}_i\hat{\mathrm{p}}_j - \hat{\mathrm{p}}_j\hat{\mathrm{r}}_i = i\hbar\delta_{ij} \quad .$$

We write

$$\underline{\epsilon}_1^* \cdot \underline{\epsilon}_2^* = \epsilon_{1\,i}^*\epsilon_{2\,i}^* = \epsilon_{1\,i}^*\epsilon_{2\,j}^*\delta_{ij} = -\frac{i}{\hbar}\epsilon_{1\,i}^*\epsilon_{2\,j}^*(\hat{\mathrm{r}}_i\hat{\mathrm{p}}_j - \hat{\mathrm{p}}_j\hat{\mathrm{r}}_i)$$

$$= -\frac{i}{\hbar}\left((\underline{\epsilon}_1^* \cdot \hat{\mathbf{r}})(\underline{\epsilon}_2^* \cdot \hat{\mathbf{p}}) - (\underline{\epsilon}_2^* \cdot \hat{\mathbf{p}})(\underline{\epsilon}_1^* \cdot \hat{\mathbf{r}}) \right) \quad .$$

The first element in Eq. (3.55) is therefore

$$\frac{\hbar}{mc^2}\langle f| \underline{\epsilon}_1^* \cdot \underline{\epsilon}_2^* |i\rangle = -\frac{i}{mc^2}\sum_\nu \Big(\langle f| \underline{\epsilon}_1^* \cdot \hat{\mathbf{r}} |\nu\rangle \langle \nu| \underline{\epsilon}_2^* \cdot \hat{\mathbf{p}} |i\rangle - \langle f| \underline{\epsilon}_2^* \cdot \hat{\mathbf{p}} |\nu\rangle \langle \nu| \underline{\epsilon}_1^* \cdot \hat{\mathbf{r}} |i\rangle \Big)$$

$$= \frac{1}{c^2}\sum_\nu \Big(\omega_{\nu i}\langle f| \underline{\epsilon}_1^* \cdot \hat{\mathbf{r}} |\nu\rangle \langle \nu| \underline{\epsilon}_2^* \cdot \hat{\mathbf{r}} |i\rangle - \omega_{f\nu}\langle f| \underline{\epsilon}_2^* \cdot \hat{\mathbf{r}} |\nu\rangle \langle \nu| \underline{\epsilon}_1^* \cdot \hat{\mathbf{r}} |i\rangle \Big) \quad .$$

Altogether we get

$$\begin{aligned}
\mathcal{M}_{NR\&lwa}^{\gamma\gamma}(i \to f) &= \frac{1}{c^2}\sum_\nu \Bigg[\left(\frac{\omega_{f\nu}\omega_{\nu\,i}}{\omega_{\nu i} + \omega_2} + \omega_{\nu i} \right) \langle f| \hat{\mathbf{r}} \cdot \underline{\epsilon}_1^* |\nu\rangle \langle \nu| \hat{\mathbf{r}} \cdot \underline{\epsilon}_2^* |i\rangle \\
&\qquad + \left(\frac{\omega_{f\nu}\omega_{\nu i}}{\omega_{\nu i} + \omega_1} - \omega_{f\nu} \right) \langle f| \hat{\mathbf{r}} \cdot \underline{\epsilon}_2^* |\nu\rangle \langle \nu| \hat{\mathbf{r}} \cdot \underline{\epsilon}_1^* |i\rangle \Bigg] \\
&= \frac{\omega_1}{c^2}\sum_\nu \Bigg[\left(\frac{\omega_{i\nu}}{\omega_{\nu i} + \omega_2} \right) \langle f| \hat{\mathbf{r}} \cdot \underline{\epsilon}_1^* |\nu\rangle \langle \nu| \hat{\mathbf{r}} \cdot \underline{\epsilon}_2^* |i\rangle \\
&\qquad - \left(\frac{\omega_{f\nu}}{\omega_{\nu i} + \omega_1} \right) \langle f| \hat{\mathbf{r}} \cdot \underline{\epsilon}_2^* |\nu\rangle \langle \nu| \hat{\mathbf{r}} \cdot \underline{\epsilon}_1^* |i\rangle \Bigg] \quad .
\end{aligned}$$

The differential decay rate is then obtained by plugging the above matrix element into Eq. (3.45):

$$\frac{\mathrm{d}\Gamma^{\lambda_1\lambda_2}}{\mathrm{d}E_1\mathrm{d}\Omega_{\boldsymbol{p}_1}\mathrm{d}\Omega_{\boldsymbol{p}_2}}\bigg|_{NR\&lwa} = \left(\frac{\alpha^2\, E_1(E_i - E_f - E_1)}{(2\pi)^3\hbar^3} \right) \Big| \mathcal{M}_{NR\&lwa}^{\gamma\gamma}(i \to f) \Big|_{E_2 = E_i - E_f - E_1}^2 \quad .$$
$$\tag{3.56}$$

Remarks and comments

The remarks we made in Sec. 3.3.4 are here similar. That is, the non-relativistic (double) dipole operator is unable to link atomic states with different spin or different parity. The parity of the intermediate state must then be opposite of the parity of the

initial and final states. Using the same notation as in Sec. 3.3.4, we may summarize as follows:

$$\Delta S = 0$$
$$\Delta m_S = 0$$
$$\Delta l = 0$$
$$J_{f(i)} \otimes 1 \otimes 1 = J_{i(f)} \quad .$$

With formula (3.56), we could account, for instance, for the two-photon decay $2s_{1/2} \to 1s_{1/2}$ in hydrogen-like atoms.

3.5.5 HYDROGEN-LIKE IONS

In this subsection, we will evaluate $\mathcal{M}^{\gamma\gamma}(i \to f)$ specifically for hydrogen-like ions. Concerning Hydrogen and hydrogen-like ions, we know the exact wavefunctions which characterize the states. The evaluation of the matrix element $\mathcal{M}^{\gamma\gamma}(i \to f)$ can be made more in detail.

Let us come back to Eq. (3.47). We insert the unit operator $\int \mathrm{d}r^3 |\boldsymbol{r}\rangle \langle \boldsymbol{r}|$ to get wavefunctions instead of ket states and we write explicitly the elements $\boldsymbol{a}_{LM}^{p*}$. We obtain:

$$
\mathcal{M}^{\gamma\gamma}(i \to f) = (2\pi) \int \mathrm{d}^3 r_1 \mathrm{d}^3 r_2 \sum_{L_1 L_2} \sum_{M_1 M_2} \sum_{\nu} (-i)^{L_1+L_2} [L_1, L_2]^{1/2}
$$

$$
\times \ D_{M_1 \lambda_1}^{L_1 *}(\varphi_{k_1}, \theta_{k_1}, 0) D_{M_2 \lambda_2}^{L_2 *}(\varphi_{k_2}, \theta_{k_2}, 0)
$$

$$
\times \ \Psi_f^\dagger(\boldsymbol{r}_1) \boldsymbol{\alpha} \cdot \left(\boldsymbol{A}_{L_1 M_1}^{(m)}(k_1, \boldsymbol{r}_1) + i\lambda_1 \boldsymbol{A}_{L_1 M_1}^{(e)}(k_1, \boldsymbol{r}_1) \right)^* \frac{\Psi_\nu(\boldsymbol{r}_1)}{\omega_{\nu i} + \omega_2}
$$

$$
\times \ \Psi_\nu^\dagger(\boldsymbol{r}_2) \boldsymbol{\alpha} \cdot \left(\boldsymbol{A}_{L_2 M_2}^{(m)}(k_2, \boldsymbol{r}_2) + i\lambda_2 \boldsymbol{A}_{L_2 M_2}^{(e)}(k_2, \boldsymbol{r}_2) \right)^* \Psi_i(\boldsymbol{r}_2) \ + \ 1 \longleftrightarrow 2 \quad ,
$$

where we introduced the notation $[L_1, L_2, ...] = (2L_1 + 1)(2L_2 + 1)...$.
Now, consider that

$$
\left(\boldsymbol{A}_{LM}^{(m)}(k, \boldsymbol{r}) + i\lambda \boldsymbol{A}_{LM}^{(e)}(k, \boldsymbol{r}) \right)^* = \left(J_L(kr) \boldsymbol{T}_{LLM}(\underline{r}) \right.
$$

$$
\left. + i\lambda J_{L-1}(k, r) \sqrt{\frac{L+1}{2L+1}} \boldsymbol{T}_{LL-1M}(\underline{r}) - i\lambda J_{L+1}(kr) \sqrt{\frac{L}{2L+1}} \boldsymbol{T}_{LL+1M}(\underline{r}) \right)^*
$$

$$
= \left(\sum_{p=0,1} \sum_{\Lambda=L-1}^{L+1} (i\lambda)^p J_\Lambda(kr) \boldsymbol{T}_{L\Lambda M}(\underline{r}) \xi_{L\Lambda}^p \right)^* \quad ,
$$

where

$$
\xi_{L\Lambda}^0 = \delta_{L,\Lambda} \quad , \qquad \xi_{L\Lambda}^1 = \begin{cases} \sqrt{\dfrac{L+1}{2L+1}} & \Lambda = L-1 \\[2mm] -\sqrt{\dfrac{L}{2L+1}} & \Lambda = L+1 \\[2mm] 0 & \text{otherwise} \end{cases} \quad .
$$

Altogether we obtain

$$
\begin{aligned}
\mathcal{M}^{\gamma\gamma}(i \to f) = \sum_{\nu} \int d^3r_1 d^3r_2 \Bigg\{ (2\pi) \sum_{L_1 L_2} \sum_{M_2 M_1} \sum_{\Lambda_1 \Lambda_2} \sum_{p_1 p_2 = 0,1} (-i\lambda_1)^{p_1} (-i\lambda_2)^{p_2} \times \\
\times \ i^{-L_1 - L_2} [L_1, L_2]^{1/2} \xi_{L_1 \Lambda_1}^{p_1} \xi_{L_2 \Lambda_2}^{p_2} D_{M_1 \lambda_1}^{L_1 *}(\varphi_{k_1}, \theta_{k_1}, 0) D_{M_2 \lambda_2}^{L_2 *}(\varphi_{k_2}, \theta_{k_2}, 0) \Bigg\}
\end{aligned}
$$

$$
\times \ J_{\Lambda_1}(k_1 r_1) J_{\Lambda_2}(k_2 r_2) \Psi_f^\dagger(\boldsymbol{r}_1) \boldsymbol{\alpha} \cdot \boldsymbol{T}_{L_1 \Lambda_1 M_1}^*(\underline{r}_1) \frac{\Psi_\nu(\boldsymbol{r}_1) \Psi_\nu^\dagger(\boldsymbol{r}_2)}{\omega_{\nu i} + \omega_1}
$$

$$
\times \ \boldsymbol{\alpha} \cdot \boldsymbol{T}_{L_2 \Lambda_2 M_2}^*(\underline{r}_2) \Psi_i(\boldsymbol{r}_2) \ + \ 1 \longleftrightarrow 2
$$

$$
= \sum_\nu \frac{C_1}{\omega_{\nu i} + \omega_1} \int d^3r_1 \, d^3r_2 J_{\Lambda_1}(k_1 r_1) J_{\Lambda_2}(k_2 r_2)
$$

$$
\times \ \Psi_f^\dagger(\boldsymbol{r}_1) \boldsymbol{\alpha} \cdot \boldsymbol{T}_{L_1 \Lambda_1 M_1}^*(\underline{r}_1) \Psi_\nu(\boldsymbol{r}_1) \Psi_\nu^\dagger(\boldsymbol{r}_2) \boldsymbol{\alpha} \cdot \boldsymbol{T}_{L_2 \Lambda_2 M_2}^*(\underline{r}_2) \Psi_i(\boldsymbol{r}_2) \quad ,
$$

$$
+ \ 1 \longleftrightarrow 2
\tag{3.57}
$$

where we used the fact that Bessel functions are real and we defined C_1, for shortening the lines, as the element enclosed in curly brackets:

$$
C_1 = \{...\} \quad .
$$

It must be clear that C_1 is not a scalar and must be left in the position where it is. We may say it is an operator.

We know from Eq. (2.8) that the Dirac hydrogenic wavefunction of the initial state, for instance, is of the type

$$
\Psi_i(\boldsymbol{r}) = \begin{pmatrix} g_{n_i \kappa_i}(r) \Omega_{j_i l_i m_{j_i}}(\underline{r}) \\ i f_{n_i \kappa_i}(r) \Omega_{j_i l_i' m_{j_i}}(\underline{r}) \end{pmatrix} = \begin{pmatrix} g_i(r) \Omega_{l_i}(\underline{r}) \\ i f_i(r) \Omega_{l_i'}(\underline{r}) \end{pmatrix} \quad ,
\tag{3.58}
$$

where, in the last step, we have grouped the quantum numbers for the sake of shortness. We have

$$
\Psi_f^\dagger(\boldsymbol{r}_1) \boldsymbol{\alpha} \Psi_\nu(\boldsymbol{r}_1) = -i f_f^* g_\nu \Omega_{l_f'}^* \boldsymbol{\sigma} \Omega_{l_\nu} + i g_f^* f_\nu \Omega_{l_f}^* \boldsymbol{\sigma} \Omega_{l_\nu'}
$$

$$
\Psi_\nu^\dagger(\boldsymbol{r}_2) \boldsymbol{\alpha} \Psi_i(\boldsymbol{r}_2) = -i f_\nu^* g_i \Omega_{l_\nu'}^* \boldsymbol{\sigma} \Omega_{l_i} + i g_\nu^* f_i \Omega_{l_\nu}^* \boldsymbol{\sigma} \Omega_{l_i'} \quad .
\tag{3.59}
$$

In the above equation, we have dropped the r_1, $\underline{r}_1$, r_2 and $\underline{r}_2$ dependence, for clearness. There is no confusion since we can restore it in the future by using the following

$$
\begin{array}{llll}
f_f^* = f_f^*(r_1) & g_f^* = g_f^*(r_1) & \Omega_{l_f'}^* = \Omega_{l_f'}^*(\underline{r}_1) & \Omega_{l_f}^* = \Omega_{l_f}^*(\underline{r}_1) \\[4pt]
f_\nu = f_\nu(r_1) & g_\nu = g_\nu(r_1) & \Omega_{l_\nu} = \Omega_{l_\nu}(\underline{r}_1) & \Omega_{l_\nu} = \Omega_{l_\nu}(\underline{r}_1) \\[4pt]
f_\nu^* = f_\nu^*(r_2) & g_\nu^* = g_\nu^*(r_2) & \Omega_{l_\nu'}^* = \Omega_{l_\nu'}^*(\underline{r}_2) & \Omega_{l_\nu}^* = \Omega_{l_\nu}^*(\underline{r}_2) \\[4pt]
f_i = f_i(r_2) & g_i = g_i(r_2) & \Omega_{l_i'} = \Omega_{l_i'}(\underline{r}_2) & \Omega_{l_i} = \Omega_{l_i}(\underline{r}_2) \quad .
\end{array}
$$

Plugging Eq. (3.59) into Eq. (3.57), we get

$$
\begin{aligned}
\mathcal{M}^{\gamma\gamma}(i \to f) &= \sum_\nu \frac{C_1}{\omega_{\nu i} + \omega_1} \int \mathrm{d}^3 r_1 \mathrm{d}^3 r_2 \, J_{\Lambda_1}(k_1 r_1) J_{\Lambda_2}(k_2 r_2) \\
&\quad \times \left(-i f_f^* g_\nu \Omega_{l_f'}^* \boldsymbol{\sigma} \Omega_{l_\nu} + i g_f^* f_\nu \Omega_{l_f}^* \boldsymbol{\sigma} \Omega_{l_\nu'} \right) \cdot \boldsymbol{T}_{L_1 \Lambda_1 M_1}^*(\underline{r}_1) \\
&\quad \times \left(-i f_\nu^* g_i \Omega_{l_\nu'}^* \boldsymbol{\sigma} \Omega_{l_i} + i g_\nu^* f_i \Omega_{l_\nu}^* \boldsymbol{\sigma} \Omega_{l_i'} \right) \cdot \boldsymbol{T}_{L_2,\Lambda_2,M_2}^*(\underline{r}_2) \\
&\quad + 1 \longleftrightarrow 2 \\[6pt]
&= \sum_\nu \frac{C_1}{\omega_{\nu i} + \omega_1} \int \mathrm{d}r_1 \mathrm{d}r_2 \, r_1^2 r_2^2 \, J_{\Lambda_1}(k_1 r_1) J_{\Lambda_2}(k_2 r_2) \\
&\quad \times \left(-i f_f^* g_\nu \langle l_f' J_f m_{J_f} | \hat{\boldsymbol{\sigma}} \cdot \boldsymbol{T}_{L_1 \Lambda_1 M_1}^*(\hat{r}_1) | l_\nu J_\nu m_{J_\nu} \rangle \right. \\
&\quad \left. + i g_f^* f_\nu \langle l_f J_f m_{J_f} | \hat{\boldsymbol{\sigma}} \cdot \boldsymbol{T}_{L_1 \Lambda_1 M_1}^*(\hat{r}_1) | l_\nu' J_\nu m_{J_\nu} \rangle \right) \\
&\quad \times \left(-i f_\nu^* g_i \langle l_\nu' J_\nu m_{J_\nu} | \hat{\boldsymbol{\sigma}} \cdot \boldsymbol{T}_{L_2 \Lambda_2 M_2}^*(\hat{r}_2) | l_i J_i m_{J_i} \rangle \right. \\
&\quad \left. + i g_\nu^* f_i \langle l_\nu J_\nu m_{J_\nu} | \hat{\boldsymbol{\sigma}} \cdot \boldsymbol{T}_{L_2 \Lambda_2 M_2}^*(\hat{r}_2) | l_i' J_i m_{J_i} \rangle \right) \\
&\quad + 1 \longleftrightarrow 2 \quad ,
\end{aligned}
$$

where the formal relation

$$
\begin{aligned}
\int \mathrm{d}\Omega \, \Omega_{l_1}^* \boldsymbol{\sigma} \Omega_{l_2} &= \int \mathrm{d}\Omega \, \langle l_1 J_1 m_{J_1} | \Omega \rangle \hat{\boldsymbol{\sigma}} \langle \Omega | l_2 J_2 m_{J_2} \rangle \\
&= \langle l_1 J_1 m_{J_1} | \hat{\boldsymbol{\sigma}} | l_2 J_2 m_{J_2} \rangle \int \mathrm{d}\Omega \, | \Omega \rangle \langle \Omega | \\
&= \langle l_1 J_1 m_{J_1} | \hat{\boldsymbol{\sigma}} | l_2 J_2 m_{J_2} \rangle
\end{aligned}
$$

has been used.

By expanding the multiplication and by replacing C_1 with his definition we finally get

$$
\begin{aligned}
\mathcal{M}^{\gamma\gamma}(i \to f) = (-2\pi) \sum_{T,T'=L,S} \sum_{J_\nu, m_{J_\nu}, l_\nu} \sum_{L_1, L_2 = 1}^{+\infty} \sum_{M_1 = -L_1}^{L_1} \sum_{M_2 = -L_2}^{L_2} \sum_{p_1, p_2 = 0, 1} \sum_{\Lambda_1 = L_1 - 1}^{L_1 + 1} \sum_{\Lambda_2 = L_2 - 1}^{L_2 + 1} \\[4pt]
\times \; (\lambda_1)^{p_1} (\lambda_2)^{p_2} i^{-L_1 - L_2 - p_1 - p_2} [L_1, L_2]^{1/2} \xi_{L_1 \Lambda_1}^{p_1} \xi_{L_2 \Lambda_2}^{p_2} \\[4pt]
\times \; D_{M_1 \lambda_1}^{L_1 *}(\varphi_{k_1}, \theta_{k_1}, 0) D_{M_2 \lambda_2}^{L_2 *}(\varphi_{k_2}, \theta_{k_2}, 0) P^T P^{T'} \\[4pt]
\times \left[\langle l_f^T J_f m_{J_f} | \hat{\boldsymbol{\sigma}} \cdot \boldsymbol{T}_{L_1 \Lambda_1 M_1}^*(\hat{r}_1) | l_\nu^{\bar{T}} J_\nu m_{J_\nu} \rangle \langle l_\nu^{T'} J_\nu m_{J_\nu} | \hat{\boldsymbol{\sigma}} \cdot \boldsymbol{T}_{L_2 \Lambda_2 M_2}^*(\hat{r}_2) | l_i^{\bar{T}'} J_i m_{J_i} \rangle \right. \\[4pt]
\left. \times \left(\int \mathrm{d}r_1 \mathrm{d}r_2 \, r_1^2 r_2^2 \, J_{\Lambda_1}(k_1 r_1) J_{\Lambda_2}(k_2 r_2) \sum_{n_\nu} \frac{U_\nu^{TT'}}{\omega_{\nu i} + \omega_1} \right) \right.
\end{aligned}
$$

$$+ \; \langle l_f^T J_f m_{J_f} | \, \hat{\boldsymbol{\sigma}} \cdot \boldsymbol{T}^*_{L_2 \, \Lambda_2 \, M_2}(\hat{r}_1) \, | l_\nu^{\bar{T}} J_\nu m_{J_\nu} \rangle \, \langle l_\nu^{T'} J_\nu m_{J_\nu} | \, \hat{\boldsymbol{\sigma}} \cdot \boldsymbol{T}^*_{L_1 \, \Lambda_1 \, M_1}(\hat{r}_2) \, | l_i^{\bar{T}'} J_i m_{J_i} \rangle$$

$$\times \; \left(\int dr_1 dr_2 r_1^2 r_2^2 J_{\Lambda_2}(k_2 r_1) J_{\Lambda_1}(k_1 r_2) \sum_{n_\nu} \frac{U_\nu^{TT'}}{\omega_{\nu i} + \omega_1} \right) \Bigg] \quad , \quad (3.60)$$

where we defined

$$U_\nu^{TT'} \;\; = \;\; \begin{cases} f_f^* g_\nu f_\nu^* g_i = f_f^*(r_1) g_\nu(r_1) f_\nu^*(r_2) g_i(r_2) & \text{for} \quad T = L, T' = L \\[4pt] f_f^* g_\nu g_\nu^* f_i = f_f^*(r_1) g_\nu(r_1) g_\nu^*(r_2) f_i(r_2) & \text{for} \quad T = L, T' = S \\[4pt] g_f^* f_\nu f_\nu^* g_i = g_f^*(r_1) f_\nu(r_1) f_\nu^*(r_2) g_i(r_2) & \text{for} \quad T = S, T' = L \\[4pt] g_f^* f_\nu g_\nu^* f_i = g_f^*(r_1) f_\nu(r_1) g_\nu^*(r_2) f_i(r_2) & \text{for} \quad T = S, T' = S \end{cases}$$

$$= \;\; h_f^{\bar{T}\,*}(r_1) \, h_\nu^T(r_1) \, h_\nu^{\bar{T}'\,*}(r_2) \, h_i^{T'}(r_2) \quad ,$$

together with

$$\bar{T} = \begin{cases} L & \text{for} \quad T = S \\ S & \text{for} \quad T = L \end{cases} \quad , \quad P^T = \begin{cases} 1 & \text{for} \quad T = L \\ -1 & \text{for} \quad T = S \end{cases}$$

$$h^T = \begin{cases} g & \text{for} \quad T = L \\ f & \text{for} \quad T = S \end{cases} \quad .$$

If one wants straight away to calculate the expression for $\mathcal{M}^{\gamma\gamma}(i \to f)$, he will soon notice that there are some technical difficulties. Indeed, there are three infinite summations: over L_1, L_2 and n_ν. Concerning the first two, one easily sees that, for any normal transition, the summations converge fast: the first two terms of each summation ($L_{1,2} = 1, 2$) represent more than the 95% of the total contribution. The serious problem is the third summation, the one over n_ν. This summation does not converge fast at all. On the contrary, quite for many transitions, even the contribution of the negative continuum part of the spectrum plays a sizeable role [49]. This summation is part of the term enclosed in parentheses, which is the radial integral of the transition. We must analyze it carefully.

First of all, we explicitly write

$$\mathcal{K}_\nu^{TT'} \equiv \sum_{n_\nu} \frac{U_\nu^{TT'}}{\omega_{\nu i} + \omega_1} \;\; = \;\; h_f^{\bar{T}\,*}(r_1) \, \hbar \left(\sum_{n_\nu} \frac{h_\nu^T(r_1) \, h_\nu^{\bar{T}'\,*}(r_2)}{E_\nu - (E_i - E_1)} \right) h_i^{T'}(r_2)$$

$$= \;\; h_f^{\bar{T}\,*}(r_1) \, \hbar \mathcal{Z}_{\nu \, (E_i - E_1)}^{TT'} \, h_i^{T'}(r_2) \quad , \tag{3.61}$$

where we defined $\mathcal{Z}_{\nu \, (E_i - E_1)}^{TT'}$ as the element enclosed in parentheses.

Then, we have seen in Eq. (2.14) how the Green function for the Dirac-Coulomb problem can be formally written as

$$G_E(\boldsymbol{r}_1, \boldsymbol{r}_2) = \sum_\nu \frac{\Psi_\nu(\boldsymbol{r}_1) \Psi_\nu^\dagger(\boldsymbol{r}_2)}{E_\nu - E} \quad .$$

With the help of Eq. (3.58), we can write the Green function above as the following matrix:

$$G_E(\boldsymbol{r}_1, \boldsymbol{r}_2) = \sum_\nu \frac{1}{E_\nu - E}$$

$$\times \begin{pmatrix} g_\nu(r_1)g_\nu^*(r_2)\,\Omega_{l_\nu}(\underline{r}_1)\Omega_{l_\nu}^*(\underline{r}_2) & -ig_\nu(r_1)f_\nu^*(r_2)\,\Omega_{l_\nu}(\underline{r}_1)\Omega_{l_\nu'}^*(\underline{r}_2) \\ if_\nu(r_1)g_\nu^*(r_2)\Omega_{l_\nu'}(\underline{r}_1)\Omega_{l_\nu}^*(\underline{r}_2) & f_\nu(r_1)f_\nu^*(r_2)\Omega_{l_\nu'}(\underline{r}_1)\Omega_{l_\nu'}^*(\underline{r}_2) \end{pmatrix} .$$

We now easily see that the radial parts of the Green function contains the elements we need in Eq. (3.61) for the definition of Z_ν.
The explicit correspondence is:

$$\begin{aligned} Z_{\nu\,(E_i-E_1)}^{LL} &= g_{\kappa\,(E_i-E_1)}^{12} & Z_{\nu\,(E_i-E_1)}^{LS} &= g_{\kappa\,(E_i-E_1)}^{11} \\ Z_{\nu\,(E_i-E_1)}^{SL} &= g_{\kappa\,(E_i-E_1)}^{22} & Z_{\nu\,(E_i-E_1)}^{SS} &= g_{\kappa\,(E_i-E_1)}^{21} \end{aligned} .$$

(3.62)

The analytical expressions of the radial elements of the Green function have been showed and derived in detail in Sec. 2.3. Therefore, equations (3.62), (3.61) and (3.60) complete the theoretical analysis of this section.

CHAPTER 4

DENSITY MATRIX APPROACH

We are never in a position to say what really is or what really happens, but we can only say what will be observed in any concrete individual case. Will we have to be permanently satisfied with this? On principle, yes. On principle, there is nothing new in the postulate that in the end exact science should aim at nothing more than the description of what can really be observed. The question is only whether from now on we shall have to refrain from tying description to a clear hypothesis about the real nature of the world. There are many who wish to pronounce such abdication even today.
But I believe that this means making things a little too easy for oneself.

Erwin Schrödinger, 1933

This makes the reality of P [momentum] and Q [position] depend upon the process of measurement carried out on the first system, which does not disturb the second system in any way. No reasonable definition of reality could be expected to permit this.

A. Einstein, B. Podolsky, N. Rosen, 1935

In quantum mechanics, a ket vector can successfully describe either one particle state or an ensemble of particles with identical states. When we have an ensemble of particles with different states, we cannot describe that ensemble by means of a ket vector. The example that it is usually made for proving this statement is the following. Imagine that we fix a z direction in the space and that we have, for instance, an ensemble of particles of which the 50% have spin state $|S_z, +\hbar/2\rangle$ and the rest 50% have spin state $|S_z, -\hbar/2\rangle$. If we then use a Stern&Gerlach (SG) apparatus for measuring the spin of the particles [50], the outcome will always be two bunches of particles in two separate directions, irrespectively of the direction along which the magnetic field of the SG apparatus is set. This results is actually the proof of the fact that the measured

ensemble is maximally unpolarized.

On the other hand, if we naively tried to associate the ket vector

$$|E\rangle = \frac{1}{\sqrt{2}}\Big(|S_z, +\hbar/2\rangle + |S_z, -\hbar/2\rangle \Big) \qquad (4.1)$$

to the ensemble, we would soon see that this description takes to wrong predictions. By using the relations

$$|S_x, +\frac{\hbar}{2}\rangle = \frac{1}{\sqrt{2}}\Big(|S_z, +\hbar/2\rangle + |S_z, -\hbar/2\rangle \Big)$$

$$|S_x, -\frac{\hbar}{2}\rangle = \frac{1}{\sqrt{2}}\Big(|S_z, +\hbar/2\rangle - |S_z, -\hbar/2\rangle \Big) \quad ,$$

which link spin states defined along the $\hat{z}$ directions with spin states defined along the $\underline{x}$ direction [25], we may rewrite Eq. (4.1) as

$$|E\rangle = |S_x, +\hbar/2\rangle \quad .$$

The predictions we would then make are that the outcome of a SG apparatus applied on measuring the spin of the ensemble should be only one bunch of particles if the magnetic field is set along the $\underline{x}$ direction. As follows from above, such predictions are wrong.

Therefore we proved that, in general, it is not possible to associate a ket vector to an ensemble of particles. The only case for which this this association is actually possible is for ensembles which are made of non-interacting particles having the same identical quantum state.

From the foregoing discussion, it follows that another formalism is needed for treating ensembles of states. On the basis of this need, the density matrix formalism was introduced into quantum mechanics in the late 1920s by Von Neumann, Dirac and Landau, who developed and applied it to quantum information theory, statistical thermodynamics and wave mechanics [51–53].

4.1 BASIC RELATIONS

Ensembles of states in quantum mechanics are described by *density operators*. The leading idea which brings to the definition of the density operator is the following. Given an ensemble χ made of N sub-ensembles, where each one of the latter is composed by particles which share the same quantum state $|\beta_i\rangle$ $(i = 1, ..., N)$, the expectation value of a certain variable o over the ensemble must reasonably be a statistical average of the expectation values of the same variable over the sub-ensembles. The statistical weight of each addend will naturally be the particles fraction (for intensive variables) or the particle number (for extensive variables) of the sub-ensemble. For any observable o, this supposition entails

$$\begin{aligned} \mathrm{E}\,(o)_\chi \;\; &\equiv\;\; \sum_{i=1}^{N} W_i\, \langle\beta_i|\,\hat{O}\,|\beta_i\rangle \\ &=\;\; \sum_{j} \langle a_j|\left(\sum_{i=1}^{N} W_i\, |\beta_i\rangle\,\langle\beta_i|\right)\hat{O}\,|a_j\rangle \;\; , \end{aligned} \qquad (4.2)$$

where $\mathrm{E}\left(o\right)_\chi$ denotes the expectation value of the variable o over the ensemble χ, $\hat{O}$ is the quantum operator related to o, W_i is the fraction or the number of particles of the ith sub-ensemble and $|a_j\rangle$ are states which form a complete basis in the quantum space where $|\beta_i\rangle$ are defined. The relation $\sum_j |a_j\rangle\langle a_j| = \hat{\mathbb{1}}$ has been used in the last step of Eq. (4.2).

It is sometimes said that ensemble of states are described by incoherent superpositions of pure states. This statement has his grounds on Eq. (4.2), where we see that the expectation values of observables over the ensemble are obtained as superposition of probabilities for the states $|\beta_i\rangle$ (incoherent superposition) and *not* as probability of a superposition of states $|\beta_i\rangle$ (coherent superposition).

From equation (4.2), it is moreover clear that what depends on the characteristics of the ensemble is enclosed in parentheses. Such quantity can be therefore assigned to be representative for the ensemble, similarly to the ket vector for a particle state and is therefore assigned the name "density operator".

Summarizing what above, we state that an ensemble of states may be described in quantum mechanics by the density operator

$$\hat{\mathrm{P}} = \sum_i W_i |\beta_i\rangle\langle\beta_i| \ ,$$

where W_i is the statistical weight of the state $|\beta_i\rangle$, or, more practically, is the fraction (for intensive variables) or the number (for extensive variables) of particles of the ensemble that share the same pure state $|\beta_i\rangle$.

The density matrix which describes the above ensemble, in a given representation $|a_i\rangle$, is obtained as

$$\rho_{ij} = \langle a_i|\hat{\mathrm{P}}|a_j\rangle \ .$$

The density matrix results of course diagonal in the representation $|\beta_i\rangle$.

When $W_i = \delta_{ij}$, the state described by the density matrix is the pure state β_j. In any other case, the state is a mixed state. When $W_i = W_0$ for any i, then the density matrix describes a maximally mixed state.

Thorough reviews of density matrices and their applications can be found in [54–57].

We give here a brief list of properties of density matrices and density operators:

- The density operator is hermitian (by definition): $\hat{\mathrm{P}}^\dagger = \hat{\mathrm{P}}$. The density matrix satisfies the equation

$$\rho_{ij}^* = \langle a_j|\hat{\mathrm{P}}|a_i\rangle = \rho_{ji} \quad .$$

- If the weights W_i represent fractions of particles, it must be true that $W_i \leq 1 \ \forall i$ and $\sum_i W_i = 1$. Then the density matrix is normalized to unity:

$$\mathrm{Tr}\left[\rho\right] = \sum_i \langle a_i|\hat{\mathrm{P}}|a_i\rangle = \sum_i \langle\beta_i|\hat{\mathrm{P}}|\beta_i\rangle = \sum_{ij} W_j \langle\beta_i|\beta_j\rangle\langle\beta_j|\beta_i\rangle$$

$$= \sum_{ij} W_j \, \delta_{ij}\delta_{ij} = \sum_i W_i = 1 \quad ,$$

where, in the second step, we used the fact that the trace of a matrix (of an operator) is independent of the used representation [25].

If W_i represent fractions of particles, it follows also

$$\text{Tr}\left[\rho^2\right] = \sum_{ijk} W_j W_k \langle a_i | \beta_j \rangle \langle \beta_j | \beta_k \rangle \langle \beta_k | a_i \rangle = \sum_{ijk} W_j W_k \langle a_i | \beta_j \rangle \delta_{jk} \langle \beta_k | a_i \rangle$$

$$= \sum_{ij} W_j^2 \langle a_i | \beta_j \rangle \langle \beta_j | a_i \rangle = \sum_{ij} W_j^2 \langle \beta_i | \beta_j \rangle \langle \beta_j | \beta_i \rangle = \sum_i W_i^2 \leq 1 \quad .$$

The equality

$$\text{Tr}\left[\rho^2\right] = 1$$

is valid if only one of the eigenvalues W_i is nonzero (and, hence, equal to unity): $W_i = \delta_{i,j}$. This is the case of a pure state.

- The expectation value of a variable over the ensemble is obtained from the density operator as in Eq. (4.2):

$$\text{E}\left(o\right)_\chi = \sum_j \langle a_j | \left(\sum_{i=1}^N W_i \, |\beta_i\rangle \, \langle\beta_i| \right) \hat{\text{O}} \, |a_j\rangle = \text{Tr}\left[\hat{\text{P}}\,\hat{\text{O}}\right] \quad .$$

- The evolution equation for a density operator is

$$\hat{\text{P}}(t) = \hat{\text{U}}(t_0, t)\hat{\text{P}}(t_0)\hat{\text{U}}^\dagger(t_0, t) \quad , \tag{4.3}$$

where $\hat{\text{U}}$ is the standard evolution operator defined in Eq. (3.1). Taking the derivative in time of both sides of Eq. (4.3), we get the *Louville equation*

$$i\hbar \frac{\partial \hat{\text{P}}(t)}{\partial t} = \left[\hat{\text{H}}, \hat{\text{P}}(t)\right] \quad .$$

For comparison, we show the evolution equation

$$\hat{\text{O}}_H(t) = \hat{\text{U}}^\dagger(t_0, t)\hat{\text{O}}_H(t_0)\hat{\text{U}}(t_0, t)$$

and the Heisemberg equation

$$i\hbar \frac{\partial \hat{\text{O}}_H(t)}{\partial t} = \left[\hat{\text{O}}_I(t), \hat{\text{H}}\right]$$

for any operator $\hat{\text{O}}_H$ in the Heisemberg representation.
Of course, $\hat{\text{H}}$ may depend on time.

4.2 QUANTUM CORRELATION AND ENTANGLEMENT

Quantum entanglement is a peculiar characteristic of quantum mechanics which has created debates since long ago. Yet nowadays, entanglement is object of deep research and is not fully accepted by the whole physics community [58].

Entanglement is the property of a quantum state of two or more physical objects. Concretely, if two physical objects are entangled, a measurement on one jeopardizes the result of the measurement on the other, independently of the distance the two objects are separated by. In quantum space, two objects are entangled if their state is not a product of the two-single states which correspond to the objects (i.e if it is not a separable quantum state).

As known, Albert Einstein himself was reluctant to accept quantum entanglement, by defining it a "spooky action at a distance"[59]. It was not until 1964 that John Stewart Bell proposed an inequality, today known with the name "Bell's inequality", which could be experimentally tested to prove whether entanglement is a property which characterizes the matter or not. This can be easily seen as a test on whether non-local or local theories exist in nature. In the 70s and 80s, several experiments have proved that the Bell's inequality is indeed violated, in nature, confirming therewith that entanglement is a inherent characteristics of nature. The most famous experiment to this aim has been maybe the one carried out by Alain Aspect [17].

Much of the current research interest concerning entanglement is focused on defining a measure for it. Generally, quantifying entanglement is indeed not a trivial question. Let us imagine we have a two-particle spin-1/2 state

$$|\Psi_{12}\rangle_a = \frac{1}{\sqrt{2}}\Big(|\uparrow\uparrow\rangle + |\downarrow\downarrow\rangle\Big) \quad .$$

Here it is easy to recognize that this state is fully entangled, as it is a Bell state. Analogously, if we have the state

$$|\Psi_{12}\rangle_b = \frac{1}{2}\Big(|\uparrow\uparrow\rangle + |\uparrow\downarrow\rangle + |\downarrow\uparrow\rangle + |\downarrow\downarrow\rangle\Big)$$

we soon understand that it does not possess any degree of entanglement, as it is a product of the two single particle states

$$|\Psi_{12}\rangle_b = \frac{1}{\sqrt{2}}\Big(|\uparrow\rangle + |\downarrow\rangle\Big) \frac{1}{\sqrt{2}}\Big(|\uparrow\rangle + |\downarrow\rangle\Big).$$

For the same reason, zero entanglement characterizes of course also the states

$$\frac{1}{\sqrt{2}}\Big(|\uparrow\uparrow\rangle + |\uparrow\downarrow\rangle\Big) = \frac{1}{\sqrt{2}}|\uparrow\rangle\Big(|\uparrow\rangle + |\downarrow\rangle\Big)$$
$$\frac{1}{\sqrt{2}}\Big(|\downarrow\uparrow\rangle + |\downarrow\downarrow\rangle\Big) = \frac{1}{\sqrt{2}}|\downarrow\rangle\Big(|\uparrow\rangle + |\downarrow\rangle\Big)$$
$$\frac{1}{\sqrt{2}}\Big(|\uparrow\uparrow\rangle + |\downarrow\uparrow\rangle\Big) = \frac{1}{\sqrt{2}}\Big(|\uparrow\rangle + |\downarrow\rangle\Big)|\uparrow\rangle$$
$$\frac{1}{\sqrt{2}}\Big(|\uparrow\downarrow\rangle + |\downarrow\downarrow\rangle\Big) = \frac{1}{\sqrt{2}}\Big(|\uparrow\rangle + |\downarrow\rangle\Big)|\downarrow\rangle \quad .$$

But what about the state

$$|\Psi_{12}\rangle_c = \left(\sqrt{\frac{2}{10}}|\uparrow\uparrow\rangle + \sqrt{\frac{5}{10}}|\uparrow\downarrow\rangle + \sqrt{\frac{3}{10}}|\downarrow\uparrow\rangle\right) \quad ?$$

How much is the entanglement it possesses? Indeed, it is not easy to answer this question. Normally, quantifying entanglement is a pure mathematical problem which

has been solved exactly for very few cases. For an ensemble composed of two particles with two degrees of freedom each (such kind of particle is called *qubit*), it has been demonstrated that a valid measure for the entanglement of their state is given by the Wootter's concurrence [60]. The Wootter's concurrence is defined as

$$\mathcal{C} = \max\left(0, \sqrt{e_1} - \sqrt{e_2} - \sqrt{e_3} - \sqrt{e_4}\right), \tag{4.4}$$

where $\sqrt{e_i}$ are the square roots of the eigenvalues of the matrix $\rho(\sigma_2^{(1)} \otimes \sigma_2^{(2)})\rho^*(\sigma_2^{(1)} \otimes \sigma_2^{(2)})$ in descending order, ρ is the density matrix characterizing the two-particle ensemble and $\sigma_2^{(1,2)}$ is the second Pauli matrix acting on the first and the second particle state, respectively.

Hence, knowing the density matrix of an ensemble of two qu-bit particles permits to investigate the entanglement properties of the pair. Since a photon has two spin states ($\lambda = +1, -1$), a photon pair represents a natural choice for investigating entanglement. We will indeed apply this approach for studying, in Sec. 5.4, the degree of entanglement of the spin state of photons emitted in two-photon decays of atoms and ions.

4.3 BUILDING THE FINAL STATE DENSITY MATRIX FOR TWO-PHOTON DECAY

In this section, we will build the polarization density matrix of the photons emitted in two-photon decays.

The initial state of the overall system, in the two-photon decay problem, is given by the photon vacuum $|\text{vac}\rangle \equiv |0,0\rangle_{i,\gamma}$, and by the excited ion (or atom) in states $|\beta_i, J_i, M_i\rangle$ with well-defined total angular momentum J_i and associated projection M_i onto the z-axis. Following the notation used in Sec. 3.5 and 3.3, β_i represents a collective label for all additional quantum numbers required to specify the state.

The magnetic sublevel population of the ion in initial states is described as a statistical mixture, by the density operator

$$\hat{\rho}_{i,\text{ion}} = \sum_{M_i} C_{M_i} |\beta_i, J_i, M_i\rangle \langle \beta_i, J_i, M_i| , \tag{4.5}$$

where C_{M_i} denotes the population of the magnetic substate $|\beta_i, J_i, M_i\rangle$. Since in most (two–photon) experiments, the initially prepared excited ionic states are unpolarized, we fix the parameters as $C_{M_i} = 1/(2J_i + 1)$. Such a realistic choice for the initial-state population will have important consequences for the (spin) entanglement of emitted photon pairs. We will see in Sec. 5.4 that, by introducing the *incoherent* mixture of initial magnetic substates as done in Eq. (4.5), also the two-photon state's coherences are jeopardized and, hence, a loss of quantum correlations will be induced.

The initial density operator of the photons is simply

$$\hat{\rho}_{i,\gamma} = |0,0\rangle_{i,\gamma\ i,\gamma}\langle 0,0| .$$

Using equation (4.3), the density operators of the initial and the final states of the overall system are connected by the standard relation [54]

$$\hat{\rho}_f = \hat{U}\, \hat{\rho}_{i,\text{ion}} \otimes \hat{\rho}_{i,\gamma}\, \hat{U}^\dagger , \tag{4.6}$$

where $\hat{\mathrm{U}}$ is the evolution operator which accounts for the interaction of the ion with the radiation field. The final-state operator (4.6) describes both the de-excited ion in some state $|\beta_f, J_f, M_f\rangle$ and the two emitted photons with wave vectors $\boldsymbol{k}_{1,2}$ and helicities $\lambda_{1,2}$.

Instead of using the final-state density operator $\hat{\rho}_f$, it is often more convenient to work with its matrix representation, i.e. the final-state density matrix. This density matrix reads

$$\langle f; \boldsymbol{k}_1\lambda_1, \boldsymbol{k}_2\lambda_2|\, \hat{\rho}_f \,|f'; \boldsymbol{k}_1\lambda_1', \boldsymbol{k}_2\lambda_2'\rangle \equiv \langle \beta_f J_f M_f; \boldsymbol{k}_1\lambda_1, \boldsymbol{k}_2\lambda_2|\, \hat{\rho}_f \,|\beta_f J_f M_f'; \boldsymbol{k}_1\lambda_1', \boldsymbol{k}_2\lambda_2'\rangle$$

$$= \frac{1}{2J_i+1} \sum_{M_i} C_i \mathcal{M}^{\gamma\gamma}_{\lambda_1\lambda_2}(i \to f) \mathcal{M}^{\gamma\gamma\,*}_{\lambda_1'\lambda_2'}(i \to f)\,,$$

where the transition amplitude $\mathcal{M}^{\gamma\gamma}_{\lambda_1\lambda_2}(i \to f)$ is the one presented in equation (3.48). The further subscript $_{\lambda_1\lambda_2}$ is used to make the polarization dependence explicit. The amplitude is related to the evolution operator by

$$\mathcal{M}^{\gamma\gamma}_{\lambda_1\lambda_2}(i \to f) = \langle \eta_f, J_f, M_f; \boldsymbol{k}_1, \lambda_1, \boldsymbol{k}_2, \lambda_2|\, \hat{\mathrm{U}} \,|\beta_i, J_i, M_i; 0,0\rangle \quad . \tag{4.7}$$

Assuming that the final magnetic sub–state of the ion remains unobserved in an experiment, we can derive the reduced density matrix which only describes the polarization state of the two photons, measured at a certain opening angle θ, with certain energies ω_1 and ω_2:

$$
\begin{aligned}
\langle \lambda_1, \lambda_2|\, \hat{\rho}_{f,\gamma} \,|\lambda_1', \lambda_2'\rangle &\equiv \sum_{M_f} \langle f; \boldsymbol{k}_1, \lambda_1, \boldsymbol{k}_2, \lambda_2|\, \hat{\rho}_f \,|f; \boldsymbol{k}_1, \lambda_1', \boldsymbol{k}_2, \lambda_2'\rangle \\
&= \frac{\mathcal{N}}{2J_i+1} \sum_{M_i,M_f} C_{M_i} \mathcal{M}^{\gamma\gamma}_{\lambda_1\lambda_2}(i \to f) \mathcal{M}^{\gamma\gamma\,*}_{\lambda_1'\lambda_2'}(i \to f)\,,
\end{aligned}
\tag{4.8}
$$

where we introduced the factor $\mathcal{N}$ to ensure the proper normalization of the matrix, $\mathrm{Tr}\,[\langle \hat{\rho}_{f,\gamma}\rangle] = 1$.

This will be the quantity we will investigate in detail in chapter 5.

CHAPTER 5

TWO-PHOTON DECAY: ADVANCED STUDIES

In physics, cumbersome formulae are quite never the most correct ones. A final formula is more likely concise and elegant.

Giorgio Immirzi, 2004

Of the two photon decay, there are many things to study. A list of the basic quantities to investigate may include: the total decay rate of the process, the spectral distribution, the angular distribution, the polarization properties of the emitted photons. In this chapter, we will accurately analyze them. We will emphasize the advanced studies which have been made on this topic by other authors as well as the original contributions of this thesis.

5.1 TOTAL CROSS SECTION AND SPECTRAL DISTRIBUTION

Many aspect of the two-photon decay process have been investigated in the past by several authors. In particular, in the second half of the last century the total cross section and the spectral distribution have been intensively studied in the context of few-electron atoms and ions. By spectral distribution, it is meant the probability density function related to the energy sharing of the two emitted photons, or, in other words, the normalized differential decay rate $d\Gamma/dE_1$, where $E1$ is the energy of one of the two emitted photons. While the sum of the two photons' energies must add up to the energy gap of the transition (due to energy conservation), the energy carried by each single photon is, in fact, not fixed.

Two-photon decay of hydrogen- and helium-like ions
In hydrogen-like ions, the two-photon decay of the $2s_{1/2}$ state has risen interests since the origins of quantum mechanics [1]. In the past century, many of the two-photon studies has been focused on such a decay.

Z	$w(M1)$	$w(2\gamma)$	$w(\text{tot})$
1	$2.49591901 \times 10^{-6}$	8.229063	8.229065
2	$2.55626238 \times 10^{-3}$	5.266042×10^{2}	5.266068×10^{2}
3	$1.47448885 \times 10^{-1}$	5.997292×10^{3}	5.997440×10^{3}
4	2.61939935	3.368840×10^{4}	3.369102×10^{4}
5	2.44075507×10^{1}	1.284703×10^{5}	1.284948×10^{5}
6	1.51219742×10^{2}	3.834621×10^{5}	3.836133×10^{5}
7	7.06964753×10^{2}	9.665073×10^{5}	9.672143×10^{5}
8	2.68960303×10^{3}	2.152429×10^{6}	2.155119×10^{6}
9	8.74246719×10^{3}	4.361002×10^{6}	4.369745×10^{6}
10	2.51003240×10^{4}	8.200570×10^{6}	8.225670×10^{6}
11	6.51818482×10^{4}	1.451723×10^{7}	1.458241×10^{7}
12	1.55805459×10^{5}	2.444948×10^{7}	2.460528×10^{7}
13	3.47395680×10^{5}	3.948826×10^{7}	3.983565×10^{7}
14	7.30032314×10^{5}	6.154224×10^{7}	6.227228×10^{7}
15	1.45779185×10^{6}	9.300828×10^{7}	9.446608×10^{7}
16	2.78454759×10^{6}	1.368469×10^{8}	1.396314×10^{8}
17	5.11524642×10^{6}	1.966626×10^{8}	2.017779×10^{8}
18	9.07769992×10^{6}	2.767891×10^{8}	2.858668×10^{8}
19	1.56211038×10^{7}	3.823790×10^{8}	3.980001×10^{8}
20	2.61488033×10^{7}	5.194978×10^{8}	5.456466×10^{8}
21	4.26945535×10^{7}	6.952229×10^{8}	7.379175×10^{8}
22	6.81531341×10^{7}	9.177457×10^{8}	9.858988×10^{8}
23	1.06578441×10^{8}	1.196478×10^{9}	1.303057×10^{9}
24	1.63563871×10^{8}	1.542164×10^{9}	1.705728×10^{9}
25	2.46724142×10^{8}	1.966992×10^{9}	2.213716×10^{9}
26	3.66298161×10^{8}	2.484712×10^{9}	2.851010×10^{9}
27	5.35897415×10^{8}	3.110759×10^{9}	3.646656×10^{9}
28	7.73430228×10^{8}	3.862374×10^{9}	4.635804×10^{9}
29	1.10222453×10^{9}	4.758729×10^{9}	5.860953×10^{9}
30	1.55241116×10^{9}	5.821062×10^{9}	7.373473×10^{9}
32	2.98171369×10^{9}	8.539707×10^{9}	1.152142×10^{10}
34	5.50996703×10^{9}	1.223449×10^{10}	1.774446×10^{10}
36	9.84022291×10^{9}	1.716321×10^{10}	2.700343×10^{10}
38	$1.70476667 \times 10^{10}$	2.362974×10^{10}	4.067741×10^{10}
40	$2.87414359 \times 10^{10}$	3.198853×10^{10}	6.072997×10^{10}
42	$4.72840541 \times 10^{10}$	4.264918×10^{10}	8.993323×10^{10}
45	$9.57795011 \times 10^{10}$	6.400027×10^{10}	1.597798×10^{11}
46	$1.19994177 \times 10^{11}$	7.281768×10^{10}	1.928119×10^{11}
47	$1.49641928 \times 10^{11}$	8.261063×10^{10}	2.322526×10^{11}
50	$2.82903863 \times 10^{11}$	1.186870×10^{11}	4.015908×10^{11}
54	$6.27019120 \times 10^{11}$	1.859758×10^{11}	8.129949×10^{11}
55	$7.58563275 \times 10^{11}$	2.069368×10^{11}	9.655000×10^{11}
58	$1.31864299 \times 10^{12}$	2.816997×10^{11}	1.600343×10^{12}
60	$1.87950004 \times 10^{12}$	3.428003×10^{11}	2.222300×10^{12}
62	$2.65095005 \times 10^{12}$	4.142831×10^{11}	3.065233×10^{12}
65	$4.36179752 \times 10^{12}$	5.438258×10^{11}	4.905623×10^{12}
66	$5.12606662 \times 10^{12}$	5.936543×10^{11}	5.719721×10^{12}
70	$9.58256840 \times 10^{12}$	8.313011×10^{11}	1.041387×10^{13}
74	$1.73921410 \times 10^{13}$	1.140289×10^{12}	1.853243×10^{13}
75	$2.01035177 \times 10^{13}$	1.230364×10^{12}	2.133388×10^{13}
78	$3.07616136 \times 10^{13}$	1.535228×10^{12}	3.229684×10^{13}
80	$4.05520829 \times 10^{13}$	1.769879×10^{12}	4.232196×10^{13}
82	$5.31771608 \times 10^{13}$	2.032135×10^{12}	5.520930×10^{13}
85	$7.91168010 \times 10^{13}$	2.482088×10^{12}	8.159889×10^{13}
86	$9.01056465 \times 10^{13}$	2.648282×10^{12}	9.275393×10^{13}
90	$1.49999200 \times 10^{14}$	3.401841×10^{12}	1.534010×10^{14}
92	$1.92403666 \times 10^{14}$	3.835980×10^{12}	1.962396×10^{14}
100	$5.03848601 \times 10^{14}$	6.008640×10^{12}	5.098572×10^{14}

Figure 5.1a: Decay rates of the $2s_{1/2}$ state (s^{-1}). Z is the nuclear charge. From Ref. [61].
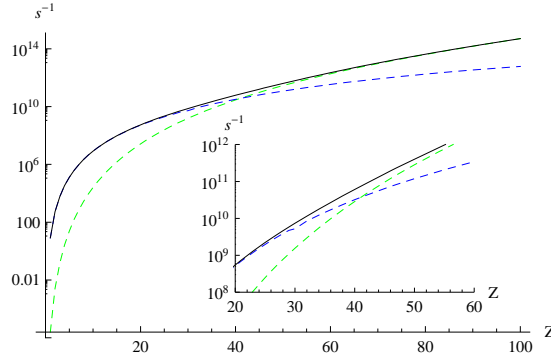

Figure 5.1b: Plot of the data in Fig. 5.1a. The green-dashed, blue-dashed and black-solid represent the single-photon, the double-photon and the total (single + double) decay rate of the state $2s_{1/2}$ in hydrogen-like ions.

Already in 1958, Shapiro and Breit derived that the two-photon decay rate of $2s_{1/2}$ state in hydrogen-like atoms can be approximately described by the relation [3]

$$W = \frac{1}{\tau} \simeq 8.226 Z^{6} \text{sec}^{-1} \quad , \tag{5.1}$$

where Z is the atomic number of the ion.

This results shows that the two-photon decay rate of $2s_{1/2}$ states grows fast with Z, spanning from about 8 sec^{-1} for hydrogen to about $4 \cdot 10^{12}$ sec^{-1} for hydrogen-like Uranium.
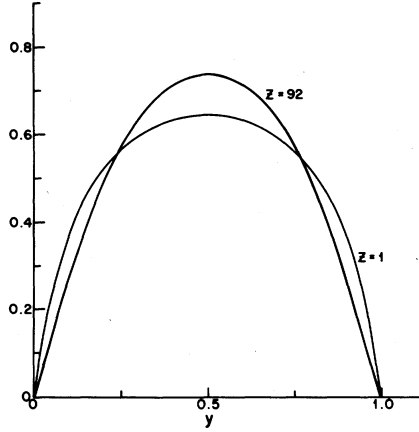
Figure 5.2: Spectral distribution of the photons in the two-photon decay of $2s_{1/2}$ in Hydrogen and hydrogen-like Uranium atoms. From Ref. [48].

Nevertheless, the single-photon decay of this state in hydrogen-like ions grows even faster with Z. For a comparison, in Fig. 5.1a we report a table from Ref. [61] which clearly shows the contribution of the single- ($w(M1)$) and double- ($w(2\gamma)$) photon decay rate to the decay of $2s_{1/2}$ state. Both contributions are plotted in Fig. 5.1b, together with the total decay rate. We see that at around $Z \simeq 40$ the single-photon decay rate ($M1$ transition) overcomes the two-photon decay rate. Formula (5.1) can be refined to give [4]

$$W_H = \frac{1}{\tau} \simeq 8.22938\, Z^6 \left(1 - \frac{m}{M}\right) \frac{1 + 3.9448(\alpha Z)^2 - 2.040(\alpha Z)^4}{1 + 4.6019(\alpha Z)^2}\, \sec^{-1}$$

and extended to the two-photon decay of the state $(1s_{1/2}\, 2s_{1/2})\, J = 0$ in helium-like ions to give [4]

$$W_{He} = \frac{1}{\tau} \simeq 16.458762\, (Z - 0.806389)^6 \left(1 + \frac{1.539}{(Z + 2.5)^2}\right)\, \sec^{-1} \quad .$$

If we define the energy gap between $2s_{1/2}$ and the ground state as ΔE, the fraction of energy carried by the first photon is

$$y = E_1/\Delta E \quad . \tag{5.2}$$

In Fig. 5.2, we see the spectral distribution for the two-photon decay of $2s_{1/2}$ state in hydrogen-like ions as a function of y.

Different transitions in hydrogen-like ions give rise to artistic and amusing pictures for the spectral distribution. See, for instance, Fig. 5.3. Those pictures can be understood if we consider that the two-photon amplitude $\mathcal{M}^{\gamma\gamma}$ contains, at the denominators, the quantity $E_\nu - E_i + E_{1,2}$. Then, for photon energies equal to $E_{1,2} \simeq E_i - E_\nu$, the contribution of the intermediate state ν becomes very big and the amplitude for the two-photon emission picks. At this point, the smart reader would argue that, within the presented formalism, the amplitude we get in these cases is infinite, which is clearly a non-physical prediction. In order to take into account these resonance cases, we must

(a) $3s_{1/2} \to 1s_{1/2}$

(b) $3d_{3/2} \to 1s_{1/2}$
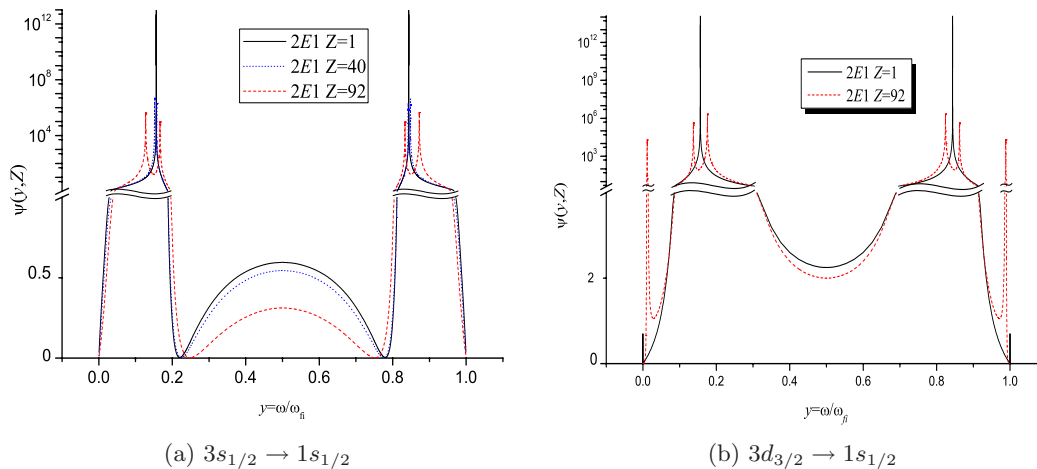
Figure 5.3: Spectral distributions for few transitions in hydrogen-like ions. From Ref. [62].

in fact slightly modify our theory. What is normally done is inserting the widths of the states in the denominators, i.e. replacing $E_\nu - E_i + E_{1,2} \to E_\nu - \frac{i}{2}\Gamma_\nu - E_i + \frac{i}{2}\Gamma_i + E_{1,2}$, where $\Gamma = \hbar/\tau$ is the state's width and τ is the state's lifetime. With this prescription, we are effectively stating that the atomic states have complex energy, to take empirically into account the fact that they are not stable:

$$\Psi_\nu \sim e^{-\frac{i}{\hbar}(E_\nu - \frac{i}{2}\Gamma_\nu)\,t} \Rightarrow \left|\Psi_\nu\right|^2 \sim e^{-\frac{\Gamma_\nu}{\hbar}\,t} = e^{-\frac{t}{\tau}} \quad .$$

The width of the initial state is usually neglected at the denominators since it is normally very small in comparison with other quantities (if the initial state decays by two-photon emission, it means it is long-lived state: $\tau_i >> \tau_\nu$). It can be showed that this way of proceeding, though not rigorous[1], takes to valid results in many cases [38]. Since the states' widths are quite small in comparison with the states' energies, at the end of the day we anyway get a huge contribution, though not infinite, from the intermediate state ν on the amplitude $\mathcal{M}^{\gamma\gamma}$, if one of the photon energies matches the gap $E_i - E_\nu$. With the foregoing analysis, we can now qualitatively understand the pictures (5.3).

The spectral distributions of hydrogen- and helium-like ions have been several times measured in the past decades, confirming theoretical predictions. See, for instance, Ref. [63, 64].

Three- or more-electron atoms

The two-photon decay of three- or more-electron ions, to my knowledge, has been much more poorly studied. This is presumably due to the difficulty in performing the infinite

---

[1]In the author's opinion, a rigorous treatment of the resonance transitions must be made by coming back to Eq. (3.42) and considering all the terms that there appear. Although this seems quite a natural statement within the framework we have drawn here, I have personally never read any discussion about it.

summation over the intermediate states to obtain the amplitude for the process.

Some effort have been devoted to study two-photon decays in K-holes in neutral atoms, both theoretically and experimentally [65–73], following the first (pioneer) work of Freund [74].

Two-photon transitions in Alkali metals have been studied by Safronova and coworkers [75].

There have been also two attempts to calculate the two-photon decay rate of $(1s^2, 2s2p)$ $^3P_0$ state in Beryllium-like ions [76, 77]. The excitation energy of this state turns out to be very small in comparison with other excitation energies, so that the summation over the intermediate states could be explicitly made by cutting it off at a certain level. In this year, I personally made a new relativistic calculation for the two-photon transition rate of $^3P_0$ state, whose results will not be here shown though they may be published in the next future.

Finally, Ref. [78] gives quite a complete overview of what has been done and what has yet to be done in the two-photon decay in heavy atoms and ions.

5.2 ANGULAR PROPERTIES OF THE EMITTED PHOTONS

In this section, we study the angular correlation of the photon pair emitted in two-photon decay of hydrogen- and helium-like atoms. By angular correlation, we mean the probability density of two photon emission with a certain angle θ between the photon directions, irrespectively of their polarizations. In Sec. 3.4, we discussed in great detail the differential decay rate for two-photon transitions. In particular, we derived (Eq. (3.45)) the decay rate differential in energy and photon spherical angles, dependent on the photon polarizations. Then, what we call here 'angular correlation' would be simply given by the same quantity summed over the photons polarizations and arbitrarily normalized.

Hydrogen-like atoms

It is known from much time ago that the angular correlation for the two-photon decay of $2s_{1/2}$ states in hydrogen-like atoms is approximately given by $\sim 1 + \cos^2 \theta$ [78–80]. A deeper analysis of this quantity has been theoretically performed by Au in 1976 [8], who calculated the angular correlation for the the same decay in hydrogen-like ions by including, apart from the leading electric dipole term ($E1E1$), some higher multipole terms and few relativistic corrections. These non-dipole and relativistic effects were found to result in an asymmetrical contribution of the type $\sim \cos \theta$ to the angular correlation's main term $\sim 1 + \cos^2 \theta$. More recently, the leading terms of the angular correlation for other few transitions have been also found [6, 69, 81]. For instance, the non-relativistic angular correlation due to the dipole term $E1E1$ in $J = 1 \rightarrow J = 0$ two-photon transitions, where J is the total angular momentum, is found to take the form $\sim 1 - 1/3 \cos^2 \theta$ [78].

The full relativistic treatment of some angular correlations has been presented for the first time, to my knowledge, by Surzhykov *et al.* in Ref. [9]. In that article, the angular correlations of photons coming from $2s_{1/2} \rightarrow 1s_{1/2}$ and $3d_{5/2} \rightarrow 1s_{1/2}$ transitions in hydrogenlike ions are presented. Their results, which are showed in Fig. 5.2, are obtained by numerically evaluating the Green function for the Dirac Hamiltonian, which we studied in great detail from Eq. (2.15) onwards. The parameter x that appears
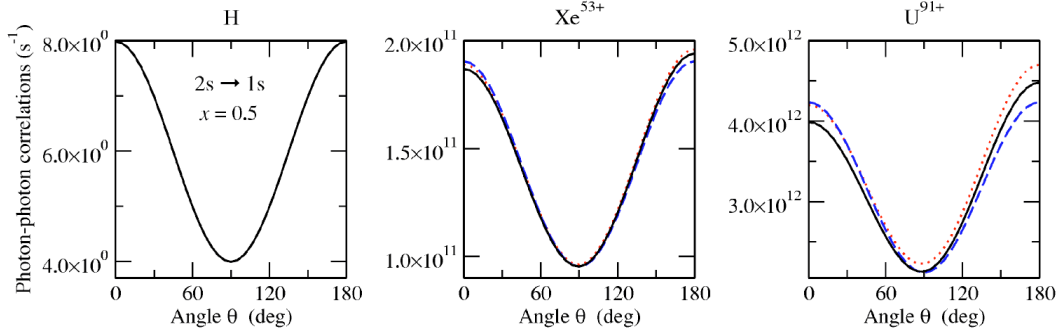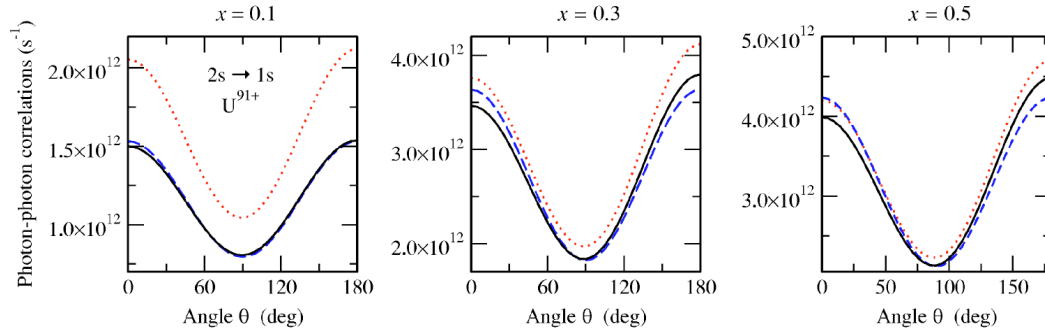
Figure 5.4: Photon-photon angular correlations in the $2s_{1/2} \to 1s_{1/2}$ two-photon decay of hydrogenlike ions. Results are presented for the relativistic theory (black-solid), nonrelativistic approximation by Au [8] (red-dotted) as well as the relativistic electric dipole (blue-dotdashed) approach for the relative photon energy y=0.5 . In the picture, the relative photon energy has been called x. From Ref. [9].

in Fig. 5.2 represents the energy fraction carried away by the first photon that in this work has been defined as y in Eq. (5.2). Thus, their results are naturally not analytic. This is the price to pay for having inserted the full relativistic and high multipoles contributions.

The angular correlation plotted in those figures is obtained by adopting the quantization ($\underline{z}$) axis along the momentum of the first photon: $\mathbf{k}_1 \parallel \underline{z}$, which is an allowed choice as long as we deal with unpolarized atoms/ions. Consequently, the equivalence

Figure 5.5: Photon-photon angular correlations in the $2s_{1/2} \to 1s_{1/2}$ two-photon decay of hydrogenlike uranium U^{91+}. The correlation functions are shown for the three relative photon energies y=0.1, 0.3, and 0.5. See Fig. 5.4 for further details.
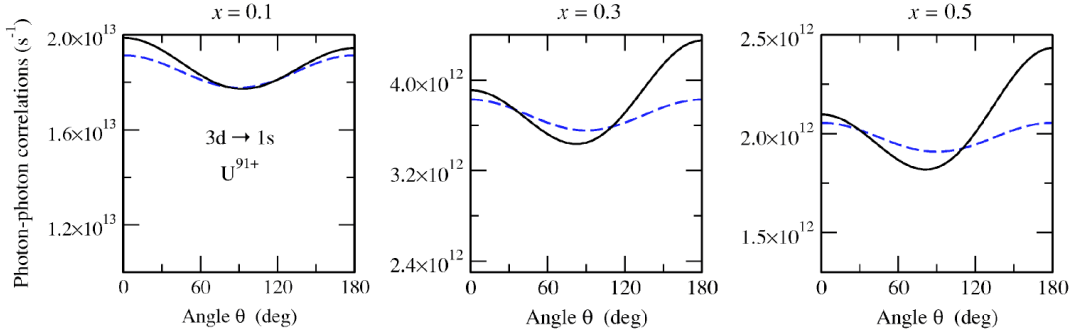
Figure 5.6: Photon-photon angular correlations in the $3d_{5/2} \to 1s_{1/2}$ two-photon decay of hydrogenlike uranium U^{91+}. The correlation functions are shown for the three relative photon energies y=0.1, 0.3, and 0.5. See Fig. 5.4 for further details.

$\theta_2 = \theta$ holds. Thus, the curves showed in the figures correspond to the expression

$$
\begin{aligned}
W^y(\theta) &\equiv \frac{d\Gamma}{dy\,d\cos\theta} \equiv 8\pi^2 \left(E_i - E_f \right) \sum_{\lambda_1,\lambda_2} \frac{d\Gamma^{\gamma_1\,\gamma_2}}{dE_1 d\Omega_{\boldsymbol{p}_1} d\Omega_{\boldsymbol{p}_2}} \Big|_{\boldsymbol{k}_1 \| \hat{z}} \\
&= \left(E_i - E_f \right) \sum_{\lambda_1,\lambda_2} \int_0^{2\pi} d\varphi_1 \int_{-1}^1 d\cos\theta_1 \int_0^{2\pi} d\varphi_2 \\
&\quad \times \frac{d\Gamma^{\gamma_1\,\gamma_2}}{dE_1 d\Omega_{\boldsymbol{p}_1} d\Omega_{\boldsymbol{p}_2}} \Big|_{\boldsymbol{k}_1 \| \hat{z}} \quad ,
\end{aligned}
\tag{5.3}
$$

where $\dfrac{d\Gamma^{\gamma_1\,\gamma_2}}{dE_1 d\Omega_{\boldsymbol{p}_1} d\Omega_{\boldsymbol{p}_2}}$ has been defined in Eq. (3.45).

As an overall comment on the figures, we notice that, in the most probable energy case y=0.5, the non-dipole and relativistic contributions add up to approximately 10% for $2s_{1/2} \to 1s_{1/2}$ two-photon transition, while to approximately 20% for $3d_{5/2} \to 1s_{1/2}$ two-photon transition. These effects lead the back-to-back emission to be slightly more probable than the collinear emission.

He-like atoms

Concerning two-electron bound systems, a recent paper of ours [10] shows the angular correlation of the photon pair for the two-photon decay of $1s_{1/2}2s_{1/2} : J = 0$, $1s_{1/2}2s_{1/2} : J = 1$ and $1s_{1/2}2p_{1/2} : J = 0$ states in helium-like Xenon Xe^{52+}, Gold Au^{77+} and Uranium U^{90+} ions. In nowadays experiments, the excited states of these ions can be efficiently populated in relativistic ion-atom collisions. For example, the formation of the metastable $1s_{1/2}2s_{1/2} : J = 0$ state during the inner-shell impact ionization of (initially) lithium-like heavy ions has been studied recently at the GSI storage ring in Darmstadt [82]. The radiative deexcitation of this state can proceed only via the two-photon transition $1s_{1/2}2s_{1/2} : J = 0 \to 1s_{1/2}^2 : J = 0$ since a single-photon decay to the $1s_{1/2}^2 : J = 0$ ground state is strictly forbidden by the conservation of angular momentum.

To best study the decay, we rewrite Eq. (3.48) as

$$
\mathcal{M}^{\gamma\gamma}(i \to f) = (2\pi) \sum_{L_1 L_2} \sum_{M_1 M_2} \sum_{p_1 p_2} (-i)^{L_1+L_2+p_1+p_2} \sqrt{(2L_1+1)(2L_2+1)}
$$

$$
\times \, (\lambda_1)^{p_1}(\lambda_2)^{p_2} D_{M_1 \lambda_1}^{L_1 *}(\varphi_{k_1}, \theta_{k_1}, 0) D_{M_2 \lambda_2}^{L_2 *}(\varphi_{k_2}, \theta_{k_2}, 0)(-1)^{p_1+p_2+M_1+M_2}
$$

$$
\times \sum_{\nu} \frac{1}{[J_i, J_\nu]^{1/2}} \Big(\langle J_\nu, m_{J_\nu}, L_1, -M_1 | J_f, m_{J_f} \rangle \langle J_i, m_{J_i}, L_2, -M_2 | J_\nu, m_{J_\nu} \rangle S^{J_\nu}(1,2)
$$

$$
+ \langle J_\nu, m_{J_\nu}, L_2, -M_2 | J_f, m_{J_f} \rangle \langle J_i, m_{J_i}, L_1, -M_1 | J_\nu, m_{J_\nu} \rangle S^{J_\nu}(2,1) \Big) \quad,
$$

$$
(5.4)
$$

where the function S^{J_ν} this time is defined as

$$
S^{J_\nu}(1,2) =
$$

$$
\sum_{\nu} \frac{\langle \beta_f, J_f \| \sum_{i=1}^{2} \boldsymbol{\alpha} \cdot \boldsymbol{a}_{L_1}^{p_1}(k_1, \hat{\mathbf{r}}_i) \| \beta_\nu, J_\nu \rangle \langle \beta_\nu, J_\nu \| \sum_{i=1}^{2} \boldsymbol{\alpha} \cdot \boldsymbol{a}_{L_2}^{p_2}(k_2, \hat{\mathbf{r}}_i) \| \beta_i, J_i \rangle}{\omega_{\nu i} + \omega_2} \quad . \qquad (5.5)
$$

It must be noticed that, since we here deal with a two-electron system, the one-particle interaction operator (3.48) has been replaced with two-particle interaction operator, which is but the sum of one-particle operators of each electron. We have already discussed the legitimacy of this prescription in Eq. (3.14).

The S element in Eq. (5.5) contains the whole information about the dynamics of the decay. The angular dependence of the decay is carried by the Clebsch-Gordan coefficients and Wigner matrices contained in the amplitude $\mathcal{M}^{\gamma\gamma}$, beside the S-elements. The notation $[L_1, L_2, ...] = \sqrt{2L_1 + 1}\sqrt{2L_2 + 1}...$ is moreover used.

In order to calculate the S-elements, we must clearly give the states $|\beta, J\rangle$. Since neither the Dirac- nor the Schrödinger-Coulomb equations for Helium are solved exactly, approximated states must be used. In the high-Z domain, the structure of few-electron ions can be reasonably well understood within the Independent Particle Model (IPM), which has been described in detail in Sec. 2.4. As explained in Eq. (2.33), the IPM takes the Pauli principle into account and decompose the many-electron wave functions into Slater determinants, built from one-particle orbitals. This model is well justified for heavy species especially, since the interelectronic effects scale with $1/Z$ and, hence, are much weaker than the electron-nucleus interaction [11, 83, 84]. We discussed IPM in great detail in Sec. 2.4.

For this particular choice of the many-electron function, all the (first- and the second-order) matrix elements can be easily decomposed into the corresponding single-electron amplitudes.

For a helium-like system, the decomposition of the S-element (Eq. (5.5)) reads:

$$
S^{J_\nu}(1,2) = -\delta_{J_\nu L_1} [J_i, J_\nu]^{1/2} \sum_{j_\nu} (-1)^{J_i+J_\nu+L_2} \left\{ \begin{array}{ccc} j_\nu & j_0 & J_\nu \\ J_i & L_2 & j_i \end{array} \right\} S^{j_\nu}(1,2), \qquad (5.6)
$$

where the one-electron matrix elements S^{j_ν} are given in Eq. (3.52).

It must be noticed that we use small and capital letters to identify the angular momentum quantum numbers of one-particle and two-particle states, respectively.
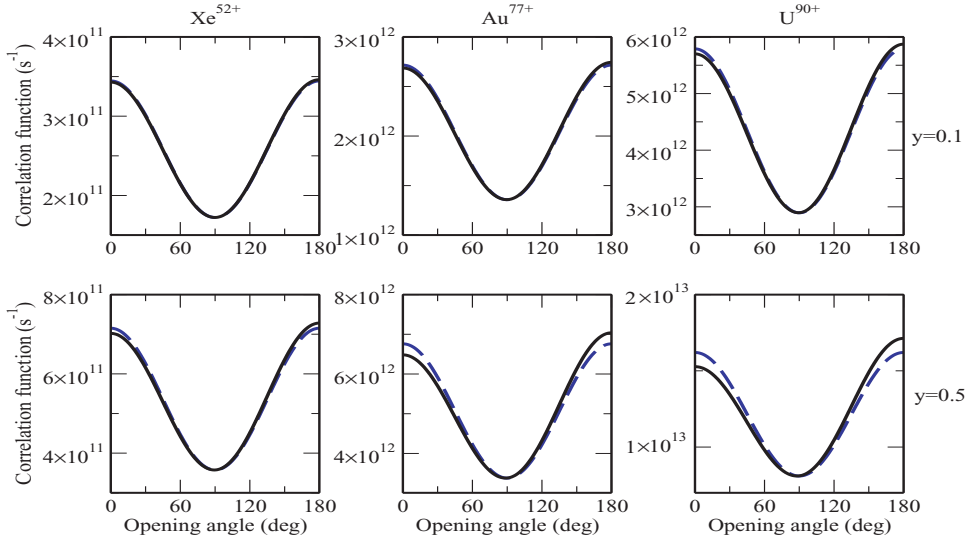
Figure 5.7: Angular correlation function (5.3) for the $1s_{1/2}2s_{1/2} : J = 0 \rightarrow 1s^2_{1/2} : J = 0$ two-photon decay of helium-like Xenon, Gold, and Uranium ions. Calculations obtained within the electric dipole $E1E1$ approximation (dashed line) are compared with those including all the allowed multipoles (solid line). Results are presented for the relative photon energies y $=$ 0.1 (upper panel) and 0.5 (lower panel). From Ref. [10].

The great advantage of formula (5.6) is that it helps us to immediately evaluate the many-electron matrix element (5.5) in terms of the (one-particle) functions $S^{j\nu}(\omega_2)$.

The summation over the complete one-particle spectrum that occurs in these functions can be performed by means of various methods. In the article, we made use of both (i) the relativistic Coulomb-Green's function we showed in Sec. 2.3 [9,85,86] and (ii) a B-spline discrete basis set [61,87–90] to evaluate all the second-order transition amplitudes. Indeed, both approaches yielded almost identical results for the angular correlation functions.

Fig. 5.7 displays the photon-photon angular correlation function, defined in Eq. (5.3), for the decay of the two-photon transition $1s_{1/2}2s_{1/2} : J = 0 \rightarrow 1s^2_{1/2} : J = 0$ in helium-like Xenon Xe^{52+}, Gold Au^{77+} and Uranium U^{90+} ions and for the two energy sharing parameters $y = 0.1$ (upper panel) and $y = 0.5$ (lower panel). Moreover, because the radiative transitions in high-Z ions are known to be affected by the higher terms of the electron-photon interaction, calculations were performed within both the exact relativistic theory (solid line) to include all allowed multipole components (p_1L_1, p_2L_2) in the amplitude (5.4) and the electric dipole approximation (dashed line), if only a single term with $L_1 = L_2 = 1$ and $p_1 = p_2 = 1$ is taken into account. In the dipole $E1E1$ approach, as expected, the angular distribution is well described by the formula $1 + \cos^2\theta$ that predicts a *symmetric* (with respect to the opening angle $\theta = 90°$) emission pattern of two photons. Within the exact relativistic theory, in contrast, an asymmetric shift in the angular correlation function is obtained. For high-Z domain, the photon emission occurs predominantly in the backward directions if the nondipole terms are taken into account, as found in Fig. 5.4. This effect becomes more pro-
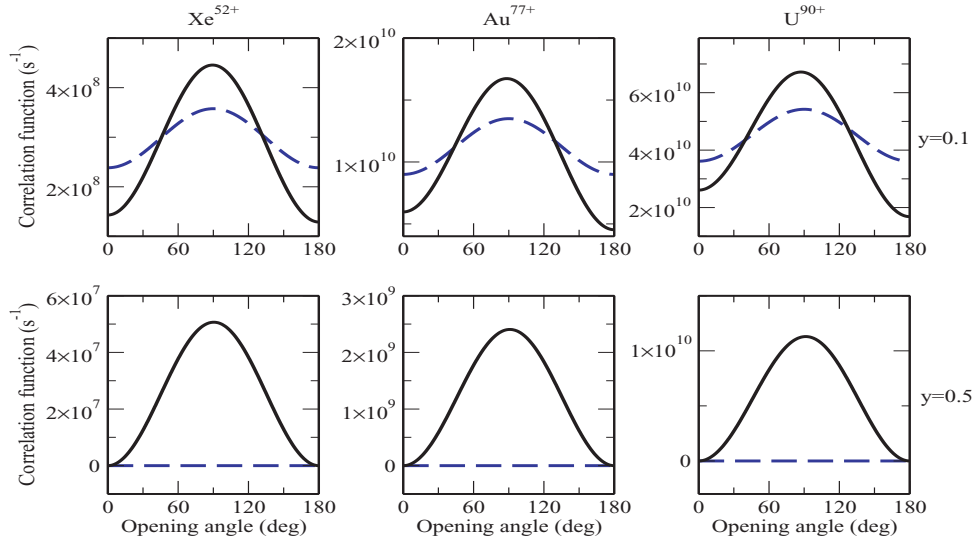
Figure 5.8: Angular correlation function (5.3) for the $1s_{1/2}2s_{1/2}$: $J = 1 \rightarrow 1s_{1/2}^2$: $J = 0$ two-photon decay of helium-like Xenon, Gold, and Uranium ions. Calculations obtained within the electric dipole $E1E1$ approximation (dashed line) are compared with those including all the allowed multipoles (solid line). Results are presented for the relative photon energies y = 0.1 (upper panel) and 0.5 (lower panel). From Ref. [10].

nounced for the equal energy sharing, as can be seen in the bottom panel of Fig. 5.7. Apart from the singlet $1s_{1/2}2s_{1/2}$: $J = 0$, the formation of the triplet $1s_{1/2}2s_{1/2}$: $J = 1$ state has been also observed in recent collision experiments at the GSI storage ring [82, 91]. Although much weaker in intensity (owing to the dominant M1 transition), the two-photon decay of this $1s_{1/2}2s_{1/2}$: $J = 1$ state has attracted recent interest and might provide an important testing ground for symmetry violations of Bose particles [11, 12]. The angular correlation between the photons emitted in this $1s_{1/2}2s_{1/2}$: $J = 1 \rightarrow 1s_{1/2}^2$: $J = 0$ (two-photon) decay is displayed in Fig. 5.8, by comparing once again the results from the exact relativistic theory with the E1E1 dipole approximation. As seen from the figure, the photon-photon correlation functions for the two-photon decay of $1s_{1/2}2s_{1/2}$: $J = 1$ state is much more sensitive with regard to higher multipoles in the electron-photon interaction than obtained for the decay of $1s_{1/2}2s_{1/2}$: $J = 0$ state. The strongest non-dipole effect can be observed for the equal energy sharing ($y = 0.5$).

Large effects due to the higher multipole contributions to the $1s_{1/2}2s_{1/2}$: $J = 1 \rightarrow 1s_{1/2}^2$: $J = 0$ two-photon transition can be observed not only for the case of equal energy sharing ($y = 0.5$) but also for the relative energy $y = 0.1$. In this latter case indeed, the photon-photon angular correlation function is found symmetric with regard to $\theta = 90°$ in the electric dipole (E1E1) approximation but becomes asymmetric in the exact relativistic theory. In contrast to the decay of $1s_{1/2}2s_{1/2}$: $J = 0$, however, a predominant *parallel emission* of both photons appears to be more likely if the higher multipoles are taken into account. For the $1s_{1/2}2s_{1/2}$: $J = 1 \rightarrow 1s_{1/2}2s_{1/2}$: $J = 0$ two-photon decay of helium-like Uranium U^{90+}, for example, the intensity ratio
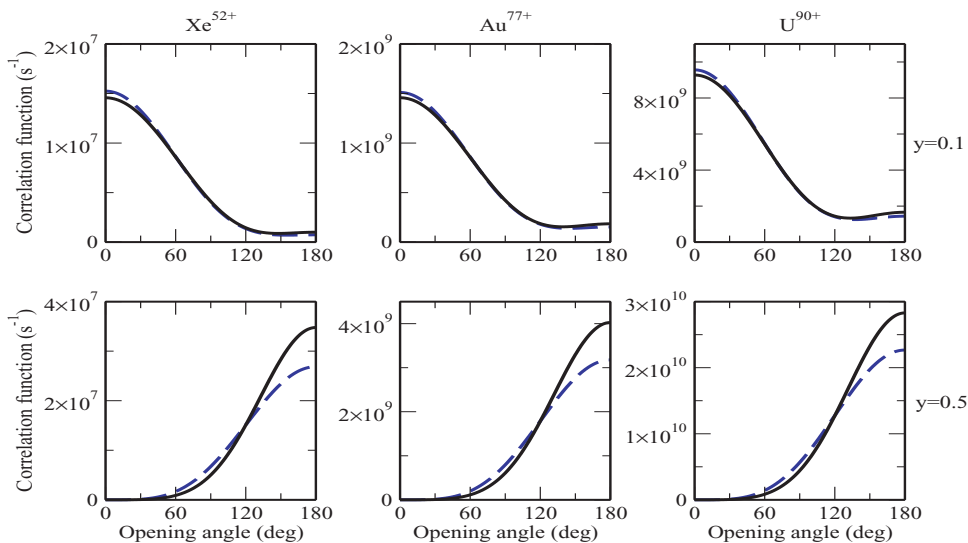
Figure 5.9: Angular correlation function (5.3) for the $1s_{1/2}2p_{1/2}$: $J = 0 \rightarrow 1s_{1/2}^2$: $J = 0$ two-photon decay of helium-like Xenon, Gold, and Uranium ions. Calculations obtained within the dipole $E1M1$ approximation (dashed line) are compared with those including all the allowed multipoles (solid line). Results are presented for the relative photon energies y = 0.1 (upper panel) and 0.5 (lower panel). From Ref. [10].

$W^{y=0.1}(\theta = 0°)/W^{y=0.1}(\theta = 180°)$ increases from unity within the electric dipole approximation to almost 1.6 in the exact relativistic treatment.

Until now we have discussed the photon-photon correlations in the decay of $1s_{1/2}2s_{1/2}$ helium-like states. Besides these (well-studied) transitions, recent theoretical interest has been focused also on the $1s_{1/2}2p_{1/2}$: $J = 0 \rightarrow 1s_{1/2}^2$: $J = 0$ two-photon decay, whose properties are expected to be sensitive to (parity violating) PNC phenomena in the atomic system [92].

The angular correlation function (5.3) for the $1s_{1/2}2p$: $J = 0 \rightarrow 1s_{1/2}^2$: $J = 0$ transition is displayed in Fig. 5.9, again for two relative photon energies $y = 0.1$ and 0.5 and for the nuclear charges $Z = 54$, 79 and 92. Calculations have been performed both within the exact theory and the ("electric and magnetic") dipole approximation which accounts for the leading E1M1-M1E1 decay channel. As seen from the figure, the emission pattern strongly depends on the energy sharing between the photons. If, for example, one of the photons is more energetic than the second one, their parallel emission becomes dominant (cfr. upper panel of Fig. 5.9). In contrast, photons with equal energies ($y = 0.5$) are more likely to be emitted back-to-back while the differential rate $W^y(\theta)$ vanishes identically for $\theta = 0°$. Such a behaviour of the photon-photon angular correlation function is caused by the interference between two pathways which appear for each multipole component of the $1s_{1/2}2p_{1/2}$: $J = 0 \rightarrow 1s_{1/2}^2$: $J = 0$ transition. For instance, the leading E1M1-M1E1 decay may proceed either via intermediate $1s_{1/2}ns_{1/2}$: $J = 1$ or $1s_{1/2}np_{1/2}$: $J = 1$ states, thus giving rise to a "double-slit" picture that becomes most pronounced for equal energy sharing.

In this section we have analyzed in detail the angular correlation of the emitted radiation in a two-photon decay in one- and two-electron bound systems. Our analysis

went through several types of two-photon decay so that general overview of the angular properties of the emitted photons should have been grasped by the reader. In the next section, we carry on our advanced analysis on the characteristics of the two-photon decay by studying the polarization properties of the emitted photons.

5.3 POLARIZATION PROPERTIES OF THE EMITTED PHOTONS

The polarization properties of the photons emitted in two-photon decays of atoms and ions represent a useful tool for studying and testing quantum mechanics of bound systems. The recent improvements in detection techniques [16], allows nowadays to measure the polarization properties of photons in x-ray regime, so as to verify theoretical predictions even in high-Z domain.

Hydrogen-like atoms
In a recent papers by Andrey Surzhykov and me [93], the polarization-polarization correlation of photons emitted in two-photon decay of $2s_{1/2}$ states in hydrogen-like ions has been studied. By 'polarization-polarization correlation', we mean the probability of measuring, in coincidence, the two emitted photons with a certain opening angle θ *and* a certain relative polarization (both photon polarizations are measured). This work has followed a slightly older study on the polarization-angle correlation of photons in $2s_{1/2} \to 1s_{1/2}$ and $3d_{5/2} \to 1s_{1/2}$ two-photon transitions, where by 'polarization-angle correlation' we mean the probability of measuring, in coincidence, the two emitted photons with a certain opening angle θ, when the polarization of one photon (of the two) is measured while the other one is not [94].
We will present here the results which have been found in Ref. [93], where I personally contributed. Moreover, the results we will present include, specifically for $2s_{1/2} \to 1s_{1/2}$ transition, the ones found in Ref. [94], since by summing the polarization-polarization correlation over the polarization outcomes of one of the two photons, one gets the polarization-angle correlation.
Prior to showing such results, we shall first agree about the geometry under which the emission of both photons is considered. Since, for the decay of unpolarized ionic states, there is no direction initially preferred for the overall system, we adopt the z axis along the momentum of the "first" photon, as done in Sec. 5.2. Together with the momentum direction of the "second" photon, this axis then defines also the reaction plane (x-z plane). A single polar angle θ, the opening angle, is required, therefore, to characterize the emission of the photons with respect to each other (cfr. Fig. 5.10).
As required by Bose-Einstein statistics, the two–photon state has to be symmetric upon exchange of the particles. Therefore, it is *a priori* not possible to address them individually. We can safely assume, however, an experimental setup in which two detectors observe, in coincidence, the photons having certain energies and propagation directions. A "click" at these detectors would correspond to the photon's collapse into energy and momentum eigenstates [95]. A clear identity can be given, therefore, to the photons: the first (second) photon is that one detected by the detector $A(B)$ (marked gray in Fig. 5.10) at a certain energy $E_{1(2)}$ and momentum $\boldsymbol{p}_{1(2)}$.
For the theoretical analysis below we shall take into account not only the emission angles and the energies but also the linear polarization states of the emitted photons. In order to observe these states, we assume that both detectors act as linear polarizers
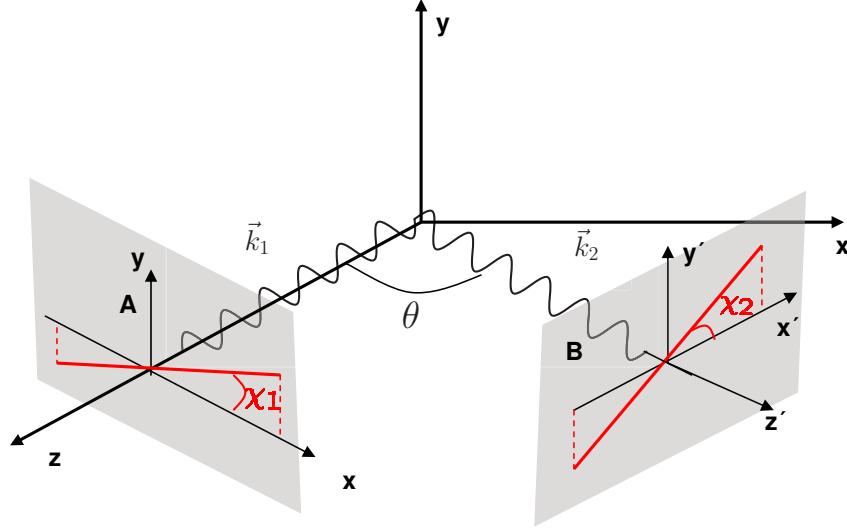
Figure 5.10: Geometry for the two–photon decay of excited ionic state.

whose transmission axes are defined in the planes that are perpendicular to the photon momenta $\boldsymbol{p}_1 = \hbar \boldsymbol{k}_1$ and $\boldsymbol{p}_2 = \hbar \boldsymbol{k}_2$ and are characterized by the angles χ_1 and χ_2 with respect to the reaction (x-z) plane. In this notation, $\chi_{1(2)} = 0°$ denotes the measured direction of the polarization of the first (second) photon within the reaction plane, as showed in figure 5.10.

As previously done, we evaluate the second-order transition amplitude (3.48) by using the Green's function for the Dirac-Coulomb Hamiltonian, as described in Sec. 2.3.

Most naturally, the polarization-polarization analysis is performed in the framework of the density matrix theory. For the decay of an unpolarized initial state $|n_i j_i\rangle$ into the level $|n_f j_f\rangle$, the two-photon spin density matrix reads

$$\langle \boldsymbol{k}_1, \lambda_1, \boldsymbol{k}_2, \lambda_2 | \, \hat{\rho}_f \, | \boldsymbol{k}_1, \lambda_1', \boldsymbol{k}_2, \lambda_2' \rangle = \frac{1}{2j_i + 1} \sum_{\mu_i, \mu_f} \mathcal{M}_{\lambda_1 \lambda_2}^{\gamma\gamma}(i \to f) \mathcal{M}_{\lambda_1' \lambda_2'}^{\gamma\gamma \, *}(i \to f) \,, \quad (5.7)$$

where $\mathcal{M}_{\lambda_1 \lambda_2}^{\gamma\gamma}$ represents the two-photon amplitude with the further subscript $\lambda_1 \lambda_2$ to make the polarization dependence explicit. We remark that $\lambda_{1,2} = \pm 1$ are the spin projections of the first and second photon onto their propagation directions, i.e. the helicities.

Instead of the helicity representation, it is more convenient[2] to re-write the density matrix (5.7) in the representation of the vectors $\underline{x} \equiv \underline{\epsilon}_L|_{\theta_s = 0}$ and $\underline{y} \equiv \underline{\epsilon}_L|_{\theta_s = 90°}$ (see Eq. (2.45) for the definition of θ_s). As showed in Sec. 2.5, such vectors denote the linear polarization of the photons respectively under the angles $\theta_s = \chi = 0°$ and $\theta_s = \chi = 90°$ with respect to the reaction plane (see Fig. 5.10). In the notation used here, the angle χ corresponds to the angle θ_s defined in Eq. (2.45).

Any linear polarization which is nowadays measured in experiments can be expressed

---

[2]The experimental investigation in this basis turns out to be easier.

in terms of these two (basis) vectors

$$\underline{\epsilon}_L(\theta_s) = \underline{\epsilon}_L(\chi) = \frac{1}{\sqrt{2}}\left(\underline{x}\,\cos\chi + \underline{y}\,\sin\chi\right)$$

$$= \frac{1}{\sqrt{2}}\left(\mathrm{e}^{-i\chi}\,\underline{\epsilon}_C^{\lambda=+1} + \mathrm{e}^{+i\chi}\,\underline{\epsilon}_C^{\lambda=-1}\right), \tag{5.8}$$

by following the decomposition of linear polarization vectors in terms of the circular polarization ones as showed in Eq. (2.45).

We can make explicit the association with ket states in the photon quantum spin space by writing

$$\underline{\epsilon}_L(\chi) \doteq |\chi\rangle = \frac{1}{\sqrt{2}}\left(\mathrm{e}^{-i\chi}\,|\lambda = +1\rangle + \mathrm{e}^{+i\chi}\,|\lambda = -1\rangle\right).$$

The density matrix (5.7) contains the complete information on the two emitted photons. It can be therefore employed to derive their polarization properties. To achieve this goal, it is natural to define the detector operator for the measurement of the photon linear polarizations:

$$\hat{\mathrm{P}} = |\boldsymbol{k}_1\chi_1\,\boldsymbol{k}_2\chi_2\rangle\,\langle\boldsymbol{k}_1\chi_1\,\boldsymbol{k}_2\chi_2|\,.$$

By taking the trace over $\hat{\mathrm{P}}$ times the density matrix (5.7) and applying Eq. (5.8), we immediately derive, as showed in Sec. 4.1, the polarization-polarization correlation function

$$\begin{aligned}\Phi_{\chi_1\chi_2}(\theta) &= \mathcal{N}\,\mathrm{Tr}(\hat{P}\hat{\rho}_f) = \frac{\mathcal{N}}{4(2j_i+1)}\sum_{\lambda_1,\lambda_1'=-1,1}\sum_{\lambda_2,\lambda_2'=-1,1}\\ &\times\quad \mathrm{e}^{i(\lambda_1-\lambda_1')\chi_1}\,\mathrm{e}^{i(\lambda_2-\lambda_2')\chi_2}\,\mathcal{M}_{\lambda_1\lambda_2}^{\gamma\gamma}(i\to f)\,\mathcal{M}_{\lambda_1'\lambda_2'}^{\gamma\gamma\,*}(i\to f)\,,\end{aligned} \tag{5.9}$$

which represents the normalized probability of a coincidence measurement of two photons with well-defined wave vectors $\boldsymbol{k}_1$ and $\boldsymbol{k}_2$ and with linearly polarization vectors characterized by the angles χ_1 and χ_2 with respect to reaction plane. Here the normalization constant $\mathcal{N}$ is chosen such that, for any value of the opening angle θ, we get the unity after having summed over the probabilities of the (four) independent photons' polarization states $|xx\rangle$, $|xy\rangle$, $|yx\rangle$, $|yy\rangle$. For the sake of brevity, we have introduced the notation $|xx\rangle = |\chi_1 = 0°\rangle\,|\chi_2 = 0°\rangle$, $|xy\rangle = |\chi_1 = 0°\rangle\,|\chi_2 = 90°\rangle$ and so forth.

In the results below, we will derive the polarization-polarization correlation Φ within the relativistic framework and by considering all the multipoles in the photon vector plane waves. Prior to doing that, however, it is useful to assume non-relativistic and long wavelength approximations and derive simple formulae, in order to get insights into the polarization properties of the photons and in order to compare, later, the relativistic as well as non-dipole effects on the polarization-polarization correlation. Within these two approximations, specifically for the transition $2s_{1/2} \to 1s_{1/2}$, we have been able to derive a simple analytic expression for the function Φ:

$$\Phi_{\chi_1\chi_2}(\theta)\Big|_{NR\&lwa} = \frac{1}{1+\cos^2\theta}\Big(\sin\chi_1\sin\chi_2 + \cos\chi_1\cos\chi_2\cos\theta\Big)^2. \tag{5.10}$$
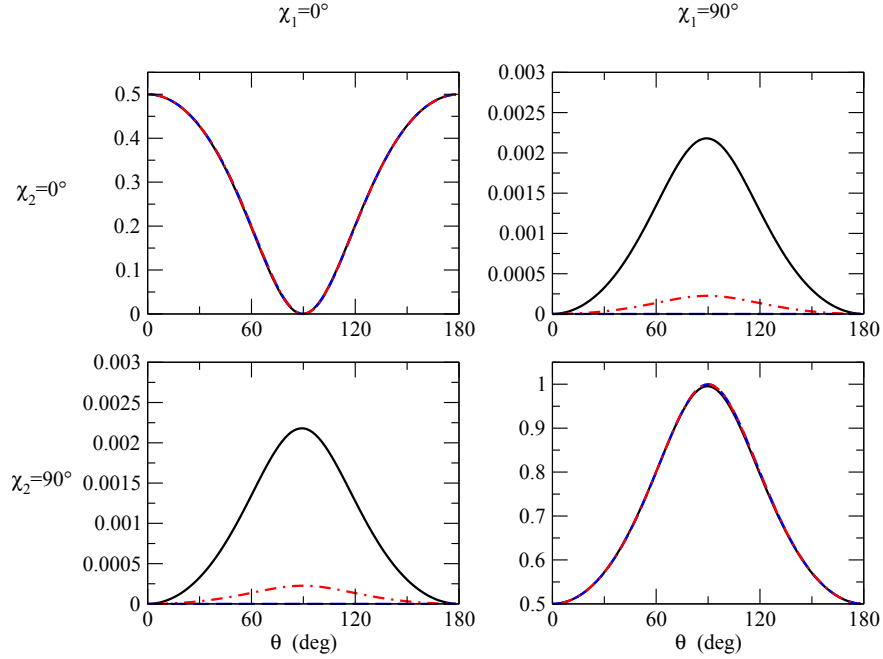
Figure 5.11: Polarization–polarization correlation of photons emitted in the $2s_{1/2} \rightarrow 1s_{1/2}$ two-photon decay. The solid line corresponds to U^{91+}, the dot-dashed line corresponds to Xe^{53+} while the dashed line corresponds *both* to H *and* to the non-relativistic calculation (the discrepancy between the two calculations is less than $10^{-10}\%$ and therefore not visible in the graph). Calculations are presented for energy sharing $y = 1/2$ and for the different polarization angles χ (cfr. Fig. 5.10).

We immediately see that the (detected) photon polarizations cannot be orthogonal to each other: For $\chi_1 = 0°(90°)$, $\chi_2 = 90°(0°)$ the polarization-polarization correlation Φ vanishes. We furthermore notice that, for the photon polarization case $\chi_{1,2} = 90°$ (both photon polarization states are along y), there is no dependence upon the opening angle θ, or, in other words, rotation around the polarization (y) axis are a symmetry of the decay process. From Eqs. (5.7) and (5.10), the photons polarization state can be derived to be pure and described by the ket vector [15]:

$$|\Psi\rangle_{NR\&lwa} = \frac{1}{1 + \cos^2\theta} \left(|yy\rangle + \cos\theta |xx\rangle\right) . \tag{5.11}$$

From this expression, it may be easier to see that the probability of measuring, in coincidence, orthogonal linear polarizations of photons within NR&*lwa* is zero.
We are now ready to show the relativistic results. Calculations have been performed for neutral Hydrogen atom H, hydrogen-like Xenon Xe^{53+} and Uranium U^{91+} ions, for various values of the energy sharing parameter y defined in Eq. (5.2).
In Fig. 5.11, for example, the polarization correlation function $\Phi_{\chi_1\chi_2}(\theta)$ is displayed for the parameter $y = 1/16$. As seen from the figure, for light ions, both the electric dipole and the fully relativistic treatments basically coincide and are well described by Eq. (5.10). For high-Z hydrogen-like ions, however, it is expected that equations (5.10) and (5.11) might not describe well the polarization properties of the emitted photons, owing to relativistic and non-dipole effects. As seen from Fig. 5.11, these effects
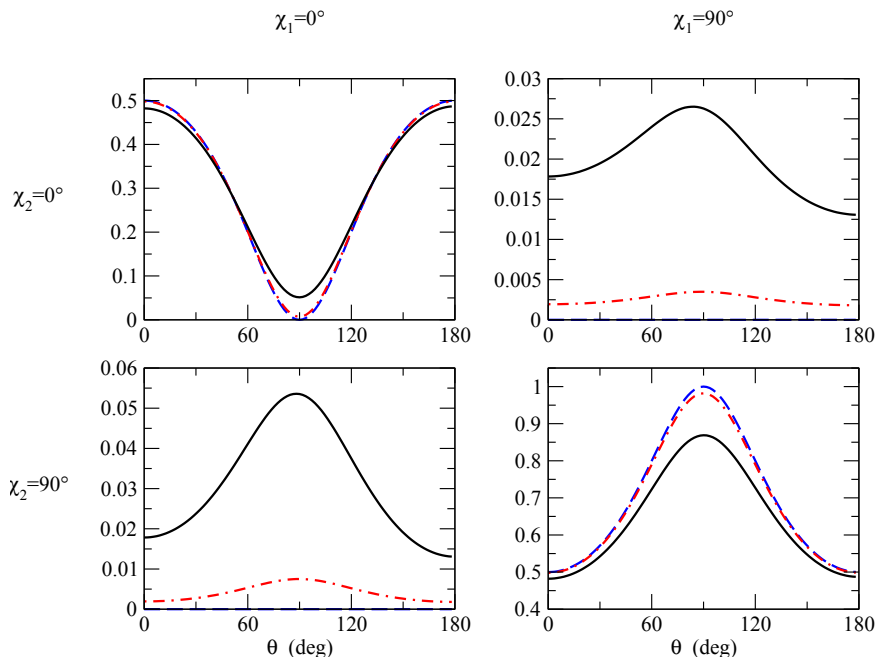
Figure 5.12: Polarization-polarization correlation of photons emitted in the $2s_{1/2} \rightarrow 1s_{1/2}$ two-photon decay. The solid line corresponds to U^{91+}, the dot-dashed line corresponds to Xe^{53+} while the dashed line corresponds *both* to H *and* to the non-relativistic calculation (the discrepancy between the two calculations is less than $10^{-10}\%$ and therefore not visible in the graph). Calculations are presented for energy sharing $y = 1/16$ and for the different polarization angles χ (cfr. Fig. 5.10).

result in a non-vanishing correlation function Φ for the "perpendicular polarization" measurements, i.e. when $\chi_2 = \chi_1 \pm 90°$. The probability of "parallel polarization" measurements consequently decreases of the same measure. We moreover notice that, in case of energy sharing $y = 1/16$ and $\theta = 90°$, events with photon polarizations *within* the reaction plane are not forbidden, in contrast to NR&*lwa*, as a consequence of relativistic and non-dipole effects. This, in turn, leads to a further reduction of the probability for those events with photon polarizations which are perpendicular to the reaction plane. For hydrogen-like Uranium ion U^{91+}, for example, the function $\Phi_{\chi_1,\chi_2}(\theta)$, as calculated at $\chi_1 = \chi_2 = 90°$ and perpendicular photon emission ($\theta = 90°$), decreases from 1 to almost 0.85 if the higher multipole terms are taken into account. While the relativistic and retardation effects are significant in high-Z domain if one of the photons is much more energetic than the second one, they become almost negligible if the photons are emitted with nearly the same energy: $\omega_1 \approx \omega_2$. As can be seen from Fig. 5.12, for energy sharing $y = 0.5$, the polarization probabilities obtained within NR&*lwa* and the rigorous relativistic approach differ in fact only of about $\sim 10^{-3}$, even for the decay of hydrogen-like Uranium ion.

Many-electron atoms

To my best knowledge, there have not been direct studies on the polarization properties of the photons coming from a two-photon decay of many-electron bound systems. The

only works I am aware of which involve photon polarizations in two-photon decay of many-electron bound states are the two works by us, [15] and [20]. The former analyzes the polarization quantum correlation of the photons, while the latter makes use of the polarization properties of the emitted photons to suggest a workable scenario to investigate parity violation phenomena in atomic physics. In the next sections, we will describe both studies in detail.

5.4 QUANTUM ENTANGLEMENT OF THE TWO EMITTED PHOTONS

In this section, we investigate the quantum correlation (entanglement) that the polarization state of photons emitted in the two-photon decay of few-electron ions possesses. The transitions we study are $2s_{1/2} \rightarrow 1s_{1/2}$ in hydrogen-like, as well as $1s_{1/2}\, 2s_{1/2} \,:\, J = 0 \rightarrow 1s_{1/2}^2 \,:\, J = 0$, $1s_{1/2}\, 2s_{1/2} \,:\, J = 1 \rightarrow 1s_{1/2}^2 \,:\, J = 0$ and $1s_{1/2}\, 2p_{1/2} \,:\, J = 0 \rightarrow 1s_{1/2}^2 \,:\, J = 0$ transitions in helium-like ions.
The geometry we refer to in what follows is the same as the one explained at the beginning of Sec. 5.3, which is, in turn, displayed in Fig. 5.10.
As underlined in Sec. 4.2, spin–correlation phenomena are most easily described within the framework of density matrix theory. Thus, we will use the spin-polarization density matrix of the two emitted photons, Eq. (4.8), to analyze the entanglement properties of the polarization state of the photons. The amplitude $\mathcal{M}^{\gamma\gamma}_{\lambda_1 \lambda_2}$ will be evaluated, once again, by using the Green function for the Dirac-Coulomb Hamiltonian, as extensively explained in Secs. 2.3 and 3.5. For transitions in He-like ions, we will make use of the independent particle model, as already done in Sec. 5.2. Thus, we will restrict ourselves to the description of transitions in highly charged ions, where such a model is adequate.

5.4.1 NON-RELATIVISTIC AND LONG WAVELENGTH APPROXIMATIONS

Before going into the relativistic analysis, we first restrict ourselves, as usual, to the non-relativistic and long wavelength approximations so as to derive approximate expressions for the description of the two-photon polarization states. As we will see later, this will provide intuitive insight into the entanglement properties of the photon pairs. Moreover, by comparing predictions of such a simplified approach with the results of the relativistic theory, we will be able to identify the relativistic and non-dipole effects in the two-photon transitions.
In this section, since we are going to describe states in the non-relativistic framework, we should consistently rename the helium-like states we are dealing with by following the non-relativistic notation:

$$1s_{1/2}^2 \,:\, J = 0 \qquad \rightarrow \quad (1s^2)\,{}^1S_0$$

$$1s_{1/2}\, 2s_{1/2} \,:\, J = 0 \quad \rightarrow \quad (1s\,2s)\,{}^1S_0$$

$$1s_{1/2}\, 2s_{1/2} \,:\, J = 1 \quad \rightarrow \quad (1s\,2s)\,{}^3S_1$$

$$1s_{1/2}\, 2p_{1/2} \,:\, J = 0 \quad \rightarrow \quad (1s\,2p)\,{}^3P_0$$

$$... \qquad\qquad \rightarrow \qquad ...$$

as explained in Sec. 2.4 and, specifically, in Eq. (2.39).

By making use of NR approximation and by restricting the intermediate-state summation over $|\nu\rangle$ to states with equal angular momentum J_ν and parity P_ν, defined by dipole selection rules, it is possible to express the density matrix (4.8) in the form [96]:

$$
\langle \lambda_1, \lambda_2 | \hat{\rho}_\gamma | \lambda_1', \lambda_2' \rangle_{NR\&lwa} = C \, \lambda_1 \lambda_2 \lambda_1' \lambda_2' \sum_{L=1}^{\infty} \sum_{\mu_1, \mu_2 = -L}^{L} d^L_{\mu_1 \mu_2}(\theta)
$$

$$
\times \langle 1, \lambda_1, 1, -\lambda_1' | L, \mu_1 \rangle \langle 1, -\lambda_2, 1, \lambda_2' | L, \mu_2 \rangle \tag{5.12}
$$

$$
\times \left(\left\{ \begin{array}{ccc} J_\nu & J_f & 1 \\ J_i & J_\nu & 1 \\ 1 & 1 & L \end{array} \right\} + \left\{ \begin{array}{ccc} 1 & 1 & L \\ J_\nu & J_\nu & J_i \end{array} \right\} \left\{ \begin{array}{ccc} 1 & 1 & L \\ J_\nu & J_\nu & J_f \end{array} \right\} \right) ,
$$

where we employed the standard notation for the Wigner $6j$- and $9j$-symbols [54], and C is a normalization constant that absorbs the radial parts of the transition amplitudes $\mathcal{M}^{\gamma\gamma}_{\lambda_1 \lambda_2}(i \to f)$. Furthermore, $d^L_{\mu_1 \mu_2}(\theta)$ are reduced Wigner matrices.

The supposition of equal angular momentum and parity for the intermediate states leads to the evident advantage of having the final-state density matrix (5.12) which depends only on the symmetry of the initial and final ionic states as well as on the photons' helicities. This supposition, however, limits the usage of the density matrix. Indeed, Eq. (5.12) can be applied only for the analysis of those transitions that proceed, within NR&lwa, via intermediate (virtual) states that have *one* particular value of total angular momentum J_ν and parity P_ν. This is the case of $(1s\,2s)\,{}^1S_0 \to (1s^2)\,{}^1S_0$ transition in helium-like ions, since, within lwa, the intermediate (virtual) states can only be[3] $(1s\,np)\,{}^1P_1$. In addition, we can use Eq. (5.12) also for $2s_{1/2} \to 1s_{1/2}$ decay in hydrogen-like ions, since, for the electric dipole E1, the angular part given by $6j$- and 9j-symbols gives the same result for the allowed intermediate states $np_{1/2}$ and $np_{3/2}$ (which suggests that the angular contribution of these states to the decay is, as expected, non-relativistically the same). In the following analysis, we shall therefore restrict the application of (5.12) to these two transitions. It happens that, for these two case-transitions, the density matrix $\langle \hat{\rho}_\gamma \rangle$ in Eq. (5.12) fulfills the relation $\mathrm{Tr}\left[\langle \hat{\rho}_\gamma^2 \rangle \right] = \mathrm{Tr}\left[\langle \hat{\rho}_\gamma \rangle \right]^2 = 1$ and, hence, it represents a pure quantum-mechanical spin state of the emitted photons (see Sec. 4.1). It can be easily found that this pure state is described by the state vector (5.11):

$$
|\Psi\rangle = -\frac{1}{2\sqrt{1 + \cos^2 \theta}} \Big[(\cos\theta - 1)(|{+}{+}\rangle + |{-}{-}\rangle) + (\cos\theta + 1)(|{+}{-}\rangle + |{-}{+}\rangle) \Big]
$$

$$
= -\frac{1}{\sqrt{1 + \cos^2 \theta}} \Big[|yy\rangle + \cos\theta \, |xx\rangle \Big] , \tag{5.13}
$$

where we have used the notation $|{\pm}\rangle \equiv |\lambda = \pm 1\rangle$, $|\chi = 90°\rangle \equiv |y\rangle$ and $|\chi = 0°\rangle \equiv |x\rangle$. The photons are identified and detected according to our discussion concerning 'labeling', which has been given at the beginning of Sec. 5.3 and which is displayed in Fig.

---

[3]One-photon transitions within lwa link initial and final states i) which satisfy the triangle rule $J_f \otimes 1 = J_i$, ii) with opposite parity and iii) with same spin (see Eq. (3.37)). Therefore, the states $(1s\,np)\,{}^3P_{0,1,2}$ are excluded from the summation over intermediate states because of 'iii', the states $(1s\,nd)\,{}^{1,2}D_{1,2,3}$ are excluded because of 'ii', the states $(1s\,nf)\,{}^{1,3}F_{2,3,4}$ (and any other) are excluded because of 'i'.

5.10.

We immediately see that, if $\theta = \pi/2$, the photon polarization state is a *product* (non-entangled, or separable) spin state. For the particular case of back-to-back photon emission ($\theta = \pi$), the vector (5.13) further simplifies to a Bell state:

$$|\Psi\rangle = \frac{1}{\sqrt{2}}(|++\rangle + |--\rangle) . \tag{5.14}$$

As seen from this expression, for the opening angle $\theta = \pi$ photons can only be detected having the same helicity. In the past, such a quantum correlation between the photons emitted in the $2s_{1/2} \to 1s_{1/2}$ decay of atomic deuterium has been employed for verifying a violation of Bell's inequality [19].

The quantitative analysis of entanglement for the emitted photon pair will be performed in the following sections, based on our general expression (5.12), as well as on the NR&*lwa* formula (5.13). Before we start such analysis, let us discuss some basic properties of the photon spin-state. We will refer to the ket vector (5.13). We recall that the typical "experimental scenario" consists of both photons detected by polarimeters whose transmission axes are characterized by the angles χ_1 and χ_2 with respect to the reaction (x-z) plane (see Fig. 5.10). Eq. (5.13) predicts that after the first photon has been detected by the detector A (the first detector) with some defined (linear) polarization angle χ_1, the state of the second photon collapses onto the ket vector

$$|\Psi\rangle \to N \left[\sin \chi_1 |y\rangle + \cos \theta \cos \chi_1 |x\rangle \right] ,$$

where N is some normalization factor. It follows from the above equation that the second photon is then found in a linearly polarized state. The direction of this linear polarization, characterized by the angle $\tilde{\chi}_2$, depends on the opening angle θ of the event and on the polarization angle χ_1 along which the polarization of the first photon had been detected. The analytical relation which links such variable is

$$\tan \tilde{\chi}_2 = \frac{1}{\cos \theta} \tan \chi_1 .$$

Trivially, this one-to-one relation between χ_1 and χ_2 does not generally imply that the photons are maximal entangled. To better understand this issue and to finally quantify the degree of entanglement we shall introduce, in a few paragraph, the 'Concurrence' measure.

5.4.2 $P_0 \to S_0$ TRANSITIONS

In contrast to the $S_0 \to S_0$ transitions we discussed above, the approximated formulae (5.12)-(5.13) cannot be applied for the analysis of the $(1s\,2p)\ ^3P_0 \to (1s^2)\ ^1S_0$ decay of helium-like ions. The principal reason for this failure is that the leading (electric-magnetic dipole) E1M1-M1E1 $(1s\,2p)\ ^3P_0 \to (1s^2)\ ^1S_0$ transition may proceed either via the intermediate $(1s\,ns)\ ^3S_1$ or via the $(1s\,np)\ ^3P_1$ states, thus invalidating the hypotheses. For this transition, we therefore come back to the relativistic treatment (and, therefore, to the relativistic notation) but we consider, at first, only the leading E1M1 dipole transition operator. By doing that, we again find the photon pair coming from $1s_{1/2}\,2p_{1/2} : J = 0 \to 1s_{1/2}^2 : J = 0$ transition are characterized by a pure spin

state of the form

$$
\begin{aligned}
|\Psi\rangle \;=\; C\Big(& -\Sigma(y)\sin^2\frac{\theta}{2}\,|++\rangle + \Delta(y)\cos^2\frac{\theta}{2}\,|-+\rangle \\
& -\Delta(y)\cos^2\frac{\theta}{2}\,|+-\rangle + \Sigma(y)\sin^2\frac{\theta}{2}\,|--\rangle \Big).
\end{aligned}
\tag{5.15}
$$

Here, C is the normalization constant while the energy–dependent functions are defined as: $\Sigma(y) = S_{E1M1}(\omega_1) + S_{E1M1}(\omega_2) + S_{M1E1}(\omega_1) + S_{M1E1}(\omega_2)$, $\Delta(y) = S_{E1M1}(\omega_1) - S_{E1M1}(\omega_2) - S_{M1E1}(\omega_1) + S_{M1E1}(\omega_2)$. The second-order reduced transition amplitudes $S_{L_1p_1,L_2p_2}(\omega)$ are defined in Eq. (5.5).
As seen from the equation above, the spin-state of the photons emitted in the $1s_{1/2}\,2p_{1/2}$: $J = 0 \to 1s_{1/2}^2$: $J = 0$ transition depends upon the energy sharing y. No simple analytical expression for this dependence can be derived in general, owing to the complicated structure of the functions $\Delta(y)$ and $\Sigma(y)$. However, if both photons carry away the same fraction of the energy, $\omega_1 = \omega_2$, the function $\Delta(y = 0.5)$ vanishes, and the vector (5.15) represents a maximally entangled (Bell) state:

$$
|\Psi\rangle = \frac{1}{\sqrt{2}}\Big(-|++\rangle + |--\rangle \Big) = -\frac{i}{\sqrt{2}}\Big(|xy\rangle + |yx\rangle \Big).
\tag{5.16}
$$

By comparing this polarization state, for $P_0 \to S_0$ He-like transitions, with the other one in Eq. (5.13), for $S_0 \to S_0$ He-like transitions, one can see that polarization properties of the former is strongly different with respect to the latter: while the photons emitted in the $S_0 \to S_0$ transitions can be only detected having *parallel* linear polarization vectors, the photons emitted in the $P_0 \to S_0$ transitions can be only detected having *orthogonal* linear polarizations. Moreover, no angular dependence arises in the state vector (5.16), which implies maximal entanglement between the photons' spins, irrespectively of the particular decay geometry.

5.4.3 ENTANGLEMENT OF THE TWO-PHOTON STATE

We are ready now to discuss the concept of entanglement for the emitted photon pairs and to introduce a proper measure for it. Let us first write the full two–photon state which accounts, not only for the spin, but also for the spatial degrees of freedom. Within NR&*lwa*, such a state, before its detection, reads

$$
\begin{aligned}
|\Phi\rangle \;=\; & N \int \mathrm{d}\omega_1\mathrm{d}\omega_2\delta(\omega_1 + \omega_2 - \Delta_\omega)f(\omega_1)\,|\omega_1\omega_2\rangle \\
& \times \int \mathrm{d}\theta_1\mathrm{d}\theta_2\,|\theta_1\theta_2\rangle + \Big(|yy\rangle\cos(\theta_1 - \theta_2)\,|xx\rangle \Big) + (1 \leftrightarrow 2),
\end{aligned}
$$

where $(1 \leftrightarrow 2)$ denotes the previous terms but with all particles' labels exchanged and the state is normalized by virtue of the constant N. Moreover, $f(\omega_{1,2})$ is the energy probability density function of the decay, $\Delta_\omega = E_i - E_f$ is the transition energy and $\theta_{1,2}$ are the angles which address the position of the first and second photon in the reaction plane, respectively. Due to the integral over angles and energies, the above state can be written as product state neither in the energies nor in the emission angles or in the polarization. It can hence be seen as highly entangled, in general.
In order to rigorously discuss entanglement, due to the identity of particles, a degree of

freedom for discrimination is needed. The energy of the photons and their opening angles are an appropriate choice, since one naturally projects onto energy and momentum eigenstates in the experiment. In the coincidence experiment displayed in Fig. 5.10, the two-photon state collapses onto a state with definite momenta. If the energies of the photons are equal and the emission directions exactly the same, we are not able to identify two separated particles between which entanglement may be defined. As long as this is not the case, we identify the particle projected on the two energies and angles as the two distinct entities to which we can safely assign an entanglement measure [95]. Hence, even though we start with a rather complex state of identical particles in which no physical subsystem structure is apparent, we can effectively deal with the two-qubit system of polarized photons projected on energy and momentum states.

Having clarified the concept of the two-photon entanglement, we shall introduce now its quantitative measure. For a photon pair, that can be seen as a "two-qubit" system, it is very convenient to describe the degree of entanglement by means of the Wootter's concurrence $\mathcal{C}$ [60]. The basic relations for this method have been explained in Sec. 4.2.

Before we discuss further the properties of the concurrence $\mathcal{C}$, we first recall that it quantifies (only) correlations that can be fully attributed to the entanglement. Bi-particle states with vanishing concurrence can still exhibit correlations which are, however, not of quantum nature.

The definition of Concurrence given in Eq. (4.4) can be simplified further if applied to a pure quantum-mechanical state described by a ket vector:

$$
\begin{aligned}
|\beta\rangle = C_{aa} |aa\rangle + C_{ab} |ab\rangle + \\
C_{ba} |ba\rangle + C_{bb} |bb\rangle \ ,
\end{aligned}
$$

where a, b are arbitrary two–dimensional basis states and C_{ij} are complex numbers. For this state, the concurrence reads

$$
\mathcal{C} = 2 \Big| C_{aa} C_{bb} - C_{ab} C_{ba} \Big| .
$$

By using the above expression and Eq. (5.13), we immediately obtain the analytical expression

$$
\mathcal{C}(\theta) = 2 \frac{|\cos\theta|}{1 + \cos^2\theta} \tag{5.17}
$$

for the spin-entanglement of the photons emitted in the $2s_{1/2} \to 1s_{1/2}$ and $(1s\,2s)\,^1S_0 \to (1s^2)\,^1S_0$ transitions. We remind that Eq. (5.17) is obtained within NR&lwa and should be questioned in high-Z domain, where higher-order and relativistic effects can play a significant role. To explore the influence of these effects on the photon spin-entanglement, we will compare, in the next paragraph, the predictions obtained from Eq. (5.17) with the rigorous relativistic calculations based on Eqs. (4.8) and (4.4). For this comparison, we will naturally make use of the table (2.39).

5.4.4 RESULTS AND DISCUSSION

Hydrogen-like ions

After having discussed the theoretical background of two-photon polarization studies, we are prepared now to analyze the influence of the relativistic and higher-multipole

effects on quantum correlations between the two photons. We start our analysis with the $2s_{1/2} \to 1s_{1/2}$ decay of hydrogen-like ions, that is well established both in theory and experiment. As shown above, the polarization properties of this transition can be described, within NR&lwa, by the state vector (5.13) and, hence, by the degree of entanglement (5.17). The theoretical predictions, obtained within such an approximated approach, are displayed in Fig. 5.13 for the decay of neutral Hydrogen as well as hydrogen-like Xenon Xe^{53+} and Uranium U^{91+} ions and are compared with the results of the rigorous relativistic treatment. The calculations are performed at two relative photon energies $y = 1/16$ (upper panel) and $y=1/2$ (lower panel). As seen from the figure, in case of equal energy sharing ($y = 1/2$), both approaches yield almost identical results along the entire isoelectronic sequence. Our calculations show that, while being maximal for the parallel ($\theta = 0$) and back-to-back ($\theta = \pi$) photon emission, the concurrence vanishes at the opening angle $\theta = \pi/2$. This behaviour is well understood from Eq. (5.13) as well as from the conservation of the projection M_{tot} of the total angular momentum J_{tot} of the overall system "ion + two photons". Namely, if no electron–spin flip were to occur during the $2s_{1/2} \to 1s_{1/2}$ decay and assuming 0 nuclear spin, the conservation law enforces that the change of the projection of the ion's total angular momentum relative to the quantization axis z (chosen along the momentum of the first photon) would be given by $M_i - M_f = 0 = \lambda_1 + M_{\gamma_2}$. In this expression, λ_1 is the helicity of the first photon and M_{γ_2} is the projection of the angular momentum of the second one. For photons emitted in parallel or back-to-back, this projection is $M_{\gamma_2} = \lambda_2$ and $M_{\gamma_2} = -\lambda_2$, correspondingly, thus leading to the conditions $\lambda_1 = -\lambda_2$ or $\lambda_1 = \lambda_2$. Moreover, owing to the spherical symmetry of s-ionic states, there is an equal probability of emission of the "first" photon with helicity $\lambda_1 = +1$ or -1. This immediately implies maximally entangled Bell states $|\Psi\rangle = (|+-\rangle + |+-\rangle)/\sqrt{2}$ for $\theta = 0$, and $|\Psi\rangle = (|++\rangle + |--\rangle)/\sqrt{2}$ for $\theta = \pi$, as predicted by Eqs. (5.13) and (5.14).

Similar to the cases of parallel and back-to-back photon emission, the conservation condition $\lambda_1 = -M_{\gamma_2}$ with the helicity of the first photon being $\lambda_1 = \pm 1$ may help to understand the behaviour of the entanglement measure $C(\theta)$ at $\theta = \pi/2$. This will require us to come back to the electric dipole decomposition for the second photon, which, analogously to Eq. (2.58), reads[4]

$$\underline{\epsilon}_C^{\lambda_2} \, e^{i\boldsymbol{k}_2\boldsymbol{r}} \;\approx\; -\lambda_2\sqrt{6\pi} \sum_{M_\gamma=-1}^{+1} \boldsymbol{A}_{1M_\gamma}^{(e)}(k,\boldsymbol{r}) \, d_{M_\gamma\lambda_2}^1(\theta) \quad . \tag{5.18}$$

For the opening angle $\theta = \pi/2$, the elements of the reduced Wigner matrix are: $d_{11}^1 = d_{1-1}^1 = d_{-11}^1 = d_{-1-1}^1 = 1/2$, implying, together with Eq. (4.7) and with the fact that the ionic states are spherically symmetric, that the probability for the second photon to have projection $M_{\gamma_2} = \mp 1$ on the quantization axis of the overall system is independent of its helicity λ_2. Thus, no correlations between the polarization (spin) states of the emitted photons appear for the perpendicular emission, leading to the vanishing entanglement $C(\pi/2) = 0$ as displayed in Fig. 5.13.

As seen from the top panel of Fig. 5.13, the accuracy of NR&lwa becomes generally worse if one of the photons has a significantly larger energy than the other one. For

---

[4]In our chosen geometry for the decay, only the spherical angle θ is required for defining the direction of the second photon.
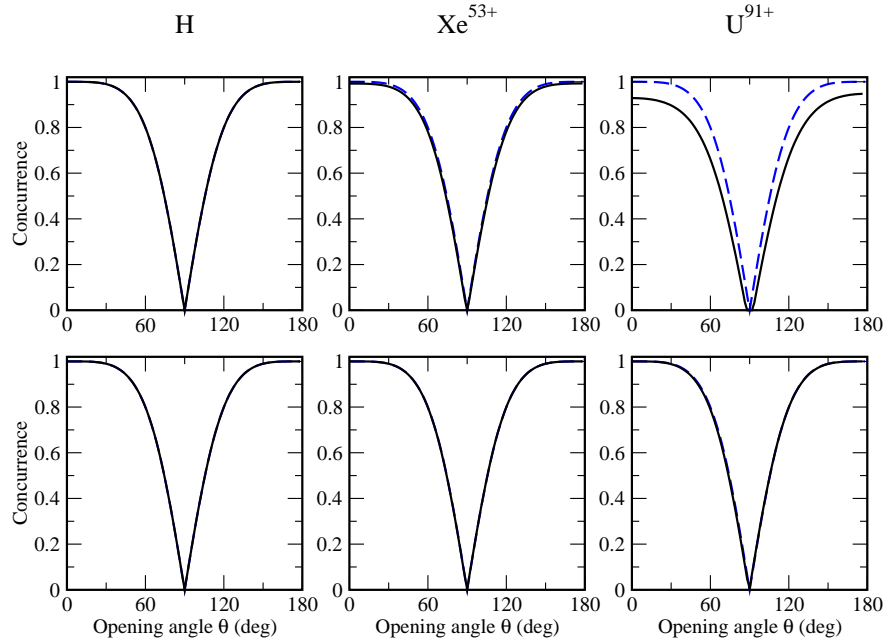
Figure 5.13: Concurrence of two photons emitted in the $2s_{1/2} \to 1s_{1/2}$ decay of neutral hydrogen and hydrogen-like Xenon and Uranium ions. Results of NR&*lwa* (dashed line) and the rigorous relativistic theory (solid line) are shown, for two relative photon energies $y = 1/16$ (upper panel) and $y = 1/2$ (lower panel).

the $2s_{1/2} \to 1s_{1/2}$ transition of hydrogen-like uranium, for example, NR&*lwa* overestimates the concurrence measure by about 10% for forward as well as backward opening angles, for an energy sharing $y = 1/16$. In order to understand better such an energy-dependent behavior, we study the *Purity* of the two-photon polarization state, which can be defined as

$$\mathcal{P} = \frac{4}{3}\,\mathrm{Tr}[\langle\hat{\rho}_\gamma\rangle^2] - \frac{1}{3}\,, \tag{5.19}$$

where $\langle\hat{\rho}_\gamma\rangle$ represents the photon density matrix (5.12). The purity varies from 0 (completely mixed state) to 1 (pure state). In Fig. 5.14 we display the purity $\mathcal{P}$ for the $2s_{1/2} \to 1s_{1/2}$ decay of U^{91+} for two relative photon energies: $y = 1/16$ (upper panel) and $1/2$ (lower panel). As seen from the figure, the purity strongly depends on the energy sharing parameter: while the purity of the two-photon state is always > 0.987 for an equal energy sharing $y = 0.5$, it is significantly reduced for $y = 1/16$. The loss of purity can be attributed to the spin-orbit coupling in hydrogen-like ions as well as to the magnetic terms in electron-photon interaction. Both these relativistic effects increase with the nuclear charge Z and with the photon energy. They lead to the fact that the decay of the unpolarized and, hence, mixed $2s_{1/2}$ level results in the emission of photons characterized by a partially mixed state. Due to complementarity of entanglement and mixedness/impurity [97], such a loss of purity causes the *reduction* of the concurrence measure that can be observed in the top panel of Fig. 5.13. Despite such a reduction, there are still quantum correlations between the polarization states of the photons.
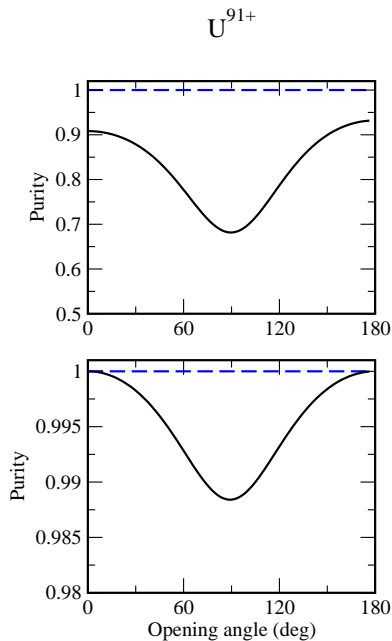
Figure 5.14: Purity (5.19) of the two-photon state in the $2s_{1/2} \rightarrow 1s_{1/2}$ decay of hydrogen-like Uranium. Results of NR&lwa (dashed line) and of the rigorous relativistic treatment (solid line) are shown, for relative photon energies $y = 1/16$ (upper panel) and $y = 1/2$ (lower panel).

Helium–like ions

In contrast to the $2s_{1/2} \rightarrow 1s_{1/2}$ decay of one-electron systems, the $1s_{1/2}\,2s_{1/2}\,:\,J = 0 \rightarrow 1s_{1/2}^2\,:\,J = 0$ transition in helium-like ions always proceeds between the pure, $J = 0$, quantum-mechanical states. Therefore, the spin-state of the photon pair emitted in such a transition will be pure at any energy sharing. The concurrence measure $C(\theta)$ of such a pure state calculated within the exact relativistic theory turns out to be almost identical to the dipole approximation (5.17). The deviation between both predictions does not exceed 1%, even for the heaviest helium-like ions and arises due to the higher, non-dipole terms in electron-photon interaction. By comparing this prediction with the calculations performed in the previous section for hydrogen-like ions, we again argue that the reduction of the spin-entanglement between the photons emitted in the $2s_{1/2} \rightarrow 1s_{1/2}$ transition shall be mainly attributed to the loss of purity of ionic states. After the above, short discussion of the $1s_{1/2}\,2s_{1/2}\,:\,J = 0 \rightarrow 1s_{1/2}^2\,:\,J = 0$ transition, we turn now to explore quantum correlations in the $1s_{1/2}\,2p_{1/2}\,:\,J = 0 \rightarrow 1s_{1/2}^2\,:\,J = 0$ decay. As one can expect from the spin-state vector (5.15), derived in leading order, "electric and magnetic" dipole approximation, these correlations should differ from those predicted for the $S_0 \rightarrow S_0$ cases. Indeed, by inserting the vector (5.15) into Eq. (5.17), we obtain, within the dipole (E1M1) approximation, the concurrence measure as

$$C(\theta, y) = \left| \frac{\Delta^2(y)\cos^4\frac{\theta}{2} - \Sigma^2(y)\sin^4\frac{\theta}{2}}{\Delta^2(y)\cos^4\frac{\theta}{2} + \Sigma^2(y)\sin^4\frac{\theta}{2}} \right| . \tag{5.20}$$
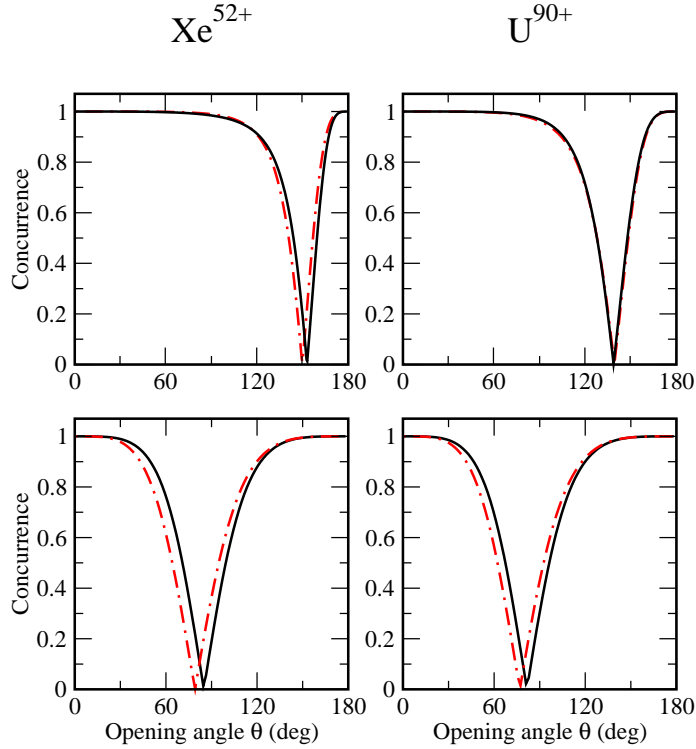
Figure 5.15: Concurrence of two photons emitted in the $1s_{1/2}\,2p_{1/2}\,:\,J=0\rightarrow 1s_{1/2}^2\,:$ $J=0$ decay of helium-like Xenon and Uranium ions. Results of the $E1M1$ dipole approximation (dash-dotted line) and of rigorous relativistic theory (solid line) are shown, for two relative photon energies $y=1/10$ (upper panel) and $y=1/4$ (lower panel).

In contrast to the polarization entanglement (5.17) between the photons emitted in the $S_0 \rightarrow S_0$ transitions, the concurrence turns out here to depend on the photons' energy sharing. To better understand such a dependence, we display the entanglement of the photons emitted in the $1s_{1/2}\,2p_{1/2}\,:\,J=0\rightarrow 1s_{1/2}^2\,:\,J=0$ decay of helium-like Xenon and Uranium ions in Fig. 5.15. Calculations are performed for two relative energies: $y=1/10$ and $1/4$ both within the dipole approximation (5.20) and by using the exact theory which accounts for the higher multipole channels. As seen from the figure, both theoretical approximations predict maximal entanglement, $\mathcal{C}=1$, for the parallel and back-to-back photon emission at *any* energy sharing y; a feature that could be expected from the conservation laws. On the contrary, the "critical" opening angle θ_c at which the concurrence vanishes, $\mathcal{C}(\theta_c)=0$, varies with the relative photon energy. By inspecting Eq. (5.20) we find the following relation for this angle:

$$\tan^2\left(\frac{\theta_c}{2}\right) = \frac{|\Delta(y)|}{|\Sigma(y)|} \,. \tag{5.21}$$

It follows from this expression that for any non-zero values of the functions $\Delta(y)$ and $\Sigma(y)$ there exists one single critical angle $\theta_c(y)$, as can also be seen, for example, from Fig. 5.15.

If the photons, emitted in the $1s_{1/2}\,2p_{1/2}\,:\,J=0\,\rightarrow\,1s^2_{1/2}\,:\,J=0$ decay, carry away the same portion of energy, $\omega_1 = \omega_2$, the function $\Delta(y)$ turns out to be zero and Eq. (5.21) cannot be applied for the determination of the critical angle θ_c. As can be seen from Eq. (5.16) and Eq. (5.20), in this case the photons state is maximally entangled (Bell state) for *any* opening angle, i.e. $\mathcal{C}(\theta, 0.5) = 1$. This behaviour differs from that of $1s_{1/2}\,2s_{1/2}\,:\,J=0\,\rightarrow\,1s^2_{1/2}\,:\,J=0$ as well as $2s_{1/2} \rightarrow 1s_{1/2}$ transitions for which no correlations appear at the opening angle $\theta = \pi/2$. In order to understand the reason for this difference, we shall return to Eq. (4.7) (and hence to Eq. (5.4)). By making use of the multipole expansion and of the properties of the Wigner matrices, we can re-write the two-photon transition amplitude in terms of reduced matrix elements (5.5) as:

$$\mathcal{M}^{\vec{k}_1 \vec{k}_2}_{fi}(\lambda_1, \lambda_2) \propto (\lambda_1 + \lambda_2)\Big(S_{E1M1}(\omega) + S_{M1E1}(\omega)\Big),$$

where, for the case of equal energy sharing, $\omega_1 = \omega_2 = \omega$.

It follows from the above equation that apart from the conservation of the projection of the total angular momentum J_{tot}, discussed in the previous paragraph, an additional selection rule arises for the $1s_{1/2}\,2p_{1/2}\,:\,J=0\,\rightarrow\,1s^2_{1/2}\,:\,J=0$ that forbids emission of the photons with opposite helicities. Together with the equal probabilities of the spin-states $|++\rangle$ and $|--\rangle$, this selection rule forces the photons polarization state to be the Bell state (5.16) and, hence, it implies maximal engagement of the photons' state.

Until now our discussion of the two-photon decay of helium-like ions was restricted to $J=0 \rightarrow J=0$ transitions. In this case, both initial and final ionic states are pure along the entire isoelectronic sequence, and, consequently, the two-photon states are pure as well. In order to underline again the effect of the loss of purity on the quantum correlations, we study the two-photon decay of the unpolarized $1s_{1/2}\,2s_{1/2}\,:\,J=1$ state. In Fig. 5.16, we display the degree of spin-entanglement for the $1s_{1/2}\,2s_{1/2}\,:\,J=1 \rightarrow 1s^2_{1/2}\,:\,J=0$ transition in helium-like Xenon and Uranium ions. Again, the exact relativistic calculations are compared with the predictions of electric dipole ($E1E1$) approach for two relative energies $y = 1/10$ and $1/4$. As seen from the figure, the general behaviour of the concurrence measure is very similar to that of the $1s_{1/2}\,2s_{1/2}\,:\,J=0 \rightarrow 1s^2_{1/2}\,:\,J=0$ and $2s_{1/2} \rightarrow 1s_{1/2}$ transitions. Namely, it changes from 1 for the parallel photon emission down to zero at $\theta = \pi/2$ and back to a maximum entanglement for $\theta = \pi$. Similar to the discussion in the previous paragraph, this can be easily understood if one applies again the momentum projection selection rules and Eq. (5.18). In contrast to the $1s_{1/2}\,2s_{1/2}\,:\,J=0 \rightarrow 1s^2_{1/2}\,:\,J=0$ and $2s_{1/2} \rightarrow 1s_{1/2}$ transitions, however, the degree of entanglement (Concurrence) for $1s_{1/2}\,2s_{1/2}\,:\,J=1 \rightarrow 1s^2_{1/2}\,:\,J=0$ transition drops down much faster for the forward $0 < \theta < \pi/3$ and backward $2\pi/3 < \theta < \pi$ angles; an effect that can be understood if we remember that the initial ionic state is prepared in an unpolarized (mixed) state.

As one can see from Fig. 5.16, spin entanglement for the $1s_{1/2}\,2s_{1/2}\,:\,J=1 \rightarrow 1s^2_{1/2}\,:\,J=0$ transition is very sensitive to higher multipoles in the electron-photon interaction. This is a direct consequence of a strong suppression of the $E1E1$ decay channel caused by the symmetry properties of the multi-photon systems (see Refs. [11–14] for further details). The non-dipole contributions become more significant for heavier ions and with increasing the energy sharing from 0 to 0.5, and result in an asymmetric shift in the concurrence.
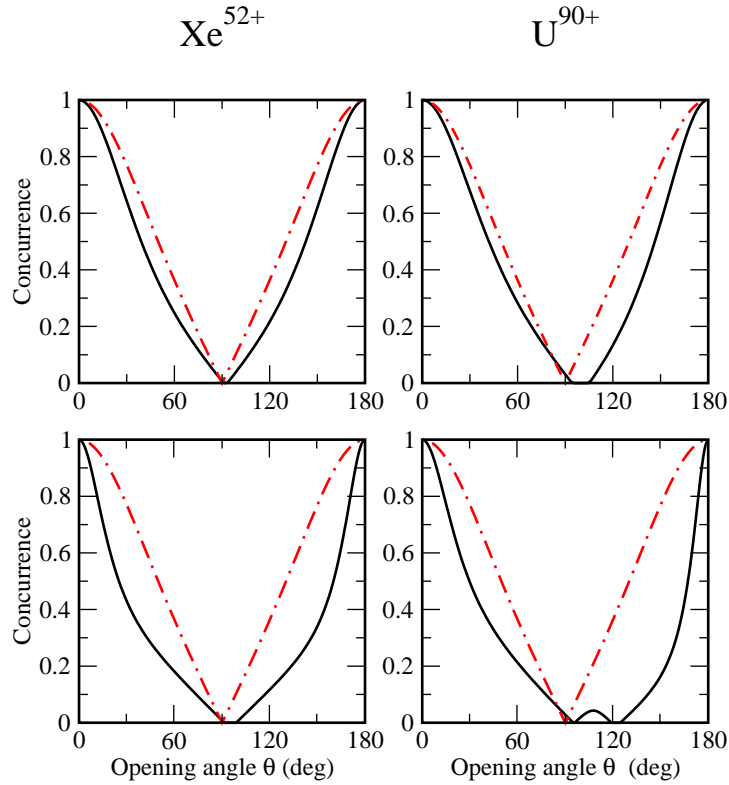
Figure 5.16: Concurrence of two photons emitted in the $1s_{1/2}\,2s_{1/2} : J = 1 \rightarrow 1s^2_{1/2} :$ $J = 0$ decay of helium-like Xenon and Uranium ions. Results of the $E1E1$ dipole approximation (dash-dotted line) and the rigorous relativistic theory (solid line) are shown, for two relative photon energies $y = 1/10$ (upper panel) and $y = 1/4$ (lower panel).

5.5 APPLICATIONS TOWARDS ATOMIC PARITY-VIOLATION STUDIES

Parity non-conservation (PNC) had been at first theoretically proposed by Lee and Yang in 1956 in order to find a way out of the so-called "$\tau - \gamma$ puzzle" [98, 99]. The next year, Wu and collaborators observed an asymmetry in nuclear beta decay ascribed to parity non-conservation in weak processes [100], and, subsequently, Lee and Yang have been forthwith awarded with the Nobel Prize. Many later experiments in nuclear and high energy physics confirmed parity violation in weak interactions and precisely recorded weak charge and other related parameters [101–104]. Although with some initial controversies, the "$\tau - \gamma$ puzzle" was also solved out by understanding that both τ and γ were two decay channels of the same parent particle, known today as the charged kaon K^+ [105, 106]. In contrast to nuclear and high energy physics, fewer experiments have been carried out in atomic physics to measure weak interaction's properties. In fact, the conflicting results of the early Bismuth experiments in the '70 [107–110] spread the conviction that nothing fundamentally useful could have ever

been extracted from atomic physics experiments. Nonetheless, renewed interest on the subject rose again in the late '80 and '90 and led to the successful measurements of the weak charge Q_w and related parameters in atomic Cesium [111–116], Thallium [117], Lead [118] and Ytterium [119]. On the theoretical side, starting from the early work of Curtis-Michel [120], several investigations of PNC have been made in the context of neutral atoms [121], few–electron ions [122, 123] and muonic atoms [124, 125]. In all the proposed studies, the little role played by PNC effects together with the need of precise measurements have been highlighted.

Parity violation in atomic physics is mainly caused by the exchange of the Z^0 boson between atomic electrons and quarks in the nucleus. All atomic states become mixtures consisting mainly of the state they are usually assigned, together with a small percentage of states possessing the opposite parity. It has been discussed some time ago the prospect for measuring the mixing between the states $1s_{1/2}2s_{1/2}$: $J = 0$ and $1s_{1/2}2p_{1/2}$: $J = 0$ in helium-like Uranium by inducing a resonant parity violating $E1E1$ transition between them [126]. The authors of the paper concluded that the proposed measurement was not feasible with the then available technology, while, nowadays, is under consideration at GSI facility in Darmstadt (Germany). With the same goal, some years later Dunford proposed an analysis based on the circular polarization asymmetry of one of the photons emitted in the two-photon decay of $1s_{1/2}2p_{1/2}$: $J = 0$ state [92]. As the author concluded, the calculations therein performed were not enough to assess whether or not the polarization asymmetry could lead to useful parity experiments.

With the same intent and similar method, we propose another route based on photon polarization properties, for the experimental determination of the mixing parameter between the states $1s_{1/2}2s_{1/2}$: $J = 0$ and $1s_{1/2}2p_{1/2}$: $J = 0$ in U^{90+}

The different polarization properties of the photons emitted in the two-photon decays of such states suggest a way to discriminate the decays and, thereby, to measure the mixing parameter between the states. However, the prospect presents some technical difficulties, widely discussed in the following, that make the experimental realization a challenge with the current state of art technologies.

Although our theoretical description of the states is relativistic, for the sake of shortness, the two states $1s_{1/2}2s_{1/2}$: $J = 0$ and $1s_{1/2}2p_{1/2}$: $J = 0$ will be briefly called, in the following, by using the non-relativistic notation, i.e. 2^1S_0 and 2^3P_0 respectively. It must be anyway clear that, since our theoretical analysis is set within a relativistic framework, the short (non-relativistic) notation (2^1S_0 and 2^3P_0) which we will use henceforth must be understood to be only a formal replacement to the full lengthy notation ($1s_{1/2}2s_{1/2}$: $J = 0$ and $1s_{1/2}2p_{1/2}$: $J = 0$).

Before explaining the ideas and goals of the prospect, a discussion on the structure of low energy states of helium-like Uranium is needed.

Helium-like Uranium ion

Heliumlike Uranium ion represents a very suitable candidate for studying PNC, due to the fact that the states 2^3P_0 and 2^1S_0 are separated by an energy difference of only few electronvolts [127, 128], out of a total binding energy of order 100 KeV. Fig. 5.17 shows the scheme of the first levels of U^{90+} [129]. 2^3P_0 state has negative parity and lifetime of about $\sim 10^{-11}$ sec, while 2^1S_0 state has positive parity and shorter lifetime of about $\sim 10^{-13}$ sec. Although 2^3P_0 can decay by single photon emission into 2^3S_1,
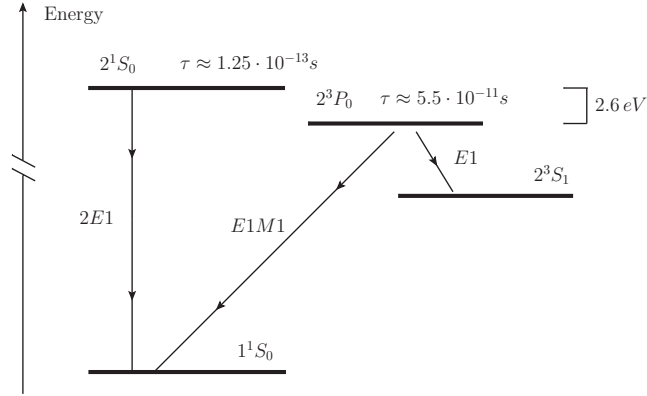
Figure 5.17: Level scheme of few low energetic states in U^{90+}.

both 2^3P_0 and 2^1S_0 decay exclusively by two–photon decay to the ground state, owing
to angular momentum conservation. Due to weak interaction between electrons and
nucleus, 2^3P_0 acquires a small admixture of 2^1S_0 and vice versa. Since the size of
the parity mixing depends inversely on the energy difference between the mixed states
[126], both 2^3P_0 and 2^1S_0 do not get any other considerable PNC contribution from
any other state. More explicitly, at the first order in perturbation theory, the "*true*"
$|2^3P_0\rangle$ and $|2^1S_0\rangle$ states can be written as [92]

$$\begin{aligned}
|2^3\widetilde{P}_0\rangle &\approx |2^3P_0\rangle + \eta\,|2^1S_0\rangle \\
|2^1\widetilde{S}_0\rangle &\approx |2^1S_0\rangle - \eta^*\,|2^3P_0\rangle \ .
\end{aligned} \tag{5.22}$$

The tilde notation is here and henceforth used to denote "true" states, in order to
differentiate them from the bare theoretical Dirac states which will be denoted without
the tilde. The mixing parameter η in Eq. (5.22) is given by

$$\eta = \frac{\langle 2^3P_0|\,\hat{H}_W\,|2^1S_0\rangle}{\Delta E_{PS}} \ , \tag{5.23}$$

where ΔE_{PS} is the energy difference between 2^3P_0 and 2^1S_0, while $\hat{H}_W$ is the operator
for the nuclear-spin-independent weak interaction [92]:

$$\hat{H}_W = \frac{G_F}{2\sqrt{2}}\left(1 - 4\sin^2\theta_w - \frac{N}{Z}\right)\rho_{el}\gamma_5 \ ,$$

where G_F is the Fermi's constant, θ_w the Weinberg angle, N the neutron number, Z the
proton number, ρ_{el} the electric charge density (normalized to Z) and $\gamma_5 = -i\alpha_1\alpha_2\alpha_3$.
Up to a very good approximation, we will neglect any parity mixing effect in any state
with the exception of 2^3P_0 and 2^1S_0. Among the low energetic states in U^{90+}, only
these two have in fact energies near enough to determine a sizeable mixing parameter
between them.

Prospective method: ideas and theory
For the purpose of measuring the parameter η in Eq. (5.23), we propose to prepare
U^{90+} in $2^3\widetilde{P}_0$ state. The efficiency of such preparation is here assumed to be 100%.

The so prepared $2^3\tilde{P}_0$ state will decay either into 2^3S_1 or into the ground state, as extensively displayed in Fig. 5.17. The two-photon decay channel $2^3\tilde{P}_0 \to 1^1S_0$, in which we are interested, can be easily selected out in experiments by requiring a (two-detector) coincidence measurement. The geometry we theoretically consider for such measurement is displayed in Fig. 5.10. It is the same geometry adopted for the previous sections, so that the reader, hopefully, may have got familiar with it.

The amplitude for this two-photon decay process, as we have widely discussed in Sec. 3.4, is the one displayed in Eq. (3.44). By introducing (5.22) into Eq. (3.44), the amplitude splits into two terms,

$$\mathcal{M}^{\gamma\gamma}_{\lambda_1\lambda_2}(2^3\tilde{P}_0 \to 1^1S_0) \approx \mathcal{M}^{\gamma\gamma}_{\lambda_1\lambda_2}(2^3P_0 \to 1^1S_0) + \eta\mathcal{M}^{\gamma\gamma}_{\lambda_1\lambda_2}(2^1S_0 \to 1^1S_0) \quad . \quad (5.24)$$

In order to suggest any experiment whose goal is the measurement of the mixing parameter η, we should be first able to theoretically discriminate the two amplitudes of the right-hand side of Eq. (5.24). The key point of the prospect is that such discrimination can be obtained by studying the polarization properties of the photons contained in those amplitudes. It has been showed in the previous sections that, in case that nearly equal energy is shared between the photons, the two-photon decay $2^3P_0 \to 1^1S_0$ is characterized by photon linear polarizations which are exclusively *orthogonal* to each other (linear polarizations of the first, second photon are detected, correspondingly, along the axes x, y' or y, x'), while the two-photon decay $2^1S_0 \to 1^1S_0$ is characterized by photon linear polarizations which are exclusively *parallel* to each other (linear polarizations of the first, second photon are detected, correspondingly, along the axes x, x' or y, y') [15, 93]. While the first assertion is true independently of the opening angle θ, the second one holds only in case the photons are recorded either collinearly or back-to-back ($\theta = 0°, 180°$). However, as it will be evident in the following, the linear polarizations of photons emitted in $2^1S_0 \to 1^1S_0$ decay can be considered parallel in the whole intervals $0° \leq \theta \lesssim 2°$ and $178° \lesssim \theta \leq 180°$, due to the fact that the (orthogonal) corrections to the polarization state are negligible in that region, even for the delicate problem under consideration. As a matter of fact, for the case $0° \leq \theta \lesssim 2°$ (or $178° \lesssim \theta \leq 180°$) and $y = 0.5$, we showed in the previous section that the polarization state of the two photons emitted in consequence of the decay of the prepared $2^3\tilde{P}_0$ state can be simply described by the ket vector [15]

$$|\Psi\rangle = O^{PS}_{f,Z,\theta}\left(|xy\rangle + |yx\rangle\right) + \eta\,O^{SS}_{f,Z,\theta}\left(|xx\rangle + |yy\rangle\right), \qquad (5.25)$$

where $\left|O^{PS}_{f,Z,\theta}\right|^2$ is the probability of detecting the emitted photons with polarizations along $\chi_1 = 0°$, $\chi_2 = 90°$ or $\chi_1 = 90°$, $\chi_2 = 0°$ while $\left|O^{SS}_{f,Z,\theta}\right|^2$ is the probability of detecting the photons with polarizations along $\chi_1 = 0°$, $\chi_2 = 0°$ or $\chi_1 = 90°$, $\chi_2 = 90°$. Both $O^{PS}_{f,Z,\theta}$ and $O^{SS}_{f,Z,\theta}$ contain the dependence on the energy sharing parameter y, the atomic number Z and the opening angle θ given respectively by the amplitudes $\mathcal{M}^{\gamma\gamma}_{\lambda_1\lambda_2}(2^3P_0 \to 1^1S_0)$ and $\mathcal{M}^{\gamma\gamma}_{\lambda_1\lambda_2}(2^1S_0 \to 1^1S_0)$.

In order to inspect the polarization properties of the photons emitted in the two-photon decay of the $2^3\tilde{P}_0$ state, we most naturally make use of the polarization-polarization correlation function, which has been defined in Eq. (5.9). The polarization-polarization correlation there showed is the physical quantity we mean to investigate.

The model we use for the calculations is once again the Independent Particle Model,

widely discussed in Sec. 2.4. Alternative and more accurate model might be, for instance the method of relativistic finite basis sets, which has been shown to be valid and efficient for accurate calculations of the two-photon E1M1 decay rate from the 2^3P_0 state [130]. The Independent Particle Model (IPM), although it treats the electrons as independent particles bound to the nucleus (the nuclear Coulomb attraction is assumed to be much stronger than the electron–electron repulsion), takes the Pauli principle into account. Moreover, as showed in Eq. (5.6), it allows a drastic simplification of the two-electron amplitude, allowing to reduce it to a summation over one-electron amplitudes. The tool we adopt here for the calculation of the latter is, as in the previous sections, the relativistic Dirac-Coulomb Green function (see Secs. 2.3 and 3.4).

The results showed below are obtained by taking into account the full multipoles contribution of the photons fields.

Finally, the *effective* nuclear charge used for the computation is $Z = 91.275$. This accounts for the electromagnetic screening that one electron makes on the other one, allowing for a basic electron-electron interaction. For details regarding how to calculate the effective charge in multi-electron atoms, see Ref. [44].

Results and discussion

After having explained the theory at the base of our prospect, we are now ready to present concretely the proposal.

In order to measure the mixing parameter η in Eq. (5.23), we propose, as previously mentioned, to prepare the Uranium ion U^{90+} in $2^3\tilde{P}_0$ state, to place two polarization detectors at a fixed position in the reaction plane and to use them as polarizer filters. While one of the two detectors will be kept at a fixed orientation (fixed transmission axis), the transmission axis of the other one will be continuously rotated to record the correlation function (5.9) for different photons polarization configurations. In order to suggest a workable experimental scenario, we must inevitably look for opening angle and energy values which enable $\eta\, O^{SS}_{f,Z,\theta}$ to be comparable with $O^{PS}_{f,Z,\theta}$, in Eq. (5.25). In other words, since η is considerably small, we must find a configuration for which the amplitude $\mathcal{M}^{\gamma\gamma}_{\lambda_1,\lambda_2}(2^3P_0 \to 1^1S_0)$ is small in comparison with $\mathcal{M}^{\gamma\gamma}_{\lambda_1,\lambda_2}(2^1S_0 \to 1^1S_0)$. On this purpose, it has been showed that the decay rate for the $2^3P_0 \to 1^1S_0$ transition is strongly suppressed for photons' opening angle $0 \leq \theta \lesssim 2°$ and equal energy sharing, whereas, for the same configuration, the decay rate $2^1S_0 \to 1^1S_0$ gets (almost) its maximum value [10, 11]. Choosing small values of θ and equal energy sharing will also ensure that the different amplitudes in Eq. (5.24) will determine different photons polarization outcomes (as remarked in the previous paragraph), which is decisive for the scope of the prospect. An optimal configuration for our purposes can be found, for instance, at $\theta = 1°$ and y=0.5. For such a configuration, the coefficients $O^{PS}_{f,Z,\theta}$ and $O^{SS}_{f,Z,\theta}$, which compose the ket vector (5.25), assume respectively the values -8.49 × 10^{-11} and 4.43 × 10^{-5}. The correlation function Φ related to such polarization state can be easily calculated:

$$
\begin{aligned}
\Phi^{y=0.5}_{\chi_1,\chi_2}(\theta = 1°) \;=\; &\mathcal{N}^2\Big[-8.49 \times 10^{-11} \left(\cos\chi_1 \sin\chi_2 + \sin\chi_1 \cos\chi_2 \right) \\
&+ \eta\, 4.43 \times 10^{-5} \left(\cos\chi_1 \cos\chi_2 + \sin\chi_1 \sin\chi_2 \right) \Big]^2.
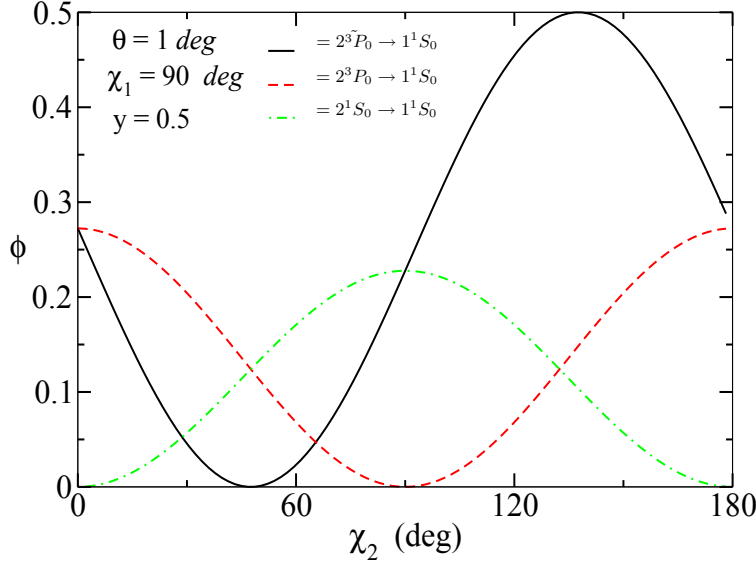\end{aligned}
\tag{5.26}
$$

Figure 5.18: Polarization-polarization correlation function (5.9) for the $2^3\tilde{P}_0 \to 1^1S_0$ two-photon decay of helium-like Uranium ion. The contribution of the different amplitudes in Eq. (5.24) are separately displayed. The dashed (red) line and the dot–dashed (green) line represent respectively the $P \to S$ and the $S \to S$ contribution to the correlation function, while the solid (black) line denotes the total $\tilde{P} \to S$ correlation function. See Fig. 5.10 for angles definitions.

We draw the above function in Fig. 5.18, where χ_1 has been arbitrarily set to $90°$, for a better visualization, while η has been fixed to the predicted theoretical value 1.75×10^{-6}, which can be obtained by correcting the value obtained in Ref. [126] with the precise calculation of the $2^1S_0 - 2^3P_0$ energy gap showed in Ref. [128]. The different contributions of the two addends in Eq. (5.24) are separately displayed, as well as the total correlation function. We can easily notice that the "parity allowed" ($|xy\rangle + |yx\rangle$) and "parity forbidden" ($|xx\rangle + |yy\rangle$) components of the photon polarization state have approximately the same magnitude. In concordance with Sec. 5.4, it can be seen in the figure, as well as from Eq. (5.26), that the amplitudes $\mathcal{M}^{\gamma\gamma}_{\lambda_1 \lambda_2}(2^1S_0 \to 1^1S_0)$ and $\mathcal{M}^{\gamma\gamma}_{\lambda_1 \lambda_2}(2^3P_0 \to 1^1S_0)$ determine respectively the probability of detecting parallel and orthogonal linearly polarized photons. In an ideal experiment, we could therefore scan the function Φ over the whole or part of the domain $\chi_{1,2} \in [0, 180°]$, in order to be then able to determine the parameter η by fitting the measured polarization correlation with the (η dependent) function (5.26).

The proposal is based on the fact that, for $y \to 0.5$ and $\theta \to 0$, the transition $2^3P_0 \to 1^1S_0$ (model-independently) vanishes. If we considered the two-photon transition $2^1\tilde{S}_0 \to 1^1S_0$, it can be easily seen from Eqs. (5.22) and (3.44), that the amplitude for that process would turn out to be equal to (5.24), with the replacement $\mathcal{M}^{\gamma\gamma}_{\lambda_1 \lambda_2}(2^1S_0 \to 1^1S_0) \leftrightarrow \mathcal{M}^{\gamma\gamma}_{\lambda_1 \lambda_2}(2^3P_0 \to 1^1S_0)$. Since, unfortunately, there exist no geometry for which the transition $2^1S_0 \to 1^1S_0$ is suppressed, the polarization of the emitted photons would be completely dominated by the "parity allowed" component that, in that case, would be ($|xx\rangle + |yy\rangle$). An initial preparation of the $2^1\tilde{S}_0$ state,

therefore, although easier from an experimental point of view [63, 82], would *not* give rise to the interference pattern shown in Fig. 5.18, for any given geometry.

Moreover, the amplitude $\mathcal{M}^{\gamma\gamma}_{\lambda_1\lambda_2}(2^1S_0 \rightarrow 1^1S_0)$ is approximately one order of magnitude larger than $\mathcal{M}^{\gamma\gamma}_{\lambda_1,\lambda_2}(2^3P_0 \rightarrow 1^1S_0)$, as can be seen from the states lifetimes displayed in Fig. 5.17. This fact represents an advantage for studying PNC effects in $2^3\widetilde{P}_0 \rightarrow 1^1S_0$ rather than in $2^1\widetilde{S}_0 \rightarrow 1^1S_0$, since such difference compensates partially for the small value of the mixing parameter η in Eq. (5.24) and so helps the two addends in the same equation to be comparable.

Although the suggested settings $y = 0.5$ and $\theta = 1°$ ensure, as needed, that the $2^3P_0 \rightarrow 1^1S_0$ channel is strongly suppressed, they determine at the same time a challenging arrangement for the experimental investigation of the prospect. Specifically, because of the required small opening angle θ, the two X-ray photon detectors would have to be placed at a relatively long distance from the source of radiation and thus the detection efficiency would be substantially decreased. An additional hindrance lies in the fact that the polarizations of both photons have to be measured at equal energy sharing ($y = 0.5$). For the case of Uranium, this fact would imply that each photon has about 50 keV (rest frame) energy. The polarization resolved experiments in this X-ray energy regime are nowadays normally performed by using Compton polarimeters [16, 131–135]. By selecting events recorded in coincidence which have the desired (Compton) scattering angle, such polarimeters can be used to measure the polarization state of the photon pair, in a similar way as in [136–139]. The selection of events can however increase considerably the statistical uncertainty.

Further experimental difficulties for the realization of the prospect might arise from the angle-energy resolution needed to record the interference pattern shown in Fig 5.18. The $P \rightarrow S$ channel rises fast, glossing over the other $S \rightarrow S$ channel in which we are interested, as soon as we depart from the (exact) theoretical proposed configuration $y = 0.5$, $\theta = 1°$. In other words, slightly different angle-energy settings would bring about a completely different polarization-polarization correlation function with respect to (5.26). As a matter of fact, the opening angle and energy resolutions needed, in order to select events for which the correlation function does not change approximately shape, would be, according to our calculations, respectively 0.5 degrees and 5 electronvolts. Even though the required angle resolution may be nowadays achieved, the energy resolution needed is approximately three orders of magnitude higher than the available resolution in current Compton polarimeters. A possible way to overcome the energy resolution limitation would be to use the so-called absorption edge technique [140]. In this technique, the photons pass through an absorption foil. The K-shell absorption edge of the foil atoms serves as a photon energy filter. The photons with the energy below the K-shell photoionization energy will have a significantly higher transmission probability than the photons with the higher energies. Since in the proposed experimental scheme both of the entangled photons have the same energy, one foil can be used as the energy filter for both of the photons. By adjusting the ion beam velocity the photon energy can be Doppler-tuned such that it is less than 5 eV below the K-edge. A Compton scattering polarimeter behind the absorption foil can be then used for the polarization analysis of the transmitted photons. Another possible experimental approach would involve high energy resolution calorimeters and a Rayleigh scattering polarimetry technique [141]. Here the energy of the Rayleigh scattered photon and its scattering direction could be measured with high resolution by an array of

x-ray calorimeters. Such arrays are currently being developed [142, 143] and likely to reach the required energy resolution at the energy of 50 keV in the near future.

The small (expected) value of the mixing coefficient η is certainly at the base of the technical difficulties explained above. A way to lighten such difficulties might be represented, for instance, by selecting a suitable isotope of U^{90+}. In virtue of the fact that the energy gap between 2^1S_0 and 2^3P_0 states varies slightly by changing the mass number of the ion [128], the mixing of the two states itself would depend on the considered isotope (cfr. Eq. (5.23)). In particular, by choosing an isotope of Uranium whose mass number is smaller than 238, we would be able to increase the mixing parameter of the two states up to a factor ≈ 1.6. However, besides the technical difficulties related to the radioactive properties that the chosen isotope might show, such improvement would be anyway not enough to bring considerable advantages to the prospect.

CHAPTER 6

SUMMARY AND OUTLOOK

In summary, we recalled in Chapter 2 the relativistic description of particles, ions and electromagnetic radiation in Quantum Mechanics. Particularly, in Secs. 2.1 and 2.2 we presented and found the solutions of the Dirac equation for free and bound states respectively. In Sec. 2.3, we investigated the Green function for the Dirac-Coulomb hamiltonian. In Sec. 2.4, we introduced the Independent Particle Model, which is the simplest endeavor to extend the relativistic description of particles in Quantum Mechanics to many-particle systems. In the last section of the second chapter, namely Sec. 2.5, a detailed (relativistic) theory of photons and radiation in Quantum Mechanics has been presented. We discussed how the angular momentum properties of photons show up naturally from the solutions of Maxwell equations and how they are linked to the photon polarization properties. We derived the electromagnetic potentials and fields that the circularly and linearly polarized radiation produces. We also derived the multipole expansion of the photon vector plane wave, which is of great usefulness, as we show later on, in dealing with transitions in bound states. We then discussed and brought out the differences of two different approximations which are usually made in dealing with the photon vector plane wave: the electric-dipole and the long wavelength approximations.

In Chapter 3, we investigated first- and second-order perturbation theory. We applied such a theory for the description of single- and double-photon decays in atoms and ions. We showed how electric-dipole and long wavelength approximations take to simple formulae, though with limited applicability. We have been able to analytically express, in hydrogen-like atoms, the amplitude for two-photon decay by employing the Dirac solutions and the Dirac-Coulomb Green function presented in Chapter 2.

In Chapter 4, we briefly showed the density matrix approach to ensembles of states in Quantum Mechanics. We discussed how density matrices enable us to investigate in a

simple manner statistical and quantum-entanglement properties of elementary ensembles of states.

We opened Chapter 5 by recalling the advanced studies which have been done, in the last decades, in studying two-photon decays. This paved the way to the original works that have been carried out by me and co-workers, during my PhD time. Indeed, in Secs. 5.2 and 5.3, we presented how the angular and polarization properties of the emitted photons in two-photon decays have been recently studied by us. We continued our thorough analysis of two-photon decay by applying the density matrix formalism to it in order to study the quantum-entanglement properties of the polarization state of the two emitted photons. These studies led us to understand how relativity and high-multipoles affect the angular, polarization and quantum-entanglement properties of the photons. Our analysis ended by showing, in Sec. 5.5, how the polarization features of the emitted photons can be brilliantly applied to investigate parity-violation phenomena in atomic physics.

Overall, this thesis suggests that two-photon transitions are a powerful tool to study the relativistic electronic structure of atoms and their inherent characteristics. From a theoretical point of view, this virtue follows from the fact that two-photon transitions are described by the second-order amplitude, which is sensible to all levels (both free and occupied) in single- and many-electron bound systems.

We wish that both theoretical and experimental efforts toward the better understanding of nature through two-photon decays is kept being pursued in the future. Thanks to new detector-technologies [16], polarization studies on two-photon decay can now open the way to exploring and understanding many and various physical areas of great interest.

APPENDICES

APPENDIX A

Here we derive that the condition

$$\boldsymbol{\nabla} \cdot \boldsymbol{A} = 0 \qquad \text{and} \qquad \Phi = 0$$

is a valid gauge condition in vacuum.

The electromagnetic fields are related to the scalar (Φ) and vector ($\boldsymbol{A}$) potentials as

$$
\begin{aligned}
\boldsymbol{E} &= -\boldsymbol{\nabla}\Phi - \frac{\partial \boldsymbol{A}}{\partial t} \quad , \\
\boldsymbol{B} &= \nabla \times \boldsymbol{A} \quad .
\end{aligned}
\tag{A.1}
$$

It is known that the electromagnetic potentials are not fully specified from the Maxwell's equations for the fields (2.40). Indeed, by choosing any regular function λ, the transformation

$$
\begin{aligned}
\boldsymbol{A} &\to \boldsymbol{A} + \boldsymbol{\nabla}\lambda \\
\Phi &\to \Phi - \frac{\partial \lambda}{\partial t}
\end{aligned}
\tag{A.2}
$$

leaves unaltered the Maxwell's equations. The transformation above is referred to as *gauge transformation*. It is therefore needed a further condition to fully specify the potentials. One of the most used is the Lorentz gauge condition

$$\boldsymbol{\nabla} \cdot \boldsymbol{A} + \frac{1}{c^2}\frac{\partial \Phi}{\partial t} = 0$$

which, together with the Maxwell's equations, fully specifies the potentials. In the vacuum, using equations (A.1) and (2.40), we get

$$0 = \boldsymbol{\nabla} \cdot \boldsymbol{E} = -\boldsymbol{\nabla}^2\Phi - \frac{\partial}{\partial t}\boldsymbol{\nabla} \cdot \boldsymbol{A} \quad .$$

If we adopt the Lorentz gauge, we get

$$0 = -\boldsymbol{\nabla}^2\Phi - \frac{\partial}{\partial t}\left(-\frac{1}{c^2}\frac{\partial \Phi}{\partial t}\right) = -\boldsymbol{\nabla}^2\Phi + \frac{1}{c^2}\frac{\partial^2 \Phi}{\partial t^2} \quad , \tag{A.3}$$

which is a wave equation for Φ.

Analogously, for the vector potential we get

$$\nabla \times \boldsymbol{B} = \frac{1}{c^2} \frac{\partial}{\partial t} \left(-\boldsymbol{\nabla}\Phi - \frac{\partial \boldsymbol{A}}{\partial t} \right) = -\boldsymbol{\nabla}\left(\frac{1}{c^2} \frac{\partial \Phi}{\partial t} \right) - \frac{1}{c^2} \frac{\partial^2 \boldsymbol{A}}{\partial t^2}$$

and

$$\nabla \times \boldsymbol{B} = \boldsymbol{\nabla} \times (\boldsymbol{\nabla} \times \boldsymbol{A}) = \boldsymbol{\nabla}(\boldsymbol{\nabla} \cdot \boldsymbol{A}) - \boldsymbol{\nabla}^2 \boldsymbol{A} \quad .$$

The two above equations lead to

$$\boldsymbol{\nabla}\left(\boldsymbol{\nabla} \cdot \boldsymbol{A} + \frac{1}{c^2} \frac{\partial \Phi}{\partial t} \right) = \boldsymbol{\nabla}^2 \boldsymbol{A} - \frac{1}{c^2} \frac{\partial^2 \boldsymbol{A}}{\partial t^2} \quad .$$

In the Lorentz gauge, we get the final equation for $\boldsymbol{A}$:

$$\boldsymbol{\nabla}^2 \boldsymbol{A} - \frac{1}{c^2} \frac{\partial^2 \boldsymbol{A}}{\partial t^2} = 0 \quad . \tag{A.4}$$

The general solutions for equations (A.3) and (A.4) are of the form[1]

$$\begin{aligned}
\Phi_L(\boldsymbol{r}, t) &= \Phi_0 \left(\eta e^{i(\boldsymbol{k r} - \omega t)} + \eta^* e^{-i(\boldsymbol{k r} - \omega t)} \right) \quad , \\
\boldsymbol{A}_L(\boldsymbol{r}, t) &= A_0 \left(\underline{\epsilon} e^{i(\boldsymbol{k r} - \omega t)} + \underline{\epsilon}^* e^{-i(\boldsymbol{k r} - \omega t)} \right) \quad ,
\end{aligned}$$

where $\boldsymbol{k}$, ω, $\underline{\epsilon}$, η, A_0, Φ_0 are parameters. We have added a subscript $_L$ to make clear that the found potentials are in the Lorentz gauge.

We notice that the equation

$$\frac{\partial^2 \Phi_L}{\partial t^2} = -\omega^2 \Phi_L$$

is satisfied.

Now, let us make a gauge transformations, from the Lorentz gauge, to another gauge. The transformation function λ we choose is

$$\lambda = -\frac{1}{\omega^2} \frac{\partial \Phi_L}{\partial t} \quad ,$$

which is surely regular, as we stated it must be.

Following the gauge transformations (A.2), we get the new potentials $\boldsymbol{A}'$ and Φ' to be

$$\begin{aligned}
\Phi' &= \Phi_L - \frac{\partial \lambda}{\partial t} = \Phi_L + \frac{1}{\omega^2} \frac{\partial^2 \Phi_L}{\partial t^2} = \Phi_L - \Phi_L = 0 \quad , \\
\boldsymbol{A}' &= \boldsymbol{A}_L + \boldsymbol{\nabla}\left(-\frac{1}{\omega^2} \frac{\partial \Phi_L}{\partial t} \right) = \boldsymbol{A}_L - \frac{1}{\omega^2} \boldsymbol{\nabla} \frac{\partial \Phi_L}{\partial t} \quad .
\end{aligned} \tag{A.5}$$

Taking the divergence of $\boldsymbol{A}'$ we get:

$$\boldsymbol{\nabla} \cdot \boldsymbol{A}' = \boldsymbol{\nabla} \cdot \boldsymbol{A}_L - \frac{1}{\omega^2} \boldsymbol{\nabla}^2 \frac{\partial \Phi_L}{\partial t} \quad .$$

---

[1] The potentials must be real so as to give rise to real electromagnetic fields.

Now we use the Lorentz condition on the first term, and the wave equation (A.3) on the second term of the rhs of the above equation. We obtain:

$$
\begin{aligned}
\boldsymbol{\nabla} \cdot \boldsymbol{A}' &= \frac{1}{c^2} \frac{\partial \Phi_L}{\partial t} - \frac{1}{\omega^2} \frac{\partial}{\partial t} \left(\frac{1}{c^2} \frac{\partial^2 \Phi_L}{\partial t^2} \right) = \frac{1}{c^2} \frac{\partial \Phi_L}{\partial t} - \frac{1}{c^2} \frac{\partial \Phi_L}{\partial t} = 0 \\
&= -\frac{1}{c^2} \frac{\partial \Phi'}{\partial t} \quad .
\end{aligned} \tag{A.6}
$$

Summarizing, we get from Eqs. (A.5) and (A.6) the following conditions for the new potentials in vacuum:

$$
\begin{aligned}
\Phi' &= 0 \quad , \\
\boldsymbol{\nabla} \cdot \boldsymbol{A}' &= 0 \quad .
\end{aligned}
$$

The above conditions represent therefore a valid gauge choice in vacuum.

APPENDIX B

The polarization tensor and multipoles, which are presented in Sec. 2.5, have some useful symmetry properties, which we here derive. In this section, the involved functions will be written without argument, for the sake of simplicity.

$$
\begin{aligned}
\boldsymbol{T}_{J L M}^* &= \sum_{m=-1}^{1} \langle L, M-m, 1, m | J, M \rangle \, Y_L^{M-m \, *} \, \xi_m^* \\
&= \sum_{m=-1}^{1} \langle L, M-m, 1, m | J, M \rangle \, (-1)^{M-m} \, Y_L^{m-M} \, (-1)^m \, \xi_{-m} \\
&= \sum_{m=-1}^{1} (-1)^{L+1-J} \langle L, m-M, 1, -m | J, -M \rangle \, (-1)^M \, Y_L^{m-M} \, \xi_{-m} \\
&\underset{m \to -m}{=} (-1)^{L+1-J+M} \sum_{m=+1}^{-1} \langle L, -M-m, 1, m | J, -M \rangle \, Y_L^{-M-m} \, \xi_m \\
&= (-1)^{L+1-J+M} \sum_{m=-1}^{+1} \langle L, -M-m, 1, m | J, -M \rangle \, Y_L^{-M-m} \, \xi_m \\
&= (-1)^{L+1-J+M} \, \boldsymbol{T}_{J L -M} \quad ,
\end{aligned}
$$

$$
\boldsymbol{A}_{L M}^{(m) \, *} = J_L \boldsymbol{T}_{L L M}^* = J_L (-1)^{L+1-L+M} \, \boldsymbol{T}_{L L -M} = (-1)^{M+1} \, \boldsymbol{A}_{L -M}^{(m)} \quad ,
$$

$$\boldsymbol{A}_{LM}^{(e)*} = J_{L-1}\sqrt{\frac{L+1}{2L+1}}\,\boldsymbol{T}_{LL-1\,M}^{*} - J_{L+1}\sqrt{\frac{L}{2L+1}}\,\boldsymbol{T}_{LL+1\,M}^{*}$$

$$= J_{L-1}\sqrt{\frac{L+1}{2L+1}}\,(-1)^{L-1+1-L+M}\,\boldsymbol{T}_{LL-1\,-M}$$

$$- J_{L+1}\sqrt{\frac{L}{2L+1}}\,(-1)^{L+1+1-L+M}\,\boldsymbol{T}_{LL+1\,-M}$$

$$= (-1)^{M}\,\boldsymbol{A}_{L-M}^{(e)}\quad,$$

$$\boldsymbol{a}_{LM}^{p*} = (-1)^{M+p+1}\,\boldsymbol{a}_{L-M}^{p}\quad,$$

$$\boldsymbol{a}_{LM}^{p} = (-1)^{M+p+1}\,\boldsymbol{a}_{L-M}^{p*}\quad,$$

$$\langle\beta_1,J_1\|\boldsymbol{\alpha}\cdot\boldsymbol{a}_L^p\|\beta_2,J_2\rangle = \left(\langle\beta_1,J_1\|\boldsymbol{\alpha}\cdot\boldsymbol{a}_L^p\|\beta_2,J_2\rangle\right)^{*} = (-1)^{p+1+J_2-J_1}\left(\frac{2J_2+1}{2J_1+1}\right)\langle\beta_2,J_2\|\boldsymbol{\alpha}\cdot\boldsymbol{a}_L^p\|\beta_1,J_1\rangle$$

$$\xi_m^{*}\cdot\xi_{m'} = \delta_{m,m'}\quad.$$

APPENDIX C

When the magnetic field ($\boldsymbol{B}$) is constant, the vector potential ($\boldsymbol{A}$) can be taken of the form

$$\boldsymbol{A} = -\frac{1}{2}\,\boldsymbol{r}\times\boldsymbol{B}\quad.$$

Proof:

$$\boldsymbol{B} \equiv \boldsymbol{\nabla}\times\boldsymbol{A} = \boldsymbol{\nabla}\times\left(-\frac{1}{2}\boldsymbol{r}\times\boldsymbol{B}\right)$$

$$= -\frac{1}{2}\boldsymbol{r}\cdot(\boldsymbol{\nabla}\cdot\boldsymbol{B}) - \boldsymbol{B}\left(\boldsymbol{\nabla}\cdot\left(-\frac{1}{2}\boldsymbol{r}\right)\right) + (\boldsymbol{B}\cdot\nabla)\left(-\frac{1}{2}\boldsymbol{r}\right) - \left(-\frac{1}{2}\boldsymbol{r}\cdot\boldsymbol{\nabla}\right)\boldsymbol{B}$$

$$= 0 + \frac{3}{2}\boldsymbol{B} - \frac{1}{2}\boldsymbol{B} + 0 = \boldsymbol{B}\quad,$$

where the first and last terms in the penultimate row disappear because of Maxwell's equations and the hypothesis of constant magnetic field, respectively.

As discussed in Sec. 3.2 and Sec. 3.3, the non-relativistic hamiltonian which accounts for the interaction of an electron with a magnetic field, at the first order in α, in the

Coulomb gauge, is

$$\hat{\mathrm{H}}' = -\frac{e}{m}\hat{\mathbf{A}} \cdot \hat{\mathbf{p}} \quad .$$

It can be easily verified that $\left[\hat{\mathbf{A}}, \hat{\mathbf{p}}\right] = 0$ and therefore the above operator is hermitian, as it is written.

By using that our magnetic field $\boldsymbol{B}$ is constant (by hypothesis), we obtain:

$$\hat{\mathrm{H}}' = +i\hbar\,\frac{e}{m}\left(-\frac{1}{2}\hat{\mathbf{r}} \times \boldsymbol{B}\right) \cdot \boldsymbol{\nabla} = +i\hbar\,\frac{e}{m}\left(+\frac{1}{2}\right)\boldsymbol{B} \cdot (\hat{\mathbf{r}} \times \boldsymbol{\nabla})$$

$$= +i\hbar\,\frac{e}{m}\left(+\frac{1}{2}\right)(\hat{\mathbf{r}} \times \boldsymbol{\nabla}) \cdot \boldsymbol{B} = \frac{e}{2m}(\hat{\mathbf{r}} \times \hat{\mathbf{p}}) \cdot \boldsymbol{B}$$

$$= +\frac{e}{2m}\hat{\mathbf{L}} \cdot \boldsymbol{B} = -\frac{q}{2m}\hat{\mathbf{L}} \cdot \boldsymbol{B}$$

where $q = -e$ is the electronic charge.

Now, as usual in non-relativistic quantum mechanics, we may add the spin contribution by hands, by adding the spin operator $\hat{\mathbf{S}}$ to $\hat{\mathbf{L}}$ and multiplying it by a constant g_s, the so-called spin g-factor. By doing that, we get

$$\hat{\mathrm{H}}' = \frac{e}{2m}\left(\hat{\mathbf{L}} + g_s\hat{\mathbf{S}}\right) \cdot \boldsymbol{B}$$

$$= +\boldsymbol{\mu}_e \cdot \boldsymbol{B} \quad ,$$

(C.1)

where

$$\boldsymbol{\mu}_e = \frac{\mu_B\,c}{\hbar}\left(\hat{\mathbf{L}} + g_s\hat{\mathbf{S}}\right)$$

is the magnetic dipole operator for the electron and $\mu_B = \dfrac{e\hbar}{2mc}$ is the Bohr magneton. Therefore, the Hamiltonian in Eq. (C.1) is the correct hamiltonian for the *non-relativistic* interaction of an electron with a *constant* magnetic field.

Bibliography

[1] M. Goeppert-Mayer, Ann. Phys. (Leipzig) **9**, 273 (1931).

[2] G. Breit and E. Teller, Astrophys. J. **91**, 215 (1940).

[3] J. Shapiro and G. Breit, Phys. Rev. **113**, 179 (1959).

[4] G.W.F. Drake, Pys. Rev. A **34**, 2871 (1986).

[5] H.W. Schäffer, *et al.*, Phys. Rev. A **59**, 245 (1999).

[6] J.H. Tung, X.M. Ye, G.J. Salamo and F.T. Chan, Phys. Rev. A **30**, 1775 (1984).

[7] M. Lipeles, R. Novick*, and N. Tolk, Phys. Rev. Lett. **15**, 690 (1965).

[8] C.K. Au, Phys. Rev. A **14**, 531 (1976).

[9] A. Surzhykov, P. Koval and S. Fritzsche, Phys. Rev. A **71**, 022509 (2005).

[10] A. Surzhykov, A. Volotka, F. Fratini, J.P. Santos, P. Indelicato, G. Plunien, Th. Stöhlker and S. Frtitzsche, Phys. Rev. A **81**, 042510 (2010).

[11] R. W. Dunford, Phys. Rev. A **69**, 062502 (2004).

[12] D. DeMille, D. Budker, N. Derr and E. Deveney, Phys. Rev. Lett. **83**, 3978 (1999).

[13] L. D. Landau, Dodkl. Akad. Nauk SSR **60**, 207 (1948).

[14] C. N. Yang, Phys. Rev. **77**, 242 (1950).

[15] F. Fratini, M.C. Tichy, Th. Jahrsetz, A. Buchleitner, S. Fritzsche, and A. Surzhykov, Phys. Rev. A **83**, 032506 (2011).

[16] S. Tashenov, Th. Stölker, D. Banas, K. Beckert, P. Beller, H.F. Beyer, F. Bosch, S. Fritzsche, A. Gumberidze, S. Hangmann, C. Kozhuharov, T. Krings, D. Liesen, F. Nolden, D. Protic, D. Sierpowski, U. Spillmann, M. Steckm, A. Surzhykov, Phys. Rev. Lett. **97**, 223202 (2006).

[17] A. Aspect, P. Grangier and G. Roger, Phys. Rev. Lett. **49**, 91 (1982).

[18] W. Perrie, A. J. Duncan, H. J. Beyer, and H. Kleinpoppen, Phys. Rev. Lett. **54**, 1790 (1985).

[19] H. Kleinpoppen, A. J. Duncan, H. J. Beyer, and Z. A. Sheikh, Phys. Scr., **T72**, 7 (1997).

[20] F. Fratini, S. Trotsenko, S. Tashenov, Th. Stöhlker and A. Surzhykov, Phys. Rev. A **83**, 052505 (2011).

[21] P.A.M. Dirac, Proc. R. Soc. London A **117**, 610 (1928).

[22] M. Massimi, *Pauli's exclusion principle: the origin and validation of a scientific principle*, Cambridge Uinversity Press, 2005, pg. 133.

[23] P.A.M. Dirac, Proc. R. Soc. London. Ser. A **133**, 60 (1931), pg. 61.

[24] C.D. Anderson, Phys. Rev. **43**, 491 (1933).

[25] J.J. Sakurai, *Modern Quantum Mechanics*, Addison-Wesley, 1994.

[26] W. Greiner, *Relativistic Quantum Mechanics: wave equations*, Spinger-Verlag, 2000.

[27] J. Meixner, Math. Zeit. **36**, 677 (1933).

[28] E.H. Weichmann and C.H. Woo, J. Math. Phys. **2**, 178 (1961).

[29] L. Hostler, J. Math. Phys. **5**, 591 (1964).

[30] J. Scwinger, J. Math. Phys. **5**, 1606 (1964).

[31] L. Hostler, J. Math. Phys. **11**, 2966 (1970).

[32] J.M. Garcia-Bondia, Phys. Rev. A **30**, 691 (1984).

[33] L. Chetouani and T.F. Hamman, J. Math. Phys. **28**, 598 (1987).

[34] R.A. Swainson and G.W.F. Drake, J. Phys. A **24**, 79 (1991).
R.A. Swainson and G.W.F. Drake, J. Phys. A **24**, 95 (1991).
R.A. Swainson and G.W.F. Drake, J. Phys. A **24**, 1801 (1991).

[35] J.C. Slater, Phys. Rev. **34**, 1293 (1929).

[36] T. Aberg, Phys. Rev. A **4**, 1735 (1971).

[37] M.E. Rose, *Elementary theory of angular momentum*, John Wiley, 1957, pg. 137.

[38] A.I. Akhiezer and V.B. Berestetskii, *Quantum Electrodynamics*, Interscience Publishers, 1965.

[39] J.D. Jackson, *Classical Electrodynamics*, John Wiley, 1998.

[40] J.C. Slater, J. Chem. Phys. **41**, 3199 (1964).

[41] A. Surzhykov, S. Fritzsche, A. Gumberidze and Th. Stölker, Phys. Rev. Lett. **88**, 153001 (2002).

[42] B. Povh, K. Rith, C. Scholz and F. Zetsche, *Particles and Nuclei: an Introduction to the Physical Concepts*, Springer, 2008.

[43] N. Bohr, Phys. Rev. **48**, 696 (1935).

[44] B.H. Bransden and C.J. Joachain, *Physics of atoms and molecules*, John Wiley, 1983.

[45] D.R. Bes, *Quantum Mechanics: A Modern and Concise Introductory Course*, Springer, Heidelberg (2007).

[46] R.P. Feynman, A.R. Hibbs, *Lectures on Physics: Quantum Mechanics and Path Integrals*, McGraw-Hill, 1965.

[47] M.E. Peskin and D.V. Schröder, *Introduction to Quantum Field Theory*, Addison-Wesley, 1995.

[48] S. P. Goldman and G. W. F. Drake, Phys. Rev. A **24**, 183 (1981).

[49] A. Surzhykov, J.P. Santos, P. Amaro and Paul Indelicato, Phys. Rev. A **80**, 052511 (2009).

[50] W. Gerlach and O. Stern, Z. Phys. **9**, 353 (1922).

[51] J. Von Neumann, Nachr. Akad. Wiss. Göttingen Math.-physik. Kl., 245 (1927).

[52] P.A.M. Dirac, Proc. Camb. Phil. Soc. **25**, 62 (1929).

[53] L.D. Landau, Z. Phys. **45**, 430 (1927).

[54] V.V. Balashov, A.N. Grum-Grzhimailo and N.M. Kabachnik, *Polarization and Correlation Phenomena in Atomic Collisions*, Kluwer Academic Plenum Publishers, New York (2000).

[55] K. Blum, *Density Matrix Theory and Applications*, Plenum Publishing Corporation, New York (1996).

[56] U. Fano, Rev. Mod. Phys. **29**, 74 (1957).

[57] R. McWeeny, Rev. Mod. Phys. **32**, 335 (1960).

[58] J. Christian, *Disproof of Bell's Theorem by Clifford Algebra Valued Local Variables*, arXiv:quant-ph/0703179.
J. Christian, *Disproof of Bell's Theorem: Further Consolidations*, arXiv:0707.1333.
J. Christian, *Can Bell's Prescription for Physical Reality Be Considered Complete?*, arXiv:0806.3078.
J. Christian, *Disproofs of Bell, GHZ, and Hardy Type Theorems and the Illusion of Entanglement*, arXiv:0904.4259.
J. Christian, *Failure of Bell's Theorem and the Local Causality of the Entangled Photons*, arXiv:1005.4932.
J. Christian, *What Really Sets the Upper Bound on Quantum Correlations?*, arXiv:1101.1958.
Tung Ten Yong, *Disproof of "Disproof of Bell's Theorem by Clifford Algebra Valued Local Variables"*, arXiv:0712.1637v1.

J. Christian, *Disproof of Bell's Theorem: Reply to Critics*,
arXiv:quant-ph/0703244v12.
D. Wallace and C.J. Timpson, *Non-locality and gauge freedom in Deutsch and Haydens formulation of quantum mechanics*, Found. Phys. Lett. **37**, 951 (2007).
D. Deutsch, *Vindication of Quantum Locality*, arXiv:1109.6223v1.
C.S. Unnikrishnan, *Is the Quantum Mechanical Description of Physical Reality Complete? Proposed Resolution of the EPR Puzzle*, Found. of Phys. Lett. **15**, 1 (2002).

[59] A. Einstein, "Letter from Einstein to Max Born, 3 March 1947" in *The Born-Einstein Letters. Correspondence between Albert Einstein and Max and Hedwig Born from 1916 to 1955*, Walker, New York (1971). (cited in Quantum Entanglement and Communication Complexity (1998), by M. P. Hobson et. al., p.1/13).
A. Einstein, B. Podolsky, N. Rosen, Phys. Rev. **47**, 777 (1935).

[60] W.K. Wootters, Phys. Rev. Lett. **80**, 2245 (1998).

[61] J. P. Santos, F. Parente, and P. Indelicato, Eur. Phys. J. D **3**, 43 (1998).

[62] P. Amaro *et al.*, Phys. Rev. A **69**, 062504 (2009).

[63] S. Trotsenko, A. Kumar, A. V. Volotka, D. Banaś, H. F. Beyer, H. Bräuning, S. Fritzsche, A. Gumberidze, S. Hagmann, S. Hess, P. Jagodziński, C. Kozhuharov, R. Reuschl, S. Salem, A. Simon, U. Spillmann, M. Trassinelli, L. C. Tribedi, G. Weber, D. Winters, and Th. Stöhlker, Phys. Rev. Lett. **104**, 033001 (2010).

[64] R. Ali *et al.*, Phys. Rev. A **55**, 994 (1997).

[65] Y.J. Wu and J.M. Li, J. Phys. B **21**, 1509 (1988).

[66] Y.B. Bannett, I. Freund, Phys. Rev. A **30**, 299 (1984).

[67] T. Aberg, in *Atomic Inner-Shell Processes*, edited by B. Crasemann, Academic Newyork (1975), p. 353.

[68] X.M. Tong, J.M. Li, L. Kissel and R.H. Pratt, Phys. Rev. A **42**, 1442 (1990).

[69] X. Mu and B. Crasemann, Phys. Rev. A **38**, 4585 (1988).

[70] Y. Bannett and I. Freund, Phys. Rev. Lett. **49**, 539 (1982).

[71] K. Ilakovac *et al.*, Phys. Rev Lett. **56**, 2469 (1986).

[72] K. Ilakovac *et al.*, Phys. Rev. A **44**, 7392 (1991).

[73] K. Ilakovac *et al.*, Phys. Rev. A **46**, 132 (1992).

[74] I. Freund, Phys. Rev. A **7**, 1849 (1973).

[75] M.S. Safronova, W.R. Johnson and U.I. Safronova, J. Phys. B: At. Mol. Opt. Phys **43**, 074014 (2010).

[76] C. Laughlin, Phys. Lett. **75**A, 199 (1980).

[77] R.W. Schmieder, Phys. Rev. A **7**, 1458 (1973).

[78] P.H. Mokler and R.W. Dunford, Phys. Scr. **69**, C1-9 (2004).

[79] S. Klarsfeld, Phys. Lett **30**A, 382 (1969).

[80] S. Klarsfeld, Lett. Nuovo Cimento **1**, 682 (1969).

[81] V. Florescu, Phys. Rev. A **30**, 2441 (1984).

[82] J. Rzadkiewicz, Th. Stöhlker, D. Banaś, H. F. Beyer, F. Bosch, C. Brandau, C. Z. Dong, S. Fritzsche, A. Gojska, A. Gumberidze, S. Hagmann, D. C. Ionescu, C. Kozhuharov, T. Nandi, R. Reuschl, D. Sierpowski, U. Spillmann, A. Surzhykov, S. Tashenov, M. Trassinelli, and S. Trotsenko, Phys. Rev. A **74**, 012511 (2006).

[83] G. W. F. Drake, Nucl. Instr. Meth. B **9**, 465 (1989).

[84] A. Surzhykov, U. D. Jentschura, Th. Stöhlker, and S. Fritzsche, Eur. Phys. J. D **46**, 27 (2008).

[85] A. Surzhykov, P. Koval, and S. Fritzsche, Comput. Phys. Commun. **165**, 139 (2005).

[86] U. D. Jentschura and A. Surzhykov, Phys. Rev. A **77**, 042507 (2008).

[87] P. Indelicato, Phys. Rev. A **51**, 1132 (1995).

[88] J. Sapirstein and W. R. Johnson, J. Phys. B **29**, 5213 (1996).

[89] V. M. Shabaev, I. I. Tupitsyn, V. A. Yerokhin, G. Plunien, and G. Soff, Phys. Rev. Lett. **93**, 130405 (2004).

[90] A. Surzhykov, J. P. Santos, P. Amaro, and P. Indelicato, Phys. Rev. A **80**, 052511 (2009).

[91] A. Kumar, S. Trotsenko, A. V. Volotka, D. Banaś, H. F. Beyer, H. Bräuning, A. Gumberidze, S. Hagmann, S. Hess, C. Kozhuharov, R. Reuschl, U. Spillmann, M. Trassinelli, G. Weber, and Th. Stöhlker, Eur. Phys. J. Special Topics **169**, 19 (2009).

[92] R. W. Dunford, Phys. Rev. A **54**, 3820 (1996).

[93] F. Fratini and A. Surzhykov, Hyp. Int. **199**, 85 (2011).

[94] A. Surzhykov, T. Radtke, P. Indelicato and S. Fritzsche, Eur. Phys. J. Special Topics **169**, 29 (2009).

[95] M. C. Tichy, F. de Melo, M. Kuś, F. Mintert, and A. Buchleitner, arXiv:0902.1684 (2009).

[96] T. Radtke, A. Surzhykov, and S. Fritzsche, Phys. Rev. A **77**, 0022507 (2008).

[97] M. Jakob and J. A. Bergou, arXiv:quant-ph/0302075 (2003).

[98] T. D. Lee and C. N. Yang, Phys. Rev. **104**, 254 (1956).

[99] G. Harris, J. Orear and S. Taylor, Phys. Rev. **100**, 932 (1955).

[100] C. S. Wu, *et al.*, Phys. Rev. **105**, 1413 (1957).

[101] J. E. Clendenin, V. W. Huges, *et al.*, Phys. Lett. **77B**, 347 (1978).

[102] J. Lang, Th. Maier, R. Müller, *et al.*, Phys. Rev. C **34**, 1545 (1986).

[103] B. Desplanques, Phys. Rep. **297**, 1 (1986).

[104] N. Tanner, Phys. Rev. **107**, 1203 (1957).

[105] S. B. Treiman and H. W. Wyld, Phys. Rev. **106**, 1320 (1957).

[106] R. H. Dalitz, AIP Conf. Proc. **300**, 141 (1994).

[107] P. E. G. Baird, M. W. S. M. Brimicombe, R. G. Hunt, G. J. Roberts, P. G. H. Sandars and D. N. Stacey, Phys. Rev. Lett. **39**, 798 (1977).

[108] L. L. Lewis, J. H. Hollister, D. C. Soreide, E. G. Lindahl and E. N. Fortson, Phys. Rev. Lett. **39**, 795 (1977).

[109] L. M. Barkov and M. S. Zolotorev, Phys. Lett. **85B**, 308 (1979).

[110] J. H. Hollister, G. R. Apperson, L. L. Lewis, T. P. Emmons, T. G. Vold and E. N. Fortson, Phys. Rev. Lett. **46**, 643 (1981).

[111] M. C. Noecker, B. P. Masterson and C. E. Wieman, Phys. Rev. Lett. **61**, 310 (1988).

[112] C. S. Wood, *et al.*, Science **275**, 1759 (1997).

[113] S. G. Porsev, K. Beloy and A. Derevianko, Phys. Rev. Lett. **102**, 181601 (2009).

[114] S. C. Bennett and C. E. Wieman, Phys. Rev. Lett. **82**, 2484 (1999).

[115] A. Derevianko. Phys. Rev. Lett. **85**, 1618 (2000).

[116] V. A. Dzuba and V. V. Flambaum, Phys. Rev. A **62**, 052101 (2000).

[117] P. A. Vetter, D. M. Meekhof, P. K. Majumder, S. K. Lamoreaux and E. N. Fortson, Phys. Rev. Lett. **74**, 2658 (1995).

[118] D. M. Meekhof, P. Vetter, P. K. Majumder, S. K. Lamoreaux and E. N. Fortson, Phys. Rev. Lett. **71**, 3442 (1993).

[119] K. Tsigutkin, D. Dounas-Frazer, A. Family, J. E. Stalnaker, V. V. Yashchuk and D. Budker, Phys. Rev. Lett. **103**, 071601 (2009).

[120] F. Courtis-Michel, Phys. Rev. **138**, B408 (1965).

[121] W. R. Johnson, S. A. Blundell, Z. W. Liu and J. Sapirstein, Phys. Rev. A **37**, 1395 (1988).

[122] M. A. Bouchiat and C. C. Bouchiat, Phys. Lett. **48B**, 111 (1974).

[123] L. N. Labzowsky, A. V. Nefiodov, G. Plunien, G. Soff, R. Marrus and D. Liesen, Phys. Rev. A **63**, 054105 (2001).

[124] P. Langacker, Phys. Lett. **256B**, 277 (1991).

[125] J. Missimer and L. M. Simons, Phys. Rep. **118**, 179 (1985).

[126] A. Schäfer, G. Soff, P. Indelicato, B. Müller and W. Greiner, Phys. Rev. A **40**, 7362 (1989).

[127] M. Maul, A. Schäfer, W. Greiner and P. Indelicato, Phys. Rev. A **53**, 3915 (1996).

[128] F. Ferro, A. Artemyev, Th. Stöhlker and A. Surzhykov, Phys. Rev. A **81**, 062503 (2010).

[129] C. T. Munger and H. Gould, Phys. Rev. Lett. **57**, 2927 (1986).

[130] G. W. F. Drake, Nucl. Instrum. and Methods B **9**, 465-470 (1985).

[131] D. Protic, E. L. Hull, T. Krings, and K. Vetter, IEEE Transactions on Nuclear Science **52**, 3181 (2005).

[132] D. Protic, Th. Stöhlker, T. Krings, I. Mohos, and U. Spillmann, IEEE Transactions on Nuclear Science **52**, 3194 (2005).

[133] U. Spillmann, H. Bräuning, S. Hess, H. Beyer, Th. Stöhlker, J.-C. Dousse, D. Protic and T. Krings, Review of Scientific Instruments **79**, 083101 (2008), pg. 8.

[134] G. Weber, H. Bräuning, S. Hess, R. Märtin, U. Spillmann and Th. Stöhlker, Journal of Instrumentation **5**, C07010 (2010).

[135] P. S. Shaw, U. Arp, A. Henins and S. Southworth, Rev. Sci. Instrum. **67**, 3362 (1996).

[136] M. H. L. Pryce and J. C. Ward, Nature **160**, 435 (1947).

[137] H. S. Snyder, S. Pasternack and J. Hornbostel, Phys. Rev. **73**, 440 (1948).

[138] C. S. Wu and I. Shaknov, Phys. Rev. **77**, 136 (1950).

[139] E. Bleuler and H. L. Brandt, Phys. Rev. **73**, 1398 (1948).

[140] Th. Stöhlker, A. Kramer, S. R. Elliott, R. E. Marrs, J. H. Scofield, Phys. Rev. A **56**, 2819 (1997).

[141] S. Tashenov et al., Nucl. Inst. Meth. A **600**, 599 (2009).

[142] F.S. Porter et al., Rev. Sci. Inst., **75** 3772 (2004).

[143] E. Silver, et al., Nucl. Instr. and Meth. A **545** 683 (2005).